1506
UNIVERSITÀ
DEGLI STUDI
DI URBINO
CARLO BO

Department of Biomolecular Sciences (DISB)

Ph.D. PROGRAMME IN: BIOMOLECULAR AND HEALTH SCIENCES

CYCLE XXXVII

Innovative and eco-friendly approaches to mitigate Microbiologically Influenced Corrosion

ACADEMIC DISCIPLINE: BIOS-15/A

Coordinator: Prof. Ferdinando Mannello

Supervisor: Prof. Emanuela Frangipani

PhD Student: Arianna Scardino

ACADEMIC YEAR

2023/2024

To my superhero Camillo, thank you for fighting the hardest battle for us.

To our baby son Mattia, the greatest gift we could ever receive.

ABSTRACT

Microbiologically influenced corrosion (MIC) is a type of corrosion caused or accelerated by the presence of microorganisms, such as bacteria, fungi, and algae. The metabolic activity of corrosive microorganisms influences the electrochemical processes that degrade materials, especially metals, leading to pitting or crevice formation that significantly increase their deterioration rate. MIC affects various industries worldwide, including oil and gas, petrochemical, water treatment, marine, aviation, and defense, as well as any system where metals are exposed to water, soil, or humid environments. Moreover, MIC causes significant expenses in terms of operational and maintenance costs and account for up to 20 % of the total global corrosion damage (*ca.* US$ 2.5 trillion/year) in the gas and oil sectors, excluding the associated safety and environmental impacts. Counteracting MIC requires a combination of preventative and corrective measures, often tailored to the specific industry and environment affected. Sulfate-reducing bacteria (SRB) are the major contributors to MIC due to their production of hydrogen sulfide, which accelerates corrosion. Effective strategies for eliminating or controlling SRB involve both physical and chemical methods. While chemical methods are the most effective, they often come with challenges such as toxicity and high disposal costs, which underscore the need for developing new and more sustainable strategies. In this PhD thesis two innovative and eco-friendly approaches have been explored with the aim of contributing to the development of novel strategies to manage and control MIC. We have initially investigated the potential use of cinnamaldehyde against the SRB model species *Desulfovibrio vulgaris*. The rationale of choosing cinnamaldehyde lies in its well-documented antimicrobial activity, as well as its efficacy to act as a green corrosion inhibitor for steels in acidic environments. We found that low concentration of cinnamaldehyde, compared to the one reported effective against representative pathogenic bacterial species (*i.e.,* 12.5 μg/ml), inhibited the growth and killed planktonic *D. vulgaris* cells and, more importantly, almost eradicate pre-formed biofilms at 50 μg/ml, by reducing biomass (> 90 %), surface area (> 85 %) and thickness (> 60 %), with comparable efficacy to the conventional biocide, glutaraldehyde. These findings are particularly relevant for strategies aimed at mitigating microbial corrosion, since sessile cells within biofilms are notoriously more difficult to eradicate than planktonic ones. Interestingly, we were able to show that cinnamaldehyde effectively disrupts pre-formed *D. vulgaris* biofilms also on representative metal coupons.

Altogether our results pave the way for the future development of green sustainable strategies involving the use of cinnamaldehyde to mitigate MIC.

Another strategy that we have pursued in this PhD thesis regards the potential role of endolysins to control the growth of SRB. Endolysins are hydrolytic enzymes encoded by bacteriophages during their lytic cycle, targeting the peptidoglycan layer of both Gram-positive and Gram-negative bacteria, thus promoting osmotic lysis. Interestingly, their fast lytic activity can also be accomplished when exogenously applied as recombinant proteins. These enzymes have garnered significant attention for their efficacy against clinically-relevant pathogens and are currently employed in clinical settings. However, the application of endolysins in environmental contexts, particularly those impacted by MIC remains largely unexplored. We have selected and tested *D. vulgaris*-specific endolysins targeting different peptidoglycan structures, demonstrating their effectiveness against *D. vulgaris* planktonic cells. Although preliminary, these promising results highlight the potential of endolysins in the sustainable management of MIC, bypassing the use of conventional toxic biocides, and opening future perspectives on the use of endolysins beyond their traditional clinical applications.

Finally, a case study highlighting the critical role of microbiological investigations as a proactive strategy to prevent MIC has been performed, to advocate for the incorporation of microbial community characterization into MIC management practices. Such proactive approaches will offer significant potential to improve early detection and mitigation strategies, protecting marine infrastructures from corrosion-related failures.

TABLE OF CONTENTS

Chapter 1

Introduction and aims

1.1. Introduction to Microbiologically Influenced Corrosion

Microbiologically influenced corrosion (MIC) has emerged as a significant issue affecting a wide range of industrial processes, materials and sectors. Unlike abiotic corrosion, which is described as the gradual degradation of a metal resulting from electrochemical reactions in the absence of biological activity (Kelly et al, 2002), MIC involves the active participation of microorganisms and both types of corrosion often occur simultaneously. MIC is an electrochemical process that can initiate, or accelerate metal corrosion reactions (Videla, 1996), enhancing their kinetic rates by 10 - 1,000 times (Lane, 2005). It is crucial to distinguish MIC from biofouling. Biofouling refers to the accumulation and growth of a wide variety of micro- and macro- organisms on a surface, including plants and/or animals (*e.g.,* algae, mussels, barnacles) (AMPP, 2023; Kniz et al., 2023), while MIC has been defined by the National Association of Corrosion Engineers (NACE) and the American Society for Testing and Materials (ASTM) as "*corrosion affected by the presence or activity, or both, of microorganisms*" (NACE-ASTM G193 2022), impacting different areas, such as petrochemical installations (Kiani Khouzani et al., 2019), gas and oil industries (Skovhus et al., 2017), water treatment facilities (Coetser, 2005), as well as the aviation and defense sectors (Lee et al., 2007) (Fig. 1).

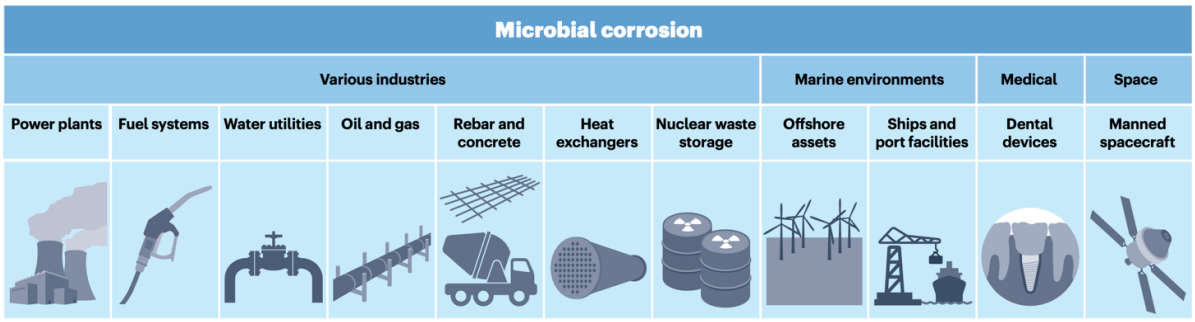

Fig. 1. Microbial corrosion affecting materials susceptible to MIC, such as various industries, as well as marine environments, medical and space sectors (Xu et al., 2023).

MIC causes significant expenses in terms of operational and maintenance costs and may account for up to 20 % of the total global corrosion damage (*ca.* US$ 2.5 trillion/year) in the oil and gas sectors, excluding the associated safety and environmental impacts (NACE, 2016). Two significant episodes in the history of MIC-related failures are considered as milestones for assessing the associated financial costs and environmental damages. The first and most well-known incident involves the Alaska pipeline leak, which caused a significant surge in global

crude oil prices. The analysis of the damage was attributed to MIC driven by sulfate reducing bacteria (SRB) (Jacobson, 2007). The leak released approximatively 750,000 liters of oil. The 27 km of the pipeline had to be rebuilt, temporarily halting production operations. The total cost, including fines imposed by the State of Alaska, exceeded US$ 700 millions (Jacobson, 2007).

The second and most recent episode regards the Aliso Canyon gas leak, one of the largest methane releases in USA history. The leak, which started in October 2015, released over 109,000 tons of methane leading to widespread evacuations and health complaints from the local residents. Subsequent investigations concluded that MIC caused by methanogens was the leading cause of the incident (Conley et al., 2016).

Understanding MIC requires the identification of interconnected mechanisms through which microbiological activity influences and/or accelerates corrosion processes. Corrosion is fundamentally linked to electrochemical processes involving oxidation (anode) and reduction (cathode) reactions. The area of the metal surface that corrodes and goes into solution is the anode, while the area that does not dissolve is the cathode. Oxidation or anodic reaction (Table 1, reaction 1) and reduction or cathodic reaction (Table 1, reaction 2) are defined as when metals gain or lose electrons, respectively.

Table 1. Electrochemical corrosion process involves both anodic and cathodic reactions.

(1) Anodic reaction	$Fe \rightarrow Fe^{2+} + 2e^-$
(2) Cathodic reaction	$2H^+ + 2e^- \rightarrow H_2$

Oxidation and reduction reactions occur in the presence of a solution, typically water. The availability and interaction of these components form the "electrochemical triangle," which allows the corrosion process to happen (Javaherdashti, 2017). Abiotic corrosion reactions and microbiological processes influencing corrosion share similarities but exhibit also differences. Both involve redox reactions driving metal degradation, but differently from abiotic corrosion, microorganisms not only facilitate these redox reactions but also integrate them into their metabolic processes by coupling energy-producing reactions to their energy dissipation (Hamilton, 2003). For MIC to occur, the presence of “three M’s” is required: Microorganisms, Media (chemical composition and physical parameters creating a conducive environment) and Metals (Little et al., 2020). The interaction of these components affects various mechanisms that influence the rate of metal corrosion, either directly or indirectly. Moreover, MIC can

manifest itself in several forms [*i.e., i)* Surface deposition due to microorganisms; *ii)* Electrical MIC (E-MIC); *iii)* Metabolite MIC (M-MIC), Fig. 2].

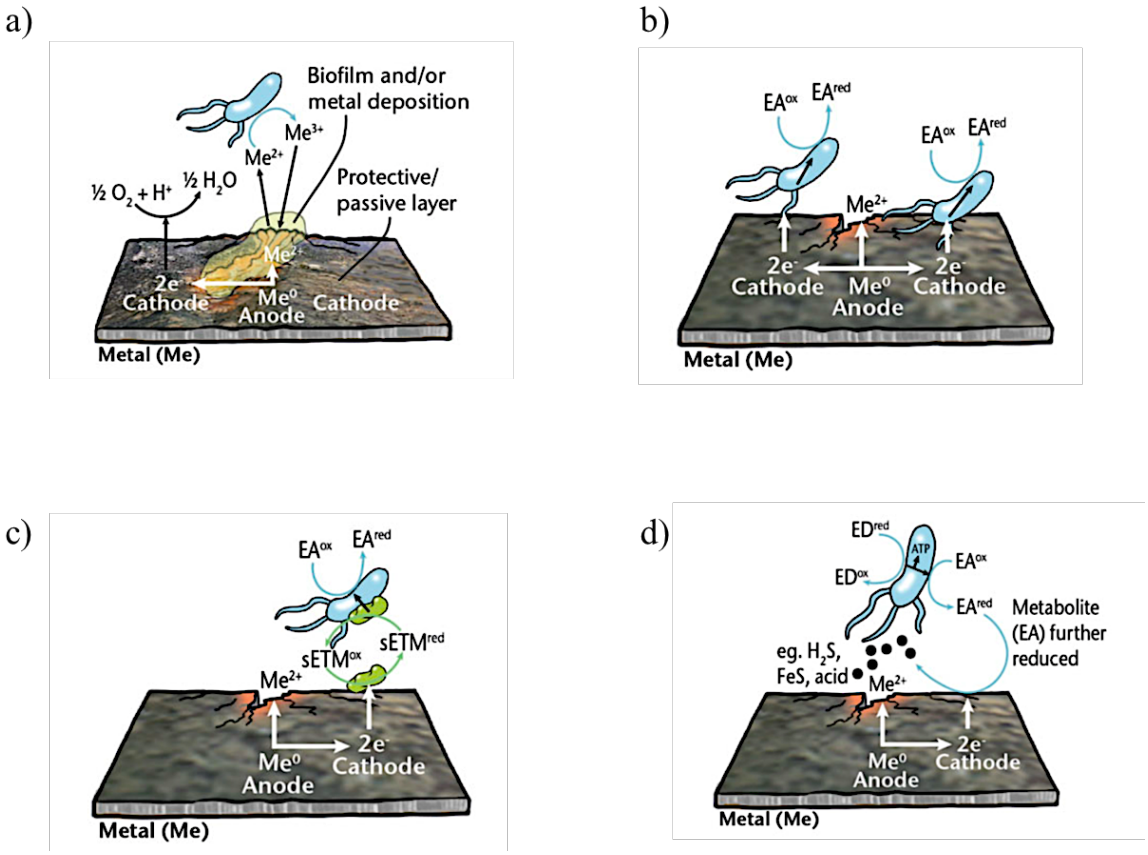

Fig. 2. Schematic representation of corrosion mechanisms influenced by microorganisms. **a)** MIC mechanism due to microbial deposits, oxygen gradient corrosion; **b)** direct and **c)** indirect electrical MIC (E-MIC). **d)** metabolite MIC (M-MIC). Me: metal; EA: electron acceptor; ED: electron donor; ox: oxidized; red: reduced; sETM: soluble electron transfer mediator (Knisz et al., 2023).

1.1.1. Surface deposition

MIC due to surface deposition is a type of localized corrosion where microorganisms can form deposits on material surfaces by attaching to them and developing biofilms (Fig. 2a). These multispecies communities are encased in a self-produces matrix of extracellular polymeric substances (EPS) (Flemming et al., 2016). MIC mechanisms can be classified based on oxygen availability, distinguishing between those occurring in oxygen-rich (aerobic) environments and those in oxygen-deprived (anaerobic) conditions. When oxygen is present, biofilm growing cells create an oxygen concentration gradient between the anodic and cathodic areas of the

surface, where oxygen acts as the electron acceptor. Anoxic regions develop when aerobic microorganisms consume oxygen faster than its diffusion back into the area. This imbalance results in localized zones of oxygen depletion, paving the way for anaerobic conditions (Hamilton, 2003). Biofilms typically exhibit a layered structure, with aerobic activity located at the surface where oxygen is rapidly depleted, while deeper layers directly in contact with the surface become anoxic, supporting and favoring the occurrence of anaerobic processes (Procópio, 2019).

1.1.2. Electrical MIC (E-MIC)

EPS secreted by the cells within biofilms exhibits redox and electrochemical properties that contribute to microbial respiration and corrosion processes. The reduction of electron acceptors occurs inside the bacterial cell, while the oxidation of electron donors happens externally. This process, known as extracellular electron transfer (EET), is a critical part of the microbial mechanism responsible for metal corrosion, and it is called Electrical MIC (E-MIC) (Enning and Garrelfs, 2014).

When the electron donor is an organic carbon source that can enter the cell, no electron transport mechanism is needed, as the electrons are already present in the bacterial cytoplasm. However, when insoluble metals are used as electron donors, they cannot directly pass through the cell membrane. Therefore, extracellular electron transport is required to facilitate their use. There are two mechanisms for this electron transfer: direct and indirect. During direct E-MIC (Fig. 2b) (Lovley, 2011), cells come into direct contact with the metal surface and accept electrons *via* cell surface enzymes, redox proteins, or membrane-bound structures, such as c-type cytochromes (Paquete et al., 2022). Additionally, some bacteria may use electrically conductive pili which allow for electron transfer between the metal and the cell (Lovley, 2017). Conversely, during indirect E-MIC (Fig. 2c), cells release soluble electron transfer mediators that facilitate electron exchange with the metal surface (Huang et al., 2018). These mediators are oxidized at the anode and then return to the cell to take part in respiratory processes (Kato, 2016).

1.1.3. Metabolite MIC (M-MIC)

During Metabolite MIC (M-MIC) (Fig. 2d), microorganisms contribute to metal deterioration processes by secreting corrosive metabolites, such as protons, organic or inorganic acids, such

as hydrogen sulfide (H_2S). When the pH is low enough, protons are directly reduced on the metal surface, and unlike E-MIC, no biocatalysts are needed for the process (Jia et al., 2018).

1.2. Microorganisms responsible of MIC

Among the various microorganisms involved in corrosion processes, such as fungi, algae, and archaea, bacteria have been the most extensively studied contributors (Lane, 2005). Indeed, the majority of MIC research has focused on bacterial species, as they play a significant role in accelerating corrosion through their metabolic activities and biofilm formation. Bacteria can interact with metals like iron, copper and certain alloys directly or indirectly, influencing electrochemical processes. These interactions can either accelerate or inhibit corrosion. A wide variety of corrosive microorganisms have been identified (Lane, 2005, Liu et al., 2023), as summarized in Fig. 3. These include acid-producing bacteria (APB), metal-oxidizing bacteria (MOB), metal-reducing bacteria (MRB), sulfate-oxidizing bacteria (SOB), nitrate-reducing bacteria (NRB), archaea, fungi, and, most notably, sulfate-reducing bacteria (SRB).

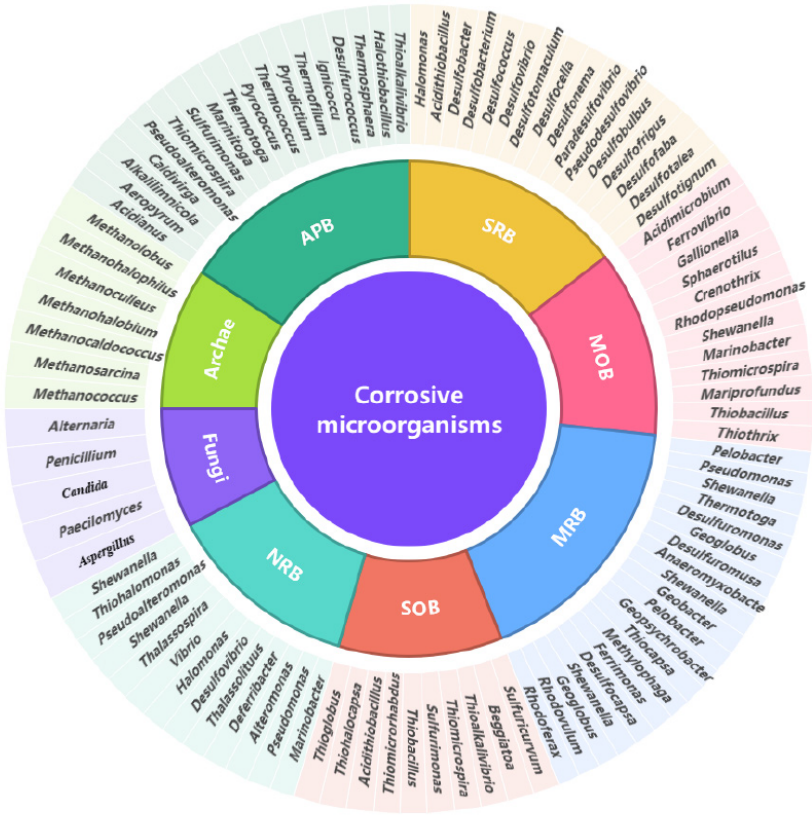

Fig. 3. Main corrosive microorganisms associated with MIC. APB: acid-producing bacteria; SRB: sulfate reducing bacteria; MOB: metal-oxidizing bacteria; MRB: metal-reducing bacteria; SOB: sulfate-oxidizing bacteria; NRB: nitrate-reducing bacteria (Liu et al., 2023).

APB produce organic or inorganic acidic metabolites that lower the pH, leading to the corrosion of metallic materials (Khan et al., 2022). The inorganic acids produced by APB include nitric acid (HNO_3), sulfurous acid (H_2SO_3), sulfuric acid (H_2SO_4), nitrous acid (HNO_2), and carbonic acid (H_2CO_3). Moreover, APB can also create favorable conditions for SRB activity by producing fatty acids that can be utilized by SRB (Telegdi et al., 2018).

MOB utilize metals such as iron and manganese as electron donors for energy metabolism, resulting in their corrosion. By oxidizing ferrous or manganese ions (*i.e.,* Mn^{2+}), they produce acidic metabolites that accelerate metal corrosion reactions. These bacteria are commonly found in corrosion pits on steel surfaces (Lane, 2005).

MRB, which can be either strictly or facultatively anaerobic, reduce insoluble metal oxides [*i.e.,* Fe(III) oxides] to Fe^{2+}, resulting in the increase of the ionic diffusion coefficient in the corrosion products and the acceleration of corrosion kinetics (Liu et al., 2023).

NRB, found in nitrate- and organic matter-rich environments, reduce nitrate and accelerate steel corrosion (Fu et al., 2021). In the gas and oil industry, nitrate addition is a strategy often used to promote NRB growth, which compete with SRB growth, by inhibiting sulfate reduction (Fida et al., 2016).

SOB oxidize sulfur (S^0) and sulfides (S^{2-}), producing the corrosive sulfuric acid (H_2SO_4) which increases acidity, hydrogen penetration and corrosion rates (Little et al., 2000). Additionally, SOB produce sulfate (SO_4^{2-}) that supports SRB growth (Norlund et al., 2006).

SRB are among the most studied bacteria associated with MIC, impacting different industrial settings and alloys. SBR comprise a group of anaerobic bacteria that obtain energy by reducing sulfate ions, producing hydrogen sulfide (H_2S), a highly toxic and corrosive compound. H_2S can then react with metal ions, such as iron, leading to the formation of metal sulfides, such as ferrous sulfide (FeS). These last are poorly soluble in aqueous environment and often appear as a dark, sludge-like residue (Telegdi et al., 2018).

MIC processes are primarily influenced by sessile cells, rather than planktonic ones in the surrounding environment. As briefly mentioned above, microorganisms often coexist within naturally occurring biofilms, which are dense aggregations of cells embedded in a self-produced EPS matrix. The EPS provides a protective environment for microbes within the biofilm, allowing them to grow, propagate, release metabolites, and communicate with other microorganisms using quorum-sensing molecules (Waters and Bassler, 2005). Within biofilms, microorganisms form synergistic communities (consortia) that collaboratively influence

electrochemical processes. The cooperative metabolism within consortia differs significantly from the activities of individual species, driving biochemical reactions that accelerate metal surface corrosion (Lee and Newman, 2003; Phan et al., 2021).

In multispecies biofilms, groups of physiologically diverse bacteria often form stratified structures, organized according to their redox processes (Fig. 4).

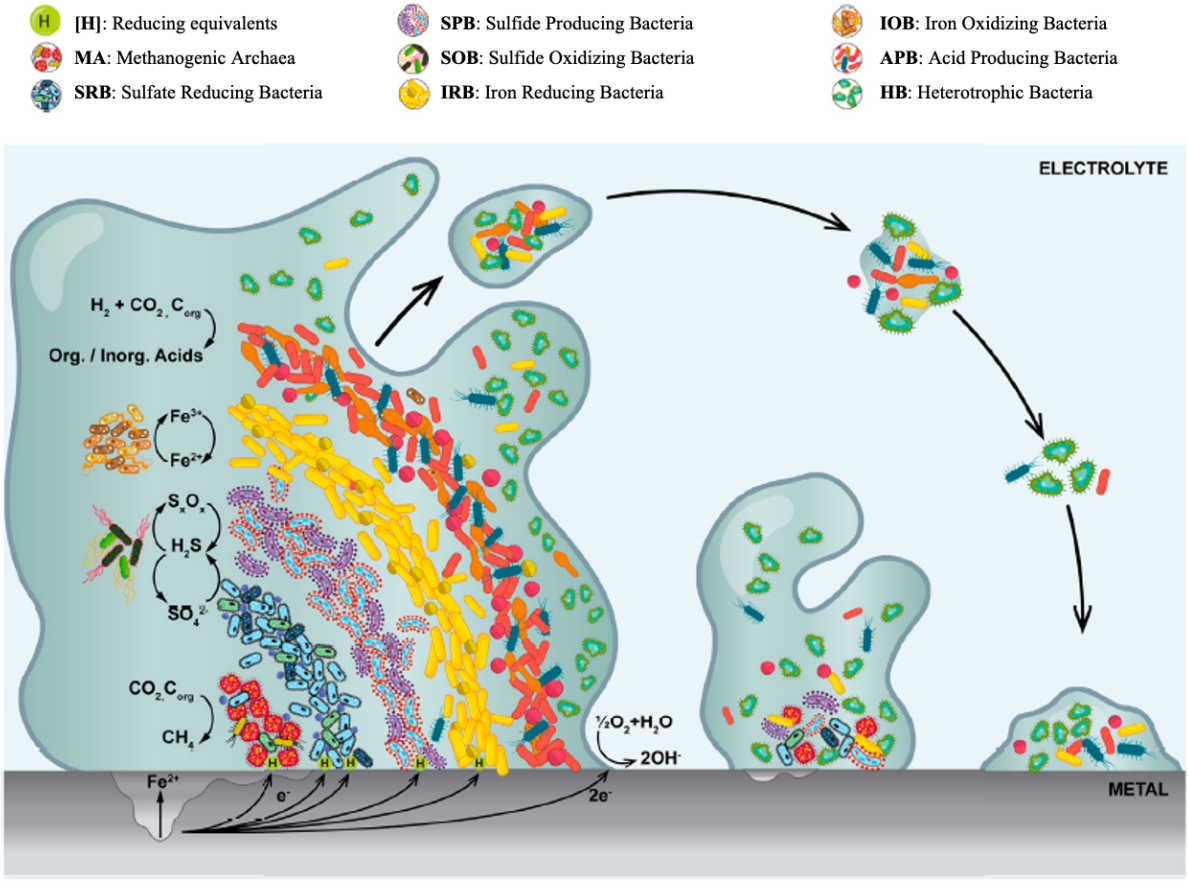

Fig. 4. Representation of a multispecies biofilm at different stages of development on a metal surface, depicting the most relevant microbial groups involved in MIC within an idealized redox zonation from the oxidized outer layers to the more anaerobic inner core. Only the most representative half reactions are shown (modified from Puentes-Cala et al., 2022).

Bacteria within biofilms can engage in cooperative or competitive interactions, both essential in accelerating metal corrosion processes (Qian et al., 2022). Microbial competition occurs when different species compete for resources, such as nutrients, oxygen, and space, resulting in the production of corrosive agents like organic acids and H_2S (Xu et al., 2023). For instance, SRB and APB, both present in the deepest layer of biofilms in direct contact with the metal surface, compete for nutrients and produce organic acids that speed up the metal corrosion in marine environments (Dang and Lovell, 2015). This dynamic within the biofilm creates a

layered structure, with the deeper layer in contact with the surface being anoxic. Indeed, initially biofilms are composed by aerobic heterotrophic bacteria species, which use the dissolved oxygen around them, generating a chemical gradient, where the outer layer presents high levels of oxygen, while the inner zone is anoxic, allowing the growth of anaerobic species (Hamilton 2003). Over time, only anaerobic bacteria that can utilize metal compounds as resources for they survival (*i.e.,* anaerobic chemolithotrophs) remain (Procópio, 2019). Iron-containing metals, such as carbon and stainless steel, are subject to corrosion processes involving both aerobic and anaerobic conditions (Fig. 4 and 5). More in detail, in the presence of oxygen the Fe^0 is abiotically oxidized to Fe^{2+}(Fig. 5a, reaction 1). These last is further oxidized to Fe(III) hydroxides, such as $Fe(OH)_3$, resulting in the rust commonly seen on corroding iron (Fig. 5a, reaction 4). Moreover, aerobic microorganisms, such as heterotrophs (*i.e.*, *Vibrio, Pseudoalteromonas, Flexibacter* and *Marinobacter* spp.), IOB (*i.e.*, *Mariprofundus, Dechloromonas* and *Sideroxydans* spp.), and SOB (*Sulfurimonas* spp.), colonize the metal surface and contribute to O_2 removal, by using it as terminal electron acceptor, generating carbon dioxide (CO_2), Fe(III) precipitates and sulfate (SO_4^{2-}), respectively. These metabolites lead to the generation of an anaerobic environment, especially in deeper layers in contact with metal surfaces, where corrosive anaerobic bacteria are able to grow (Usher et al., 2014) (Fig. 5b). In O_2 deprived conditions it is possible to find anaerobic Fe^0 oxidants, such as protons (H^+), nitrate (NO_3^-), Fe(III), SO_4^{2-}, CO_2 and H_2S. Only H^+ and H_2S can abiotically react with Fe^0 to oxide and corrode it, producing H_2 (Tang et al., 2019) (Fig. 5a, reactions 2-3), while the remaining Fe^0 oxidants require microbial catalysis, in which bacteria accept electrons from Fe^0 to support their anaerobic respiration (Fig. 5a). These electron reactions are promoted by anaerobic bacteria through various mechanisms, such as the production of metabolites leading to the H_2 formation; H_2-mediated electron transfer between the metal and the microorganisms; direct electron transfer between metal and microorganisms; and redox-active organic molecules shuttling electrons between Fe^0 and microorganisms. H_2 formation is favored by the release of hydrogenases during cell lysis or by its secretion outside the cell (Tsurumaru et al., 2018). Microorganisms such as NRB, iron reducing bacteria (IRB), SRB, methanogens and acetogens, possess the capacity to reduce nitrate, Fe(III), SO_4^{2-} and CO_2, respectively, by oxidizing H_2 produced from fermentative bacteria or Fe^0 (Fig. 5b). Regarding the direct electron transfer between metals and microorganisms, this mechanism happens when the initial electron acceptor for electrons derived from Fe^0 is an outer-surface electrical contact on the cell surface (*i.e.*, *c*-

type cytochromes) (Tang et al., 2019). An alternative to H_2 is represented by redox-active organic molecules (*i.e.,* flavins, phenazines and pyocyanins) acting as electron shuttles between Fe^0 and microorganisms (Lovley and Holmes, 2022). All these mechanisms influence and accelerate metal corrosion processes.

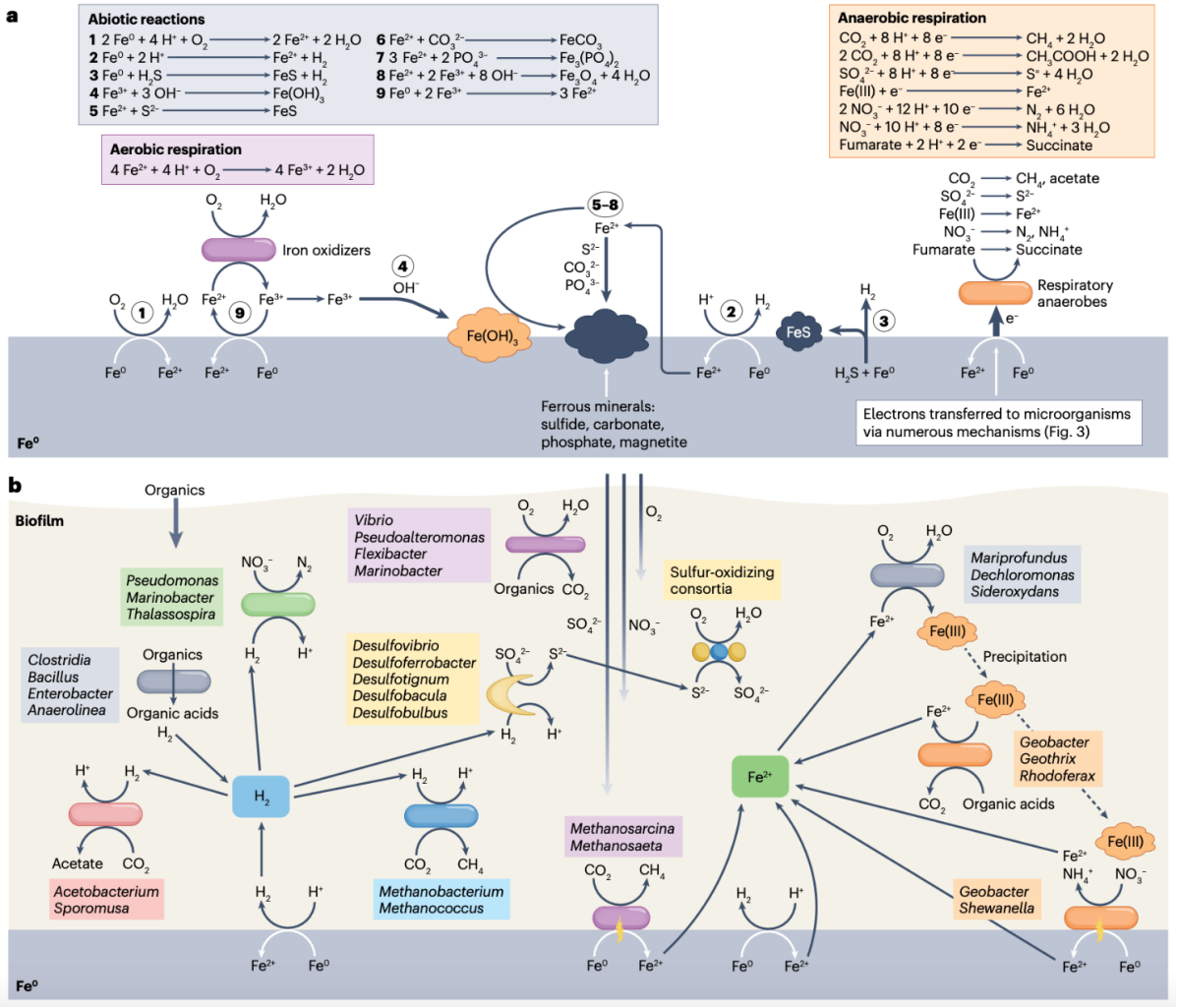

Fig. 5. Key reactions and microorganisms involved in the corrosion of Fe^0-containing metals. **a)** Key reactions associated with microbial corrosion of iron metals, with numbers 1-9 representing abiotic reactions. **b**) Microbial diversity and spatial organization within a biofilm drive MIC process. Hydrogen (H_2), released abiotically from iron (Fe^0) and also produced by fermentative bacteria (in grey box), is consumed by various microbial groups, including NRB (green box), SRB (yellow box), methanogens (light blue box) and acetogens (red box). Aerobic microorganisms, such as heterotrophs (magenta box), SOB (yellow box) and IOB (grey box), consume O_2 at the surface of biofilm promoting anaerobic corrosion conditions. Electroactive methanogens (magenta box) and IRB (orange boxes) directly extract electrons from Fe^0 generating ferrous ion (Fe^{2+}) that iron oxidizers convert to Fe(III) oxides that serve as an additional electron acceptor for Fe(III) reducers. The diffusion of organic compounds and electron acceptors, such as O_2, NO_3^-, SO_4^{2-}, from the environment into the biofilm, along with their preferential consumption (O_2 first, followed by NO_3^-, and then SO_4^{2-}), creates vertical heterogeneity stratification within the biofilm, with Fe^0 as an electron donor at the base of the biofilm (modified from Xu et al., 2023).

1.2.1 Sulfate Reducing Bacteria

SRB, strict anaerobes, are among the most extensively studied microorganisms in MIC research due to their significant role in sulfur cycle (Jorgensen and Kasten, 2006). Sulfur, one of the most abundant elements on the Earth, can be present in various forms, including pyrite (FeS_2) or gypsum ($CaSO_4$) in rocks and sediments, as well as sulfate (SO_4^{2-}) in seawater (Jasińska et al., 2012). With a broad range of oxidation states ranging from -2 (completely reduced) to +6 (completely oxidized), sulfur supports various metabolic processes. SRB perform dissimilatory sulfate reduction, using SO_4^{2-} as the terminal electron acceptor in their energy metabolism to produce H_2S. The dissimilatory sulfate reduction reactions, inhibited by the presence of oxygen, confine SRB only to O_2-depleted environments (Fareleira et al., 2003). Indeed, in anoxic zones of marine sediments SRB are predominant due to the high sulfate concentration in seawater (~ 28 mM). They are also found in freshwater sediments, where sulfate concentrations are lower (~ 1 mM) but maintained through redox cycling of H_2S to sulfate at the oxic-anoxic interface, facilitated by chemolithotrophic and phototrophic bacteria, respectively (Holmer and Stoskholm, 2001) (Fig. 6, Table 2).

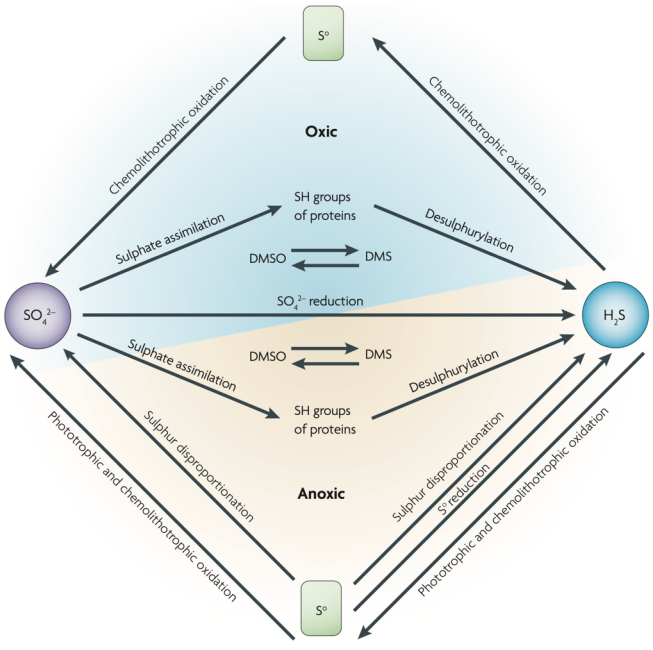

Fig. 6. Sulfur transformation by SRB. SRB reduce sulfate (SO_4^{2-}) to hydrogen sulfide (H_2S). Then the sulfide can be oxidized aerobically by SOB (*i.e.*, *Thiobacillus* or *Beggiatoa* spp.) or anaerobically by phototrophic sulfur bacteria (*i.e.*, *Chlorobium* spp.) to sulfur (S^0) and SO_4^{2-}. Other sulfur transformations include assimilation of SO_4^{2-} and S^0 disproportionation (*Desulfovibrio sulfodismutans*) and reduction (*Desulfuromonas* spp.). Moreover, organic sulfur compounds, such as dimethylsulfoxide (DMSO) can be transformed into dimethylsulfide (DMS) and vice versa by several groups of microorganisms (Muyzer and Stams, 2008).

Table 2. Processes and microorganisms involved in the sulfur cycle.

Process	Reaction and microorganisms involved
Sulfur oxidation • Aerobic • Anaerobic	$H_2S \rightarrow S^0 \rightarrow SO_4^{2-}$ • Chemolithotrophic sulfur-bacteria (*i.e*, *Thiobacillus*) • Phototrophic and some chemolithotrophic bacteria (*i.e.*, *Chlorobium* spp.)
Sulfate reduction (Anaerobic)	$SO_4^{2-} \rightarrow H_2S$ *Desulfovibrio, Desulfobacter, Archeoglobus* (*Archea*)
Sulfur reduction (Anaerobic)	$S^0 \rightarrow H_2S$ *Desulforomonas*
Sulfur disproportionation	$S_2O_3^{2-} \rightarrow H_2S \rightarrow SO_4^{2-}$ *Desulfovibrio* and others
Organic sulfur compounds oxidation and reduction	$CH_3SH \rightarrow CO_2 + H_2S$ DMSO → DMS Various microorganisms
Desulfurylation	Organic compound-S → H_2S Various microorganisms

Pathways to reduce sulfate include both assimilatory and dissimilatory sulfate reduction reactions. Assimilatory sulfate reduction plays an important role in biomolecular synthesis by providing reduced sulfur, essential for the production of sulfur-containing compounds. This process is particularly important for the synthesis of the amino acids cysteine and methionine, which requires energy-intensive steps within assimilatory pathways. However, only a small fraction of sulfite synthetized during sulfate reduction is incorporated into sulfur-containing amino acids. On the other hand, the majority of sulfate undergoes reduction to sulfide through the dissimilatory sulfate reduction driven by SRB (Li et al., 2019), which occurs in two distinct steps. From a chemical point of view, sulfate is an unfavorable electron acceptor for microorganisms due to the redox potential ($E^{0'}$) of the sulfate-sulfite pair being -516 mV, which is too low to be reduced by common intracellular electron carriers like ferritin or NADH. Therefore, in the first step of dissimilatory sulfate reduction, SO_4^{2-} is activated by the enzyme sulfate adenylyl transferase (Sat), forming adenosine-5'-phosphosulfate (APS) at the cost of two ATP equivalents. APS reductase then reduces APS to bisulfite (HSO_3^-) using two electrons (Table 3, reactions 1 and 2). This activation is facilitated by the hydrolysis of the released pyrophosphate ($HP_2O_7^{3-}$, PPi), which drives the reaction forward (Table 3, reaction 3). The redox potential ($E^{0'}$) of the APS-sulfite plus AMP pair is -60 mV, enabling its reduction through reduced ferredoxin or NADH.

Table 3. Dissimilatory sulfate reduction reactions

(1)	$SO_4^{2-} + ATP + H^+ \rightarrow APS + HP_2O_7^{3-}$
(2)	$APS + 2e^- + 0.5H^+ \rightarrow 0.5HSO_3^- + AMP$
(3)	$HP_2O_7^{3-} + H_2O \rightarrow H_2PO_4^{2-}$
(4)	$0.5HSO_3^- + 0.5SO_3^{2-} + 6e^- + 7H^+ \rightarrow 0.5HS^- + 0.5H_2S + 3H_2O$
(5)	$SO_4^{2-} + ATP + 8e^- + 8.5H^+ \rightarrow 0.5\ HS^- + 0.5\ H_2S + AMP + HPO_4^{2-} + 2H_2O$

In the second step, bisulfite reductase reduced HSO_3^- to sulfide (HS^-) using six electrons (Reaction 4). The $E^{0'}$ of the sulfite-sulfide redox pair is -116 mV. Overall, the sulfate reduction process requires 8 moles of electrons and 8.5 moles of protons to reduce 1 mole of sulfate (Reaction 5) (Keller and Wall, 2011).

1.2.2 Dissimilatory sulfate reductase

Research on metabolism and biochemistry of SRB has predominantly focused on the genus *Desulfovibrio*, a member of the *∂*-proteobacteria class (Postgate, 1984). In particular, the species *Desulfovibrio vulgaris* Hildenborough has been used as a model microorganism for studying SRB energy metabolism (Heidelberg et al., 2004) (Fig. 7).

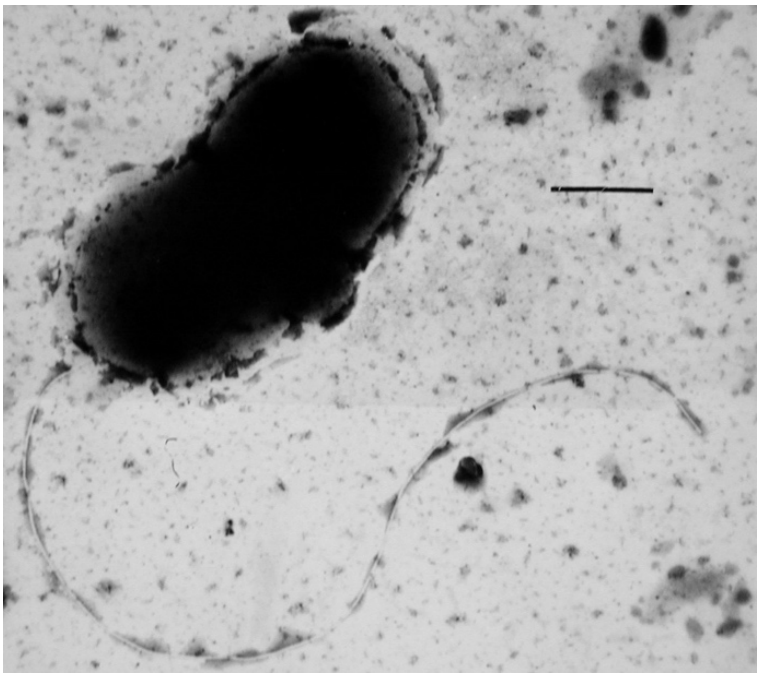

Fig. 7. Transmission electron microscopy (TEM) image of *D. vulgaris* Hildenborough cell. Scale bar, 0.5 μm. Image courtesy of Wikimedia Commons/Graham Bradley (In This Issue, 2014).

In SRB, dissimilatory sulfite reductase (Dsr) is the key enzyme involved in dissimilatory sulfate reduction, allowing them to obtain energy (Fig. 8).

SO_4^{2-} ions can enter the cell *via* specialized transport systems, including ATP-binding cassette (ABC)-type (SulT) and superfamily-type (SulP) transporters, which facilitate their passage across the cytoplasmatic membrane (Kertesz, 2001). Once inside, SO_4^{2-} is activated in adenosine-5′-phosphosulfate (APS) by the enzyme sulfate adenylyl transferase (Sat) (Fig. 8, reaction I). APS reductase, encoded by the *apsAB* genes, subsequently reduces APS to sulfite (SO_3^{2-}) using two electrons (Fig. 8, reaction II). Dsr is composed of two subunits, namely DsrA and DsrB, encoded by the *dsrA* and *dsrB* genes, respectively (Müller et al., 2014). DsrAB activity is also supported by DsrC, a protein encoded by *dsrC* that is universally present in SRB genomes containing *dsrAB*. DsrC acts as a substrate for sulfite reduction and possesses two conserved cysteine residues, crucial for its function (Oliveira et al., 2008). During the reduction process, sulfite binds to the active site of DsrAB, where it is converted into a sulfur (S^0) intermediate bound to DsrC, to form DsrC trisulfide (Fig. 8, reaction III). The membrane complex DsrMKJOP facilitates the dissociation of the trisulfide intermediate from DsrC, enabling further reduction of S^0 to sulfide (HS^-/S^{2-}). Concurrently, DsrC is released and recycled for subsequent reactions (Fig. 8, reaction IV) (Santos et al., 2015). Overall, in dissimilatory sulfate reduction, sulfite can be reduced to a mixture of products, including trithionate ($S_3O_6^{2-}$), thiosulfate ($S_2O_3^{2-}$) and sulfide (HS^-/S^{2-}), mediated by DsrAB (Ferreira et al., 2022).

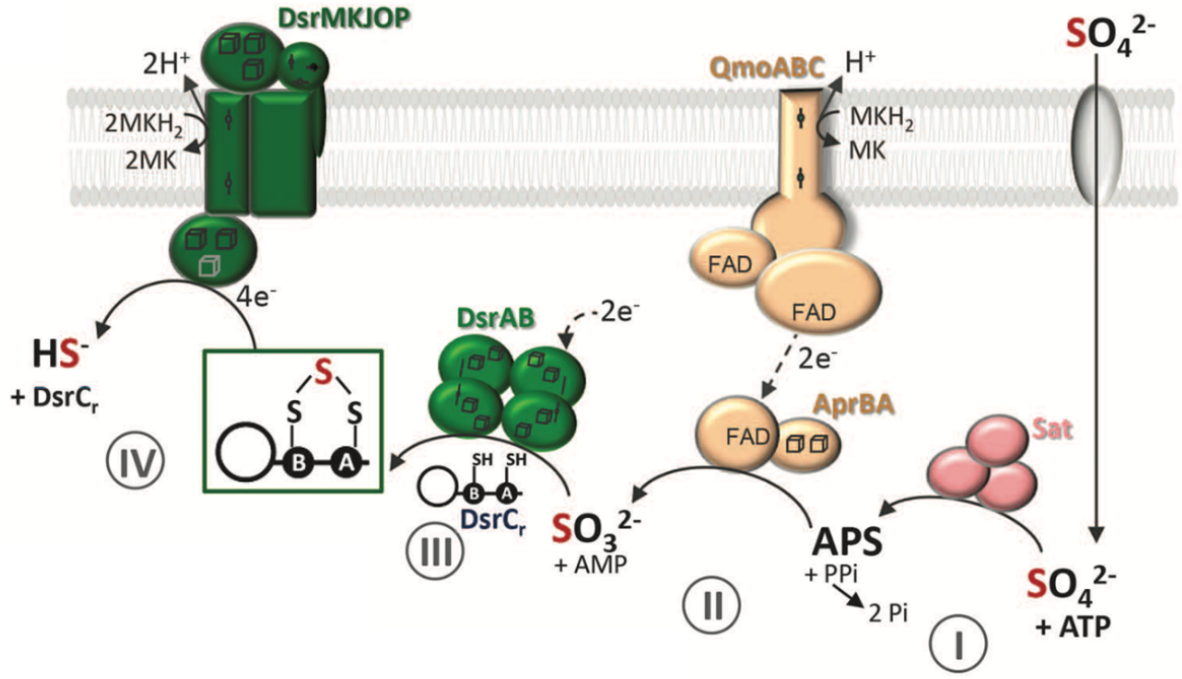

Fig. 8. Sulfate respiratory pathway by SRB. The pathway involves the import of sulfate; activation of SO_4^{2-} to adenosine-5'-phosphosulfate (APS) (I); reduction of APS to sulfite by APS reductase (II); reduction of sulfite to DsrC trisulfide by DsrAB/DsrC (III); reduction of the trisulfide to sulfide (IV) (Santos et al., 2015).

1.2.3 Mechanisms of MIC due to SRB

The MIC mechanism consequent to the metabolic activity of SRB (Fig. 9) starts with iron dissolution leading to a loss of 8 electrons (Table 4, reaction 1). This reaction occurs extracellularly since insoluble iron cannot diffuse into SRB cells.

Table 4. Anodic depolarization mechanism of metal corrosion.

(1) Anodic reaction	$4Fe \rightarrow 4Fe^{2+} + 8e^-$
(2) Water dissociation	$8H_2O \rightarrow 8H + 8OH^-$
(3) Cathodic reaction	$8H^+ + 8e^- \rightarrow 8H + 4H_2$
(4) Anodic depolarization	$3Fe^{2+} + 6OH^- \rightarrow 3Fe(OH)_2$
(5) Hydrogen oxidation	$SO_4^{2-} + 4H_2 \rightarrow H_2S + 2H_2O + 2OH^-$
(6) Dissociation of hydrogen sulfide	$H_2S \rightarrow S^2 + 2H_2$
(7) Anodic depolarization	$Fe^{2+} + S^2 \rightarrow FeS$
Total reaction	$4Fe + SO_4^{2-} + 4H_2O \rightarrow FeS + 3Fe(OH)_2 + 2OH^-$

The electrons generated in the anodic reaction (Table 4, reaction 1) and the generated H^+ through the H_2O dissociation (Table 4, reaction 2), lead to the formation of H_2 molecules thanks to a cathodic polarization process (Table 4, reaction 3). The main corrosion product is $Fe(OH)_2$

(Table 4, reaction 4). SRB metabolism reduces SO_4^{2-} to H_2S by consuming H_2 (Table 4, reaction 5). Then, the H^+ concentration in the cathodic area increases with the dissociation of H_2S (Table 4, reaction 6). Thanks to an anodic depolarization a new corrosion product, *i.e.,* iron-sulfide (FeS), is formed (Table 4, reaction 7).

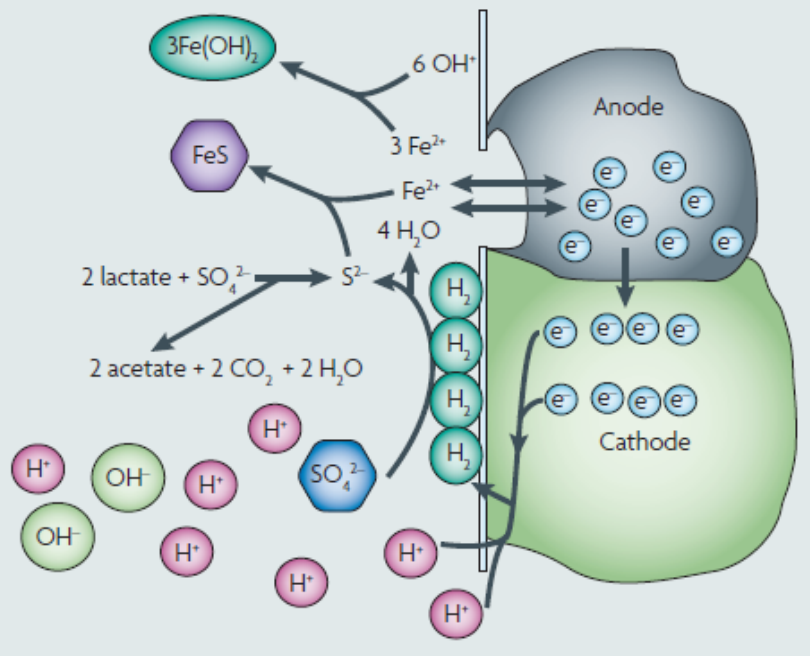

Fig. 9. Depolarization mechanisms of metal corrosion influenced by SRB (Muyzer and Stams, 2008).

On the other hand, at the cathode where sessile SRB are present in contact with the metal and reduce SO_4^{2-} to S^{2-}, protons act as electron acceptors (Fig. 9). By the SRB hydrogenase, hydrogen adsorbing on the metal surface is removed. An organic carbon nutrient, such as lactate, can diffuse into SRB cytoplasm and its oxidation releases electrons in the same location where SO_4^{2-} is reduced to S^{2-} (Fig. 9). It is reasonable that at the metal surface, when in lack of organic carbon, SRB may derive energy from iron oxidation for survival (Xu and Gu, 2011). Central to this electrochemical process is the extracellular electron transfer across the SRB cell wall which is required to couple the extracellular oxidation of iron to the intracellular SO_4^{2-} reduction (Li et al., 2018). When the SRB cell wall is in direct contact with the metal surface, extracellular electrons are transferred into the cytoplasm thanks to the presence of SRB redox-active proteins, such as *c*-cytochromes, providing electrons for the reduction of metal ions (Heidelberg et al., 2004).

1.3. Methods to prevent and mitigate MIC

To prevent and mitigate MIC, multiple strategies are currently in use aiming at fighting the adhesion and biofilm formation of the microorganisms on metal surfaces. MIC can be controlled using different ways: I) physical methods (*i.e.*, cleaning by means of piggins; UV-radiation; ultrasonic treatments), II) chemical methods (*i.e.*, use of biocides); III) electrochemical methods (*i.e.*, cathodic protection; coating) (Fig. 10).

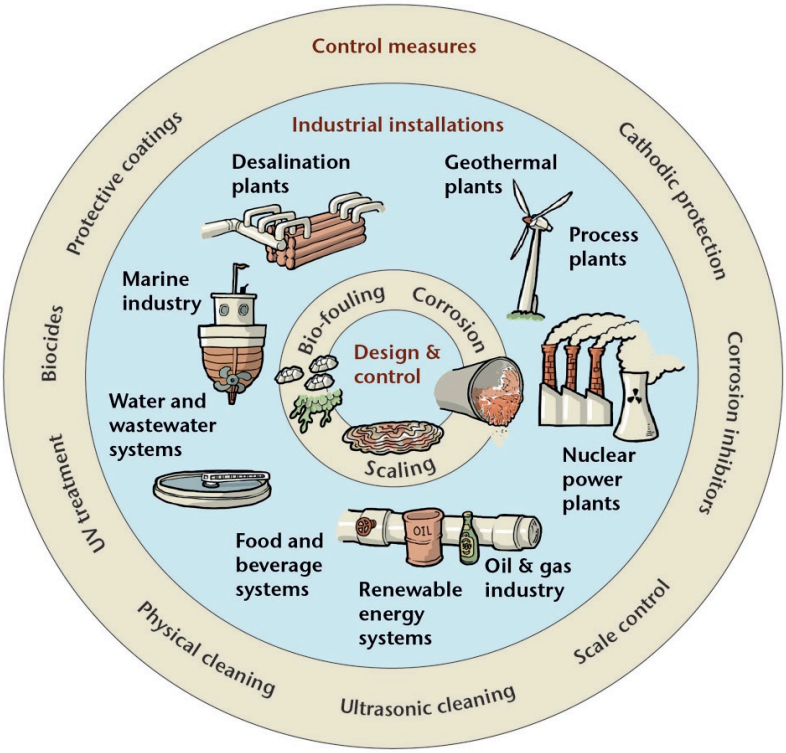

Fig. 10. Examples of various strategies to control and mitigate MIC (Knisz et al., 2023).

Physical methods are widely employed in MIC mitigation by applying mechanical forces with the aim to scrap the biofilm from metal surfaces. One of the most commonly used tools for cleaning the inner surface of the oil and gas pipelines is the so-called “pig”. These devices are primarily utilized for inspecting pipelines, cleaning their surfaces, and supplying chemicals (Javaherdashti, 2017). When biofilms form inside the pipelines, pigging can mechanically scrape them off. However, they cannot entirely remove bacterial colonization, allowing microorganisms to regrow and reestablish biofilms over time. A limitation of pigging arises in the context of localized corrosion, where bacterial cells penetrate into pits within the pipe walls.

The brushes on pigs are unable to access these deep pits effectively, leaving the colonized areas untreated (Cote et al., 2014). While pigging remains a recommended non-destructive method for pipeline inspection and cleaning, its inability to completely prevent MIC, limits its effectiveness as a standalone solution.

Another physical method explored for MIC control is UV treatment. UV radiations damage microbial proteins and membranes and indirectly affect DNA by inducing the formation of reactive oxygen compounds (*i.e.*, H_2O_2, O^{2-}). These damages cause DNA breaks, leading to microorganism death (Elasri and Miller, 1999). However, the efficacy of UV treatment is restricted to microorganisms directly exposed to the radiation, while those shielded within corrosion products or embedded in deeper biofilm layers remain unaffected. Moreover, while UV irradiation can inactivate microorganisms, it does not remove them from the biofilm. Dead cells will then serve as a nutrient source for other bacteria, including MIC-promoting ones (Little et al., 2020). Practical challenges also arise in applying UV treatment to long pipelines, further limiting its utility.

Ultrasonic treatment is another technique in MIC mitigation, utilizing acoustic pressure to generate cavitation bubbles in liquid environments. When these bubbles collapse, they produce localized high-pressure and high-temperature conditions that damage microbial cells. Despite its potential, the application of ultrasonic treatment to MIC-specific contexts remains unexplored, with limited supporting data (Pound et al., 2005).

Chemical methods to mitigate MIC prominently involve the use of biocides, which are highly effective in addressing MIC issue, including the removal of biofilms. Biocides act by either killing microorganisms or inhibiting their growth. They can be categorized as oxidizing (*e.g.*, chlorine, ozone, bromine) or non-oxidizing (*e.g.,* isothiazolones, quaternary ammonium salts, aldehydes such as glutaraldehyde and acrolein) (Videla, 2002, Struchtemeyer et al., 2012; Xu et al., 2017; Sharma et al., 2018). Oxidizing biocides operate by penetrating and releasing free radicals, which disrupt cellular components and lead to cell death. Non-oxidizing biocides, while also capable of penetrating cell membrane, work differently by directly targeting and destroying the cell structure. However, the application of biocides has drawbacks, as they can corrode equipments, thus exacerbating maintenance issues. For example, glutaraldehyde is known to directly corrode carbon steel (Eid et al., 2018). Moreover, although highly effective, biocides are unfriendly for the environment due to their toxicity, leading to high disposal costs (Videla, 2002).

Electrochemical methods, including cathodic protection and coatings, play a crucial role in mitigating MIC. Cathodic protection, a widely applied corrosion mitigation technique, involves applying a negative potential to the metal surface. This negative charge repels negatively charged bacteria, reducing their attachment to the surface. Simultaneously, cathodic reactions generate hydroxyl ions, increasing the pH around the metal and creating an alkaline environment that inhibits bacterial growth (Javaherdashti, 2017). The concept of "protection potential" refers to the specific electrical potential needed to reduce or eliminate generalized corrosion in a corrosive environment (Bertolini et al., 1998). However, the effectiveness of cathodic protection in mitigating MIC remains uncertain. In certain cases, the technique may inadvertently provide electrons that electroactive microorganisms can exploit, potentially exacerbating microbial corrosion instead of preventing it (Liduino et al., 2021). Corrosion inhibitors offer another chemical strategy for MIC mitigation. These compounds are highly effective in reducing corrosion by adsorbing onto metal surfaces through functional groups. Common inhibitors include surfactants and heterocyclic organic compounds enriched with heteroatoms (*i.e.,* N, O and S) or groups with π-shared electrons (Feng et al., 2022). The inhibitors work by forming a protective barrier through physical adsorption (via Van der Waals forces) or chemical bonding. This barrier isolates the metal surface from corrosive agents, reducing bacterial adhesion and biofilm formation (Kokalj, 2022). Physical adsorption is associated with weaker interactions compared to chemical bonding, which creates more robust and stable bonds on the metal surface. Protective coating is also a standard practice, especially for underground pipelines. Coatings prevent corrosion by forming a physical barrier over the metal. To be effective, a coating must be adherent, non-porous, and mechanically resistant. Polymer-based coatings, such as polyurethanes, fluorinated compounds, epoxy resins, and silicones, are commonly used in MIC protection. These coatings must withstand harsh chemicals like sulfuric and acetic acids produced SRB and acidogenic bacteria, respectively, during the corrosion process (Abdolahi et al., 2014). The primary challenge with coatings lies in ensuring their integrity, as their disbandment can lead to corrosion failure.

Chemical biocides and coating, while effective in MIC mitigation, often come with significant energy demands due to the use of reactive substances and the generation of manufacturing waste. In contrast, microbial or plant-based synthesis present a potentially more sustainable alternative, both environmentally and energetically. Bio-based methods could lead to the development of less toxic products, making them more eco-friendly. Moreover, targeted

biological interventions or strategic environmental modifications to suppress or eliminate highly corrosive microbial populations offer a promising avenue for sustainable MIC control (Fig. 11).

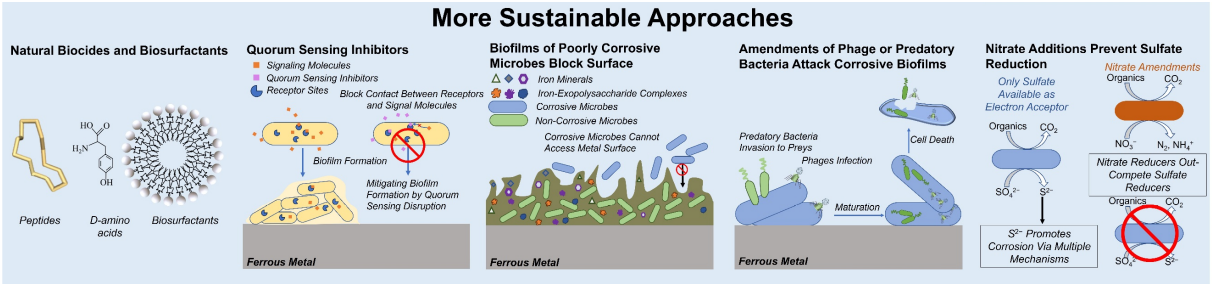

Fig. 11. Representative sustainable green corrosion mitigation alternatives (modified from Wang et al., 2023).

Microbial and plant-based production of corrosion inhibitors represent sustainable alternatives to the chemical synthesis of traditional biocides, often offering lower human toxicity and broader environmental applicability (Fig. 11).

For instance, the citrus-derived compound D-limonene enhances the biological efficacy of tetrakis(hydroxymethyl)phosphonium sulfate (THPS) against oilfield biofilms in laboratory studies (Unsal et al., 2022). Similarly, D-amino acids serve as biofilm dispersal agents (Genchi, 2017), boosting the efficacy of commercial biocides like THPS and alkyldimethylbenzylammonium chloride (ADBAC) (Jia et al., 2017). Peptide A, a cyclic peptide inspired by natural proteins, has shown extended activity against oilfield and marine biofilms when used with 2,2-dibromo-3-nitrilopropionamide (DBNPA) (Herzberg et al., 2021). Biosurfactants offer another promising approach, derived from microorganisms, plants, or natural raw materials (Plaza and Achal, 2020; Farias et al., 2021; Verma et al., 2023) (Fig. 11). For example, rhamnolipids, produced by *Pseudomonas aeruginosa*, form a protective barrier on metal surfaces, inhibiting biofilm formation and protecting carbon steel from corrosive microbes like *Bacillus licheniformis* (Li, Yuan et al., 2022). Similarly, biosurfactants from *Bacillus* spp. common in oil reservoirs prevent biofilm adhesion and eradicate existing *Pseudomonas* spp. biofilms (Purwasena et al., 2019). Quorum-sensing inhibitors disrupt microbial communication necessary for biofilm formation, offering another innovative strategy (Lamin et al., 2022). For instance, plant-derived methyl eugenol disintegrates *Desulfovibrio* spp. biofilms on stainless steel, while other inhibitors reduce biofilm-associated gene expression in *D. vulgaris* (Scarascia et al., 2019). Despite promising laboratory results, large-scale field trials are essential to evaluate these strategies in real-world applications. Using

microbes to combat corrosion caused by other microorganisms or abiotic factors is an intriguing and cost-effective alternative to traditional methods. Protective microbial biofilms and extracellular products can act as barriers, preventing oxygen and corrosive agents from reaching metal surfaces. For example, marine *Vibrio* spp. form uniform biofilms that block oxygen and metabolites, reducing corrosion (Gao et al., 2021; 2022). Similarly, *Pseudoalteromonas lipolytica* produces biomineralized films containing calcite and extracellular polymeric substances (EPS), inhibiting carbon steel corrosion (Guo et al., 2019). *Tenacibaculum mesophilum D-6* forms oxygen-consuming biofilms that hinder the diffusion of corrosive species like chloride ions, thereby protecting carbon steel (Li et al., 2023). Additionally, *Vibrio* spp. deposit iron-EPS complexes, reducing steel corrosion (Moradi et al., 2015). However, fostering and maintaining protective biofilms in diverse, competitive microbial environments poses significant challenges. Insights from natural phenomena, such as low corrosion rates in iron sheet piles linked to mineral deposits from *Methanobacterium* spp., could guide future strategies (Kip et al., 2017). Further studies of such microbial activities may enable sustainable microbial corrosion mitigation.

Phage therapy also shows potential for targeting specific bacteria within microbial communities to mitigate corrosion (Goldman et al., 2009) (Fig. 11). Lytic bacteriophages have been used to reduce populations of *Sphaerotilus natans* and *Haliscomenobacter hydrossis*, the primary culprits of sludge bulking in wastewater systems (Choi et al., 2011; Kotay et al., 2011). Phages specific to *Salmonella enterica*, a hydrogen sulfide producer in sewage, reduced both bacterial numbers and hydrogen sulfide production in synthetic sewage (Salim et al., 2021). In oil pipeline environments, bacteriophages inhibited the growth of *Stenotrophomonas maltophilia* PBM-IAUF-2, a corrosive microbe, though their direct impact on corrosion was not assessed (Pedramfar et al., 2017). Predatory bacteria, such as *Bdellovibrio bacteriovorus*, reduced corrosion caused by SRB by 80% (Qiu et al., 2016). While these methods show promise, their application to complex, diverse microbial biofilms remain underexplored. Further research is necessary to evaluate their efficacy and practical implementation, given their environmentally friendly and non-toxic potential.

1.4. Aims of thesis

The work presented in this thesis aims to contribute to the development of novel methods for MIC prevention, mitigation and control. For this purpose, two complementary environmentally-friendly approaches have been pursued, namely the investigation of the role of essential oils in eradicating *D. vulgaris* biofilms, and an innovative strategy based on the production of recombinant endolysins. Each of the following Chapters will be proceeded by a short summary aimed at presenting the submitted manuscript (Chapter 2), the manuscript in preparation (Chapter 3) and the publication (Chapter 4) collected in this PhD thesis.

Chapter 2 of this work investigates the potential use of cinnamaldehyde as an environmentally friendly biocide against the model SRB microorganism, *D. vulgaris*. Cinnamaldehyde was chosen for its dual role as an antimicrobial agent and as a well-documented corrosion inhibitor. This study demonstrates that cinnamaldehyde effectively eradicates biofilm-grown *D. vulgaris* similarly to the well-known biocide glutaraldehyde, highlighting its potential as a green alternative biocide for MIC mitigation.

Chapter 3 investigates a novel approach to MIC control, through the use of bacteriophage-derived endolysins, as green biocides. While endolysins are well-known for their efficacy in treating bacterial infections in clinical settings, their potential in environmental applications, particularly in the MIC field, remains unexplored. Therefore, this work has been focused on selecting and testing *in vitro D. vulgaris*-specific endolysins, demonstrating their effectiveness against planktonic cells and underscoring their potential application for controlling SRB-driven MIC.

Finally, in Chapter 4, a study characterizing bacterial communities in offshore and nearshore marine sediments, with a focus on the bacterial groups primarily responsible for MIC, has been performed. This study promotes proactive strategies to detect MIC at its early stages and offers insights into mitigating MIC through community profiling.

By addressing these aims, this thesis seeks to advance the knowledge required to MIC control and mitigation through sustainable and innovative solutions.

Chapter 1 references

- Abdolahi A, Hamzah E, Ibrahim Z, Hashim S. **(2014)**. Application of Environmentally-Friendly Coatings Toward Inhibiting the Microbially Influenced Corrosion (MIC) of Steel: A Review. *Polymer Reviews, 54*, 702-745. https://doi.org/ 10.1080/15583724.2014.946188
- AMPP. (**2023)**. Corrosion Terminology.. https://www.ampp.org/resources/what-is-corrosion/corrosion-terminology-glossary
- Bertolini L, Bolzoni F, Pedeferri P. *et al.* **(1998)**. Cathodic protection and cathodic preventionin concrete: principles and applications. *Journal of Applied Electrochemistry* **28**, 1321–1331. https://doi.org/10.1023/A:1003404428827
- Choi J, Kotay SM, Goel R. **(2011)**. Bacteriophage-based biocontrol of biological sludge bulking in wastewater. *Bioengineered bugs*, *2*(4), 214–217. https://doi.org/10.1016/j.watres.2010.08.038
- Coetser SE, Cloete TE. **(2005)**. Biofouling and Biocorrosion in Industrial Water Systems. *Critical Reviews in Microbiology*, *31*(4), 213–232. https://doi.org/10.1080/10408410500304074
- Conley S, Franco G, Faloona I, Blake DR, Peischl J, Ryerson TB. **(2016)**. Methane emissions from the 2015 Aliso Canyon blowout in Los Angeles, CA. Science, 351, 1317–1320. http://doi:10.1126/SCIENCE.AAF2348
- Cote C, Rosas O, Sztyler M, Doma J, Beech I, Basseguy R. **(2014)**. Corrosion of low carbon steel by microorganisms from the 'pigging' operation debris in water injection pipelines. *Bioelectrochemistry*, *97*, 97–109. https://doi.org/10.1016/j.bioelechem.2013.11.001
- Dang H, Lovell CR. **(2015)**. Microbial Surface Colonization and Biofilm Development in Marine Environments. *Microbiology and molecular biology reviews: MMBR*, *80*(1), 91–138. https://doi.org/10.1128/MMBR.00037-15
- Eid MM, Duncan KE, Tanner RS. **(2018)**. A semi-continuous system for monitoring microbially influenced corrosion. *Journal of microbiological methods*, *150*, 55–60. https://doi.org/10.1016/j.mimet.2018.05.018
- Elasri MO, Miller RV. **(1999)**. Study of the response of a biofilm bacterial community to UV radiation. *Applied and environmental microbiology*, *65*(5), 2025–2031. https://doi.org/10.1128/AEM.65.5.2025-2031.1999
- Enning D, Garrelfs J. **(2014)**. Corrosion of iron by sulfate-reducing bacteria: new views of an old problem. *Applied and environmental microbiology*, *80*(4), 1226–1236. https://doi.org/10.1128/AEM.02848-13
- Fareleira P, Santos BS, António C, Moradas-Ferreira P, LeGall J, Xavier AV, Santos H. **(2003)**. Response of a strict anaerobe to oxygen: survival strategies in *Desulfovibrio gigas*. *Microbiology*, *149*(Pt 6), 1513–1522. https://doi.org/10.1099/mic.0.26155-0
- Farias CBB, Almeida FCG, Silva IA, Souza TC, Meira HM, da Silva S. *et al.* **(2021)**. Production of green surfactants: market prospects. *Electronic Journal of Biotechnology*, 51, 28–39. https://doi.org/10.1016/j.ejbt.2021.02.002
- Feng L, Zhu H, Ma X, *et al.* **(2022)**. Chapter10 - Inhibitors for microbiologically influenced corrosion (MIC). Eco-Friendly Corrosion Inhibitors. Principles, Designing and Applications;137–54. https://doi.org/10.1016/B978-0-323-91176-4.00001-5
- Ferreira D, Barbosa ACC, Oliveira GP, Catarino T, Venceslau SS, Pereira IAC. **(2022)**. The DsrD functional marker protein is an allosteric activator of the DsrAB dissimilatory sulfite reductase. *Proceedings of the National Academy of Sciences of the United States of America*, *119*(4), e2118880119. https://doi.org/10.1073/pnas.2118880119

- Fida TT, Chen C, Okpala G, Voordouw G. **(2016)**. Implications of Limited Thermophilicity of Nitrite Reduction for Control of Sulfide Production in Oil Reservoirs. *Applied and environmental microbiology*, *82*(14), 4190–4199. https://doi.org/10.1128/AEM.00599-16
- Flemming HC, Wingender J, Szewzyk U, Steinberg P, Rice SA, Kjelleberg S. **(2016)**. Biofilms: an emergent form of bacterial life. *Nature reviews. Microbiology*, *14*(9), 563–575. https://doi.org/10.1038/nrmicro.2016.94
- Fu Q, Xu J, Wei B, Qin Q, Gao L, Bai Y, Yu C, Sun C. **(2021)**. The effect of nitrate reducing bacteria on the corrosion behavior of X80 pipeline steel in the soil extract solution of Shenyang. *International Journal of Pressure Vessels and Piping*; 190, 104313. http://dx.doi.org/10.1016/j.ijpvp.2021.104313
- Gao Y, Feng D, Moradi M, Yang C, Jin Y, Liu D. *et al.* **(2021)**. Inhibiting corrosion of aluminum alloy 5083 through *Vibrio* species biofilm. *Corrosion Science*, 180, 109188. https://doi.org/10.1016/j.corsci.2020.109188
- Gao Y, Zhang M, Fan Y. *et al.* **(2022)**. Marine *Vibrio* spp. protect carbon steel against corrosion through secreting extracellular polymeric substances. *npj Mater Degrad* **6**, 6. https://doi.org/10.1038/s41529-021-00212-2
- Genchi G. **(2017)**. An overview on D-amino acids. *Amino acids*, *49*(9), 1521–1533. https://doi.org/10.1007/s00726-017-2459-5
- Goldman G, Starosvetsky J, Armon R. **(2009)**. Inhibition of biofilm formation on UF membrane by use of specific bacteriophages. J. Membr. Sci. 342, 145–152. https://doi.org/10.1016/j.memsci.2009.06.036
- Guo Z, Wang W, Guo N, Zeng Z, Liu T, Wang X. **(2019)**. Molybdenum-- mediated chemotaxis of *Pseudoalteromonas lipolytica* enhances biofilm-induced mineralization on low alloy steel surface. *Corrosion Science*, 159, 108123. https://doi.org/10.1016/j.corsci.2019.108123
- Hamilton WA. **(2003)**. Microbially Influenced Corrosion as a Model System for the Study of Metal Microbe Interactions: A Unifying Electron Transfer Hypothesis. Biofouling, 19(1), 65–76. https://doi.org/10.1080/0892701021000041078
- Heidelberg JF, Seshadri R, Haveman SA, Hemme CL, Paulsen IT, Kolonay JF, Eisen JA, Ward N, Methe B, Brinkac LM, Daugherty SC, Deboy RT, Dodson RJ, Durkin AS, Madupu R, Nelson WC, Sullivan SA, Fouts D, Haft DH, Selengut J, Peterson JD, Davidsen TM, Zafar N, Zhou L, Radune D, Dimitrov G, Hance M, Tran K, Khouri H, Gill J, Utterback TR, Feldblyum TV, Wall JD, Voordouw G, Fraser CM. **(2004)**. The genome sequence of the anaerobic, sulfate-reducing bacterium Desulfovibrio vulgaris Hildenborough. *Nature biotechnology*, *22*(5), 554–559. hsttp://doi:10.1038/nbt959
- Herzberg M, Berglin M, Eliahu S, Bodin L, Agrenius K, Zlotkin A, Svenson J. **(2021)**. Efficient Prevention of Marine Biofilm Formation Employing a Surface-Grafted Repellent Marine Peptide. *ACS applied bio materials*, *4*(4), 3360–3373. https://doi.org/10.1021/acsabm.0c01672
- Holmer M, Storkholm P. **(2001)**. Sulphate reduction and sulphur cycling in lake sediments: a review. Freshwater Biology, 46: 431-451. https://doi.org/10.1046/j.1365-2427.2001.00687.x
- Huang Y, Zhou E, Jiang C *et al*. **(2018)**. Endogenous phenazine-1-carboxamide encoding gene PhzH regulated the extracellular electron transfer in biocorrosion of stainless steel by marine *Pseudomonas aeruginosa*. *Electrochem Commun*; 94:9–13. https://doi.org/10.1016/j.elecom.2018.07.019

- In This Issue. **(2014)**. Proceedings of the National Academy of Sciences of the United States of America, 111(41), 14637–14638. https://doi.org/10.1073/iti4114111
- Jacobson GA. **(2007)**. Corrosion at Prudhoe Bay: a lesson on the line. *Materials performance, 46*(8).
- Jasińska A, Burska D, Bolałek J. **(2012)**. Sulfur in the marine environment. *Ocean and Hydro*, **41**, 72–82. https://doi.org/10.2478/s13545-012-0019-x
- Javaherdashti R. **(2017)**. Microbiologically Influenced Corrosion: An Engineering Insight, 2nd ed. Springer International Publishing, AG, Cham, Switzerland. http://dx.doi.org/10.1007/978-3-319-44306-5.
- Jia R, Tan JL, Jin P, Blackwood DJ, Xu D, Gu T. **(2018)**. Effects of biogenic H_2S on the microbiologically influenced corrosion of C1018 carbon steel by sulfate reducing *Desulfovibrio vulgaris* biofilm. Corros. Sci., 130, 1-11. https://doi.org/10.1016/j.corsci.2017.10.023
- Jia R, Yang D, Li Y, Xu D, Gu T. **(2017)**. Mitigation of the *Desulfovibrio vulgaris* biofilm using alkyldimethylbenzylammonium chloride enhanced by d-amino acids. International Biodeterioration & Biodegradation, 117, 97–104. https://doi.org/ 10.1016/j.ibiod.2016.12.001
- Jørgensen BB, Findlay AJ, Pellerin A. **(2019)**. The Biogeochemical Sulfur Cycle of Marine Sediments. *Frontiers in microbiology*, *10*, 849. https://doi.org/10.3389/fmicb.2019.00849
- Kato S. **(2016)**. Microbial extracellular electron transfer and its relevance to iron corrosion. *Microbial biotechnology*, *9*(2), 141–148. https://doi.org/10.1111/1751-7915.12340
- Keller KL, Wall JD. **(2011)**. Genetics and molecular biology of the electron flow for sulfate respiration in desulfovibrio. *Frontiers in microbiology*, *2*, 135. https://doi.org/10.3389/fmicb.2011.00135
- Kelly R, Scully J, Shoesmith D, Buchheit R. **(2002)**. Electrochemical techniques in corrosion science and engineering (1st Edition). Boca Raton: CRC Press. https://doi.org/10.1201/9780203909133
- Kertesz MA. **(2001)**. Bacterial transporters for sulfate and organosulfur compounds. *Research in microbiology*, *152*(3-4), 279–290. https://doi.org/10.1016/s0923-2508(01)01199-8
- Khan MS, Liang T, Liu Y, Shi Y, Zhang H, Li H, Guo S, Pan H, Yang K, Zhao Y. **(2022)**. Microbiologically Influenced Corrosion Mechanism of Ferrous Alloys in Marine Environment. *Metals*, *12*(9), 1458. https://doi.org/10.3390/met12091458
- Kiani Khouzani M, Bahrami A, Hosseini-Abari A, Khandouzi M, Taheri P. **(2019)**. Microbiologically Influenced Corrosion of a Pipeline in a Petrochemical Plant. *Metals*.; 9(4):459. https://doi.org/10.3390/met9040459
- Kip N, Jansen S, Leite MFA, de Hollander M, Afanasyev M, Kuramae EE, Veen JAV. **(2017)**. Methanogens predominate in natural corrosion protective layers on metal sheet piles. *Scientific reports*, *7*(1), 11899. https://doi.org/10.1038/s41598-017-11244-7
- Knisz J, Eckert R, Gieg LM, Koerdt A, Lee JS, Silva ER, Skovhus TL, An Stepec BA, Wade SA. **(2023)**. Microbiologically influenced corrosion-more than just microorganisms. *FEMS microbiology reviews*, *47*(5), fuad041. https://doi.org/10.1093/femsre/fuad041
- Kokalj A. **(2022)**. Corrosion inhibitors: physisorbed or chemisorbed? Corros Sci;196:109939. https://doi.org/10.1016/j.corsci.2021.109939
- Kotay SM, Datta T, Choi J, Goel R. **(2011)**. Biocontrol of biomass bulking caused by Haliscomenobacter hydrossis using a newly isolated lytic bacteriophage. *Water research*, *45*(2), 694–704. https://doi.org/10.1016/j.watres.2010.08.038

- Lamin A, Kaksonen AH, Cole IS, Chen XB. **(2022)**. Quorum sensing inhibitors applications: A new prospect for mitigation of microbiologically influenced corrosion. *Bioelectrochemistry*, *145*, 108050. https://doi.org/10.1016/j.bioelechem.2022.108050
- Lane RA. **(2005)**. Under the microscope: Understanding, detecting, and preventing microbiologically influenced corrosion. *J. Fail. Anal. Prev.*;5, 10–12
- Lee AK, Newman DK. **(2003)**. Microbial iron respiration: impacts on corrosion processes. *Applied microbiology and biotechnology*, *62*(2-3), 134–139. https://doi.org/10.1007/s00253-003-1314-7
- Li J, Cai MH, Miao Y, Luo G, Li WT, Li Y, Li AM. **(2019)**. Bacterial community structure and predicted function in an acidogenic sulfate-reducing reactor: Effect of organic carbon to sulfate ratios. *Bioresource technology*, *293*, 122020. https://doi.org/10.1016/j.biortech.2019.122020
- Li Y, Xu D, Chen C, Li X, Jia R, Zhang D, Sand W, Wang F, Gu T. **(2018)**. Anaerobic microbiologically influenced corrosion mechanisms interpreted using bioenergetics and bioelectrochemistry: A review[J]. J. Mater. Sci. Technol., 34(10): 1713-1718. https://doi.org/10.1016/j.jmst.2018.02.023
- Li Z, Xu Y, Zhang J, Feng D, Fan Y, Xu D. *et al.* **(2023)**. Living marine bacterium *Tenacibaculum mesophilum* D-- 6 inhibits crevice corrosion of X70 carbon steel. *Corrosion Science*, 215, 111012. https://doi.org/10.1016/j.corsci.2023.111012
- Li Z, Yuan X, Sun M, Li Z, Zhang D, Lei Y. *et al*. **(2022)**. Rhamnolipid as an eco-friendly corrosion inhibitor for microbiologically influenced corrosion. *Corrosion Science*, 204, 110390. https://doi.org/10.1016/j.corsci.2022.110390
- Liduino V, Galvão M, Brasil S, Sérvulo E. **(2021)**. SRB-mediated corrosion of marine submerged AISI 1020 steel under impressed current cathodic protection. *Colloids and surfaces. B, Biointerfaces*, *202*, 111701. https://doi.org/10.1016/j.colsurfb.2021.111701
- Little BJ, Blackwood DJ, Hinks J *et al*. **(2020)**. Microbially influenced corrosion—any progress?, Corros Sci;170:108641. https://doi.org/10.1016/j.corsci.2020.108641
- Little BJ, Ray RI, Pope RK. **(2000)**. Relationship Between Corrosion and the Biological Sulfur Cycle: A Review. *CORROSION* 1; 56 (4): 433–443. doi: https://doi.org/10.5006/1.3280548
- Liu P, Zhang H, Fan Y, Xu D. **(2023)**. Microbially Influenced Corrosion of Steel in Marine Environments: A Review from Mechanisms to Prevention. *Microorganisms*, *11*(9), 2299. https://doi.org/10.3390/microorganisms11092299
- Lovley DR, Holmes DE. **(2022)**. Electromicrobiology: the ecophysiology of phylogenetically diverse electroactive microorganisms. *Nature reviews. Microbiology*, *20*(1), 5–19. https://doi.org/10.1038/s41579-021-00597-6
- Lovley DR. **(2011)**. Live wires: direct extracellular electron exchange for bioenergy and the bioremediation of energy-related contamination. *Energy Environ. Sci.*,4, 4896-4906. https://doi.org/10.1039/C1EE02229F
- Lovley DR. **(2017)**. Electrically conductive pili: biological function and potential applications in electronics. Curr Opin Electrochem 4:190–198. https://doi.org/10.1016/j.coelec.2017.08.015
- Moradi M, Song Z, Tao X. **(2015)**. Introducing a novel bacterium, *Vibrio neocaledonicus* sp., with the highest corrosion inhibition efficiency. *Electrochemistry Communications*, 51, 64–68. https://doi.org/10.1016/j.elecom.2014.12.007

- Müller AL, Kjeldsen KU, Rattei T, Pester M, Loy A. **(2015)**. Phylogenetic and environmental diversity of DsrAB-type dissimilatory (bi)sulfite reductases. *The ISME journal*, *9*(5), 1152–1165. https://doi.org/10.1038/ismej.2014.208
- Muyzer G, Stams AJ. **(2008)**. The ecology and biotechnology of sulphate-reducing bacteria. *Nature reviews. Microbiology*, *6*(6), 441–454. https://doi.org/10.1038/nrmicro1892
- NACE IMPACT Study. **(2016)**. impact.nace.org (Accessed September 16th, 2023).
- NACE-ASTM G193-**2022**, Standard Terminology and Acronyms Relating to Corrosion.
- Norlund KL, Southam G, Tyliszczak T, Hu Y, Karunakaran C, Obst M, Hitchcock AP, Warren LA. **(2009)**. Microbial architecture of environmental sulfur processes: a novel syntrophic sulfur-metabolizing consortia. *Environmental science & technology*, *43*(23), 8781–8786. https://doi.org/10.1021/es803616k
- Oliveira TF, Vonrhein C, Matias PM, Venceslau SS, Pereira IA, Archer M. **(2008)**. The crystal structure of Desulfovibrio vulgaris dissimilatory sulfite reductase bound to DsrC provides novel insights into the mechanism of sulfate respiration. *The Journal of biological chemistry*, *283*(49), 34141–34149. https://doi.org/10.1074/jbc.M805643200
- Paquete CM, Morgado L, Salgueiro CA, Louro RO. **(2022)**. Molecular Mechanisms of Microbial Extracellular Electron Transfer: The Importance of Multiheme Cytochromes. *Frontiers in bioscience (Landmark edition)*, *27*(6), 174. https://doi.org/10.31083/j.fbl2706174
- Pedramfar A, Beheshti Maal K, Mirdamadian SH. **(2017)**. Phage therapy of corrosion--producing bacterium *Stenotrophomonas maltophilia* using isolated lytic bacteriophages. *Anti-Corrosion Methods and Materials*, 64, 607–612. https://doi.org/10.1108/ACMM-02-2017-1755
- Phan HC, Blackall LL, Wade SA. **(2021)**. Effect of Multispecies Microbial Consortia on Microbially Influenced Corrosion of Carbon Steel. *Corrosion and Materials Degradation*. 2(2):133-149. https://doi.org/10.3390/cmd2020008
- Płaza G, Achal V. **(2020)**. Biosurfactants: Eco-Friendly and Innovative Biocides against Biocorrosion. *International Journal of Molecular Sciences*, *21*(6), 2152. https://doi.org/10.3390/ijms21062152
- Postgate JR. **(1984)**. The Sulphate-Reducing Bacteria, edn. 2, vol. 130 (Cambridge University Press, London).
- Pound BG, Gorfu Y, Schattner P, Mortelmans KE. **(2005)**. Ultrasonic Mitigation of Microbiologically Influenced Corrosion. Corrosion 61, 452–463, https://doi.org/10.5006/1.3280645
- Procópio L. **(2019)**. The role of biofilms in the corrosion of steel in marine environments. *World journal of microbiology & biotechnology*, *35*(5), 73. https://doi.org/10.1007/s11274-019-2647-4
- Puentes-Cala E, Tapia-Perdomo V, Espinosa-Valbuena D, Reyes-Reyes M, Quintero-Santander D, Vasquez-Dallos S, Salazar H, Santamaría-Galvis P, Silva-Rodríguez R and Castillo-Villamizar G. **(2022)**. Microbiologically influenced corrosion: The gap in the field. *Front. Environ. Sci.*10:924842. https://doi.org/10.3389/fenvs.2022.924842
- Purwasena IA, Astuti DI, Ardini Fauziyyah N, Putri DAS, Sugai Y. **(2019)**. Inhibition of microbial influenced corrosion on carbon steel ST37 using biosurfactant produced by Bacillus sp. *Materials Research Express*, *6*(11), Article 115405. https://doi.org/10.1088/2053-1591/ab4948

- Qian PY, Cheng A, Wang R, Zhang R. **(2022)**. Marine biofilms: diversity, interactions and biofouling. *Nature reviews. Microbiology*, *20*(11), 671–684. https://doi.org/10.1038/s41579-022-00744-7
- Qiu L, Mao Y, Gong A, Zhang W, Cao Y, Tong L. **(2016)**. Inhibition effect of *Bdellovibrio bacteriovorus* on the corrosion of X70 pipeline steel induced by sulfate-reducing bacteria. *Anti-Corrosion Methods and Materials*, Vol. 63 No. 4, pp. 269-274. https://doi.org/10.1108/ACMM-10-2014-1447
- Salim A, Madhavan A, Babu P, Porayath C, Kesavan M, Hely S. *et al.* **(2021)**. Bacteriophage-based control of biogenic hydrogen sulphide produced by multidrug resistant *Salmonella enterica* in synthetic sewage. *Journal of Environmental Chemical Engineering*, 9, 105797. https://doi.org/10.1016/j.jece.2021.105797
- Santos AA, Venceslau SS, Grein F, Leavitt WD, Dahl C, Johnston DT, Pereira IA. **(2015)**. A protein trisulfide couples dissimilatory sulfate reduction to energy conservation. *Science (New York, N.Y.)*, *350*(6267), 1541–1545. https://doi.org/10.1126/science.aad3558
- Scarascia G, Lehmann R, Machuca LL, Morris C, Cheng KY, Kaksonen A, Hong PY. **(2019)**. Effect of Quorum Sensing on the Ability of *Desulfovibrio vulgaris* To Form Biofilms and To Biocorrode Carbon Steel in Saline Conditions. *Applied and environmental microbiology*, *86*(1), e01664-19. https://doi.org/10.1128/AEM.01664-19
- Sharma M, Liu H, Chen S. *et al.* **(2018)**. Effect of selected biocides on microbiologically influenced corrosion caused by *Desulfovibrio ferrophilus* IS5. *Sci Rep* 8, 16620. https://doi.org/10.1038/s41598-018-34789-7
- Skovhus T, Enning D, Lee J. **(2017)**. Microbiologically influenced corrosion in the upstream oil and gas industry. 1st Edn. Boca Raton FL: CRC Press. http://doi:10.1201/9781315157818
- Struchtemeyer CG, Morrison MD, Elshahed MS. **(2012)**. A critical assessment of the efficacy of biocides used during the hydraulic fracturing process in shale natural gas wells. *International Biodeterioration & Biodegradation* 71:15–21. https://doi.org/10.1016/j.ibiod.2012.01.013
- Tang HY, Holmes DE, Ueki T, Palacios PA, Lovley DR. **(2019)**. Iron Corrosion via Direct Metal-Microbe Electron Transfer. *mBio*, *10*(3), e00303-19. https://doi.org/10.1128/mBio.00303-19
- Telegdi J, Shaban A, Vastag G. **(2018)**. Biocorrosion-Steel. Encyclopedia of Interfacial Chemistry. Surface Science and Electrochemistry. 28-42.
- Tsurumaru H, Ito N, Mori K, Wakai S, Uchiyama T, Iino T, Hosoyama A, Ataku H, Nishijima K, Mise M, Shimizu A, Harada T, Horikawa H, Ichikawa N, Sekigawa T, Jinno K, Tanikawa S, Yamazaki J, Sasaki K, Yamazaki S, Fujita N, Harayama S. **(2018)**. An extracellular [NiFe] hydrogenase mediating iron corrosion is encoded in a genetically unstable genomic island in Methanococcus maripaludis. *Scientific reports*, *8*(1), 15149. https://doi.org/10.1038/s41598-018-33541-5
- Unsal T, Wang D, Kijkla P, Kumseranee S, Punpruk S, Mohamed ME, Saleh MA, Gu T. **(2022)**. Food-grade D-limonene enhanced a green biocide in the mitigation of carbon steel biocorrosion by a mixed-culture biofilm consortium. *Bioprocess and biosystems engineering*, *45*(4), 669–678. https://doi.org/10.1007/s00449-021-02685-6
- Usher KM, Kaksonen AH, MacLeod ID. **(2014)**. Marine rust tubercles harbour iron corroding archaea and sulphate reducing bacteria. Corros. Sci. 83, 189–197. https://doi.org/10.1016/j.corsci.2014.02.014

- Verma C, Hussain CM, Quraishi MA, Alfantazi A. **(2023)**. Green surfactants for corrosion control: Design, performance and applications. *Advances in colloid and interface science*, *311*, 102822. https://doi.org/10.1016/j.cis.2022.102822
- Videla HA. **(1996)**. Manual of Biocorrosion, 1st ed. CRC-Press, pp 13–45.
- Videla HA. **(2002)**. Prevention and control of biocorrosion. Int. Biodeterior. Biodegrad. 49, 259–270. https://doi.org/10.1016/S0964-8305(02)00053-7
- Wang D, Zhou E, Xu D, Lovley DR. **(2023)**. Burning question: Are there sustainable strategies to prevent microbial metal corrosion?. *Microbial biotechnology*, *16*(11), 2026–2035. https://doi.org/10.1111/1751-7915.14347
- Waters CM, Bassler BL. **(2005)**. Quorum sensing: cell-to-cell communication in bacteria.*Annual review of cell and developmental biology*, *21*, 319–346. https://doi.org/10.1146/annurev.cellbio.21.012704.131001
- Xu D., Gu T. **(2011)**. Bioenergetics explains when and why more severe MIC pitting by SRB can occur. Corrosion/2011. Paper No. 11426. Houston: NACE International.
- Xu D, Gu T, Lovley DR. **(2023)**. Microbially mediated metal corrosion. Nat. Rev. Microbiol., 1–14. https://doi.org/10.1038/s41579-023-00920-3
- Xu D, Jia R, Li Y, Gu T. **(2017)**. Advances in the treatment of problematic industrial biofilms. *World journal of microbiology & biotechnology*, *33*(5), 97. https://doi.org/10.1007/s11274-016-2203-4

Chapter 2

Potential use of cinnamaldehyde against *Desulfovibrio vulgaris* biofilm to mitigate microbiologically influenced corrosion

Arianna Scardino[1], Gianmarco Mangiaterra[1], Barbara Citterio[1], Sarah Hijazi[1], Caterina Ciacci[1], Mauro Fehervari[2], Emanuela Frangipani[1*]

[1]*Department of Biomolecular Sciences, University of Urbino Carlo Bo, Urbino (PU), Italy*

[2]*Fano offshore R&D Engineering, Saipem SpA, Fano (PU), Italy*

Manuscript submitted to *Applied and Environmental Microbiology* on November 11th, 2024

Current stage: resubmission with minor revision

Preface to Chapter 2

Microbiologically influenced corrosion is an electrochemical process driven by the presence and/or activity of microorganisms, impacting a wide range of industrial sectors. Sulfate reducing bacteria (SRB) are among the key contributors to this type of corrosion. SRB are anaerobic microorganisms that thrive in anoxic environments and produce corrosive compounds such as ferrous sulfide (FeS) and hydrogen sulfide (H_2S). Current methods to prevent and mitigate microbiologically influenced corrosion involve the use of biocides, such as glutaraldehyde. However, these biocides have drawbacks, including high toxicity and disposal costs. Moreover, glutaraldehyde was reported to also be corrosive to low-carbon steel materials, highlighting the urgent need for innovative, effective and environmentally-friendly options. Essential oils, known for their potent antimicrobial properties and low toxicity, may offer a promising alternative. Yet, their potential application against SRB remains poorly investigated. This Chapter focuses on cinnamaldehyde, a compound selected both for its antimicrobial properties as well as its documented efficacy as a corrosion inhibitor. Specifically, the results reported in this Chapter have been recently resubmitted with minor revision as a Research Article to *Applied and Environmental Microbiology*. In this work the effectiveness of cinnamaldehyde in eradicating biofilm-grown *Desulfovibrio vulgaris,* an SRB model microorganism, was investigated and compared to the well-known reference glutaraldehyde, proving insights into the potential of cinnamaldehyde as a sustainable alternative. To avoid misunderstanding, in this Chapter, the acronym MIC is used to denote "Minimum Inhibitory Concentration", while Microbiologically Influenced Corrosion has never been shortened.

Manuscript #	AEM02200-24
Current Revision #	0
Submission Date	2024-11-11 07:16:04
Current Stage	Waiting for Revision
Title	Potential use of cinnamaldehyde against *Desulfovibrio vulgaris* biofilm to mitigate microbiologically influenced corrosion
Manuscript Type	Full-Length Text
Special Section	N/A
Journal Section	Environmental Microbiology
Corresponding Author	Prof. Emanuela Frangipani (Universita degli Studi di Urbino Carlo Bo Dipartimento di Scienze Biomolecolari)
Contributing Authors	Ms. Arianna Scardino , Dr. Gianmarco Mangiaterra , Dr. Barbara Citterio , Dr. Sarah Hijazi , Dr. Caterina Ciacci , Dr. Mauro Fehervari , Prof. Emanuela Frangipani (corr-auth)
Abstract	Microbiologically influenced corrosion poses significant challenges to various industries, as metal surfaces degrade due to the formation of microbial biofilms. Sulfate-reducing bacteria (SRB) are key contributors to this process in anoxic environments (*e.g.,* oil and gas pipelines), by producing highly corrosive hydrogen sulfide. Current prevention methods involving biocides often have drawbacks such as high toxicity and disposal costs, calling for novel environmentally-friendly alternatives. Essential oils with their antimicrobial properties and biodegradability may represent promising candidates against microbial corrosion. In this study, cinnamaldehyde was selected both for its antimicrobial activity and its well-documented role as corrosion inhibitor; then its antibiofilm activity was investigated against *Desulfovibrio vulgaris*, in comparison with the well-known reference biocide glutaraldehyde. Both compounds were bactericidal against *D. vulgaris* at 12.5 µg/ml. *D. vulgaris* biofilms were developed and monitored by confocal microscopy, then 72 h-old biofilms were exposed to serial cinnamaldehyde and glutaraldehyde concentrations (12.5 - 100 µg/ml) for further 48 h, to evaluate their disruptive effects. Both compounds caused a significant disruption of pre-formed biofilms, at 50 µg/ml. The reduction compared to the untreated controls was ca. 90 % vs 85 % for biomass, 60 % vs 45 % for average thickness, and 85 % vs 80 % for surface area, respectively. Interestingly, cinnamaldehyde applied to a *D. vulgaris* biofilm grown on representative metal coupons completely inhibited the recovery of viable adherent cells. These data, altogether, highlight the potential of cinnamaldehyde as an effective alternative for controlling and mitigating microbiologically influenced corrosion, with comparable efficacy to glutaraldehyde.
Importance	The increasing environmental and health concerns associated with the use of conventional biocides to manage and control microbiologically influenced corrosion highlight the need for eco-friendly alternatives. SRB represent the main players in this process, by adhering and proliferating as biofilms on metal infrastructures, producing metabolites that accelerate corrosion. Essential oils have long been regarded as potent antimicrobials endowed with low toxicity, however there is limited knowledge about their potential use against anaerobic bacteria responsible for corrosion. This study focuses on the antimicrobial activity of cinnamaldehyde and shows its efficacy in eradicating biofilm-grown *D. vulgaris*, a model species to study SRB energy metabolism. Notably, cinnamaldehyde is also a well-known corrosion inhibitor, which makes it an appealing candidate for industrial applications, particularly where SRB-induced corrosion is prevalent. Altogether our results pave the way for the future development of green sustainable strategies involving the use of cinnamaldehyde to mitigate microbiologically influenced corrosion.
Editor	Prof. Arpita Bose
Suggested Reviewers to Include	Elisa Taviani (Università degli Studi di Genova), Christoph Keel (University of Lausanne), Martina Cappelletti (University of Bologna)
Suggested Reviewers to Exclude	N/A
Keywords	Desulfovibrio vulgaris, Sulfate reducing bacteria, Microbiologically influenced corrosion, Biofilm, Cinnamaldehyde, Eco-friendly alternatives
Research Areas	Antimicrobial Chemotherapy, Applied and Industrial Microbiology, Environmental Microbiology
PubMed Similar Manuscripts	(expand)
Preprint Server	No
Biorxiv Preprint	No
Funding Sources	No Funders
Decision	Minor Modifications / 2025-01-07
Electronic Forms	0 of 1 forms complete - View Electronic Forms Status

Potential use of cinnamaldehyde against *Desulfovibrio vulgaris* biofilm to mitigate microbiologically influenced corrosion

Arianna Scardino[1], Gianmarco Mangiaterra[1], Barbara Citterio[1], Sarah Hijazi[1], Caterina Ciacci[1], Mauro Fehervari[2], Emanuela Frangipani[1*]

[1]*Department of Biomolecular Sciences, University of Urbino Carlo Bo, Urbino (PU), Italy*

[2]*Fano offshore R&D Engineering, Saipem SpA, Fano (PU), Italy*

*Corresponding author. Department of Biomolecular Sciences, University of Urbino, Via Santa Chiara 27, 61029 Urbino (PU), Italy. Phone: +39 0722 303544. E-mail: emanuela.frangipani@uniurb.it.

ABSTRACT

Microbiologically influenced corrosion poses significant challenges to various industries, as metal surfaces degrade due to the formation of microbial biofilms. Sulfate-reducing bacteria (SRB) are key contributors to this process in anoxic environments (*e.g.,* oil and gas pipelines), mainly by producing highly corrosive hydrogen sulfide. Current prevention methods involving biocides often have drawbacks such as high toxicity and disposal costs, calling for novel environmentally-friendly alternatives. Essential oils with their antimicrobial properties and biodegradability may represent promising candidates against microbial corrosion. In this study, cinnamaldehyde was selected both for its antimicrobial activity and its well-documented role as corrosion inhibitor; then its antibiofilm activity was investigated against *Desulfovibrio vulgaris*, in comparison with the well-known reference biocide glutaraldehyde. Both compounds were bactericidal against *D. vulgaris* at 12.5 µg/ml. *D. vulgaris* biofilms were developed and monitored by confocal microscopy, then 72 h-old biofilms were exposed to serial cinnamaldehyde and glutaraldehyde concentrations (12.5 - 100 µg/ml) for further 48 h, to evaluate their disruptive effects. Both compounds caused a significant disruption of pre-formed biofilms, at 50 µg/ml. The reduction compared to the untreated controls was *ca.* 90 % *vs* 85 % for biomass, 60 % *vs* 45 % for average thickness, and 85 % *vs* 80 % for surface area, respectively. Interestingly, cinnamaldehyde applied to a *D. vulgaris* biofilm grown on

representative metal coupons completely inhibited the recovery of viable adherent cells. These data, altogether, highlight the potential of cinnamaldehyde as an effective alternative for controlling and mitigating microbiologically influenced corrosion, with comparable efficacy to glutaraldehyde.

IMPORTANCE

The increasing environmental and health concerns associated with the use of conventional biocides to manage and control microbiologically influenced corrosion highlight the need for eco-friendly alternatives. SRB represent the main players in this process, by adhering and proliferating as biofilms on metal infrastructures, producing metabolites that accelerate corrosion. Essential oils have long been regarded as potent antimicrobials endowed with low toxicity, however there is limited knowledge about their potential use against anaerobic bacteria responsible for corrosion. This study focuses on the antimicrobial activity of cinnamaldehyde and shows its efficacy in eradicating biofilm-grown *D. vulgaris*, a model species to study SRB energy metabolism. Notably, cinnamaldehyde is also a well-known corrosion inhibitor, which makes it an appealing candidate for industrial applications, particularly where SRB-induced corrosion is prevalent. Altogether our results pave the way for the future development of green sustainable strategies involving the use of cinnamaldehyde to mitigate microbiologically influenced corrosion.

KEYWORDS

Desulfovibrio vulgaris, Sulfate reducing bacteria, Microbiologically influenced corrosion, Biofilm, Cinnamaldehyde, Eco-friendly alternatives.

Introduction

Microbiologically influenced corrosion is an electrochemical process in which microorganisms can initiate, or accelerate metal corrosion reactions (Videla, 1996), enhancing its kinetic rates by 10 - 1,000 times (Lane, 2005). Indeed, it has been defined by the National Association of Corrosion Engineers (NACE) and the American Society for Testing and Materials (ASTM) as "*corrosion affected by the presence or activity, or both, of microorganisms*" (NACE-ASTM G193 2022), impacting a wide range of industrial processes, materials and sectors, such as petrochemical installations (Kiani Khouzani et al., 2019), gas and oil industries (Skovhus et al., 2017), water treatment facilities (Coetser, 2005), as well as the aviation and defense sectors (Lee et al., 2007). Microbiologically influenced corrosion causes significant expenses in terms of operational and maintenance costs and may account for up to 20 % of the total annual global corrosion damage in the oil and gas sectors, excluding the associated safety and environmental impacts (NACE, 2016). Various microorganisms play a role in this type of corrosion (Lane, 2005), with sulfate reducing bacteria (SRB) being identified as the primary contributors, especially in anoxic environments (Gu et al., 2019). SRB contribute to corrosion through multiple mechanisms, the main one being the metabolic production of hydrogen sulfide (H_2S) during cellular respiration, by reducing the electron acceptor sulfate (Postgate, 1965). The presence of H_2S leads to serious operational problems by reacting with metal ions (mainly iron) and producing ferrous sulfide (FeS), which is poorly soluble in aqueous environments and, together with slime, cause dark-colored sludge that hinders the flow in oil and gas pipelines, and also complicates maintenance efforts, contributing to clogging issues during cleaning operations (Telegdi et al., 2017). Additionally, some SRB species may also generate organic acids, such as acetic and propionic acids, further acidifying the environment and accelerating metal corrosion (Gu, 2014).

Typical SRB include *Desulfovibrio* spp., *Desulfobacter* spp., and *Desulfotomaculum* spp., which are detected on the inner surface of steel rust layers, where the abundance index of SRB is much higher compared to other bacteria species (Li et al., 2017). To study SRB energy metabolism and their impact on metal corrosion, the Gram-negative bacterium *Desulfovibrio vulgaris* Hildenborough ATCC 29579 has been widely used as a model microorganism (Heidelberg et al., 2004). Moreover, *D. vulgaris* has been extensively studied due to its ability to form biofilms (*i.e.,* dense aggregations of microorganisms embedded in a self-produced

extracellular matrix). Bacterial biofilms strongly adhere to metallic surfaces, thereby generating and maintaining oxygen-deprived zones that select, promote and support the growth of specific anaerobic bacteria, such as SRB, thus positively affecting the kinetics of the microbial corrosion process (Procopio, 2019). Indeed, biofilms facilitate the local presence of high concentrations of bacteria on metal surfaces, leading to severe degradation, especially on carbon steel materials, which are more vulnerable to SRB biofilms compared to stainless steel ones (Chen et al., 2015). Moreover, biofilm-growing bacteria exhibit a very high tolerance to external stresses, and their recurrent exposure to biocides used during cleaning and disinfection procedures raises concern about the adaptation routes they might evolve, both at single-cell and community levels (Cloete et al., 1998). When SRB grow as biofilms, they influence the electrochemical conditions of metal surfaces (*e.g.,* carbon steel) by acting as a cathodic depolarizers. Indeed, some SRB possess hydrogenases that reduce sulfate to H_2S, thus accelerating the dissolution of the metal (*i.e.,* iron) (Blackwood, 2018). Moreover, SRB biofilms create localized microenvironments with altered pH and ion concentrations, physically interact with metal surfaces via cell wall components or extracellular polymeric substances (EPS), potentially disrupting protective oxide films and increasing susceptibility to localized corrosion (Jin and Guan, 2014).

To prevent and limit microbiologically influenced corrosion in industrial applications, multiple strategies are currently in use aiming at fighting the adhesion and biofilm formation of microorganisms on metallic surfaces. To these aims, a conventional approach involves the use of biocides (*i.e.,* compounds that kill microorganisms or inhibit their growth), that can be both inorganic compounds (*e.g.*, chlorine, ozone, bromine) and organic ones (*e.g.,* isothiazolones, quaternary ammonium salts, aldehydes such as glutaraldehyde and acrolein) (Videla, 2002; Struchtemeyer et al., 2012; Xu et al., 2017; Sharma et al., 2018). Glutaraldehyde is widely used as a biocide, due to its broad-spectrum activity, solubility and stability across a wide pH and salinity range (Javaherdashti, 2017). Moreover, glutaraldehyde is also cost-effective and can be used individually or in combination with other compounds such as quaternary amines and nitrites, to reduce the concentration needed to control SRB growth (Greene et al., 2006). However, glutaraldehyde is toxic to aquatic organisms with long lasting effects, requiring expensive and complex disposable procedures (Pereira et al., 2014). The environmental apprehensions linked to the documented hazards to human health, together with the reported evidence that glutaraldehyde can be as corrosive to low-carbon steel materials as to SRB (Eid

et al., 2018), underscore the need for innovative, effective and environmentally safe alternatives to replace toxic biocides. This need aligns with the mission area of the Horizon Europe framework program, specifically focusing on the health of oceans, seas, coastal, and inland waters, started in 2021 **(**European Commission, Directorate-General for Research and Innovation et al., 2021**)**. In this context, the development of bio-inhibitors, such as plant extracts, demonstrated significant potential as effective corrosion inhibitors in various harsh environments (Quraishi, 1999; Swaroop, 2016). Plant extracts serve as a valuable source of naturally-occurring chemical compounds that are biodegradable and can be extracted using simple and low-cost methods (Hossain et al., 2019). The effectiveness of these natural compounds in inhibiting corrosion largely depends on the type of metal and their interaction with the surface. Cinnamaldehyde, a naturally bioactive compound, is widely available in the environment, primarily from the bark of cinnamon trees (Rieger et al., 2014). It exhibits antibacterial, antifungal, insecticidal, acaricidal and nematocidal properties (Kalemba and Kunicka, 2003; Haddi et al., 2017; OuYang et al., 2019; Lu et al., 2020; Marchesini et al., 2020; Pang et al., 2021; Catani et al., 2023; D'Addabbo et al., 2024). Cinnamaldehyde is primarily used in agriculture, food, medical, and flavor and fragrance industries. Its low toxicity, eco-friendliness, and well-known strong adsorption properties make it a promising candidate as an effective green corrosion inhibitor. Moreover, beside its antibacterial activity, cinnamaldehyde has been reported to inhibit acid corrosion (*i.e.,* HCl 10 % w/w), due to its ability to form a protective macroscopic film on metal surfaces (Avdeev et al., 2013; Cabello et al., 2013; Negm et al., 2013; Keles et al., 2014; Jafferji et al., 2018; Bouraoui et al., 2019; Hossain et al., 2019; Wang et al., 2019; Saad et al., 2024). Interestingly, while numerous studies have highlighted the wide antibacterial properties of plant extracts and essential oils (EOs), very few studies have been focused on bacteria involved in microbial corrosion, especially on SRB (Korenblum et al., 2013; Bhola et al., 2014; Souza et al., 2017). The innate ability of EOs as well as cinnamaldehyde to inhibit corrosion, its minimal toxicity combined with its antibacterial properties, offers a compelling approach to managing the proliferation of SRB in natural settings. In this study, the activity of cinnamaldehyde against biofilm-growing *D. vulgaris* on glass and metal surfaces, has been investigated for the first time, and compared to the well-known biocide, glutaraldehyde. Cinnamaldehyde was found to be bactericidal at concentrations ranging from 12.5 µg/ml to 100 µg/ml both on planktonic and sessile *D. vulgaris* cultures, with a comparable efficacy to the conventional biocide glutaraldehyde. Moreover, cinnamaldehyde

caused a significant disruption of pre-formed *D. vulgaris* biofilms, highlighting its potential as an effective environmentally-friendly alternative for controlling and mitigating microbial corrosion.

Experimental Procedures

Bacterial strain and culture conditions

Desulfovibrio vulgaris Hildenborough strain ATCC 29579 (DSM 644) was obtained from the Leibniz Institute DSMZ (Braunschweig, Germany) and grown anaerobically in Hungate tubes filled with Desulfovibrio (Postgate) medium, prepared according to the DSMZ guidelines (Medium N. 63), with minor modifications. Indeed, $FeSO_4$ x $7H_2O$ concentration was lowered from 0.5 g/L to 0.02 g/L, to limit FeS precipitates formed during *D. vulgaris* growth. Each Hungate tube containing the medium was purged with a N_2 flux to remove dissolved O_2 and obtain anoxic conditions, and then sterilized by autoclaving. For solid media preparation, 15 g/L of agar was added prior to autoclaving. *D. vulgaris* was incubated in a standard anaerobic environment for 48-72 h at 37 °C using a BD GasPak™ EZ Standard Incubation Container equipped with a BD GasPak EZ Container System Sachet with Indicator. All culture manipulations were performed into "La Petite" Glove Box (Plas Labs, Inc.™), to limit O_2 concentration. *D. vulgaris* stock solutions were kept as 15 % glycerol suspensions at -80 °C.

Determination of Minimum Inhibitory Concentration (MIC) and Minimum Bactericidal Concentration (MBC)

Cinnamaldehyde (W228613, Sigma-Aldrich) and glutaraldehyde (G6257, Sigma-Aldrich) were used for susceptibility testing. The minimum inhibitory concentration (MIC) of the selected compounds was determined by following the broth macrodilution method, according to the Clinical and Laboratory Standards Institute guidelines (CLSI, 2018). Briefly, 100 mg/ml stock solutions of cinnamaldehyde and glutaraldehyde dissolved in dimethyl sulfoxide (DMSO) and ddH_2O, respectively, were serially diluted in 2 ml of sterile Postgate medium, to the lowest concentration of 1.56 µg/ml. *D. vulgaris* was grown for 48 h at 37 °C in Postgate medium, and further diluted in each assay tube, to achieve a final inoculum of 5 x 10^5 CFU/ml. The MIC was determined as the lowest amount of antimicrobial agent that did not result in the rise of turbidity and/or in blackish color of the medium caused by FeS precipitation, indicative of bacterial growth (Fig. 1). From each test tube previously used for MIC determination, in which no growth was visible, 1 ml of broth was mixed with 9 ml of Postgate solid medium, poured in a Petri dish and anaerobically incubated at 37 °C for 72 h. MBC was determined as the first antibacterial

dilution for which no visible growth of *D. vulgaris* as colonies on solid media was obtained at the end of the incubation period. The MBC/MIC ratio was subsequently calculated, considering a MBC/MIC ratio > 4 or ≤ 4, indicative of a bacteriostatic or bactericidal effect, respectively (Pankey and Sabath, 2004).

D. vulgaris biofilm formation and disruption on glass cover slips

D. vulgaris biofilms were allowed to form on sterile glass coverslips (13 mm diameter, VWR International s.r.l., Italy) previously treated with 70 % v/v ethanol, then washed with ddH_2O, and air-dried before autoclaving. Briefly, a 72 h culture of *D. vulgaris* was diluted to an OD_{600} of 0.007 (corresponding to *ca.* 1 x 10^6 CFU/ml) in Postgate medium and used to inoculate a 24-well flat-bottom microtiter plate equipped with a glass cover slip in each well. Biofilms formation occurred during static anaerobic incubation at 37 °C for 96 h and was inspected every 24 h by confocal laser scanning microscopy (CLSM). Prior to CLSM visualization, planktonic cells were removed by gently washing each cover slip with sterile PBS, followed by acridine orange staining. Biofilms were observed with a Leica TCS SP5 confocal microscope equipped with a 40x oil immersion objective, and biofilm spatial characteristics were quantified using COMSTAT version 2.1, analyzing at least five image stacks per condition (Heydorn et al., 2000; Vorregaard 2008; Runci et al., 2017).

To investigate the disruptive effect of cinnamaldehyde and glutaraldehyde on *D. vulgaris* biofilms, 72 h-old biofilms were gently washed in PBS to remove planktonic cells, and then transferred to a new 24-well flat-bottom microtiter plate containing different cinnamaldehyde and glutaraldehyde dilutions (100, 50, 25, 12.5 µg/ml) in Postgate medium. Plates were incubated at 37 °C without shaking for further 48 h under anaerobic conditions. Then, CLSM biofilm visualization was performed as described above.

D. vulgaris biofilm formation and disruption on metal coupons

Metal coupons (18 mm diameter, 2 mm of thickness - material code: S355J2G3 - chemical composition: 0.20 % C, 0.20 % Si, 0.037 % Al, 0.005 % S, 0.02 % Cu, 0.98 % Mn, 0.009 % P, 0.005 % N, 0.02 % Cr, 0.36 % CEV, 0.01 % Ni, Rometec Srl, Roma, Italy) were treated with 70 % EtOH for 10 min, washed with ddH_2O and dry heat sterilized (3 h at 180°C). Coupons were then placed in a 12-well flat-bottom microtiter plate containing 3 ml of Postgate medium

inoculated with 1 x 10^6 CFU/ml of *D. vulgaris*. Biofilm formation was allowed during static anaerobic incubation at 37 °C for 72 h. Every 24 h three coupons were removed, washed twice with sterile PBS to remove planktonic cells, and subjected to two rounds of sonication followed by serial dilution and vital count, to quantify adherent bacterial cells (Fig. S1).

To investigate the disruptive effect of cinnamaldehyde on *D. vulgaris* biofilms formed on metal coupons, 48 h-old biofilms were gently washed in PBS to remove planktonic cells, and then transferred to a new 12-well flat-bottom microtiter plate containing 100 µg/ml of cinnamaldehyde (*i.e.,* 8X MIC) in Postgate medium. Plates were incubated anaerobically at 37 °C without shaking for further 48 h. Adherent cells were then quantified by viable cell count (CFU/ml), as detailed (Fig. S1).

Statistical analysis

Statistical analysis was performed with the GraphPad Prism software, version 10.2.0, by using one-way ANOVA, followed by the Dunn's multiple-comparison test. Differences among treatments and untreated controls (NT) were considered statistically significant with a P-value ≤ 0.001, indicated with *.

Results

Susceptibility of *D. vulgaris* to cinnamaldehyde and glutaraldehyde

D. vulgaris susceptibility to cinnamaldehyde and glutaraldehyde was initially investigated by determining the MIC in Postgate medium. After 72 h of incubation in anaerobic conditions at 37 °C, bacterial growth was monitored by turbidimetry. Test tubes containing a compound concentration ≤ 6.125 µg/ml showed a turbidity increase comparable to the one of the positive control devoid of any compound, whereas at concentrations ≥ 12.5 µg/ml no change in turbidity was recorded in comparison to the negative control (*i.e.,* not-inoculated medium), indicative of bacterial growth inhibition. Thus, the MIC of both cinnamaldehyde and glutaraldehyde was determined to be 12.5 µg/ml (Fig. 1). MBC determination showed lack of bacterial growth at the MIC, leading to a MBC/MIC ratio of 1, indicating a bactericidal activity of both cinnamaldehyde and glutaraldehyde.

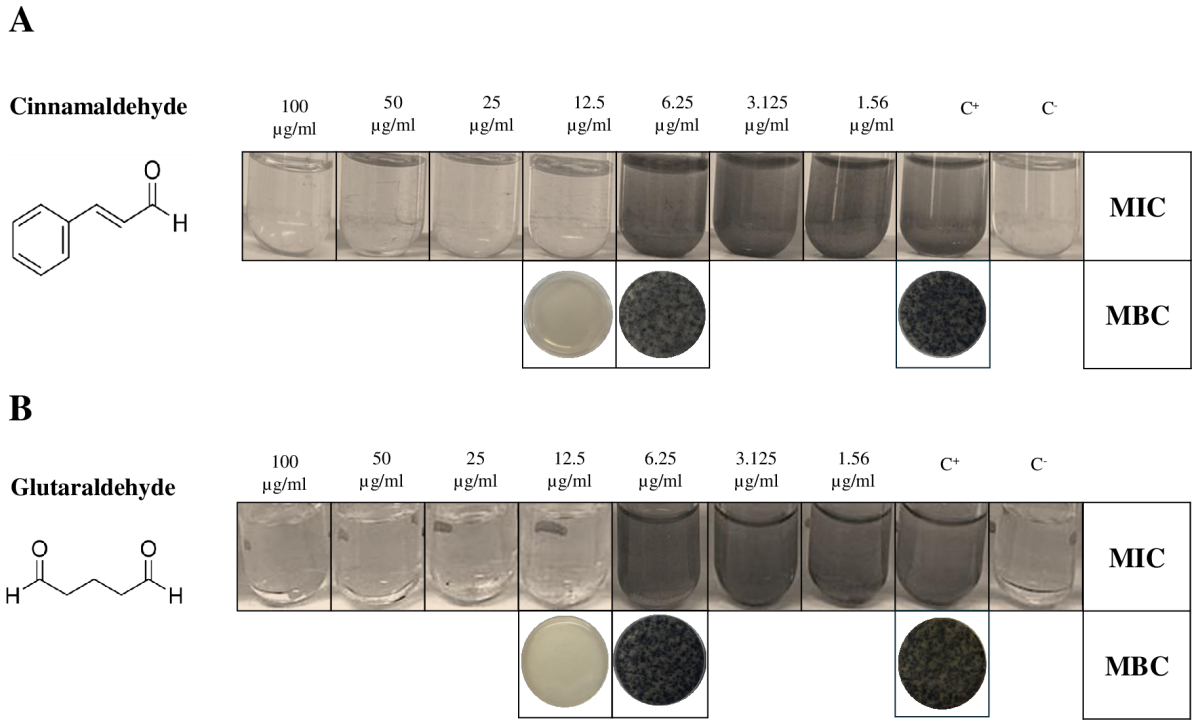

Fig. 1. Minimum inhibitory concentration (MIC) and minimum bactericidal concentration (MBC) determination. The MIC of cinnamaldehyde and glutaraldehyde was determined by the broth macrodilution method as the lowest amount of compound that did not result in the rise of turbidity and/or in blackish color of the medium, after 48 h of incubation. The MBC was determined as the first compound dilution for which no visible growth of *D. vulgaris* as colonies on solid media was obtained (representative plates are shown). C^+ and C^- indicate positive and negative controls, respectively. DMSO (*i.e.,* cinnamaldehyde solvent) did not affect growth, at all concentrations tested (data not shown).

In order to examine the disruptive effect of cinnamaldehyde and glutaraldehyde on *D. vulgaris* biofilm, the biofilm formation dynamics of *D. vulgaris* was carefully investigated over 96 h post-inoculum in Postgate medium at 37 °C, on glass cover slips under anaerobic conditions, using CLSM. Patches of *D. vulgaris* cell aggregates began to appear at 48 h, progressively expanding to obtain a thick and confluent layer after 72 h, followed by the onset of dispersion at 96 h (Fig. 2A). Analyses of biofilm architecture showed that biomass increased progressively up to 72 h, reaching a maximum of *ca.* 7 $\mu m^3/\mu m^2$, along with an increase of thickness and surface area (17 µm and 3 x 10^6 μm^2, respectively) (Fig. 2B). The decrease of all biofilm spatial characteristics observed after 96 h is likely due to nutrient exhaustion and catabolite buildup, leading to the dispersal of the mature biofilm, as confirmed by CLSM observations (Fig. 2A).

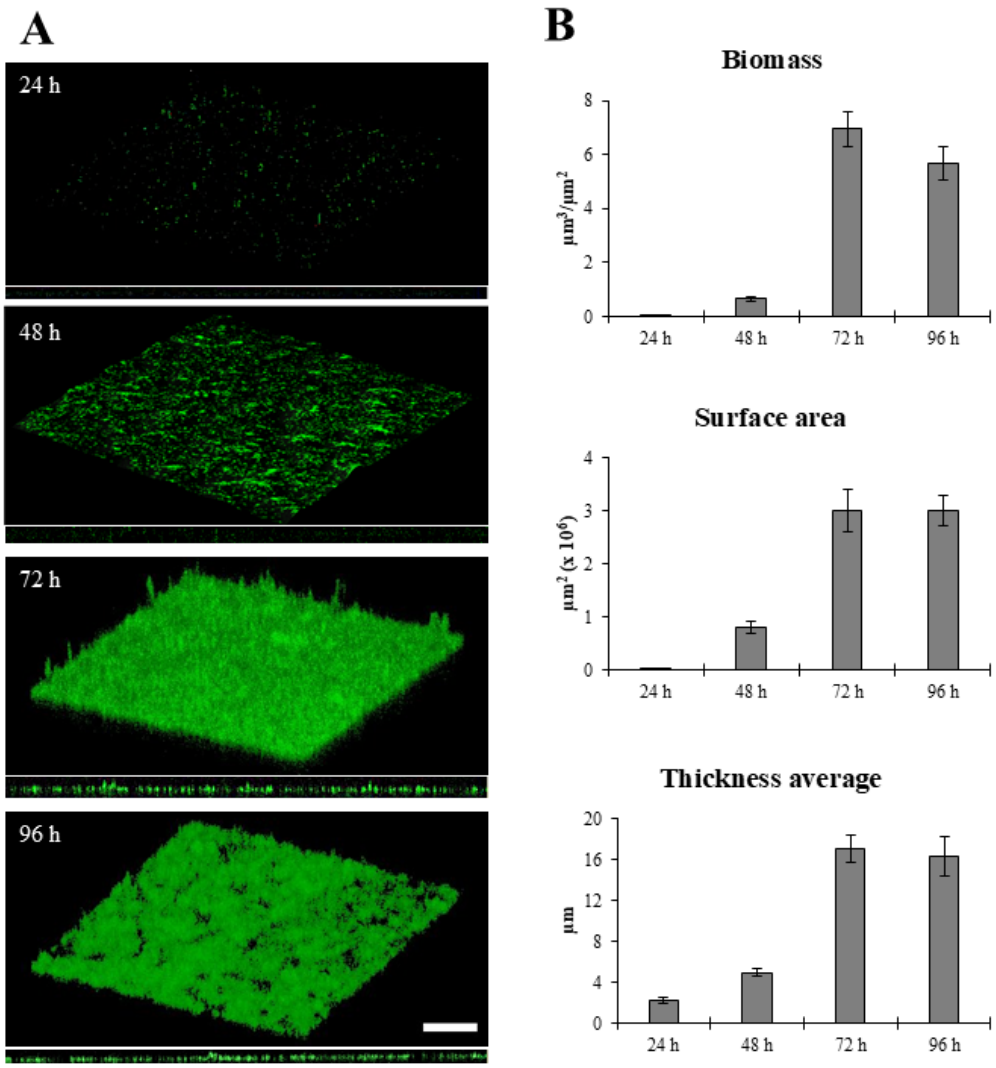

Fig. 2. Time course of *D. vulgaris* biofilm formation in Desulfovibrio (Postgate) medium. (A) Representative confocal microscope images of biofilms (x-y plane and orthogonal view) stained with acridine orange. Scale bar, 50 µm. (B) Quantification of biofilm spatial characteristics determined by analysis with COMSTAT, version 2.1. At least five image stacks were analyzed per condition.

Effect of cinnamaldehyde and glutaraldehyde against preformed *D. vulgaris* biofilms

To investigate the disruptive effect of cinnamaldehyde and glutaraldehyde on *D. vulgaris* preformed biofilms, 72 h-old mature biofilms were exposed to different concentrations of each compound (ranging from the MIC to 8X MIC) for further 48 h, under anaerobic conditions, prior to confocal microscopy analysis. Both cinnamaldehyde and glutaraldehyde caused evident disruption of preformed *D. vulgaris* biofilms in a concentration-dependent manner (Fig. 3A) consistent with a reduction in biofilm biomass, surface area and average thickness (Fig. 3B). Notably, treatment with 4X MIC of cinnamaldehyde and glutaraldehyde caused a significant disruption of preformed biofilms compared to the untreated biofilm, with a reduction of *ca* 90 % *vs* 85 % for biomass, 85 % vs 80 % for surface area and 60 % vs 45 % for average thickness, respectively (Fig. 3B). Since cinnamaldehyde was dissolved in DMSO, differently from glutaraldehyde which was soluble in ddH_2O, the potential disruptive effect of DMSO on *D. vulgaris* biofilm was also investigated, to rule out a solvent-dependent effect. To this aim, mature *D. vulgaris* biofilms were exposed to different DMSO concentrations (1 %, 0.5 %, 0.25 % and 0.125 % of DMSO corresponding to the DMSO contained in the 8X MIC, 4X MIC, 2X MIC and MIC treatments, respectively) for 48 h, under anaerobic conditions (Fig. 4A). DMSO at concentrations of 0.125 %, 0.25 % and 0.5 % did not significantly reduce the biofilm biomass compared to the untreated control, thus confirming the potential of cinnamaldehyde, rather than its solvent, in eradicating pre-formed *D. vulgaris* biofilms. When used at the concentration of 1 %, however, DMSO caused a statistically significant reduction in biomass and surface area (*ca.* 40 % and 15 % compared to NT, respectively) (Fig. 4B), confirming that DMSO can be toxic to microorganisms and should not be used at concentration higher than 2 % (Wang et al., 2023).

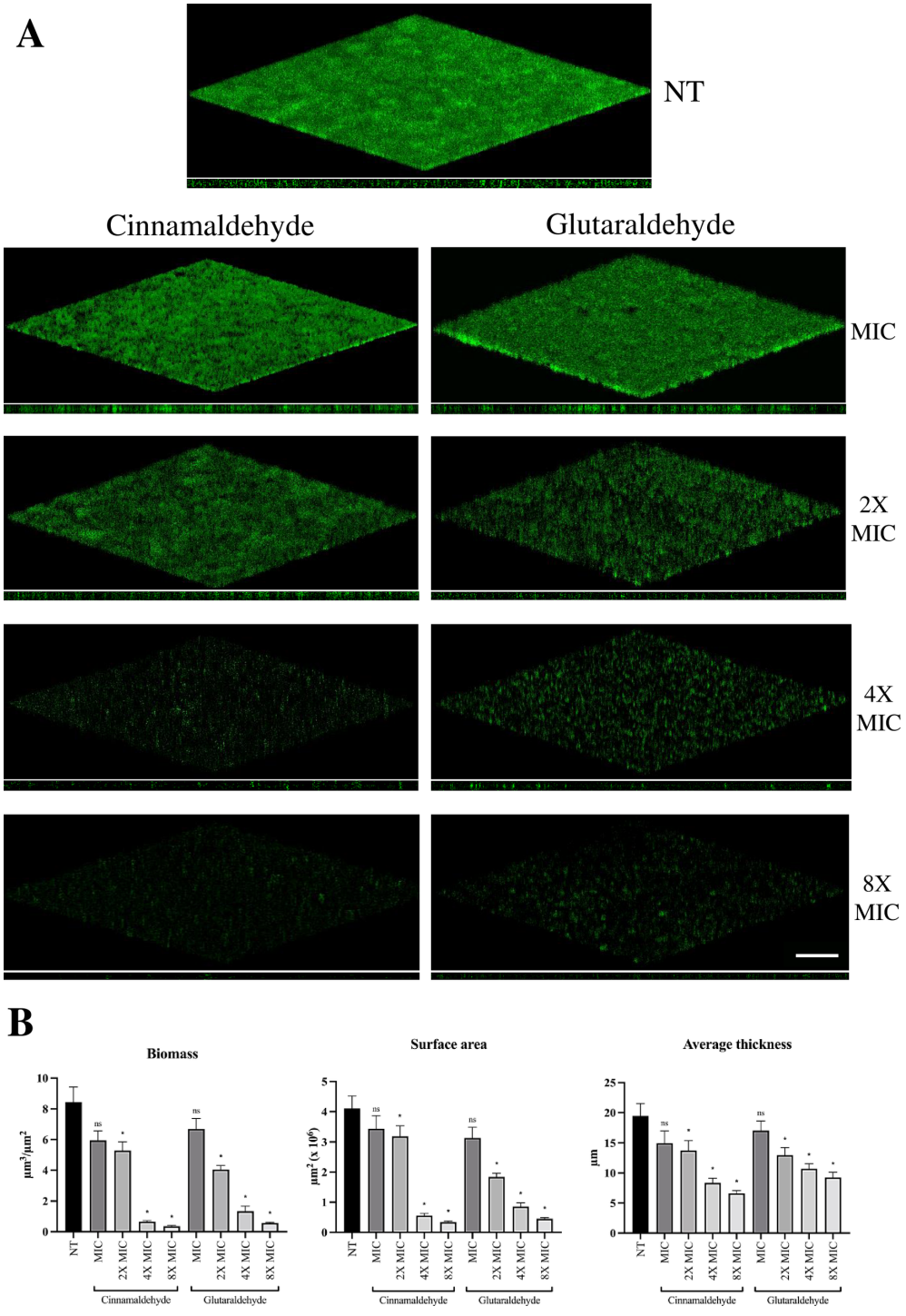

Fig. 3. Effect of cinnamaldehyde and glutaraldehyde on 72 h-old *D. vulgaris* biofilms (A) Representative confocal microscope images of *D. vulgaris* biofilm developed for 72 h (top) and treated with cinnamaldehyde (left) and glutaraldehyde (right) concentrations ranging from MIC to 8X MIC (12.5, 25, 50 and 100 µg/ml) for further 48 h at 37 °C in anaerobic conditions (x-y plane and orthogonal view). Scale bar, 50 µm. **(B)** Quantification of biofilm spatial characteristics determined by analysis with COMSTAT, version 2.1. At least five image stacks were analyzed per condition. Statistical analysis was performed with the GraphPad Prism software, by using one-way ANOVA, followed by the Dunn's multiple-comparison test. Differences among treatments and untreated control (NT) were considered highly statistically significant (*) with a P-value ≤ 0.001; not significant (ns) indicate a P > 0.001. Black columns indicate untreated control (NT), all other columns represent treatments with either cinnamaldehyde or glutaraldehyde, at the indicated concentrations (MIC, 2X MIC, 4X MIC, 8X MIC).

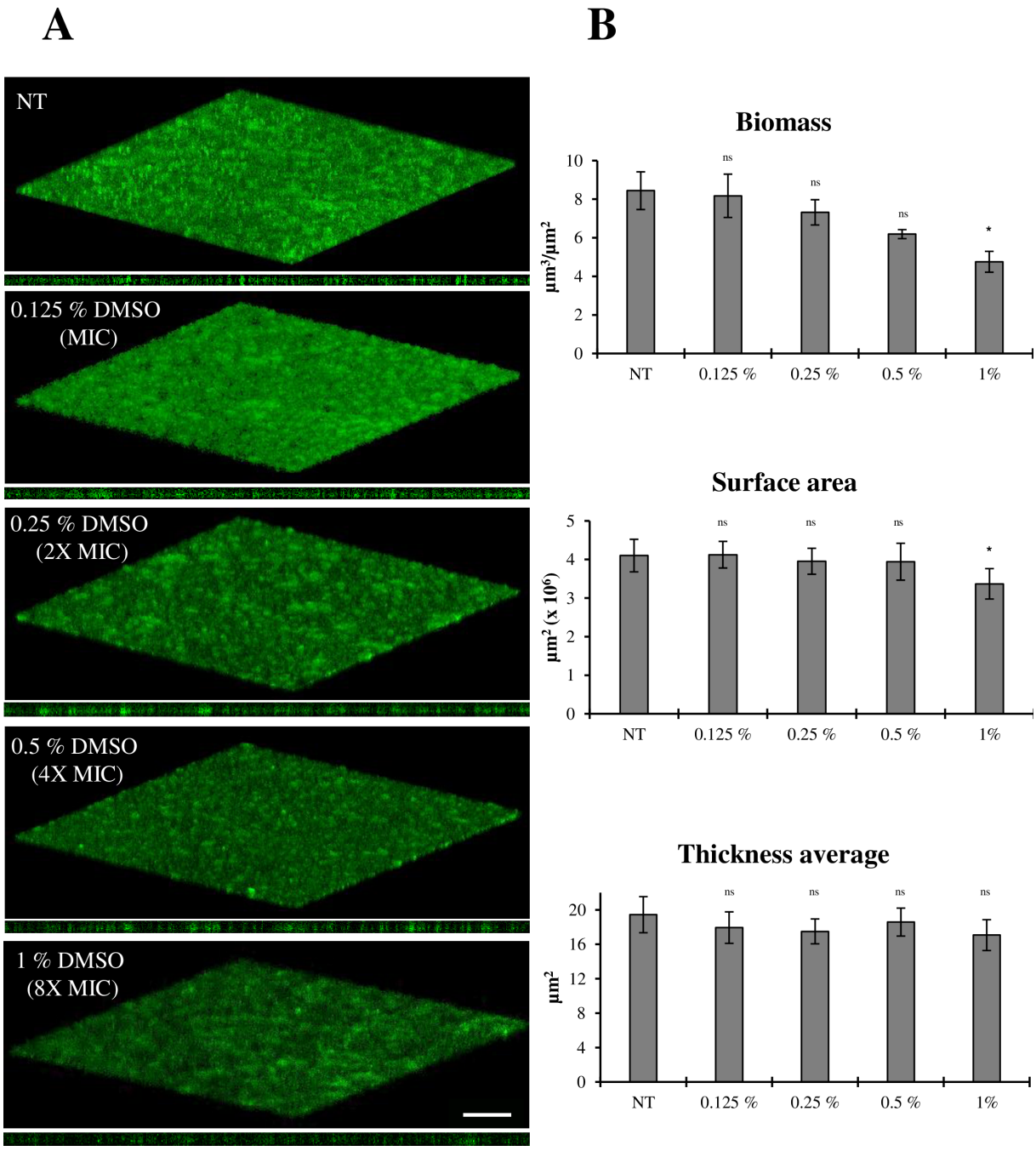

Fig. 4. Effect of DMSO on 72-old *D. vulgaris* biofilms. (A) Representative confocal microscope images of *D. vulgaris* biofilm developed for 72 h and treated or not (NT) for 48 h with DMSO at the same concentrations present during treatments with cinnamaldehyde (0.125 %, 0.25 %, 0.5 % and 1 % of DMSO, corresponding to the amount present at MIC, 2X MIC, 4X MIC and 8X MIC, respectively). Treatments were performed under anaerobic conditions and biofilm were stained with acridine orange. Scale bar, 50 µm. (B) Quantification of biofilm spatial characteristics determined by analysis with COMSTAT, version 2.1. At least five image stacks were analyzed per condition. Statistical analysis was performed with the GraphPad Prism software, by using one-way ANOVA, followed by the Dunn's multiple-comparison test. Differences among treatments and untreated control (NT) were considered highly statistically significant (*) with a P-value ≤ 0.001; not significant (ns) indicate a P > 0.001.

D. vulgaris biofilm formation and disruption of preformed biofilms on metal coupons

Since SRB-mediated corrosion mainly affects carbon steel surfaces (Javed et al., 2015), the antibiofilm activity of cinnamaldehyde was investigated on representative metal coupons on which *D. vulgaris* biofilms were allowed to form for 72 h. To this aim, metal coupons inoculated with *D. vulgaris* were initially analyzed for cell adhesion/biofilm formation every 24 h for 72 h. Unlike glass cover slips, biofilm formation on metal coupons could not be analyzed using CLSM due to the weight and thickness of the coupons. Consequently, every 24 h, three inoculated metal coupons were sacrificed, and the biofilm present on each coupon was detached using cycles of vortex and sonication (Fig. S1), and the resulting supernatant was serially diluted for *D. vulgaris* CFU enumeration.

After 48 h, *D. vulgaris* viable cell count reached *ca*. 1.5 x 10^7 CFU/ml, which decreased to *ca.* 1 x 10^6 CFU/ml at 72 h (Fig. 5A). Therefore, the *D. vulgaris* 48 h-old biofilm was chosen as the optimal condition to evaluate the disruptive effect of cinnamaldehyde at the highest concentration tested on cover glasses (*i.e.,* 8X MIC). The same volume of DMSO present at 8X MIC (*i.e.,* 1 %) was included as control, to confirm that the observed effect was solely due to cinnamaldehyde rather than the solvent. *D. vulgaris* 48 h-old biofilms were incubated for an additional 48 h under anaerobic conditions, after which a viable count was performed. Interestingly, no difference was observed between the untreated (NT) samples and those treated with 1 % DMSO (Fig. 5B). In contrast, no CFU/ml were detected at 8X MIC, indicating a bactericidal effect of cinnamaldehyde even on *D. vulgaris* biofilms developed on metal surfaces (Fig. 5C).

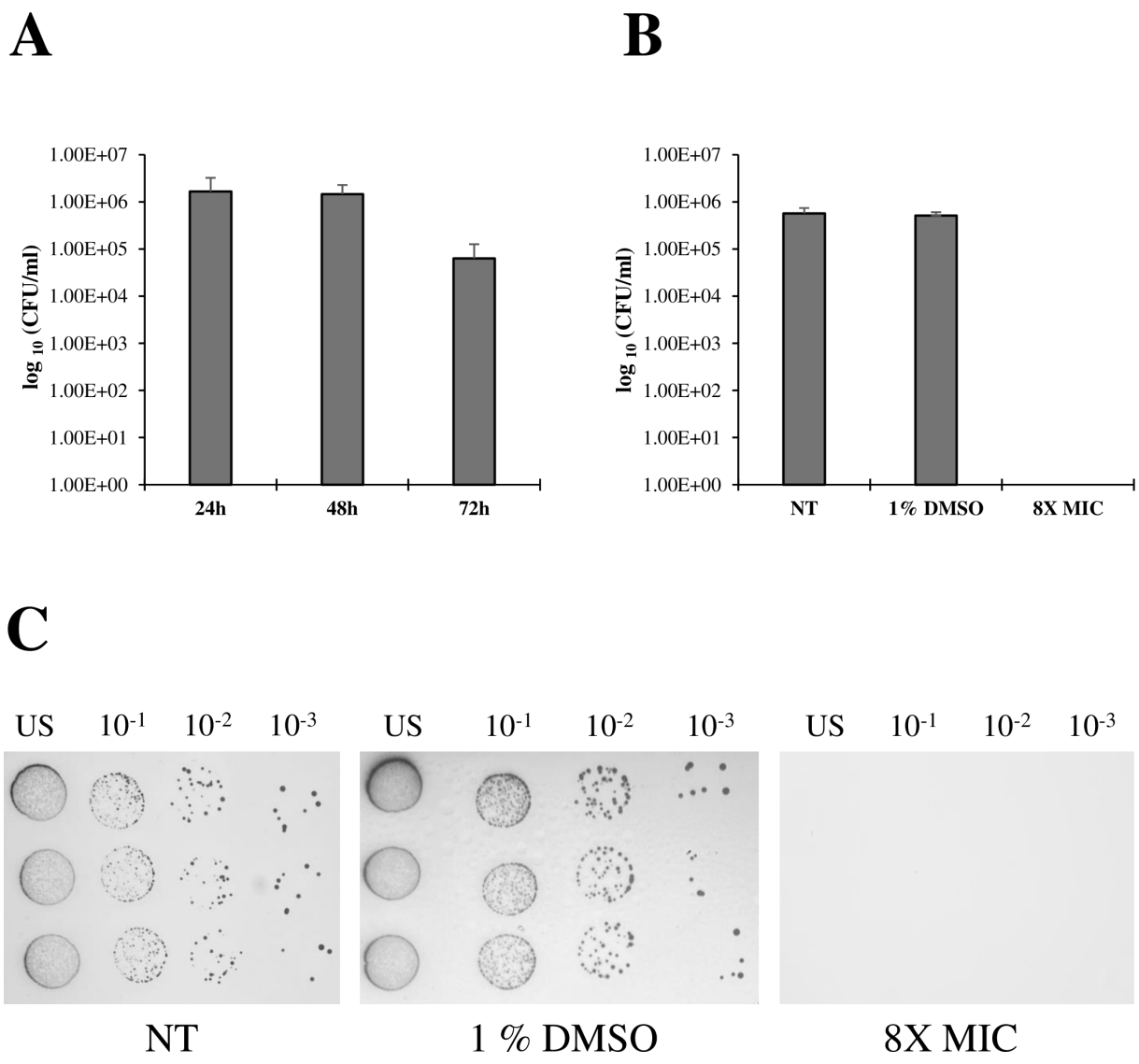

Fig. 5. *D. vulgaris* biofilms on metal coupons: formation, disruption and vital count. (A) *D. vulgaris* biofilm formation on metal coupons for 72 h followed by vital count after biofilm detachment; **(B)** Disruption (measured as CFU/ml after biofilm detachment from the metal coupons) of 48-old *D. vulgaris* biofilms treated with the maximum concentration of cinnamaldehyde (8X MIC) as well as 1 % DMSO, compared to the untreated (NT) control; **(C)** Representative images of serially-diluted (up to 10^{-3}, US: undiluted sample) bacterial suspensions (10 µl) obtained after biofilm detachment from metal coupons, spotted onto Postgate agar medium.

Discussion

Investigating the dynamics of biofilm formation in SRB responsible for microbiologically influenced corrosion is essential for the development of eco-friendly strategies to replace the use of toxic biocides, as part of corrosion mitigation strategies. In this study, we demonstrate for the first time that cinnamaldehyde exhibits promising antibacterial and antibiofilm properties against *D. vulgaris*, an SRB model microorganism. Indeed, cinnamaldehyde showed comparable efficacy to the well-known reference biocide, glutaraldehyde, which is however toxic to the environment, particularly to aquatic ecosystems (Sano et al., 2005; Pereira et al., 2014). Cinnamaldehyde is well-known for its wide spectrum of antimicrobial activity, however, planktonic growth inhibition of relevant pathogenic species, has been documented for concentration ≥ 250 µg/ml, including *Escherichia coli* (MIC = 250 µg/ml, Firmino et al., 2018; MIC = 310 µg/ml, Ye et al., 2013; Shen et al., 2015; MIC = 780 µg/ml, Pereira et al., 2021); *Staphylococcus aureus* (MIC = 250 µg/ml, Firmino et al., 2018; MIC = 310 µg/ml, Ye et al., 2013; MIC = 500 µg/ml; Ferro et al., 2016, Ferrando et al., 2024); *Pseudomonas aeruginosa* (MIC = 250 µg/ml, Firmino et al., 2018; MIC = 800 µg/ml, Song et al., 2023; MIC = 1000 µg/ml, Subhaswaraj et al., 2018, Ferrando et al., 2024; MIC = 1024 µg/ml, Tetard et al., 2019) and *Enterococcus faecalis* (MIC = 250 µg/ml, Ferro et al., 2016; MIC = 1000 µg/ml, Ferrando et al., 2024).

In this work we found that a > 20 times lower concentration of cinnamaldehyde (*i.e.,* 12.5 µg/ml) inhibited the growth and killed planktonic *D. vulgaris* cells (Fig. 1) and, more importantly, a concentration as low as 50 µg/ml (*i.e.*, 4X MIC) almost completely disrupt biofilm-grown cells, by reducing biomass (> 90 %), surface area (> 85 %) and thickness (> 60 %) (Fig. 3). These findings are particularly relevant for strategies aimed at mitigating microbial corrosion, since sessile cells within biofilms are notoriously more difficult to eradicate than planktonic ones. Indeed, in field applications, very high concentrations of biocides are typically required to eradicate sessile cells due to biofilms' multiple defense mechanisms such as the presence of a diffusional barrier that slows biocide penetration, the reduced metabolic rates that limit biocide uptake, and the upregulation of efflux pumps to expel biocides (Li et al., 2016).

Since SRB-mediated corrosion mainly affects steel surfaces, the effect of cinnamaldehyde was also tested against *D. vulgaris* 48 h-old biofilms grown on metal coupons. Cinnamaldehyde exposure (100 µg/ml) for 48 h resulted to be bactericidal against *D. vulgaris* adherent cells, as revealed by viable count determination (Fig. 5). Differently from cover glass slips (Fig. 4), no

difference was observed between untreated samples and those treated with 1 % DMSO (Fig. 5). Although the different experimental setting between glass cover slips and metal coupons does not allow a direct comparison on the biofilm-disruptive effect of cinnamaldehyde, the results observed might suggest that while 1 % DMSO seems to affect *D. vulgaris* biofilms in terms of spatial features (*i.e.,* biomass and surface area) it does not affect cell viability, as also observed in the preliminary MIC determination experiments (data not shown).

Interestingly, while numerous studies have highlighted the broad-spectrum antibacterial properties of plant extracts and EOs, very few are focused on bacteria directly involved in microbial corrosion, such as SRB. It has been demonstrated that lemongrass essential oil (LEO) and its principal component, citral, can effectively control both planktonic and sessile cultures of *Desulfovibrio alaskensis* strain NCIMB 13491, with a MIC of 170 µg/ml, a > 10 times higher concentration than the cinnamaldehyde one used in this study. Additionally, both LEO and citral exhibited anti-biocorrosion effects on carbon steel (Korenblum et al., 2013). Other major components of EOs, such as linalool, geraniol, nerol, eugenol R-limonene, and S-limonene, have also been tested against *D. alaskensis* NCIMB 13491, showing MIC values ranging from 78 to 2,500 µg/ml (Souza et al., 2017), much higher (*i.e.,* from 6 to 200 times) than the cinnamaldehyde concentration effective against *D. vulgaris*.

Given the limited knowledge about the application of EOs or their components on SRB biofilms, the present study aimed at investigating the potential effect of cinnamaldehyde, which has not previously been applied in this specific area of research. The rationale of choosing cinnamaldehyde lies in its well-documented efficacy as a green corrosion inhibitor for steels in acidic environments (Hossain et al., 2019; Kumar et al., 2022). Indeed, cinnamaldehyde is able to adsorb onto the metal surface, forming a protective macroscopic film (Avdeev et al., 2013; Cabello et al., 2013; Negm et al., 2013; Keles et al., 2014; Jafferji et al., 2018; Hossain et al., 2019; Wang et al., 2019; Saad et al., 2024). This adsorbed layer acts as a barrier, effectively slowing down the corrosive attack from the surrounding aggressive environment (Mouaden et al., 2020). Moreover, cinnamaldehyde has also been regarded as a quorum-sensing inhibitor in biofouling seawater bacteria, able to reduce biofilm formation at the high concentration of 1,200 µg/ml (Katebian et al., 2016), and as a potential antifouling coating in combination with the conventionally-used non-toxic polydimethylsiloxane (Guo et al., 2024).

We have demonstrated that cinnamaldehyde effectively disrupts pre-formed *D. vulgaris* biofilms both on glass coverslip and metal coupons, paving the way for further studies on its

long-term effects and performance under different environmental conditions. Cinnamaldehyde's dual function as both an antimicrobial agent and a corrosion inhibitor makes it an appealing candidate for industrial applications, particularly in environments where SRB-induced corrosion is prevalent. By mitigating both microbial proliferation and metal degradation caused by the corrosive agents produced by SRB metabolism (*e.g.,* H_2S), cinnamaldehyde may offer a safer and environmentally-friendly approach for controlling SRB activity and managing biofilm-related corrosion, making it a viable replacement for more hazardous traditionally used biocides.

Acknowledgements

G.M. salary was co-financed by the European Union – PON Ricerca e Innovazione 2014-2020 pursuant to art. 24, lett. a, of Law 30 December 2010, n. 240 and subsequent amendments and integration of the D. M. 10 August 2021, n. 1062 (CUP H31B21009620007). This work was partially financed by Saipem SpA, Fano (PU), Italy.

References

- Avdeev YG, Kuznetsov YI, Buryak AK. **(2013)**. Inhibition of steel corrosion by unsaturated aldehydes in solutions of mineral acids. Corros. Sci. 69, 50–60.
- Bhola SM, Alabbas FM, Bhola R et al. **(2014)**. Neem extract as an inhibitor for biocorrosion influenced by sulfate reducing bacteria: A preliminary investigation. Engineering Failure Analysis 36, 92-103. https://doi.org/10.1016/j.engfailanal.2013.09.015.
- Blackwood DJ. **(2018)**. An electrochemist perspective of microbiologically influenced corrosion. *Corrosion and Materials Degradation*, *1*(1), 59-76. https://doi.org/10.3390/cmd1010005
- Bouraoui MM, Chettouh S, Chouchane T, Khellaf N. **(2019)**. Inhibition Efficiency of Cinnamon Oil as a Green Corrosion Inhibitor, Journal of Bio- and Tribo-Corrosion 5:28. https://doi.org/10.1007/s40735-019-0221-0
- Cabello G, Funkhouser GP, Cassidy J, Kiser CE, Lane J, Cuesta A. **(2013)**. CO and trans-cinnamaldehyde as corrosion inhibitors of I825, L80–13Cr and N80 alloys in concentrated HCl solutions at high pressure and temperature. Electrochim. Acta **97**, 1–9
- Catani L, Manachini B, Grassi E, Guidi L, Semprucci F. **(2023)**. Essential Oils as Nematicides in Plant Protection—A Review. *Plants*.; 12(6):1418. https://doi.org/10.3390/plants12061418
- Chen Y, Tang Q, Senko JM, Cheng G, Newby BZ, Castaneda H, Ju LK. **(2015)**. Long-term survival of *Desulfovibrio vulgaris* on carbon steel and associated pitting corrosion. Corrosion Science 90; 89–100
- Clinical and Laboratory Standards Institute. **(2018)**. Methods for Dilution Antimicrobial Susceptibility Tests for Bacteria That Grow Aerobically, 11th ed.; CLSI: Wayne, PA (approved standard M07-A10).
- Cloete TE, Jacobs L, Brözel VS. **(1998)**. The chemical control of biofouling in industrial water systems. *Biodegradation*. 9(1):23-37. doi:10.1023/a:1008216209206
- Coetser SE, Cloete TE. **(2005)**. Biofouling and Biocorrosion in Industrial Water Systems. *Critical Reviews in Microbiology*, *31*(4), 213–232. https://doi.org/10.1080/10408410500304074
- D'Addabbo T, Laquale S, Veronico P, Avato P, Argentieri MP. **(2024)**. Nematicidal activity of the essential oil from *Cinnamomum cassia* and *(E)*-cinnamaldehyde against phytoparasitic nematodes.
- Eid MM, Duncan KE, Tanner RS. **(2018)**. A semi-continuous system for monitoring microbially influenced corrosion. Journal of Microbiological Methods 150, 55-60
- European Commission, Directorate-General for Research and Innovation, Lacroix, D., Boero, F., Ligtvoet, A. *et al*. **(2021)**. Mission area, healthy oceans, seas, and coastal and inland waters – Foresight on demand brief in support of the Horizon Europe mission board. Publications Office of the European Union, **https://data.europa.eu/doi/10.2777/054595**
- Ferrando N, Pino-Otín MR, Ballestero D, Lorca G, Terrado EM, Langa E. **(2024)**. Enhancing Commercial Antibiotics with Trans-Cinnamaldehyde in Gram-Positive and Gram-Negative Bacteria: An In Vitro Approach. *Plants*. 13(2):192. https://doi.org/10.3390/plants13020192
- Ferro TAF, Araújo JMM, dos Santos Pinto BL, dos Santos JS, Souza EB, da Silva BLR, Colares VLP, Novais TMG, Filho CMB, Struve C, Calixto JB, Monteiro-Neto V, da Silva LCN and Fernandes ES. **(2016)**. Cinnamaldehyde Inhibits *Staphylococcus aureus* Virulence

Factors and Protects against Infection in a *Galleria mellonella* Model. Front. Microbiol. 7:2052. doi: 10.3389/fmicb.2016.02052

- Firmino DF, Cavalcante TTA, Gomes GA, *et al*. **(2018)**. Antibacterial and Antibiofilm Activities of Cinnamomum Sp. Essential Oil and Cinnamaldehyde: Antimicrobial Activities. ScientificWorldJournal. 7405736. Published 2018 Jun 6. doi:10.1155/2018/7405736
- Greene EA, Brunelle V, Jenneman GE, Voordouw G. **(2006)**. Synergistic inhibition of microbial sulfide production by combinations of the metabolic inhibitor nitrite and biocides. Appl. Environ. Microbiol. 72, 7897–7901. http://dx.doi.org/10.1128/AEM.01526-06.
- Gu, T. **(2014)**. Theoretical modeling of the possibility of acid producing bacteria causing fast pitting biocorrosion. *J. Microb. Biochem. Technol*, *6*(2), 068-074. http://dx.doi.org/10.4172/1948-5948.1000124
- Gu T, Jia R, Unsal T, Xu D. **(2019)**. Toward a better understanding of microbiologically influenced corrosion caused by sulfate reducing bacteria. *Journal of Materials Science & Technology* 35, 631-636.
- Guo Y, Yan M, Zhao W. **(2024)**. Cinnamaldehyde grafted porous Aerogel-Organ gel liquid infused surface for achieving difunctional long-term dynamic antifouling. Journal of Colloidal and Interface Science. 653, 833-843.
- Haddi K. Faroni LRA, Oliveira EE. **(2017)**. Cinnamon Oil. In: Nollet L.M.L., Rathore H. S., (eds). Green Pesticides Handbook CRC Press, Taylor & Francis Group. 117—151
- Heidelberg JF, Seshadri R, Haveman SA, *et al*. **(2004)**. The genome sequence of the anaerobic, sulfate-reducing bacterium *Desulfovibrio vulgaris* Hildenborough. *Nat Biotechnol*. 22(5):554-559. doi:10.1038/nbt959
- Heydorn A, Nielsen AT, Hentzer M, Sternberg C, Givskov M, Ersbøll BK, Molin S. **(2000)**. Quantification of biofilm structures by the novel computer program COMSTAT. Microbiology 146:2395–2407. https://doi.org/ 10.1099/00221287-146-10-2395.
- Hossain SZ, Al-Shater A, Kareem SA, Salman A, Ali RA, Ezuber H, Razzak SA. **(2019)**. Cinnamaldehyde as a green inhibitor in mitigating AISI 1015 carbon steel corrosion in HCl. Arabian Journal for Science and Engineering, 44, 5489-5499.
- Jafferji H, Sharifi NP, Schneider EM, Sakulich AR. **(2018)**. Investigation of incorporating cinnamaldehyde into lightweight aggregate for potential corrosion reduction in cementitious materials. Cem. Concrete Compos. 87, 1–9
- Javaherdashti R. **(2017)**. Microbiologically Influenced Corrosion: An Engineering Insight, 2nd ed. Springer International Publishing, AG, Cham, Switzerland. http://dx.doi.org/10.1007/978-3-319-44306-5.
- Javed MA, Stoddart PR, Wade SA. **(2015)**. Corrosion of carbon steel by sulphate reducing bacteria: Initial attachment and the role of ferrous ions. Corrosion Science. 93, 48-57.
- Jin J, Guan Y. **(2014)**. The mutual co-regulation of extracellular polymeric substances and iron ions in biocorrosion of cast iron pipes. *Bioresource technology*, *169*, 387-394. https://doi.org/10.1016/j.biortech.2014.06.05
- Kalemba D, Kunicka A. **(2003)**. Antibacterial and antifungal properties of essential oils. *Curr Med Chem*. 10(10):813-829. doi:10.2174/0929867033457719
- Katebian L, Gomez E, Skillman L, Li D, Ho G, Jiang SC. **(2016)**. Inhibiting quorum sensing pathways to mitigate seawater desalination RO membrane biofouling. Desalination. 393, 135-143. https://doi.org/10.1016/j.desal.2016.01.013

- Keles H, Keles M. **(2014)**. Electrochemical investigation of a Schiff base synthesized by cinnamaldehyde as corrosion inhibitor on mild steel in acidic medium. Res. Chem. Intermed. 40, 193–209.
- Kiani Khouzani M, Bahrami A, Hosseini-Abari A, Khandouzi M, Taheri P. **(2019)**. Microbiologically Influenced Corrosion of a Pipeline in a Petrochemical Plant. *Metals*. 9(4):459. https://doi.org/10.3390/met9040459
- Korenblum E, Regina de Vasconcelos Goulart F, de Almeida Rodrigues I, Abreu F, Lins U, Alves PB, Blank AF, Valoni E, Sebastián GV, Alviano DS, Alviano CS, Seldin L. **(2013)**. Antimicrobial action and anti-corrosion effect against sulfate reducing bacteria by lemongrass (Cymbopogon citratus) essential oil and its major component, the citral. AMB Express. 3(1):44. doi: 10.1186/2191-0855-3-44.
- Kumar D, Muralidhar V, Jain V, Rai B. **(2022)**. Integrating experiments, DFT and characterization for comprehensive corrosion inhibition studies – A case for cinnamaldehyde as an excellent green inhibitor for steels in acidic media. Corrosion Science 208, 110623. https://doi.org/10.1016/j.corsci.2022.110623
- Lane RA. **(2005)**. Under the microscope: Understanding, detecting, and preventing microbiologically influenced corrosion. *J. Fail. Anal. Prev.* 5, 10–12
- Lee JS, Ray RI, Little BJ. **(2007)**. Microbiologically influenced corrosion in military environments, Publ. Domain Rep. http://www.dtic.mil/cgi-bin/GetTRDoc?AD=ADA470709
- Li H, Zhou E, Zhang D *et al.* **(2016)**. Microbiologically Influenced Corrosion of 2707 Hyper-Duplex Stainless Steel by Marine *Pseudomonas aeruginosa* Biofilm. *Sci Rep* 6, 20190. https://doi.org/10.1038/srep20190
- Li X,Duan J,Xiao H,Li Y,Liu H, Guan F and Zhai X (2017) Analysis of Bacterial Community Composition of Corroded Steel Immersed in Sanya and Xiamen Seawaters in China via Method of Illumina MiSeq Sequencing. Front. Microbiol. 8:1737. doi: 10.3389/fmicb.2017.01737
- Lu L, Shu C, Chen L, *et al*. **(2020)**. Insecticidal activity and mechanism of cinnamaldehyde in *C. elegans*. *Fitoterapia*. 146:104687. doi:10.1016/j.fitote.2020.104687
- Marchesini P, Novato TP, Cardoso SJ, et al. Acaricidal activity of (E)-cinnamaldehyde and α-bisabolol on populations of Rhipicephalus microplus (Acari: Ixodidae) with different resistance profiles. *Vet Parasitol*. 2020;286:109226. doi:10.1016/j.vetpar.2020.109226
- Mouaden KEL, Chauhan DS, Quraishi MA, Bazzi L, Hilali M. **(2020)**. Cinnamaldehyde-modified chitosan as a bio-derived corrosion inhibitor for acid pickling of copper: Microwave synthesis, experimental and computational study. International Journal of Biological Macromolecules 164, 3709–3717. https://doi.org/10.1016/j.ijbiomac.2020.08.137
- NACE IMPACT Study, **(2016)**. impact.nace.org(Accessed September 16th, 2023).
- NACE-ASTM G193-2022, Standard Terminology and Acronyms Relating to Corrosion.
- Negm NA, Yousef MA, Tawfik SM. **(2013)**. Impact of synthesized and natural compounds in corrosion inhibition of carbon steel and aluminium in acidic media. Recent Patents Corros. Sci. 3, 58–68
- OuYang Q, Duan X, Li L, Tao N. **(2019)**. Cinnamaldehyde Exerts Its Antifungal Activity by Disrupting the Cell Wall Integrity of *Geotrichum citri-aurantii*. Front Microbiol. 2019 Jan 30;10:55. doi:10.3389/fmicb.2019.00055.
- Pang D, Huang Z, Li Q, *et al*. **(2021)**. Antibacterial Mechanism of Cinnamaldehyde: Modulation of Biosynthesis of Phosphatidylethanolamine and Phosphatidylglycerol in

Staphylococcus aureus and *Escherichia coli*. *J Agric Food Chem*. 69(45):13628-13636. doi:10.1021/acs.jafc.1c04977

- Pankey GA, Sabath LD. **(2004)**. Clinical relevance of bacteriostatic versus bactericidal mechanisms of action in the treatment of Gram-positive bacterial infections. Clin Infect Dis. 38(6):864-70. doi:10.1086/381972.
- Pereira SPP, Oliveira R, Coelho S, Musso C, Soares AMVM, Domingues I, Nogueira AJA. **(2014)**. From sub cellular to community level: Toxicity of glutaraldehyde to several aquatic organisms. Science of the Total Environment 470–471, 147–158.
- Pereira WA, Pereira CDS, Assunção RG, *et al*. **(2021)**. New Insights into the Antimicrobial Action of Cinnamaldehyde towards *Escherichia coli* and Its Effects on Intestinal Colonization of Mice. *Biomolecules*. 11(2):302. doi:10.3390/biom11020302
- Postgate JR. **(1965)**. Recent Advances in the Study of the Sulfate-Reducing Bacteria, Bacteriological Reviews, Vol 26, No 4
- Procopio L. **(2019)**. The role of biofilms in the corrosion of steel in marine environments. World Journal of Microbiology and Biotechnology, 35:73 https://doi.org/10.1007/s11274-019-2647-4
- Quraishi MA. **(1999)**. Investigation of some green compounds as corrosion and scale inhibitors for cooling systems. Corrosion 55, 493–497
- Rieger KA, Schiffman JD. **(2014)**. Electrospinning an essential oil:cinnamaldehyde enhances the antimicrobial efficacy of chitosan/poly (ethylene oxide) nanofibers. Carbohydr. Polym. 113, 561–568
- Runci F, Bonchi C, Frangipani E, Visaggio D, Visca P. **(2016)**. Acinetobacter baumannii Biofilm Formation in Human Serum and Disruption by Gallium. Antimicrob Agents Chemother. 61(1):e01563-16. doi: 10.1128/AAC.01563-16.
- Saad WA, El-Shamy AM. **(2023)**. Unlocking the Potential of Cinnamaldehyde: A Comprehensive Study on Its Dual Role as an Effective Inhibitor Against Corrosion and Microbial Corrosion of Mild Steel in Saline Environments. Journal of Bio- and Tribo-Corrosion. 10:14 https://doi.org/10.1007/s40735-024-00817-5
- Sano LL, Krueger AM, Landrum PF. **(2005)**. Chronic toxicity of glutaraldehyde: differential sensitivity of three freshwater organisms. Aquatic Toxicology 71, 283–296. doi:10.1016/j.aquatox.2004.12.001
- Sharma M., Liu H., Chen, S. *et al.* Effect of selected biocides on microbiologically influenced corrosion caused by *Desulfovibrio ferrophilus* IS5. *Sci Rep* 8, 16620 (2018). https://doi.org/10.1038/s41598-018-34789-7
- Shen S, Zhang T, Yuan Y, Lin S, Xu J, Ye H. **(2015)**. Effects of cinnamaldehyde on *Escherichia coli* and *Staphylococcus aureus* membrane. Food Control 47, 196e202. http://dx.doi.org/10.1016/j.foodcont.2014.07.003
- Skovhus T, Enning D, and Lee J. **(2017)**. Microbiologically influenced corrosion in the upstream oil and gas industry. 1st Edn. Boca Raton FL: CRC Press. doi:10.1201/9781315157818
- Song L, Yang H, Meng X, *et al*. **(2023)**. Inhibitory Effects of Trans-Cinnamaldehyde Against *Pseudomonas aeruginosa* Biofilm Formation. *Foodborne Pathog Dis*. 20(2):47-58. doi:10.1089/fpd.2022.0073
- Souza PM, Goulart FRV, Marques JM, Bizzo HR, Blank AF, Groposo C, Sousa MP. **(2017)**. Vólaro V, Alviano CS, Moreno DSA, Seldin L. Growth Inhibition of Sulfate-Reducing Bacteria in Produced Water from the Petroleum Industry Using Essential Oils. Molecules. 22(4):648. doi: 10.3390/molecules22040648.

- Struchtemeyer CG, Morrison MD, Elshahed MS. **(2012)**. A critical assessment of the efficacy of biocides used during the hydraulic fracturing process in shale natural gas wells. Int. Biodeterior. Biodegrad. 71, 15–21.
- Subhaswaraj P, Barik S, Macha C, Chiranjeevi PV, Siddhardha B. **(2018)**. Anti quorum sensing and anti biofilm efficacy of cinnamaldehyde encapsulated chitosan nanoparticles against *Pseudomonas aeruginosa* PAO1. LWT - Food Science and Technology 97, 752–759. https://doi.org/10.1016/j.lwt.2018.08.011
- Swaroop BS, Victoria SN, Manivannan R. **(2016)**. Azadirachta indica leaves extract as inhibitor for microbial corrosion of copper by Arthrobacter sulfureus in neutral pH conditions—a remedy to blue green water problem. J. Taiwan Inst. Chem. Eng. 64, 269–278
- Telegdi J, Shaban A, Trif L. **(2017)**. Microbiologically influenced corrosion (MIC). *Trends in Oil and Gas Corrosion Research and Technologies*. 191-214.
- Tetard A, Zedet A, Girard C, Plésiat P, Llanes C. **(2019)**. Cinnamaldehyde Induces Expression of Efflux Pumps and Multidrug Resistance in *Pseudomonas aeruginosa*. Antimicrob Agents Chemother 63:10.1128/aac.01081-19. https://doi.org/10.1128/aac.01081-19
- Videla HA. **(2002)**. Prevention and control of biocorrosion. International Biodeterioration & Biodegradation 49, 259–270
- Videla HA. **(1996)**. Manual of Biocorrosion, 1st ed. CRC-Press, pp 13–45.
- Videla HA, Herrera LK. **(2009)**. Understanding microbial inhibition of corrosion. A comprehensive overview. *International Biodeterioration & Biodegradation*, *63*(7), 896-900. https://doi.org/10.1016/j.ibiod.2009.02.002
- Vorregaard M. **(2008)**. Comstat2—a modern 3D image analysis environment for biofilms, in informatics and mathematical modelling. Technical University of Denmark, Kongens Lyngby, Denmark.
- Wang D, Yang C, Zheng B, Yang M, Gao Y, Jin Y, Dong Y, Liu P, Zhang M, Zhou E, Gu T, Xu D, Wang F. **(2023)**. Microbiologically influenced corrosion of CoCrFeMnNi high entropy alloy by sulfate-reducing bacterium *Desulfovibrio vulgaris*. Corrosion Science. 223, 111429. https://doi.org/10.1016/j.corsci.2023.111429
- Wang Z, Wang T, Zhu J, Wei L, Shen Y, Li N, Hu J. **(2019)**. Synergistic effect and mechanism of copper corrosion inhibition using cinnamaldehyde and vanillin in HCl solution: an experimental and theoretical approach. Colloids Surfaces A Physicochem. Eng. Asp. 563, 246–254.
- Xu D, Jia R, Li Y, Gu T. **(2017)**. Advances in the treatment of problematic industrial biofilms. *World J Microbiol Biotechnol*. 33(5):97. doi:10.1007/s11274-016-2203-4
- Ye H, Shen S, Xu J, Lin S, Yuan Y, Jones GS. **(2013)**. Synergistic interactions of cinnamaldehyde in combination with carvacrol against food-borne bacteria. Food Control 34, 619e623

Supplementary materials

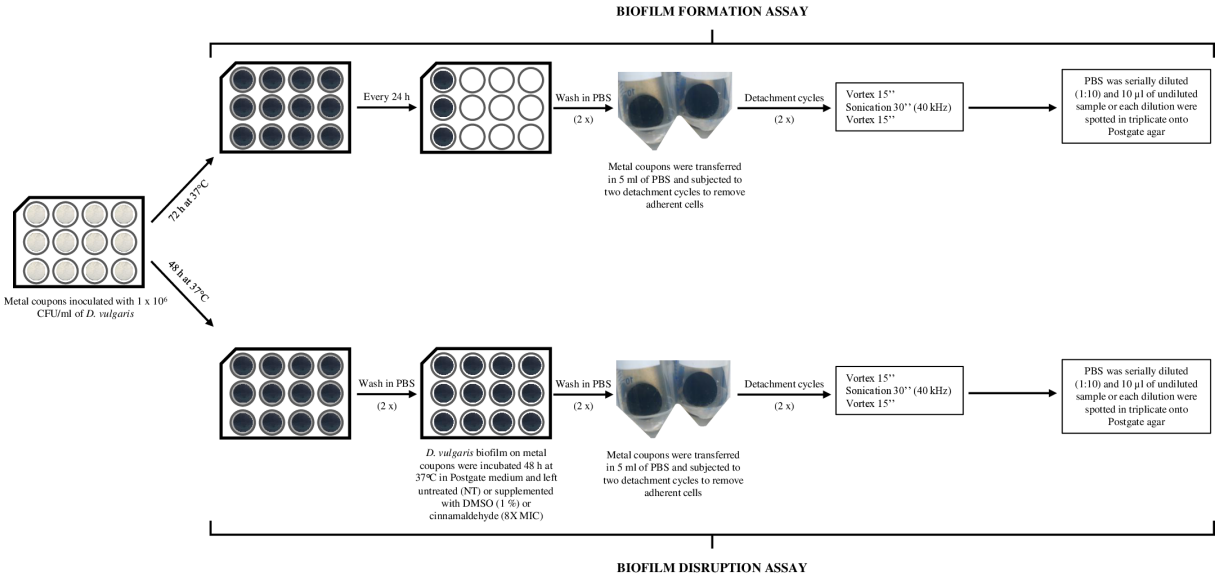

Fig. S1. Workflow of *D. vulgaris* biofilm formation and disruption on metal coupons.

Chapter 3

Bacteriophage-derived endolysins as green biocides against Microbiologically Influenced Corrosion

Preface to Chapter 3

Endolysins are hydrolytic enzymes encoded by bacteriophages during their lytic cycle, targeting the peptidoglycan layer of both Gram-positive and Gram-negative bacteria, thus promoting cell osmotic lysis. However, their fast lytic activity can also be accomplished when exogenously applied as recombinant proteins. These enzymes have garnered significant attention for their efficacy against clinically-relevant pathogens and are currently employed in clinical settings. However, the application of endolysins in environmental contexts, particularly those impacted by microbiologically influenced corrosion (MIC) driven by sulfate reducing bacteria (SRB), remains largely unexplored. In this context, Chapter 3 introduces a novel approach to MIC control using bacteriophage-derived endolysins as environmentally friendly alternatives to conventional biocides. This work focuses on the selection and *in vitro* testing of *Desulfovibrio vulgaris*-specific endolysins targeting different peptidoglycan structures and demonstrates their effectiveness against *D. vulgaris* planktonic cells. This study has been performed in collaboration with Dr. Roberto Vazquez Fernandez, Prof. Yves Briers (University of Gent, Belgium) and Prof. Rob Lavigne (University of Leuven, Belgium), supported by a FEMS research and training grant. Although preliminary, this study underscores the potential of endolysins to revolutionize MIC management in an environmentally sustainable manner, bypassing the use of conventional toxic biocides, and paves the way for the use of endolysins beyond clinical applications.

3.1 Introduction

The escalating threat posed by multidrug-resistant (MDR) bacteria is a global public health concern, intensified by the scarcity of novel antibiotics. If comprehensive global measures are not implemented, the World Health Organization (WHO) estimates suggest that by 2050, antibiotic-resistant bacteria could cause over 10 million deaths, surpassing the mortality associated with cancer. Recognizing this crisis, the WHO has emphasized that antimicrobial resistance (AMR) is a serious issue requiring a One Health approach, integrating efforts across human health, animal health, food production, and the environment (WHO, 2023).

Bacteriophages (phages) and phage-derived enzymes distinctly satisfy all four innovation criteria defined by the WHO, serving as a novel class of "non-traditional" antibiotics characterized by a unique mode of action, target, and an absence of known cross-resistance (WHO, 2020). Bacteriophages are viruses that only infect bacteria. They are ubiquitous in the environment and are considered as the most abundant organisms in the biosphere (Clokie et al., 2011. They were independently discovered in 1915 by Frederick Twort in England (Twort, 1915) and in 1917 by Félix d'Hérelle in France (d'Hérelle, 1917). Phages are solely composed of a nucleotide string carrying their genetic information (*i.e.,* DNA or RNA) surrounded by a protein shell or capsid. They can propagate through a lytic or lysogenic life cycle. During the lytic cycle phages can infect, multiply within a host cell, generating a numerous progeny that is liberated upon cell lysis, causing the rapid death of the bacterial host cell. Conversely, during the lysogenic life cycle some phages, called temperate, can integrate their genome into the host chromosome thus replicating within the host cell for several generations before undergoing the lytic cycle (Little, 2005) (Fig. 1).

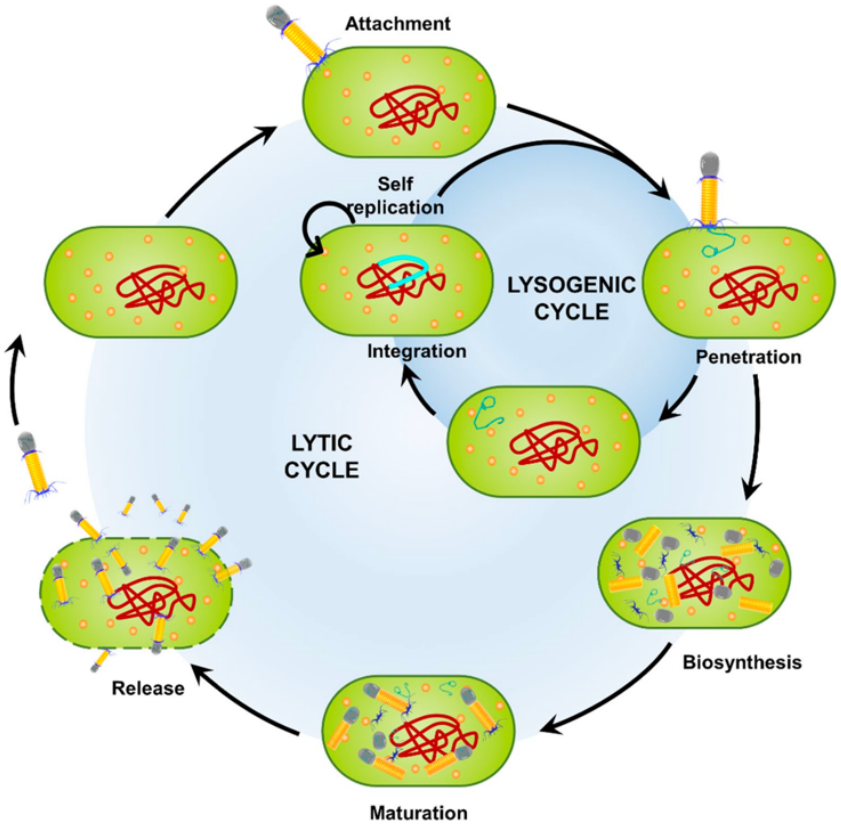

Fig. 1. Lytic and lysogenic cycle of bacteriophages. Lytic phages reproduce through a six-step process: attachment, penetration, biosynthesis, maturation, and lysis of the host cell, which releases new phage progeny leading to the death of the infected bacterium. In contrast, the lysogenic cycle involves the integration of the phage genome into the bacterial DNA, forming a prophage. This integrated genome replicates within the bacterial cell and can switch back to the lytic cycle when conditions are favorable (Bisen et al., 2024).

Phages can be seen as a natural toolbox offering several potential biotechnological tools, such as:

- RNA polymerases used in driving protein expressions (Butler and Chamberlin, 1982; Tabor and Richardson, 1985)
- phage receptor binding proteins (RBPs) involved in host-phage interactions, for bacterial endotoxin detection and removal (Santos, 2018)
- exopolysaccharide (EPS) depolymerases for disruption of the bacterial biofilm matrix (Topka-Bielecka et al., 2021)
- phage integrases and recombinases to mediate unidirectional site-specific recombination between two DNA recognition sequences and for precise genome editing (Groth and Calos, 2004; Murphy, 2012)

- proteins that block the action of bacterial Clustered Regularly Interspaced Short Palindromic Repeats (CRISPR)-Cas systems, by targeting the bacterial Cas proteins used by bacteria for genome editing (Stanley and Maxwell, 2018).

Phages offer several potential advantages compared to antibiotics. Their primary benefit lies in their specificity for target bacteria, minimizing damage to the host's flora. Phages are self-limiting, relying on their hosts for continuous growth; without specific hosts, their survival is short-lived. Phages possess a narrow host range, making it difficult to look for suitable phages for a given bacterium (Hibstu et al., 2022). On the other hand, the extensive use of bacteriophages may promote the selection of phage-resistant bacteria through spontaneous mutations, acquisition of restriction-modification systems, adaptive immunity, and other mechanisms (Gondil et al., 2020).

The interest in phage-encoded peptidoglycan (PG) hydrolases, commonly known as endolysins, has surged over the past decade, largely due to the critical demand for new antibacterial agents to address the rise of MDR bacterial pathogens. Endolysins are hydrolytic enzymes encoded by bacteriophages which play a specific role in the release of phage progeny, by degrading the PG of the host bacterium thus promoting cell osmotic lysis (Sao-José, 2018). These endolysins efficiently cleave the specific peptide bonds of bacterial PG from the inside of the host cell, however their fast activity can also be accomplished when exogenously applied as recombinant proteins (Vázquez and Briers, 2023). Indeed, the term "Enzybiotics" designates phage lysins intended for use as antimicrobial agents (Nelson et al., 2001). The therapeutic application of recombinant lysins in eliminating bacterial infections has been already assayed both *in vitro* and in *clinical trials* (Fischetti, 2005; Fenton et al., 2010; Briers et al., 2014a; Murray et al., 2021; Liu et al., 2023), and interestingly, the development of bacterial resistance by the accumulation of point mutations has never been observed (Chang, 2020). Given the many potential applications of endolysins, several biotechnology companies have started to investigate the use of phage-derived and engineered lysins in various fields. Indeed, endolysins have been applied not only as novel therapeutics, but also as novel food preservation tools in the field of food safety (Dy et al., 2018; Nazir et al., 2023).

However, to the best of our knowledge, the potential of endolysins for the biocontrol of aquaculture or other environmentally relevant issues remains largely unexplored (De Romero et al., 2004). Therefore, this chapter is focused on the potential application of endolysins against

D. vulgaris, a model microorganism of the environmental issue constituted by microbiologically influenced corrosion

3.1.1 Bacteriophage-encoded peptidoglycan hydrolases

Bacteriophage-encoded PG degrading hydrolases, known as endolysins, are proteins that degrade bacterial cell wall and play a crucial role in the lytic replication cycle, facilitating the release of phage progenies (Fischetti, 2005). First, at the beginning of lytic cycle, phages can inject their genetic material into bacterial cells by degrading PG thanks to the virion-associated PG hydrolases (VAPGHs) (Rodríguez-Rubio et al., 2013). Secondly, phages require endolysins express inside the bacterial host, at the end of their infection cycle. The phage release is complicated by the presence of a stronger barrier constituted by the bacterial cell wall. The most of lytic double-stranded DNA (dsDNA) phages (belonging to the *Caudovirales* order) have overcome this structural obstacle by adopting the endolysin-holin two component system (Fig. 2) to lyse the bacterial host in an optimal time (Stone, 2002). Holins are small hydrophobic proteins encoded by phages, synthetized during the late phase of the phage infection cycle and accumulated in the inner membrane of the bacterial cell in the form of homodimers (Grundling et al., 2001). Once endolysins reach a critical concentration, a triggering event occurs, leading to the formation of holes and subsequent collapse of the proton motive force of the cell membrane (Savva et al., 2014). Holins are considered biological clock, as they regulate the initiation of cell lysis. By controlling the access of endolysins to the cell wall (Young, 1992) they favor the consequent break down of the host PG, leading to cell lysis and the release of the phage progeny particles (De Smet et al., 2017) (Fig. 2).

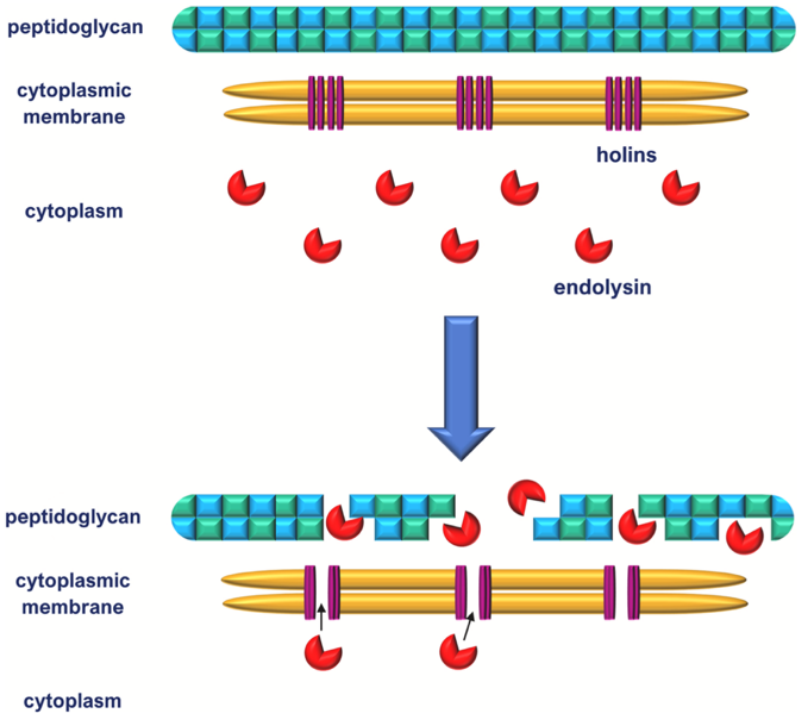

Fig. 2. Model of endolysin-holin two component system. Holins form pores in the cytoplasmic membrane that allow the export of endolysins accumulated in cytoplasm into periplasm, across the cytoplasmic membrane. Once outside the cell, endolysins degrade the PG structure (Grabowski et al., 2021).

3.1.2 Structural composition of phage endolysins

The structure of endolysins can be either modular or globular (Fig. 3). Modular endolysins, which are encoded by Gram-positive bacteria infecting phages, consist of two domains: an enzymatically active domain (EAD) and a cell wall binding domain (CBD). The EAD carries out the catalytic function by targeting specific chemical bonds within the PG, while the CBD directs endolysin to a specific cell wall substrate, such as lipoteichoic acids (Schmelcher et al., 2012). Typically, modular endolysins have one or two EADs at the N-terminal and a single CBD at the C-terminal end, with the domains connected by a flexible inter-domain sequence (linker) that ensures an autonomous function of both domains (Briers et al., 2008, 2009; Fischetti, 2010; Oliveira et al., 2013). In contrast, globular endolysins, which are encoded by Gram-negative infecting phages, differ in structure from modular ones, since they consist of a single EAD digesting the PG layer and lack a CBD (Briers et al., 2007).

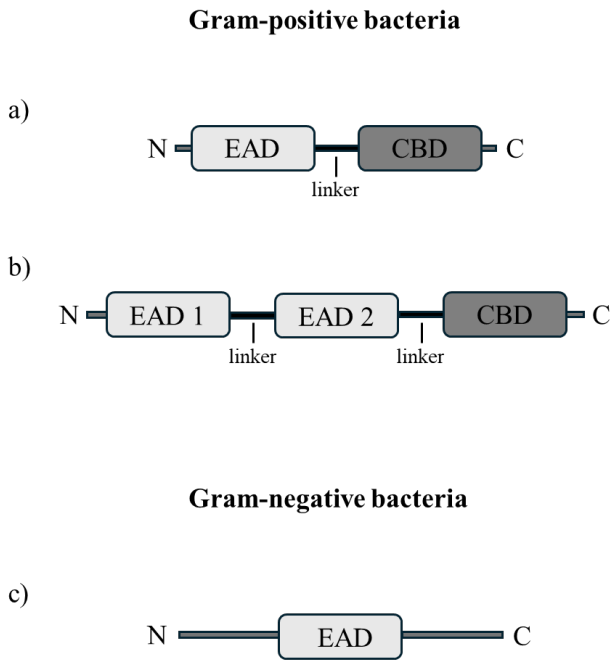

Fig. 3. Modular configuration models of most commonly found phage endolysins. (**a**) Modular endolysin with one N-terminal enzymatically active domain (EAD) and a C-terminal cell wall-binding domain (CBD). (**b**) Modular endolysin with two EADs and a C-terminal CBD. (**c**) Simple globular model of an EAD with no CBD.

3.1.3 Lytic activity of endolysins

Endolysins exhibit broad lytic activities against Gram-positive and Gram-negative bacterial cells. Catalytic domains of phage endolysins can be classified into different enzymatic activities that target glycosidic, amide or peptide bonds present in the PG structure.

Endolysins can be classified into five groups based on the specific bonds they cleave, and include: (I) muramidases, (II) glucosaminidases, (III) transglycosylase, (IV) amidase and (V) endopeptidases (Fig. 4).

(I) N-acetyl-β-D-muramidases (similar to lysozyme) cleave the β-1,4 bond between N-acetylmuramic acid (NAM) and N-acetylglucosamine (NAG) in the glycan strand, while (II) N-acetyl-β-D-glucosaminidases hydrolyze the other β-1,4 glycosidic bond between NAG and NAM. Both of these hydrolases require H_2O for bond cleavage. In contrast, (III) lytic transglycosylases also cleave the β-1,4 linkages between NAM and NAG but through an intramolecular reaction that forms of a 1,6-anhydromuramoyl product, without H_2O presence for reaction catalysis. (IV) N-acetylmuramoyl-L-alanine amidases cleave the amide bond between sugar NAM and the peptide (L-alanine), detaching the glycan polymer from the peptide, thus destabilizing the PG. Endopeptidases cleave peptide bonds within crosslinks.

They include (V) L-alanoyl-D-glutamate endopeptidases, (Va) interpeptide bridge-specific endopeptidases that directly cross-link the L-diaminopimelic (DAP) acid-to the D-alanine terminal of the opposite peptide chain, and (Vb) γ-D-glutaminyl-L-lysine endopeptidases, which target bonds within the peptide stem connecting PG strands in gram-positive bacteria (Loessner, 2005; Briers et al., 2007; Fischetti, 2010; Fenton et al., 2010). The most common, universal and broad spectrum endolysins comprise amidase or muramidase activities, since they target the most conserved PG bonds. In contrast, endopeptidases are more species-specific, hydrolyzing the most variable parts of the PG, such as interpeptide bridges and crosslinks (Schmelcher et al., 2012)

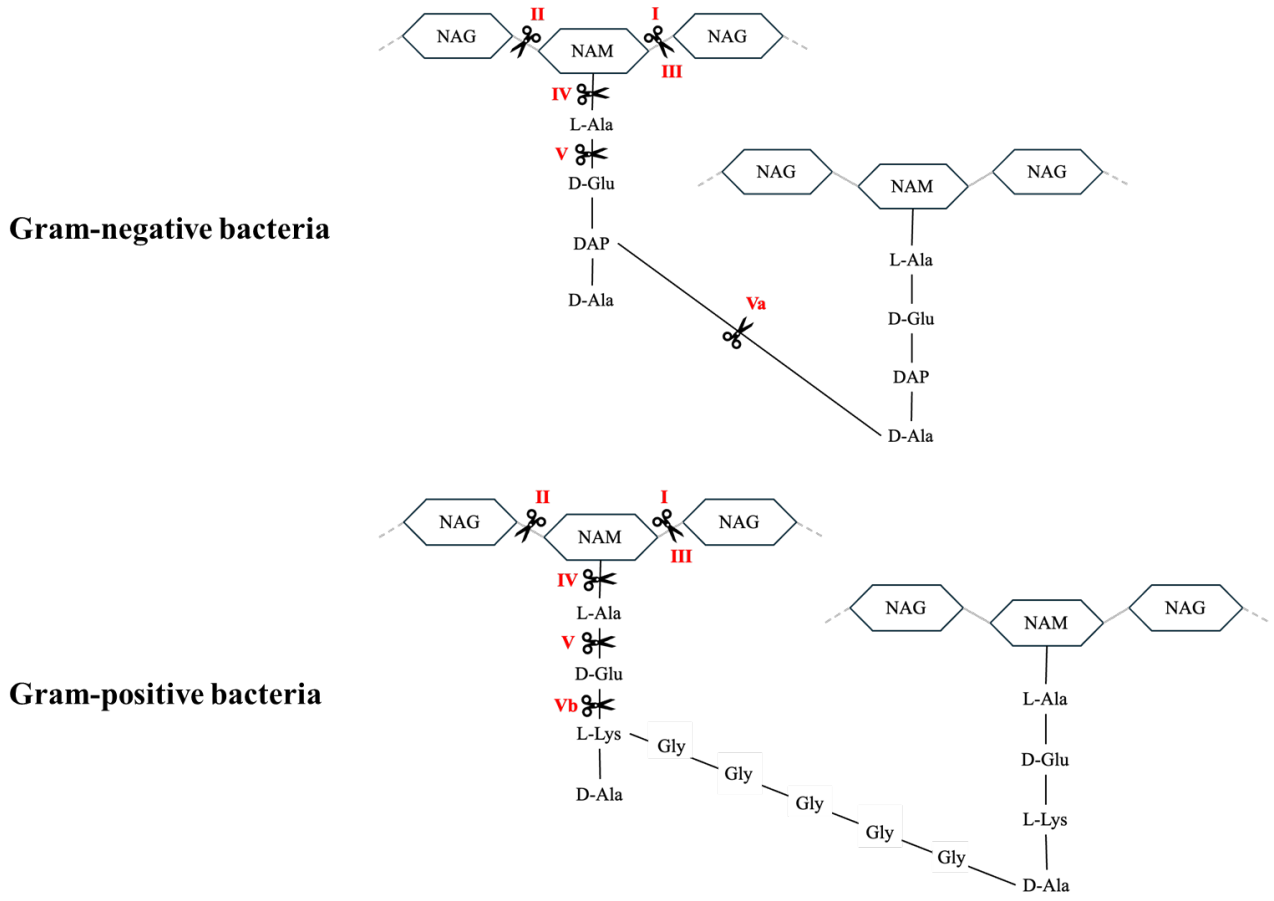

Fig. 4. Enzymatic activities of phage endolysins on PG structure. PG is a complex molecule consisting of alternating residues of β-(1,4) linked N-acetylglucosamine (NAG) and N-acetylmuramic acid (NAM) sugars. Attached to NAM there is an oligopeptide chain that can be cross-linked by peptide bonds to the peptide chain of another strand, forming a 3D structure that surrounds the bacterial cell. The bonds that can be cleaved by the EADs of endolysins are indicated. I) N-acetyl-β-D-muramidases; II) N-acetyl-β-D-glucosaminidases; III) Transglycosylases; IV) N-acetylmuramoyl-L-alanine amidases; V) L-alanoyl-D-glutamate endopeptidase; Va) interpeptide bridge-specific endopeptidase between DAP and D-Ala; Vb) interpeptide bridge-specific endopeptidase γ-D-glutaminyl-L-lysine endopeptidase. L-Ala: L-alanine; D-Glu: D-glutamate; DAP: acid-L-diaminopimelic; L-Lys: L-lysine; D-Ala: D-alanine; Gly: Glycine.

3.1.4 Possible strategies to overcome the outer membrane barrier

Gram-negative bacteria possess a protective outer membrane (OM) that distinguishes them from Gram-positive ones and hinders the access of both hydrophobic and hydrophilic molecules into the cell, including endolysins. Only the smallest molecules (< 600 Da) can pass through embedded porins (Exner et al., 2017). The OM is an asymmetric lipid bilayer, with phospholipids (PLs) in the inner part and a glycolipid known as lipopolysaccharide (LPS) in the outer layer (Funahara and Nikaido, 1980; Sun et al., 2022) linked by divalent cations (Mg^{2+} and Ca^{2+}). LPS can be subdivided in three regions: the O-polysaccharide part as outermost layer, the core polysaccharide as intermediate region and the lipid A as the most inner part (Raetz and Whitfield, 2002). The OM integrity can be mechanically or chemically disrupted, allowing the endolysins access to the PG layer. Mechanical means involving the use of high hydrostatic pressure that permeabilize the OM results in a bactericidal effect, and this approach has been applied in the preservation of not-pasteurized fresh food products (Nakimbugwe et al., 2006). When combined with endolysin activity, high hydrostatic pressure achieved up to a 4-log reduction in cell numbers. Endolysins reduce the necessary pressure, thereby lowering the associated equipment and energy costs needed for complete sterilization (Briers et al., 2008). On the other side, chemical means (*e.g.,* EDTA) involve the use of outer membrane permeabilizers (OMP) causing the disintegration of the LPS layer by chelating divalent cations (Ca^{2+} and Mg^{2+}) that bridge adjacent LPS molecules, with the consequent OM disruption (Vaara, 1992; Briers et al., 2011). OMP themselves may not be bactericidal, but they may potentiate the activity of other compounds, such as endolysins, thus acting synergistically (Vaara, 1999; Briers et al., 2011; Antonova et al., 2019). Weak organic acids, such as citric acid, exhibit chelating and permeabilizing effects, mainly in their protonated form. Moreover, citric acid can acidify the medium, potentially damaging the OM (Oliveira et al., 2014; Helander and Mattila-Sandholm, 2000).

3.1.5 Endolysin-based antimicrobials

Endolysins were recognized by the WHO as a novel and non-traditional antimicrobial approach (WHO, 2022) to treat various MDR-bacteria causing infections and diseases in clinical settings. The first documented use of purified endolysin was reported in 1959 (Freimer et al., 1959), while the first *in vivo* application was published in 2001, introducing the term “Enzybiotics” to describe endolysins as antimicrobial agents (Nelson et al., 2001). Clinical trials involving

endolysins have demonstrated promising results (Table 1), with no bacterial resistance observed (recently reviewed by Pattnaik et al., 2024). ContraFect, a biotech company of the Rockefeller University, obtained ownership rights to nine endolysins and has focused on developing endolysin therapies for bacterial infections. ContraFects conducted a phase III clinical trial (ClinicalTrials.gov Identifier #NCT04160468) on Exebacase (CF-301), a recombinant endolysin targeting various *Streptococcus* and *Staphylococcus* species, including methicillin-resistant *Staphylococcus aureus* (MRSA). In the phase II clinical trial, Exebacase, primarily developed for infective endocarditis, showed a 42.8 % improvement in recovery rates when combined with standard-of-care antibiotics (SOC) (Watson et al., 2019; Traczewski et al., 2021) . Notably, in February 2020, the Food and Drug Administration (FDA) recognized ContraFect CF-301 phase III study as a "Breakthrough Therapy", marking it as the first recombinant endolysin to enter human clinical trials in the United States.

Another advancement in the field is the endolysin N-Rephasin® SAL200, developed by Intron Biotechnology Inc. (ClinicalTrials.gov Identifier #NCT03089697). This endolysin, evaluated for intravenous administration, exhibited high safety and tolerance profiles during its phase IIa clinical trial. SAL200, specifically targeting MRSA, did not cause significant adverse effects in the endolysin pharmacokinetics study in humans, highlighting its potential as adjuvant to conventional antibiotics (Jun et al., 2017).

Additionally, GengaGen Inc. has advanced the field with clinical trials of the phage-derived endolysin P128, conducted up to phase I and phase II to assess safety and efficacy (ClinicalTrials.gov Identifier #NCT01746654). Administered intranasally, P128, an endolysin targeting both coagulase-negative and coagulase-positive *Staphylococci*, demonstrated effectiveness in both *in vitro* and *in vivo* studies.

The first commercially endolysin-containing product, Staphefekt SA.100. (ClinicalTrials.gov Identifier #NCT02840955) was developed by Micreos Human Health. Staphefekt SA.100 is a synthetic phage endolysin designed for topical skin application, to counteract persistent and recurring *S. aureus* related skin infections. Staphefekt is currently registered as a (class 1) medical device in Europe and is readily accessible over the counter as a cetomacrogol-based cream and gel (Tottè et al., 2017).

Table 1: Studies showing the *in vivo* efficacy of phage-derived and modified endolysins (Pattnaik et al., 2024).

Target pathogens and model used	Endolysin/derivatives	Route of administration	Outcomes	Clinical trials
Staphylococus aureus (MRSA) Mouse	P128 (chimeric lysin)	Intraperitoneal	The combination of P128 and oxacillin resulted in the inhibition of 4 MRSA strains and could kill biofilm-embedded bacteria.	Phase I/II completed (NCT01746654)
Staphylococcus epidermidis Mouse	LysGH15	Intraperitoneal	Bacteria in blood and organs were reduced by 4 and 3 logs, respectively after treatment when compared with untreated control mice.	-
Streptococcus pneumonia Mouse	ClyJ-3 (chimeric lysin with an improved linker)	Intraperitoneal	Superior to the parental enzyme ClyJ, demonstrating 20 % more efficacy, with the linker sequence also having a significant impact on the chimeric lysin's activity.	Pre-clinical
Streptococcus pneumonia Mouse	ClyJ (chimeric lysin)	Intraperitoneal	100 % and 20 % survival when treated 1 h and 3 h post-infection, respectively; No resistance to the chimeric lysine was observed even after doubling the concentration of ClyJ for 8 consecutive days.	Pre-clinical
Streptococcus pneumonia Zebrafish	Cpl-711 and PL3 (chimeric lysins)	Intraperitoneal	77.8 % survival was observed with the combination treatment; 50 % survival for PL3 alone; 44.4 % survival for Cpl-711 alone; compared to 27.8 % survival for the control group.	Pre-clinical
Streptococcus pneumonia Mouse and zebrafish	Cpl-711 (chimeric lysin)	subcutaneous	58 % of mice survived as compared to 53 % for the control group; 100 % survival was observed when the Cpl-711 was combined with cefotaxime (67 % for cefotaxime alone). In the case of zebrafish, 100 % survival was achieved compared to 23 % in the control group.	Pre-clinical
Streptococcus agalactiae Mouse	ClyV (chimeric lysin)	Intraperitoneal	100 % survival was observed in the mouse model as compared to the 29%survaival rate in the case of control models. No adverse effects were observed even after administration of higher dose of ClyV.	–
Streptococcus suis Mouse	Ply5218	Intraperitoneal	80–90 % survival rate after immediate treatment; 70–80 % survival rate with delayed triple treatment as compared to 10–20 % survival in the case of the control group after 7 days of infection. Bacterial burden was found to be less in the case of both triple and immediate treatment when compared to the group treated after 1 and 2 h post-infection.	–
Streptococcus suis Piglet	Ply5218	Intramuscular	Bacterial burden in the blood was significantly reduced than in the control untreated group; reduced body temperature, clinical scores, and pro-inflammatory cytokines were observed in the treated group.	–
Acinetobacter baumannii Mouse	LysSS	Intraperitoneal	40 % survival after treatment with 125 μg of LysSS; a high mortality rate was seen after treatment with 500 μg when compared with the control group.	–
	Ply6A3		70 % survival (0 % for the control); reduced white blood cell counts, IL-10, and procalcitonin levels were observed after treatment.	Pre-clinical (ALM01856)
Pseudomonas aeruginosa Mouse	PyS2-GN4 (pyocin-endolysin fusion protein)	Intraperitoneal	73 %, 80 %, 93 %, and 100 % survival rate was observed in infected mouse treated with 2.5, 5, 12.5, and 25 mg/kg lysocin respectively as compared to the control group with 37 % survival rate, organs of the surviving lysocin injected mice had no sign of bacterial infection.	–
Staphylococus aureus (MRSA and MSSA) Mouse and	SAL200 (N-Rephasin)	Intravenous and intraperitoneal	~1.2 log reduction of CFU/ml in blood and up to 1.8 log reduction in bacteremia when combined with antibiotics.	Phase IIa terminated (NCT03089697)

Target pathogens and model used	Endolysin/derivatives	Route of administration	Outcomes	Clinical trials
Galleria mellonella larvae			After 96 h post-infection, the combination also improved the *Galleria mellonella* larvae's survival rate.	
Staphylococcus aureus *Mouse*	ABD_M23 (chimeric lysin fused to albumin-binding domain)	Intravenous	~2 log reduction of *S. aureus* in blood post 48 h when administered with ABD-M23 (featuring extended serum half-life) as compared to ~1 log reduction of bacteremia in case of parental M23.	–
Bacillus anthracis Mouse	PlyB	Intravenous	Control murine models administered with only buffer after infection had a survival rate of 14 % that increased to 28 % and 100 % at 0.625 mg/kg and 5 mg/kg of PlyB respectively with no significant side effects. The synergistic effect of single doses of PlyB and PlyG increased the survival rate to 71 % (28 % survival rate in case of either PlyB or PlyG administered alone at 0.625 mg/kg).	PlyG is in pre-clinical stage (PFW40491)
Staphylococus aureus (MRSA) Rat and rabbit	CF-301 (Exebacase)	Intravenous	~6 log drop in bacterial densities was observed in the case of both rat and rabbit at 10 mg/kg (~2600 μg/animal) & 0.09–0.18 mg/kg (~210–420 μg/animal) of CF-301 respectively when compared to 3 log reduction in control having administered with only daptomycin.	Phase III completed (NCT04160468)
Staphylococus aureus (MRSA) Rabbit	CF-301 (Exebacase)	Intravenous	3 log reduction of MRSA vegetation in the control group that increased to >8 log reduction when daptomycin was combined with the exebacase.	Phase III completed (NCT04160468)
Staphylococus aureus (MRSA and MSSA) Mouse	SAL200 (N-Rephasin)	Intranasal	~10-fold reduction of bacterial density in the lungs of the mouse when treated with SAL200 when compared to the control group (90–95 % survival rate in the treated group compared to 10–40 % in the control group), recovery from pneumonia was observed in histopathological studies after treatment.	Phase IIa terminated (NCT03089697)
Bacillus anthracis, Mouse	LysB4	Intranasal	100 % survival was observed in a high dose LysB4-treated group with 100μg/head at 6, 24, and 48h post-infection whereas a low dose of 10μg/head extended the onset of death improving the survival rate. Reduced bacterial numbers in lungs (<1 log) and other organs (2–3 log) compared to control.	–
Acinetobacter baumannii, Galleria mellonella and mouse	ElyA1	Intranasal	When treated with combination of colistin (1/4 MIC) and 25 g/ml ElyA, infected wax moth larvae demonstrated a higher survival rate than those treated with colistin alone. <1 log reduction of *A. baumannii* when treated with ElyA1 and colistin on the skin of infected mouse compared to <0.5 log reduction when treated with colistin alone.	–
Pseudomonas aeruginosa Mouse	PlyPa91	2 intranasal or 1 each intranasal and intratracheal	70 % survival after intranasal plus intratracheal treatment whereas 20 % after 2 intranasal treatments (having the same amount of lysin) indicating that the mice's survival rate was significantly influenced by the delivery method.	–
Streptococcus pneumonia Mouse	Cpl-711 (chimeric lysin)	Intranasal	~2 log reduction of nasopharyngeal carriage, independent of strain and treatment regime; superior to parental endolysin Cpl-1	Pre-clinical
Clostridioides difficile Mouse	LHD (phage lysin–human defensin fusion protein)	Oral (gavage)	100 % survival rate observed in *C. difficile* infected mice as that of 60 % survival for the control, reduced percentage of diarrhea, and significantly reduced concentration of *C. difficile* spores and toxins in the feces of infected mice.	–

Target pathogens and model used	Endolysin/derivatives	Route of administration	Outcomes	Clinical trials
Staphylococus aureus (MRSA) Rat	CF-301 (Exebacase)	Intravenous	0.48 log reduction of MRSA in the bone compared to control (1.56 log reduction when combined with daptomycin) The treated group of rats (with daptomycin, exebase, and a combination of both) had a mean bacterial density of 4.09 (±0.37), 4.65 (±0.65), and 3.57 (±0.48) $\log_{10}$ CFU/g of bone as compared to control group having a bacterial density of 5.13 (±0.34) $\log_{10}$ CFU/g of bone.	Phase III completed (NCT04160468)
Klebsiella pneumonia Rat	LysECD	Intraperitoneal	>1 log reduction of viable bacteria in biofilms within the implant; significantly reduced biofilm mass observed in LysECD treated rats.	–
Staphylococcus aureus Mouse	SEP_TAT and LST_TAT (lysins fused to cell-penetrating peptides, CPPs)	Subcutaneous (peripheral)	>2.2 log reduction of bacteria within abscesses treated with lysin-CPP cocktail when compared to control ones with 1 log reduction, significant reduction of intracellular bacteria in the pus	–
Staphylococus aureus Mouse	S25-3LYS-his	Topical	A significant decrease (1–2 logs) in intraepidermal *Staphylococci* numbers and the size of pustules in impetigo mice with increased skin microbiota diversity.	–
Staphylococus aureus (MRSA) Mouse	LysGH15	Topical (ointment)	The mean bacterial count of *S. aureus* on the skin of infected mice was ~10^2 CFU/mg after 18 h of treatment which became undetectable after 96 h (10^5 CFU/ml bacterial count in control groups); accelerated wound healing in the mouse model by reducing the levels of pro-inflammatory cytokines.	Pre-clinical (ADG26756)
Staphylococcus aureus Mouse	TSPphg	Topical	~3 log reduction of *S. aureus* on the skin of infected mice with accelerated wound closure.	–
Pseudomonas aeruginosa Mouse	PlyPa03, PlyPa91	Topical	*P. aeruginosa* was reduced by > 2 logs (PlyPa03) and 1 log (PlyPa91) on infected mouse skin when compared to control, and 20 % and 70 % of mice treated with PlyPa91 in two intranasal instillations and mice treated with one intranasal and one intratracheal instillation, respectively, survived lung infection. These results suggest that the route of delivery is important for increased efficacy.	–
Mycobacterium ulcerans Mouse	LysB	Subcutaneous	~1 log reduction of bacteria in footpads compared to the control group along with the production of IFN-γ and TNF in the draining lymph node.	–
Staphylococus aureus, S. epidermidis Zebrafish and mouse	LysRODI	Intramammary (preventive treatment)	In protein-treated groups, zebrafish embryos had a survival rate of >92 % survival in presence of LysRODI and CHAPSH3b, indicating a non-toxic effect. 3-4 log units' reduction in bacterial burden when compared with the control group, improved mammary gland health.	–
Streptococcus mutans and S. sobrinus Rat	ClyR (chimeric lysin)	Oral	Continuous administration of ClyR showed a significant reduction in the severity of caries (56 %) in rat models.	–
Fusobacterium necrophorum Rabbit	LysAm24, LysAp22, and LysECD7 (gel)	Topical	The lifetime of the infected rabbits was enhanced by approximately two times compared to the placebo-treated rabbits after the topical gel was administered twice daily for five days. Less acute infection and a delay in the course of infection were also noted in the gel-treated rabbit model.	–
Staphylococcus aureus (MRSA) Mouse	LysP108	–	*In vivo* tests showed that compared to monotherapy, the subcutaneous abscess that was produced in the mice was greatly diminished when treated with LysP108 plus vancomycin. This was further supported by H&E (hematoxylin and eosin) staining, which	Preclinical (YP_009099525)

Target pathogens and model used	Endolysin/derivatives	Route of administration	Outcomes	Clinical trials
			demonstrated that combined therapy did not result in the persistence of the abscess and inflammatory response as compared to the control groups.	
Streptococcus pneumonia *Mouse*	Cpl-1 loaded chitosan nanoparticles	–	Histopathological and inflammatory analysis showed that treatment with Cpl-1 loaded chitosan nanoparticles resulted in the lowest bacterial load in the lungs of infected animals when compared to the control group treated with Cpl-1 and chitosan nanoparticles alone, and that treatment groups had lower concentrations of pro-inflammatory and anti-inflammatory cytokines than other groups at 48 and 72 h.	–
Streptococcus suis and *Streptococcus agalactiae* Mouse	Ply0643	–	80 % survival rate from lethal bacteremia was observed in *Streptococcus suis* infected mice when treated with Ply0643 (total 0.8 mg/ mouse) and *Streptococcus agalactiae* infected mice showed a significant reduction in bacterial infection in mammary glands.	–
Klebsiella pneumoniae Mouse	LysCA and LysG24	Intranasal	The infected mice treated with LysCA at the onset of symptoms showed full recovery after 48 h with no signs of abnormality in the lung tissue, but their mental condition and mobility were affected as compared to untreated ones. The mice treated with LysG24 showed partial recovery of mental status and mobility after 48 h which was not good as that of mice treated with LysCA, slight congestion and edema were also observed in the lungs of this group of mice.	–
Staphylococcus aureus (MRSA) Mouse	XZ.700 (Chimeric endolysin)	Topical cream and gel	*In vivo* bioluminescence experiment showed that male mice were 2 times more efficient in eliminating the bacterial load than the female when treated with XZ.700. *In vivo* bioluminescence analysis also revealed that both cream and gel were capable of reducing a significant amount of bacterial numbers in the skin-infected mice as compared to untreated control.	Pre-clinical

- Means no information available on clinical trials.

Despite significant progress in treating Gram-positive bacteria, addressing Gram-negative bacteria remains challenging due to the presence of the OM. Indeed, exogenous addition of recombinant endolysins molecules is successfully being used to quickly kill Gram-positive pathogens due to turgor pressure, but these molecules are too large to pass the OM of Gram-negative bacteria. To this aim, a novel class of engineered enzyme-based antibacterials, coined as Artilysins, with great potential as antibiotic alternatives/adjuvant, was recently developed (Czaplewski et al., 2016). Artilysins are known to be active against drug-resistant Gram-negative and Gram-positive bacteria (Gerstmans et al., 2016), since they can pass through the OM and reach the PG layer, where they exert their action. Artilysins are generated by fusing an OMP peptide with the EAD of an endolysin. This approach leverages the physicochemical

properties of OMP peptides to locally disrupt the OM, enabling lysin entry and subsequent osmotic lysis through PG degradation (Briers et al. 2014a; Briers et al. 2014b, Briers and Lavigne, 2015). Artilysins are currently commercialized by Lysando AG, as a new antimicrobial platform technology under the registered mark Artilysin®. These engineered lysins act rapidly upon contact, are highly bactericidal, active against persisters, show no cross-resistance with existing resistance mechanisms (including colistin) and do not elicit resistance development upon serial exposure to subinhibitory doses (Briers et al., 2014; Briers et al., 2014b). An example of Artilysin is Art-175, a broad-spectrum Artilysin composed of a *P. aeruginosa* lysin (KZ144) encoded by the bacteriophage ΦKZ, which was fused at its N-terminal with a potent antimicrobial peptide, (*i.e.,* the sheep myeloid 29 aa peptide SMAP-29) (Skerlavaj et al., 1999; Briers et al., 2014; Defraine et al., 2016). The SMAP-29 peptide leads to the destabilization of the OM, allowing the enzymatic domain of KZ144 to gain access to and degrade the underlying PG (Fig. 5).

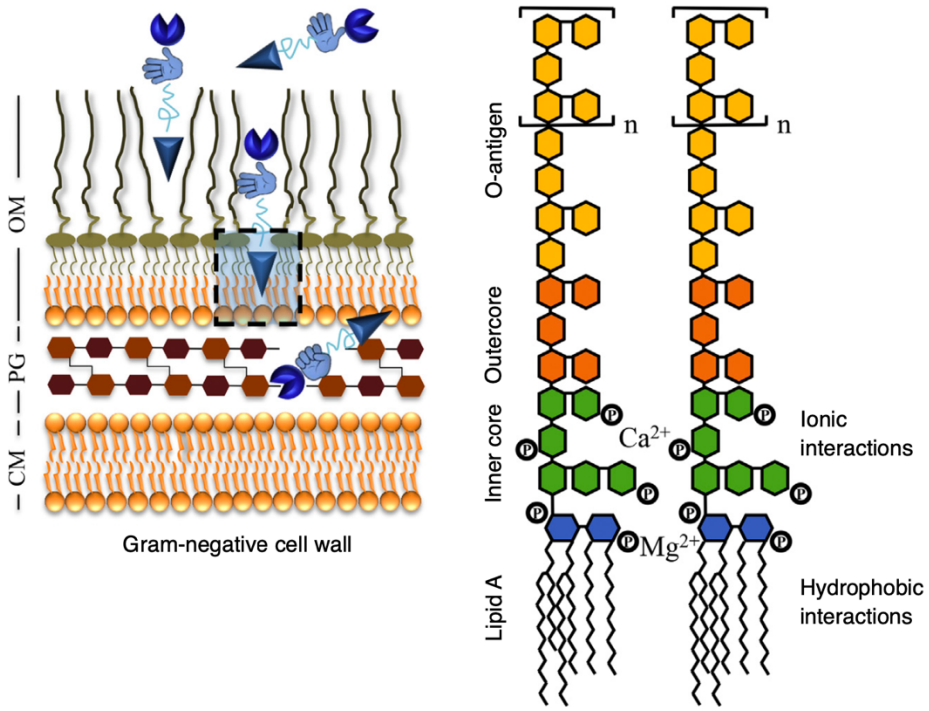

Fig. 5. Artilysin mechanism of action. Artilysins are engineered lysins fused with OMP peptides that possess cationic, hydrophobic, or amphipathic properties. These peptides disrupt the stabilizing forces within the LPS layer, primarily targeting ionic interactions between divalent cations (Ca^{2+}, Mg^{2+}) and phosphate groups present on sugars of the lipid A or inner core. They also interfere with hydrophobic and van der Waals forces between the fatty acids of the lipid A. The OMP peptide destabilizes the OM, allowing the enzymatic domain of Artilysin to reach and degrade the underlying PG. CM: cytoplasmic membrane; PG: peptidoglycan; OM: outer membrane (Gutiérrez and Briers, 2020).

3.2 Materials and Methods

3.2.1 Bacterial strains and culture conditions

Pseudomonas aeruginosa ATCC 15692 (PAO1) and *Acinetobacter baumannii* 19606 (Janssen et al., 1997) used in this study were present in the strain collection of the University of Urbino Carlo Bo (Urbino, Italy). *Desulfovibrio vulgaris* Hildenborough ATCC 29579 (DSM 644) was obtained from the Leibniz Institute DSMZ (Braunschweig, Germany). *Escherichia coli* BL21(DE3)pLysS and *E. coli* Arctic Express were provided by R. Lavigne from the University of Leuven, Belgium. All strains were grown in Luria Bertani (LB) broth, except *D. vulgaris*, which was grown in Desulfovibrio (Postgate) medium, prepared according to the DSMZ guidelines (Medium N. 63), with minor modifications. Indeed, $FeSO_4$ x $7H_2O$ concentration was lowered from 0.5 g/L to 0.02 g/L, to limit FeS precipitates formed during *D. vulgaris* growth. The Postgate medium, after sterilization by autoclaving, was placed into the Whitley A35 anaerobic workstation (Don Withley Scientific Ltd., Shipley UK) the day before its use, to obtain an anaerobic medium. All strains were grown with shaking at 37°C, except for *D. vulgaris* which was grown on static condition. All media were solidified by supplementing 15 g/L agar, prior autoclaving. For protein expression in *E. coli* strains, ampicillin (Ap) and gentamicin (Gm) were used at 100 µg/ml and 20 µg/ml, respectively.

3.2.2 Endolysins expression and purification

All nucleotide sequences used were optimized for *E. coli* codon usage and are listed in Appendix I. *D. vulgaris* endolysin sequences were retrieved from Fernandez-Ruiz et al. (2018), by Vazquez Fernandez R., Briers Y. and Lavigne R. (unpublished results).

Recombinant endolysins were expressed in both *E. coli* BL21(DE3)pLysS and Arctic Express (Stratagene, USA), from at least 500 ml of bacterial culture. Briefly, a preculture of each expressing *E. coli* strain (10 ml LB in 50 ml flask inoculated from fresh plate) was grown overnight at 37 °C. The cells were diluted into fresh medium at OD_{600} = 0.1 and grown at 37 °C to OD_{600} = 0.6. Next, protein expression was induced with 1 mM isopropyl-β-d-thiogalactopyranoside (IPTG) at 37 °C for 3h for *E. coli* BL21(DE3)pLysS and at 16 °C for 18 h for *E. coli* Arctic Express cells. Recombinant Art-175 was purified as previously described (Briers et al., 2014a). Concerning *D. vulgaris* endolysins (Appendix I), all *E. coli* induced

bacterial cultures were harvested by centrifugation (4,000 x *g* for 45 min at 4 °C), and the obtained cell pellet was resuspended in 20 ml of lysis buffer (20 mM NaH_2PO_4 x $2H_2O$, 500 mM NaCl, 20 mM imidazole [pH 7.4] supplemented with 25 µg/ml DNaseI). Cell disruption was performed by sonication (Bandelin Sonopuls HD3200) under the following conditions: 40% maximum amplitude for 4 min with 1s/1s pulse for 30'' break steps, on ice. Cell debris were separated by centrifugation at 26,000 × *g* for 10 min at 4 °C, and the supernatant was then filtered (Filtropur S 0.2, PES-membrane, 0.2 µm pore size; Sarstedt AG & Co., Germany) before applying it to a Poly-Prep® Chromatography Column (Bio-Rad; Hercules, California, USA) filled with Ni-NTA His Bind® beads (Merck). Bound proteins were washed using buffer A (20 mM NaH_2PO_4 x $2H_2O$, 500 mM NaCl, 20 mM and 50 mM imidazole [pH 7.4]) and eluted with a linear gradient to 100 % buffer B (20 mM NaH_2PO_4 x $2H_2O$, 500 mM NaCl, 500 mM imidazole [pH 7.4]). The endolysin containing fractions were pooled and dialyzed against buffer C (20 mM NaH_2PO_4 x $2H_2O$, 500 mM NaCl [pH 7.4]). After dialysis, the protein concentration was determined spectrophotometrically in silica cuvettes at 280 nm (Jasco V-650; Jasco Corporation, Tokyo, Japan), as well as by the Bradford assay (Bradford, 1976).
Protein expression and localization were determined by running cell fractions in 15 % (w/v) SDS-PAGE with Coomassie blue staining (Brunelle and Green, 2014). Immunoblot analysis was performed with monoclonal Anti-6xHis antibody (1:3000) (Sigma-Aldrich, Cat.# H1029), using Anti-Mouse IgG, HRP conjugate secondary antibody (1:2500) (Promega, Cat.#4021).

3.2.3 *In vitro* antibacterial assay

P. aeruginosa, A. baumannii and *D. vulgaris* strains were grown to the mid-exponential phase (OD_{600}, 0.6), harvested by centrifugation (16,000 x *g* for 5 min), washed, and 10-fold diluted in 20 mM HEPES (pH 7.4) to a final concentration of 10^8 cells/ml. For *P. aeruginosa* and *A. baumannii* 50 µl of the bacterial cell dilutions were incubated at 25 °C, with shaking, with 50 µl of a protein solution containing 10 µg, 20 µg and 30 µg of Art-175 in 20 mM HEPES buffer (pH 7.4). After a 60-min incubation, appropriate dilutions of the cell suspensions were plated on LB agar in triplicate. Colonies were counted after overnight incubation at 37 °C. For *D. vulgaris*, 500 µl of bacterial cell dilution was incubated at 25 °C, with shaking, with 500 µl of a protein solution containing 200 µg Art-175 in 20 mM HEPES buffer (pH 7.4). After a 120-

min incubation, appropriate dilutions of the cell suspensions were plated on Postgate agar. Colonies were counted after 72 h incubation at 37 °C in anaerobic conditions.

For *D. vulgaris* specific endolysins, the procedure detailed by Briers et al. (2007) was employed with minor modifications. Briefly, bacterial cells were pre-treated with chloroform (0.5 % *v/v*) for 15 min (in static conditions) to permeabilize the outer membrane, then cells were harvest by centrifugation (8,000 x *g*, 20 min) and washed with ddH_2O twice. Bacterial pellets were resuspended in 50 mM Tris-HCl buffer containing 0.1 % Triton X-100 (pH 8.2) and adjusted to an OD_{600} = 0.8. A total of 50 µl of a protein solution containing 10, 20, 30, 40 or 50 µg of *D. vulgaris* specific endolysins were added to 150 µl of bacterial suspension (OD_{600} = 0.8). The same volume of Tris-HCl buffer containing 0.1 % Triton X-100 without any endolysin was used as negative control. After 60-min of incubation at 37 °C in anaerobic and static conditions, appropriate dilutions of the cell suspensions were plated on Postgate agar in triplicate. The antibacterial activity was quantified as Log reduction, by calculating the ratio $Log_{10}[N_0/N_i]$ (with N_0 as the initial number of untreated cells and N_i as the number of residual cells counted after treatment).

3.3 Results and Discussion

3.3.1 Art-175 antibacterial activity against *Pseudomonas aeruginosa*¸ *Acinetobacter baumannii* and *Desulfovibrio vulgaris*

Art-175 is a recombinant endolysin in which a *P. aeruginosa* bacteriophage ΦKZ endolysin (KZ144), is fused at the N-terminus with the sheep myeloid 29-amino acid (SMAP-29, Skerlavaj et al., 1999) peptide, that targets and transports the endolysin across the outer membrane of Gram-negative bacteria (Briers et al., 2014a). KZ144 is a modular endolysin with a N-terminal PG binding domain and a C-terminal catalytic domain with transglycosylase activity (Briers et al., 2014a). The nucleotide sequence of Art-175 (Appendix I) was synthetized into the expression vector pET-21a+ (Bio-Fab Research s.r.l., Rome - Italy), expressed and purified by metal affinity chromatography as previously described by Briers et al. (2014a) (Fig. 6).

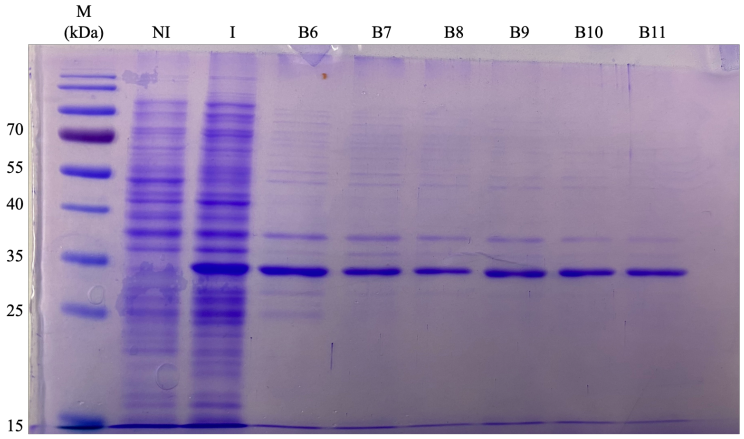

Fig. 6. SDS-PAGE analysis and purification of Art-175. M, molecular size marker; uninduced (NI) *E. coli* BL21(DE3)pLysS/pET21a-Art-175 whole cells; induced (I) *E. coli* BL21(DE3)pLysS/pET21a-Art-175 whole cells; Art-175 fractions obtained after AKTA purification (from B6 to B11).

The B6 fraction (Fig. 6), containing the highest amount of Art-175 (molecular weight 33.4 kDa), was tested at 10, 20 and 30 µg against *P. aeruginosa* (Fig. 7A**)** and *A. baumannii* (Fig. 7B) (Briers et al., 2014a; Defraine et al., 2016). After 60-min of incubation Art-175 confirmed its well-known bactericidal activity already at 10 µg (Briers et al., 2014a) displaying complete killing (> 5 log reduction compared to the untreated control) against *P. aeruginosa* (Fig. 7A). Moreover, since Art-175 was also shown to be active against other Gram-negative bacteria, its antibacterial activity was also tested against *A. baumannii* (Fig. 7B). Art-175 displayed an

almost complete killing at all concentrations tested (*ca.* 3 log reduction compared to the untreated control) for *A. baumannii* (Fig. 7B), thus confirming literature data (Defraine et al., 2016).

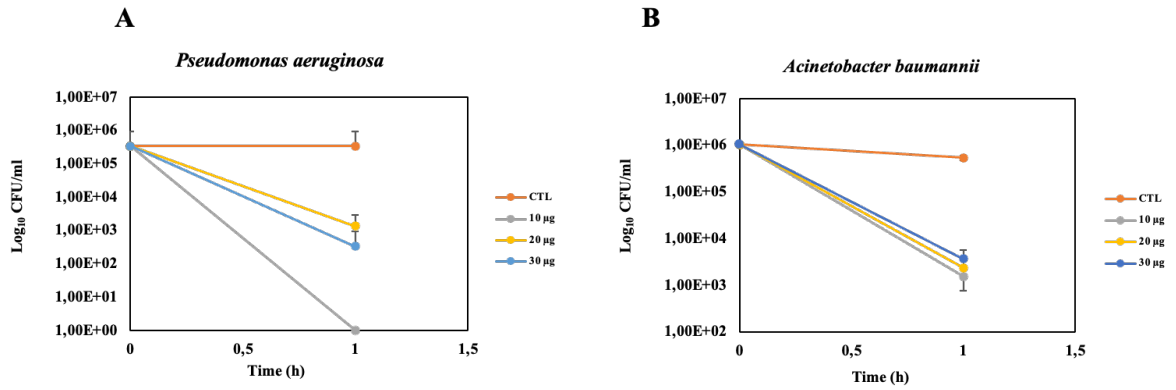

Fig. 7. Time-kill assay of *P. aeruginosa* **(A)** and *A. baumannii* **(B)** strains, resuspended in 20 mM HEPES (pH 7.4) and exposed to 10, 20 or 30 µg of purified Art-175. Untreated cells were exposed to HEPES buffer without Art-175 (orange lines, CTL). Cells treated with 10, 20, 30 ug of Art-175 are indicated in grey, yellow and blues lines, respectively. Bacteria were enumerated by vital count (Log_{10} CFU/ml) and Art-175 antibacterial activity was assessed after 60 min of exposure. Each value represents the mean ± standard deviation of three replicates.

Despite being a recombinant endolysin based on the *P. aeruginosa* phage ΦKZ, Art-175 has shown a broad activity within Gram-negative bacteria, therefore its potential to control the growth of bacteria involved in microbiologically influenced corrosion has been investigated. To this aim, different concentrations of Art-175 (ranging from 200 µg/ml to 6.25 µg/ml) were tested against *D. vulgaris*, an anerobic Gram-negative model microorganism used for the study of sulfate reducing bacteria (SRB) energy metabolism. The buffer in which Art-175 is resuspended (20 mM HEPES), was also tested against *D. vulgaris* as control (Fig. 8A). The MIC value of Art-175 determined against *D. vulgaris* was 200 µg/ml (Fig. 8A). Time-kill experiments of *D. vulgaris* planktonic cultures treated with 200 µg/ml Art-175 or 20 mM HEPES buffer were performed (Fig. 8B). Unlike the previously observed results about the bactericidal activity of Art-175 against *P. aeruginosa* and *A. baumannii*, Art-175 did not kill *D. vulgaris* planktonic cells, in spite of the low tonicity of the 20 mM HEPES buffer, blowing up the cells, and making them more sensitive to the action of phage lysins. Indeed, no log reduction, in term of viable cells, was observed compared to the untreated control, after 2 h of incubation (Fig. 8B). The enzymatic activity of Art-175 was also determined by using a turbidimetry reduction assay (Fig. 8C). The OD_{600} of a *D. vulgaris* culture was measured both

at the beginning (T_0) and at the end (T_2) of the antibacterial assay. Surprisingly, a raise in turbidimetry was observed in *D. vulgaris* cells treated with 200 µg/ml Art-175 compared to the untreated and HEPES controls (Fig. 8C). Indeed, treated *D. vulgaris* cultures resulted to be darker than the control ones (Fig. 8D). These results suggest that Art-175 may weaken the outer membrane without killing the bacterium, thus causing the release of iron complexes formed during cellular respiration, that are likely to accumulate in the periplasmic space (Park et al., 2008).

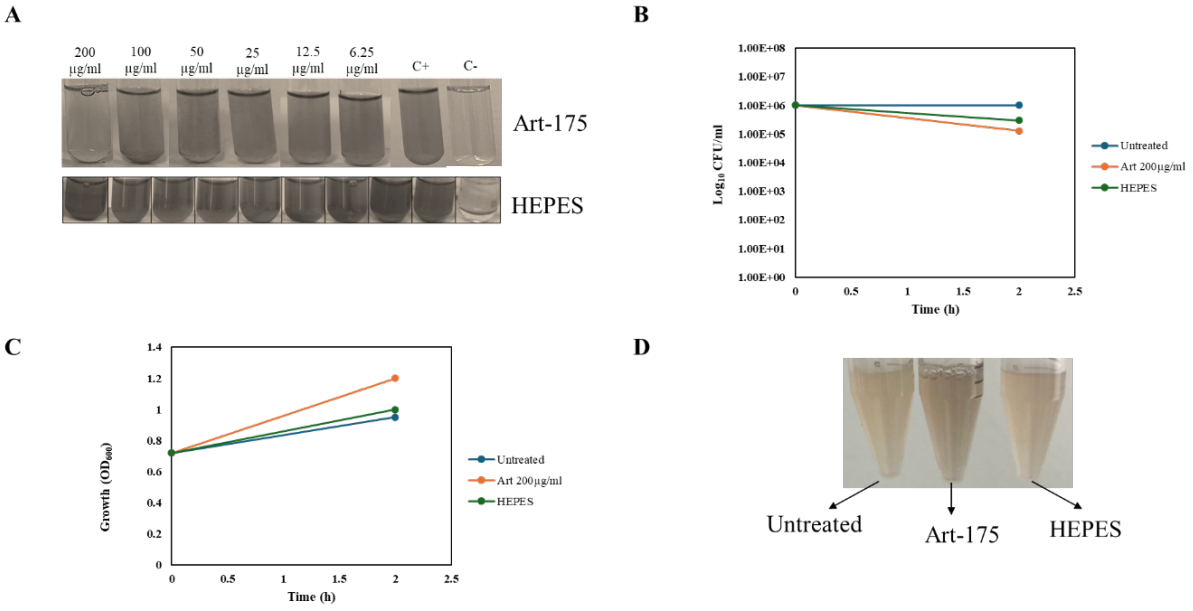

Fig. 8. (A) Minimum Inhibitory Concentration (MIC) determination of Art-175 (ranging from 200 µg/ml to 6.25 µg/ml) against *D. vulgaris* planktonic cultures. Positive (C+) and negative (C-) control represent unamended Postgate medium with or without *D. vulgaris*, respectively. The buffer in which Art-175 is resuspended (20 mM HEPES), was also included. **(B)** Time-kill experiments of *D. vulgaris* treated with 200 µg/ml Art-175 (orange line), and HEPES buffer (green line) at pH 7.4. Bacteria were enumerated by vital count (Log_{10} CFU/ml). The untreated control (blue line) was also included. **(C)** The enzymatic activity of Art-175 was determined by using a turbidity reduction assay with 200 µg/ml Art-175 and HEPES as control. **(D)** Representative image showing the blackening of *D. vulgaris* cultures treated with 200 µg/ml Art-175.

3.3.2 *In vitro* antibacterial activity of *D. vulgaris* endolysins

Although Art-175 exhibited broad-spectrum activity against several Gram-negative bacteria, it has proven ineffective against *D. vulgaris* planktonic cells. Consequently, the potential use of endolysins encoded by bacteriophages targeting *D. vulgaris* may represent a promising direction for overcoming this limitation. To this aim, all *D. vulgaris* endolysin sequences (Appendix I) were retrieved from a database of uncultured viral genomes containing 2,628

putative endolysins (Fernández-Ruiz et al., 2018) and obtained in collaboration with Dr. Roberto Vazquez Fernandez, Prof. Yves Briers (University of Gent, Belgium) and Prof. Rob Lavigne (University of Leuven, Belgium), supported by a FEMS research and training grant. For each *D. vulgaris* specific endolysin the nucleotide sequence (Appendix I) was codon-optimized for the *E. coli* to enhance soluble expression efficiency. Furthermore, since these 9 selected endolysins have not been previously characterized, an *in silico* analysis was conducted to predict their functional domains and structures, by using InterProScan (Mulder and Apweiler, 2007), and Alphafold predictions with ChimeraX_Daily: alphafold21_predict_colab.ipynb (Mirdita et al., 2022), respectively (Appendix I). All nine *D. vulgaris* endolysins were expressed in *E. coli* BL21(DE3)pLysS and only proteins present in the soluble fractions were subjected to purification by metal affinity chromatography. The remaining *D. vulgaris* endolysins were also expressed in *E. coli* Arctic Express to overcome protein insolubility, however only endolysin RVLD1983 was successfully expressed in the soluble fractions and purified.

The nine endolysins specific for *D. vulgaris* are listed in Fig. 9 and have different PG targets. Two of them (*i.e.,* RVLD 1528 and RVLD 1699) are predicted amidases (A), thus able to cleave the amide bond between the sugar-derivative (glycan, MurNAc) and the peptide moiety (L-alanine). RVLD 1601 is a predicted peptidase (P), targeting peptide bonds within PG crosslinks. RVLD 1985, RVLD 2367, RVLD 1984 full length (FL), RVLD 1984 without N-terminal helix (WONH), RVLD 1983 FL and RVLD 1984 WONH are all predicted soluble lytic transglycosylases (SLT), cleaving the β-1,4 bonds between MurNAc and GlcNac present in the PG structure by forming of a new 1,6-anhydro bond.

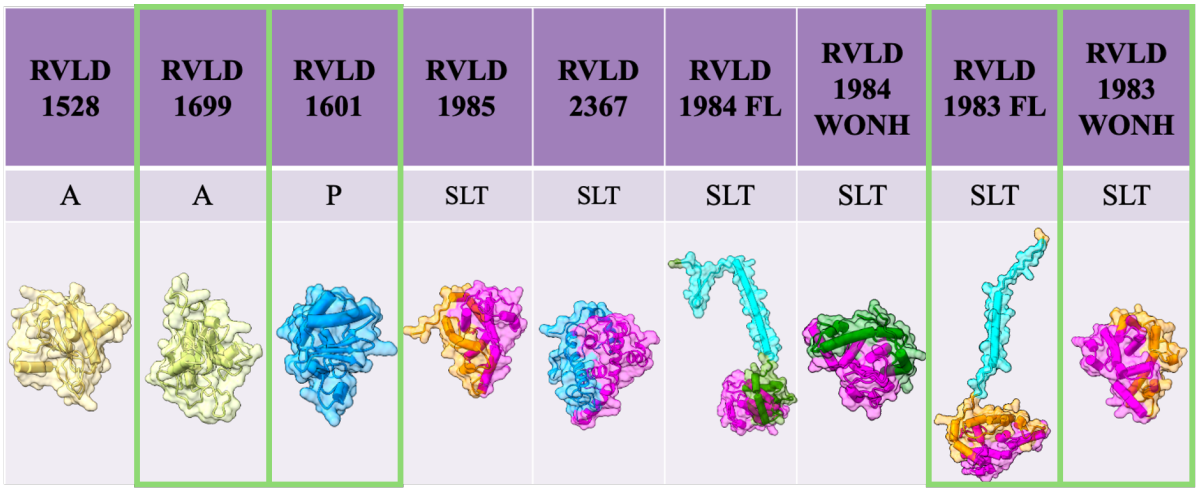

Fig. 9. Scheme depicting all *D. vulgaris* endolysins identified in this study. Proteins highlighted in green were successfully purified and tested against *D. vulgaris* planktonic cultures. A= Amidase; P= Peptidase; SLT: Soluble Lytic Transglycosylase.

Of all these endolysins (Fig. 9), RVLD 1699, RVLD 1601, RVLD 1983 FL and RVLD 1983 WONH were successfully expressed, purified and tested *in vitro* against *D. vulgaris* planktonic cultures (Fig. 10).

The preliminary results have been achieved during a 3 months secondment in the Laboratory of Gene Technology in Leuven (Belgium) under the supervision of Prof. Rob Lavigne.

Initially, the activities of purified proteins were tested against *D. vulgaris* planktonic cells with the same procedure used in the antibacterial assay with Art-175 (Fig. 8). No log reduction, in terms of viable cells, was observed in *D. vulgaris* cells treated with specific endolysins compared the untreated ones (data not shown). The lack of activity is most likely due to the inability of endolysins to cross the outer membrane of *D. vulgaris*. Therefore, to favor endolysins entrance in *D. vulgaris* cells, a pre-treatment with chloroform (0.5%. *v/v*) was employed to destabilize the outer membrane and allow the access of selected endolysins to their target (*i.e.*, the PG), as previously described (Briers et al., 2007), with minor modifications as detailed in the Materials and Methods section. Starting from the same stock containing *D. vulgaris* cells treated with chloroform, an aliquot was used as negative control exposing it to Tris-HCl buffer containing 0.1% Triton X-100 without endolysins, while the other one was treated with different concentrations of purified endolysins suspended in the same buffer, ranging from 10 to 50 µg of protein (Fig. 10).

The antibacterial activity of RVLD 1699 was evaluated by testing protein concentrations of 10, 20, 30, 40 and 50 µg against *D. vulgaris*, resulting in a > 2 log reduction compared to the negative control (CTL). Specifically, a > 2 log reduction was achieved with 10 and 20 µg, while concentrations of 30, 40 and 50 µg led to a > 3 log reduction (Fig. 10).

For RVLD1601, the antibacterial assay also demonstrated a ≥ 2 log reduction with all concentrations tested (*i.e.,* 10, 20, 30, 40 and 50 µg) when compared to the untreated cells (Fig. 10).

In the case of RVLD 1983 FL, only 10 µg of the protein were tested, due to the limited availability of the purified protein. Nevertheless, even at this low concentration, a log reduction > 3 was observed compared to the negative control (Fig. 10).

Finally, the antibacterial activity of RVLD 1983 WONH also resulted in a consistent log reduction (> 3 log) across all tested concentrations, when compared to the negative control (Fig. 10), in line with what observed for the full length endolysin (RVLD 1983 FL). These results suggest that the predicted transmembrane N-terminal helix is dispensable for the enzymatic

activity but may play a role in the bacterial cell lysis from within. Indeed, expression of the full-length protein (*i.e.,* RVLD 1983 FL) led to a smaller amount of purified protein compared to the yield of RVLD 1983 WONH, suggesting a mild toxicity in *E. coli* expressing cells. Notably, given the impurities of the purified RVLD 1983 FL (Fig. 10) the amount tested (*i.e.,* 10 µg) is a rough estimate of the amount of endolysin present in the assay.

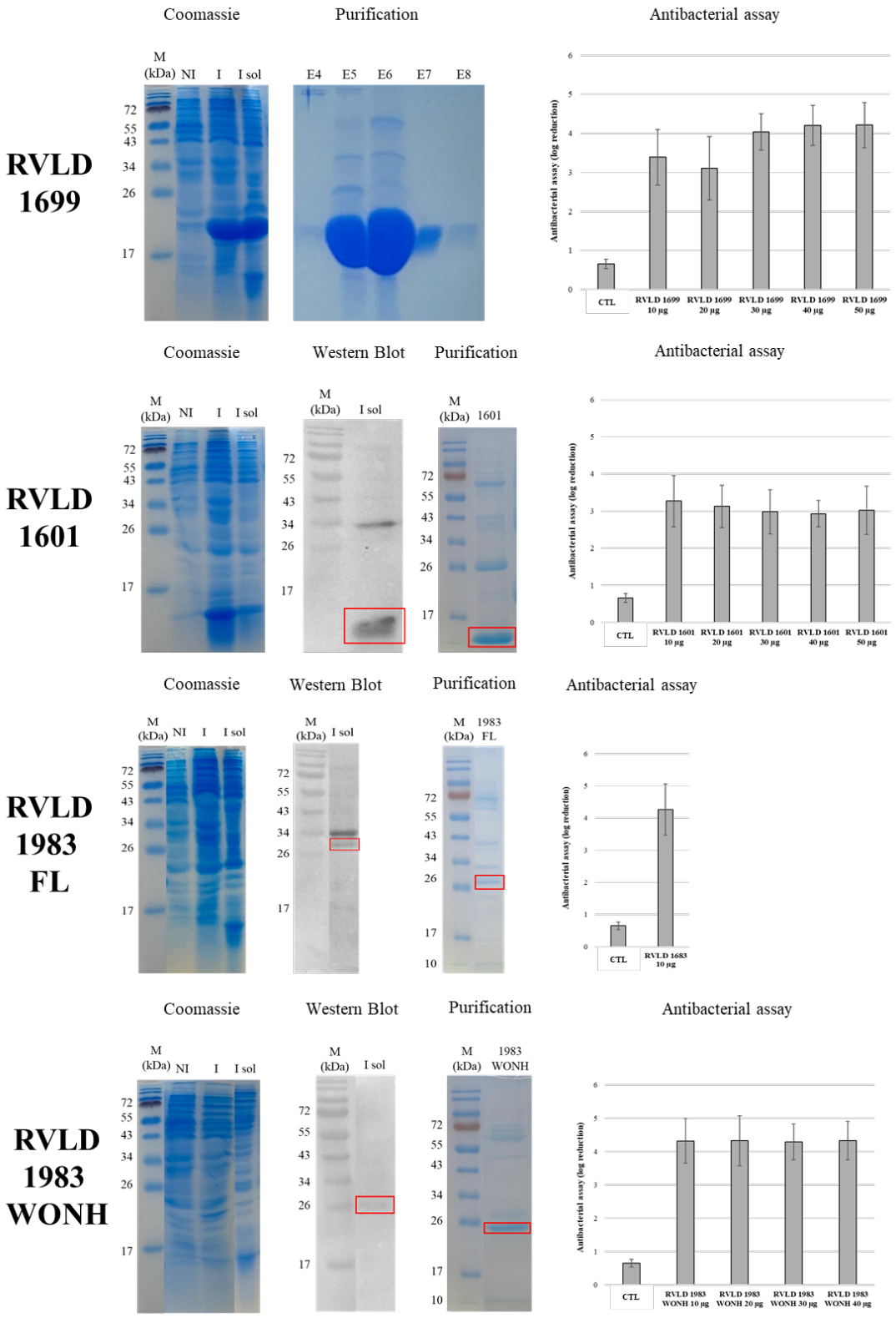

Fig. 10. Expression and purification of *D. vulgaris* specific endolysins used in this study. SDS-page analyses (Coomassie blue staining) of *E. coli* overexpressing cell lysates; Western blot analyses targeting the His_6 tag of each recombinant protein; SDS-page analyses of purified protein fractions obtained by Poly-Prep® Chromatography; Antibacterial assay against *D. vulgaris* planktonic cells pre-treated with chloroform (5% *v/v*). M= molecular weight marker; NI: not induced; I: induced; I sol: induced soluble fraction; CTL: bacterial cells not treated with endolysin (negative control).

Although preliminary, these results pave the way for the development of engineered endolysins specifically targeting *D. vulgaris*. The addition of an OMP peptide that mimics the destabilizing action of chloroform, may lead to the development of recombinant endolysins that will enable their EAD to reach and degrade the PG layer more effectively. To this aim *D. vulgaris* specific lysins libraries for the rapid assembling and high-throughput screening of customized modular lysins for the development of new antibacterials could be generated, by using the VersaTile technique (Gerstmans et al., 2020; Duyvejonck et al., 2021). This technique is a new DNA assembly method for the rapid construction of combinatorial libraries of engineered lysins that involves a two-step approach: *i)* the construction of a collection of all modules, referred to as tiles (*i.e.,* a coding sequence for a specific module such as OMP, linker, CBD, or EAD) and *ii)* the assembly of all tiles in a directed or random manner (Gerstmans et al., 2020; Duyvejonck et al., 2021). The specific *D. vulgaris* engineered endolysins obtained with VersaTile could provide a more effective mean to mitigate SRB-associated issues, offering a novel and innovative strategy for targeted microbial control.

3.4 **Appendix I**

Nucleotide, amino acid sequences and *in silico* structure prediction of all endolysins used in this study

Art-175

Nucleotide sequence

CATATGCGTGGTCTGCGTCGTCTGGGTCGTAAAATCGCGCACGGTGTTAAAAAATACGGTCC
GACCGTTCTGCGTATCATCCGTATCGCGGGCGGTTCTAAAGTTCTGCGTAAAGGTGACCGTG
GTGACGAAGTTTGCCAGCTGCAGACCCTGCTGAACCTGTGCGGTTACGACGTTGGTAAACCG
GACGGTATCTTCGGTAACAACACCTTCAACCAGGTTGTTAAATTCCAGAAAGACAACTGCCT
GGACTCTGACGGTATCGTTGGTAAAAACACCTGGGCGGAACTGTTCTCTAAATACTCTCCGC
CGATCCCGTACAAAACCATCCCGATGCCGACCGCGAACAAATCTCGTGCGGCGGCGACCCCG
GTTATGAACGCGGTTGAAAACGCGACCGGTGTTCGTTCTCAGCTGCTGCTGACCTTCGCGTC
TATCGAATCTGCGTTCGACTACGAAATCAAAGCGAAAACCTCTTCTGCGACCGGTTGGTTCC
AGTTCCTGACCGGTACCTGGAAAACCATGATCGAAAACTACGGTATGAAATACGGTGTTCTG
ACCGACCCGACCGGTGCGCTGCGTAAAGACCCGCGTATCTCTGCGCTGATGGGTGCGGAACT
GATCAAAGAAAACATGAACATCCTGCGTCCGGTTCTGAAACGTGAACCGACCGACACCGACC
TGTACCTGGCGCACTTCTTCGGTCCGGGTGCGGCGCGTCGTTTCCTGACCACCGGTCAGAAC
GAACTGGCGGCGACCCACTTCCCGAAAGAAGCGCAGGCGAACCCGTCTATCTTCTACAACAA
AGACGGTTCTCCGAAAACCATCCAGGAAGTTTACAACCTGATGGACGGTAAAGTTGCGGCGC
ACCGTAAACTCGAG

Amino acid sequence (predicted MW including His_6-tag = 33.4 kDa)

MRGLRRLGRKIAHGVKKYGPTVLRIIRIAGGSKVLRKGDRGDEVCQLQTLLNLCGYDVGKPD
GIFGNNTFNQVVKFQKDNCLDSDGIVGKNTWAELFSKYSPPIPYKTIPMPTANKSRAAATPV
MNAVENATGVRSQLLLTFASIESAFDYEIKAKTSSATGWFQFLTGTWKTMIENYGMKYGVLT
DPTGALRKDPRISALMGAELIKENMNILRPVLKREPTDTDLYLAHFFGPGAARRFLTTGQNE
LAATHFPKEAQANPSIFYNKDGSPKTIQEVYNLMDGKVAAHRKLEHHHHHH

In silico structure prediction with InterProScan and Alphafold

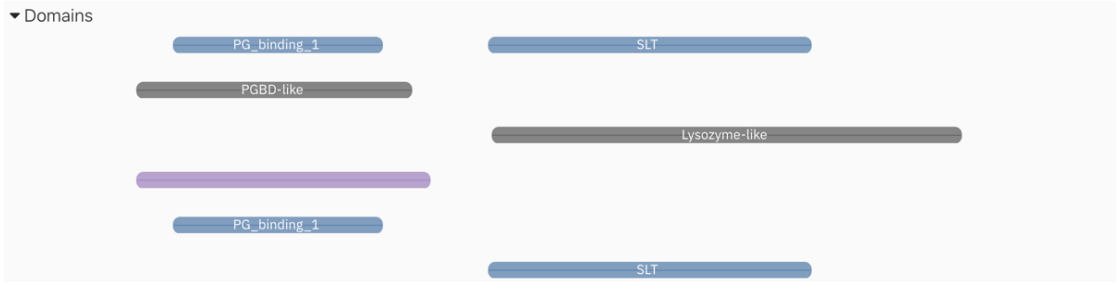

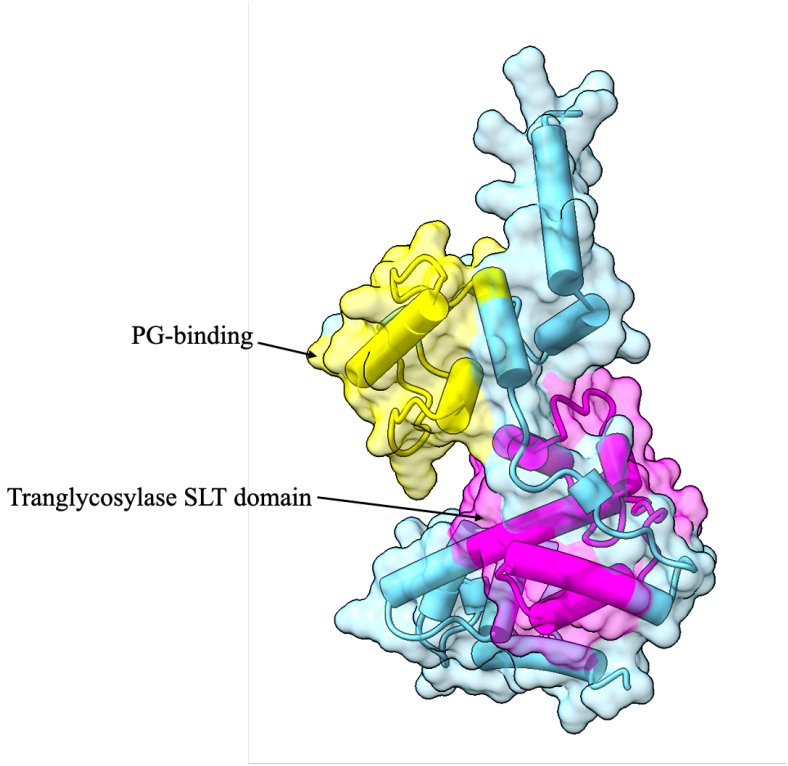

Nucleotide, amino acid sequences and *in silico* structure prediction (InterProScan, Mulder and Apweiler, 2007) and Alphafold prediction with ChimeraX_Daily: alphafold21_predict_colab.ipynb, (Mirdita et al., 2022) of Art-175.
NdeI site encompassing the ATG and the XhoI site of Art-175 gene are highlighted in pink and green, respectively. DNA sequence was cloned in the NdeI/XhoI site of pET21a (Novagen), that allows the insertion of an in-frame His_6-tag at the C-terminal of protein. PG: Peptodoglycan; SLT; Soluble Lytic Transglicosilase.
In the InterProScan figure protein representative domains are highlighted, such as the PG-binding and SLT (lysozyme-like) domains.

RVLD_1601

Nucleotide sequence

CATATGAGCTTTAAATACTTCAAACTGGAAGAATTCGACTGTCAGGAAACCGGCAAGAATAA
CATGTCTGAAGGCTTCATCCATAAGCTGGACGAACTGCGTGAAGCGTGTGGTTTCCCGTTTA
CCATCACTTCCGGTTACCGTGATCCGTCCCACTCTGTAGAGAAATCCAAGAAAAAAGGTGGT
CAGCATACCCTGGGTATCGCTGCTGACATCCGTATTCACTCTGGTGACGACCGCTATACCAT
CGTTCAGAAAGCGATGGAACTGGGCTTCACCGGTATTGGTATCGCAAAAACCTTCGTTCACG
TTGATCTGCGTGTTACCACGCCGGTTATTTGGACCTACCTCGAG

Amino acid sequence (predicted MW including His_6-tag = 13.85 kDa)

MSFKYFKLEEFDCQETGKNNMSEGFIHKLDELREACGFPFTITSGYRDPSHSVEKSKKKGGQ
HTLGIAADIRIHSGDDRYTIVQKAMELGFTGIGIAKTFVHVDLRVTTPVIWTYLEHHHHHH

In silico structure prediction with InterProScan and Alphafold

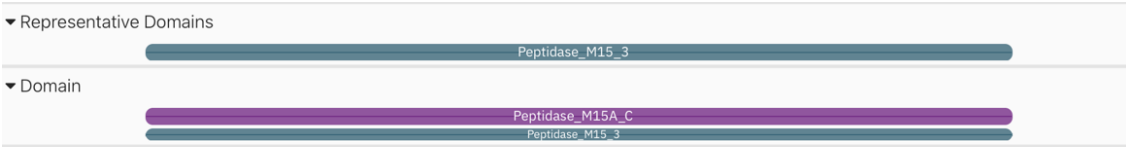

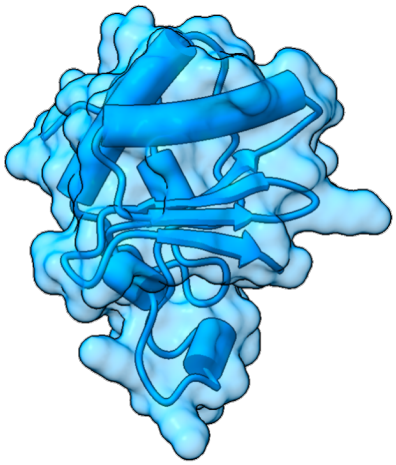

Nucleotide, amino acid sequences and *in silico* structure prediction (InterProScan, Mulder and Apweiler, 2007) and Alphafold prediction with ChimeraX_Daily: alphafold21_predict_colab.ipynb, (Mirdita et al., 2022) of RVLD_1601. NdeI site encompassing the ATG and the XhoI site of RVLD_1601 gene are highlighted in pink and green, respectively. DNA sequence was cloned in the NdeI/XhoI site of pET21a (Novagen), that allows the insertion of an in-frame His6-tag at the C-terminal of protein.
In the InterProScan figure protein representative domains are highlighted, such as peptidase_M15_3 domain.

RVLD_1699

Nucleotide sequence

CATATGAAAAACGGCAAGATCGACCTGCGTGACAAAACCAACTATATTGTTGTGCACTGCGC
TGCGACTAAACCGAGCATGGATATCGGTGCCGCAGAAATTCGCAAATGGCATACTGACCCGC
CTCGTAACTGGGATGATATCGGTTACCACTTTGTCATCACGCGTGATCGCAACCCGATCATC
GAACTGGGTCGTCACGTTTCCGTACCAGGCGCTCATGTTGCGAAACACAACTGGGAATCCGT
TGGCATTTGTCTGGTTGGCGGTATGGCCGAAGATGGCACCTCCGAAAACAACTTCACGAACA
ATCAGATGGCAGCACTGCACGACCTGATCCGTGTTCTGATGATGATTTACCCGCAGGCAGAA
GTAGTTGGCCACTGCGATCTGGATCCGGACAACAAGGCTGATTGTCCAGGTTTCGACGTTGG
TGAATGGTTCGCTGAAGAATTCATCGGTCTGACCAACGAAAGCATCCTCGAG

Amino acid sequence (predicted MW including His_6-tag = 18.59 kDa)

MKNGKIDLRDKTNYIVVHCAATKPSMDIGAAEIRKWHTDPPRNWDDIGYHFVITRDRNPIIE
LGRHVSVPGAHVAKHNWESVGICLVGGMAEDGTSENNFTNNQMAALHDLIRVLMMIYPQAEV
VGHCDLDPDNKADCPGFDVGEWFAEEFIGLTNESILEHHHHHH

In silico structure prediction with InterProScan and Alphafold

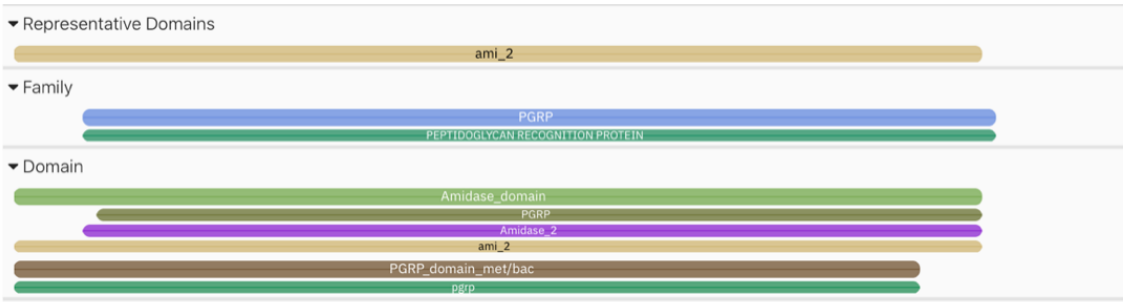

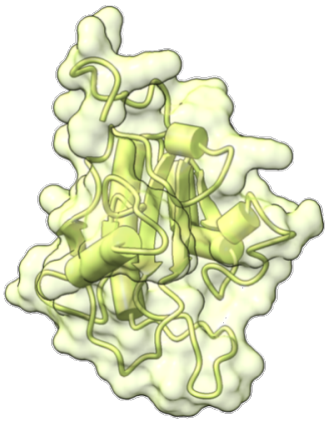

Nucleotide, amino acid sequences and *in silico* structure prediction (InterProScan, (Mulder and Apweiler, 2007) and Alphafold prediction with ChimeraX_Daily: alphafold21_predict_colab.ipynb, (Mirdita et al., 2022) of RVLD_1699. NdeI site encompassing the ATG and the XhoI site of RVLD_1699 gene are highlighted in pink and green, respectively. DNA sequence was cloned in the NdeI/XhoI site of pET21a (Novagen), that allows the insertion of an in-frame His6-tag at the C-terminal of protein.
In the InterProScan figure protein representative domains are highlighted, such as amidase domain.

RVLD_1983_FL

Nucleotide sequence

CATATGCCAGACGTGACCCTGAAAGTAGAAACTAGCCCGACCTGGAAAGAAATCCTGGTGCA
GGCGCTGTGTTGCTGCGCACGTTGGATCCTGCGTGGCTTTCTGCTGTTCATCGGTTTCTACC
TGGCAAGCCTGTGGCTGCCGATCTCCGCGAAAGCGGCGGAAGTGACCATTCCGCGTGCTGCA
CAGCAGTACCGTGCGACCCTGGTTCGTGCTGCTCATGCCACCTGGGGTCTGGATGCACCGGT
TGCGGTATTTGCTGCCCAGGTTCACACGGAGAGCTGGTGGCGTAACGACACCGTGTCCCATG
TGGGTGCCCAGGGTCTGGCTCAGTTCATGCCAGCTACCGCTCGCTGGCTGCCGTCTGTTGCG
CCGGAGACTGGTAAACCGGCTCCGTTTAACCCGGGTTGGTCCCTGCGTGCTCTGTGTGTTTA
CGATAAGTGGCTGTGGGACCGCGTTGCCGGCCATTCTGATTTCGAACGTATGGCGTTCACCC
TGTCCGCTTATAACGGTGGCCTGGGTTGGGTGAACCGTGATCGTAAGAAGGCTCGTGCTCTG
GGCGTTGACGATCGCCGCTGGTTCGGTGCAGTTGAAAACGTTAACGCGGGTCGTTCCAAGGC
CGCTTTCCGTGAAAACCGTAACTATCCGCGTCTGATCCTGGAGGAACGCCAGTACGCATACA
TCAAAGCAGGCTGGGGTCCGGGCGTGGAAGATGAAGCGCGTCTGCTCGAG

Amino acid sequence (predicted MW including His_6-tag = 27.95 kDa)

MPDVTLKVETSPTWKEILVQALCCCARWILRGFLLFIGFYLASLWLPISAKAAEVTIPRAAQ
QYRATLVRAAHATWGLDAPVAVFAAQVHTESWWRNDTVSHVGAQGLAQFMPATARWLPSVAP
ETGKPAPFNPGWSLRALCVYDKWLWDRVAGHSDFERMAFTLSAYNGGLGWVNRDRKKARALG
VDDRRWFGAVENVNAGRSKAAFRENRNYPRLILEERQYAYIKAGWGPGVEDEARLLEHHHHH
H

In silico structure prediction with InterProScan and Alphafold

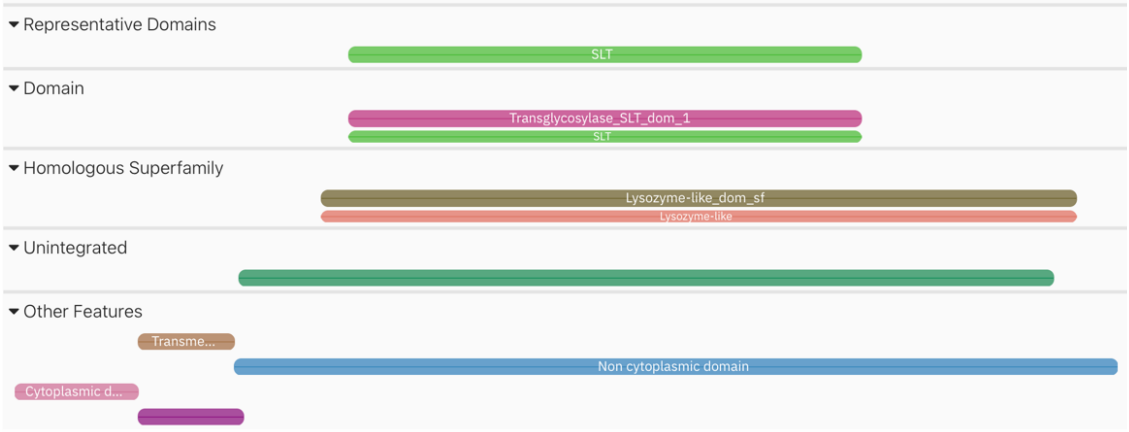

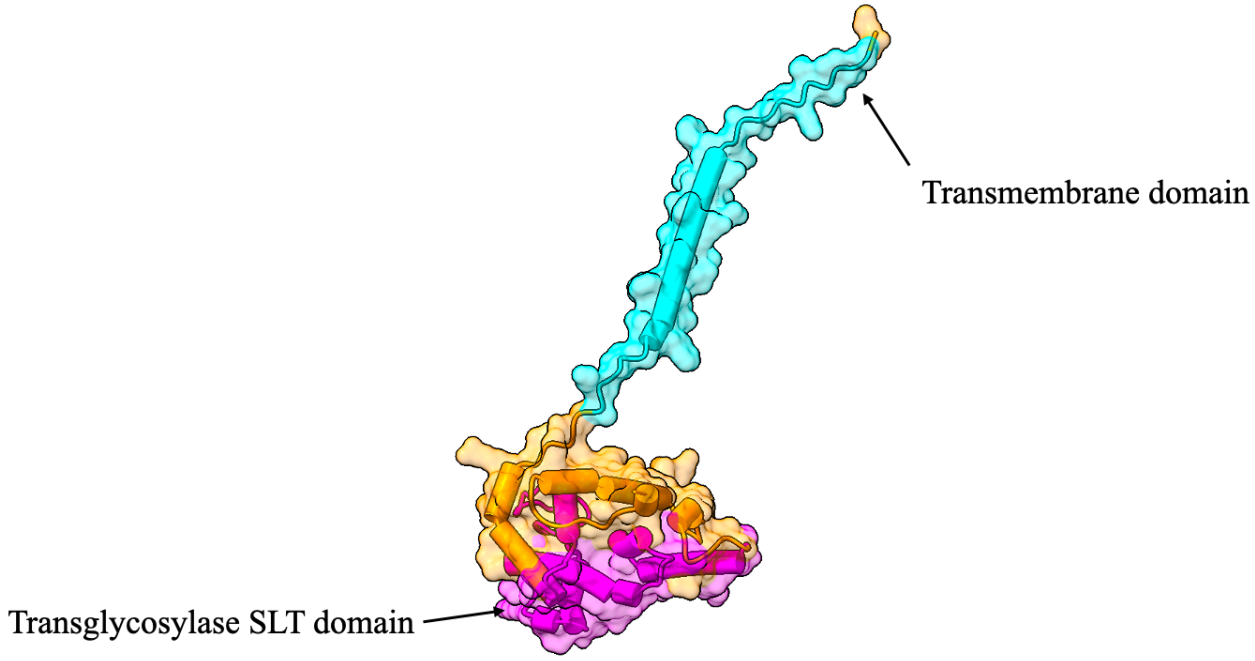

Nucleotide, amino acid sequences and *in silico* structure prediction (InterProScan, (Mulder and Apweiler, 2007) and Alphafold prediction with ChimeraX_Daily: alphafold21_predict_colab.ipynb, (Mirdita et al., 2022) of RVLD_1983 FL. NdeI site encompassing the ATG and the XhoI site of RVLD_1983 FL gene are highlighted in pink and green, respectively. DNA sequence was cloned in the NdeI/XhoI site of pET21a (Novagen), that allows the insertion of an in-frame His6-tag at the C-terminal of protein. SLT; Soluble Lytic Transglicosilase.
In the InterProScan figure protein representative domains are highlighted, such as SLT (lysozyme-like) domain.

RVLD_1984_FL

Nucleotide sequence

CATATGGGTTTTCACAAAGGTTATCGTGCCATTCGTCTGCCGTTCGGTTGGGAGGTATGGGT
GTGGCCACCTGCGCCGGCTACGCCATTCGGTCGCCGCCTGGCAACCCTGTTTGTGTCTGCGG
CGCTGTCCTTTCTGGGTTGGTGTCTGGAGGCACTGCGTGTTCTGGGTATCGCTCTGCTGGCA
GCGATCCTGCTGCACCTGTGGTTCGGCTATTCCGCACACGCGGCTACTATCCCGCGCGAGGC
ACAGGCTCACCGTTCCGTCCTGGTCCGCGCCGCGCGTCTGGAATGGGGTCTGGGTGCACCGG
TTGCCACCTTCGCGGCGCAAGTACACCAGGAATCTGAGTGGCGCCCGGATGCTGTCTCTCCG
GTGGGCGCCCAGGGTCTGGCACAGTTTATGCCGAGCACGGCTCGTTGGCTGCCGTCCGTTGC
GCCGCAGACCGGTCAGCCGGCTCCATTTAACCCGGCGTGGGCGCTGCGTGCTGTTGTGGCGT
ACGACCTGTGGCTGCACCAGCGCGTACGTGCAGCTACCCCGTGTGACCGTATGGCCATGGCT
CTGGCAGCATACAACGGTGGCCTGGGCTGGGTTCAGCGTGACGTTCGTCTGGCGGCAACCCG
TGGTCGTAACCCAGCAGCTTGGTGGGGCAACGTCGAAGCGGTTAACGCCGGTCGTAGCGCAA
ACGCATTCCGCGAGAACCGCGGCTACCCGCGCCGCATCCTGCTGACGCTGGAACCGGTGTAC
GAAGCGGCTGCATGGGGCGGTGGTAGCTGCGACGGCGGTCGTAGCTCGAG

Amino acid sequence (predicted MW including His_6-tag = 29.32 kDa)

MGFHKGYRAIRLPFGWEVWVWPPAPATPFGRRLATLFVSAALSFLGWCLEALRVLGIALLAA
ILLHLWFGYSAHAATIPREAQAHRSVLVRAARLEWGLGAPVATFAAQVHQESEWRPDAVSPV
GAQGLAQFMPSTARWLPSVAPQTGQPAPFNPAWALRAVVAYDLWLHQRVRAATPCDRMAMAL
AAYNGGLGWVQRDVRLAATRGRNPAAWWGNVEAVNAGRSANAFRENRGYPRRILLTLEPVYE
AAAWGGGSCDGGRLEHHHHHH

In silico structure prediction with InterProScan and Alphafold

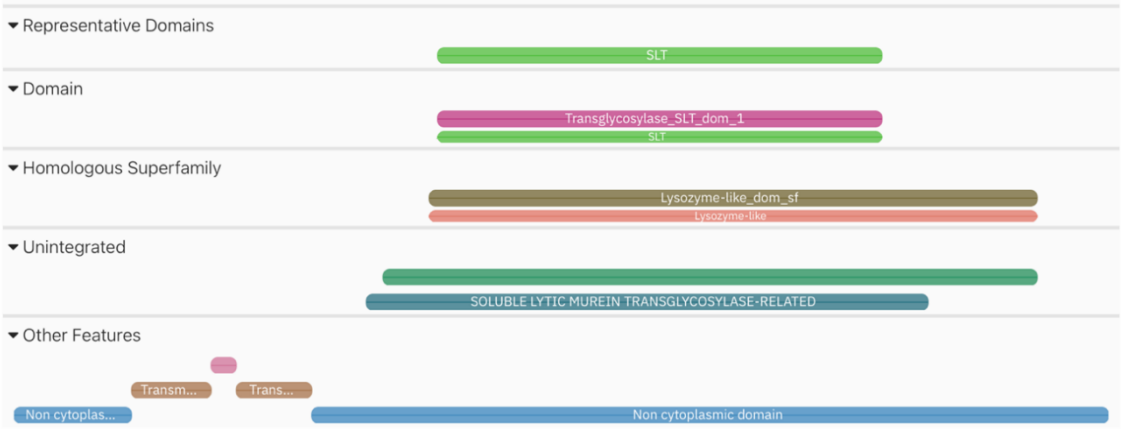

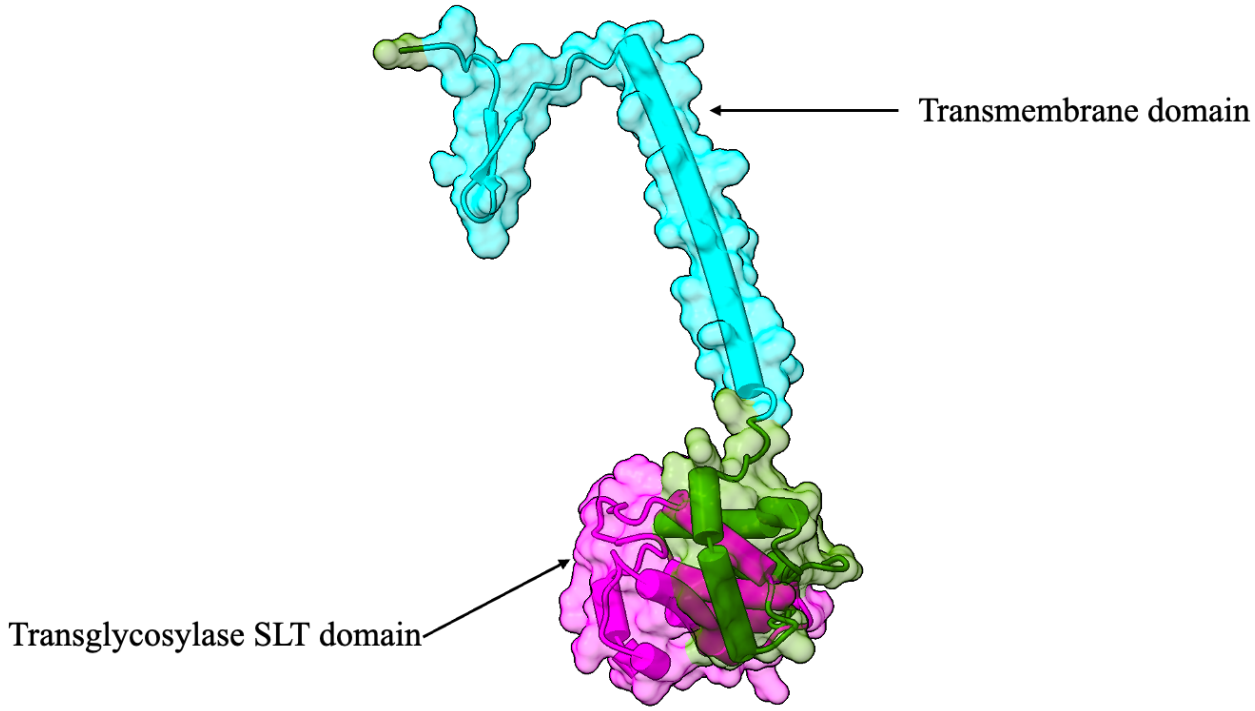

Nucleotide, amino acid sequences and *in silico* structure prediction (InterProScan, (Mulder and Apweiler, 2007) and Alphafold prediction with ChimeraX_Daily: alphafold21_predict_colab.ipynb, (Mirdita et al., 2022) of RVLD_1984 FL. NdeI site encompassing the ATG and the XhoI site of RVLD_1984 FL gene are highlighted in pink and green, respectively. DNA sequence was cloned in the NdeI/XhoI site of pET21a (Novagen), that allows the insertion of an in-frame His6-tag at the C-terminal of protein. SLT; Soluble Lytic Transglicosilase.
In the InterProScan figure are protein representative domains are highlighted, such as SLT (lysozyme-like) domain.

RVLD_2367

Nucleotide sequence

CATATGGCCACCATCCCTCCAGACGCACTGTGTCACCGCGCAACCCTGACTCGTGAAGCGCG
TTTCCGTTTCGGTATGGACGCTCCGGTTGCCACGTTCGCTGCGCAGATCCACCAGGAAAGCG
AATGGCGTGCGGGCGCAGTGTCCCCAGTTGGTGCTCAGGGTCTGGCACAGTTTATGCCGGGT
ACGGCGCGTTGGCTGCCAACCGTGATGCCAGACACCGGCCAACCGGCCCCTTTTAACCCGGC
CTGGGCGATTCGCGCACTGGTGGCCTACGATTGGTGGATCCTGCAGCGTGTTCGTGCCGCAA
CTCCGTGCGACCGTATGGCCAAAGGTCTGGCAGGCTACAACGGCGGTCCGGGCTGGCTGACT
CGTGACGAACGTAAGGCCGCAGCACAGGGCCTGGACCCGGATGTTTGGTGGGGTAGCGTGGA
AACCGTTAACGCGGGTCGCAGCCGTGCCGCGTTTCGTGAAAACCGTGGCTACCCGCGCCGTA
TCCTGCTGGTGCTGGAACCTGTATACATGGCCGCTGGTTGGGGCGCGGGCTCCTGTCCAGCT
CAGGGTGGTCGCTCTCTCGAG

Amino acid sequence (predicted MW including His_6-tag = 21.47 kDa)

MATIPPDALCHRATLTREARFRFGMDAPVATFAAQIHQESEWRAGAVSPVGAQGLAQFMPGT
ARWLPTVMPDTGQPAPFNPAWAIRALVAYDWWILQRVRAATPCDRMAKGLAGYNGGPGWLTR
DERKAAAQGLDPDVWWGSVETVNAGRSRAAFRENRGYPRRILLVLEPVYMAAGWGAGSCPAQ
GGRSLEHHHHHH

In silico structure prediction with InterProScan and Alphafold

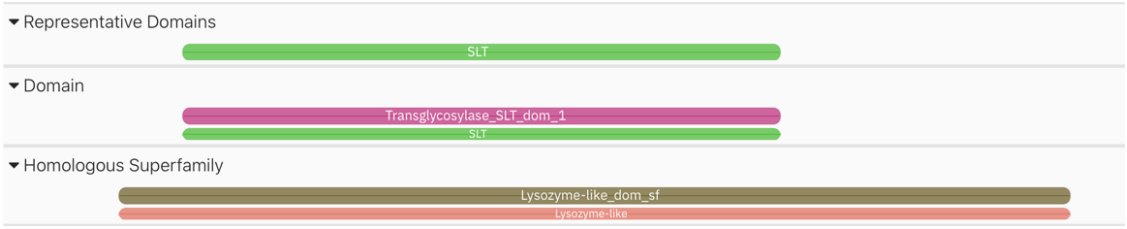

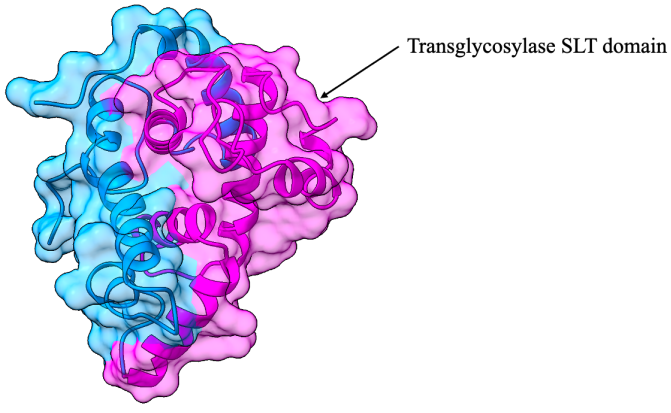

Nucleotide, amino acid sequences and *in silico* structure prediction (InterProScan, (Mulder and Apweiler, 2007) and Alphafold prediction with ChimeraX_Daily: alphafold21_predict_colab.ipynb, (Mirdita et al., 2022) of RVLD_2367. NdeI site encompassing the ATG and the XhoI site of RVLD_2367 gene are highlighted in pink and green, respectively. DNA sequence was cloned in the NdeI/XhoI site of pET21a (Novagen), that allows the insertion of an in-frame His6-tag at the C-terminal of protein. SLT; Soluble Lytic Transglicosilase.
In the InterProScan figure protein representative domains are highlighted, such as SLT (lysozyme-like) domain.

RVLD_1984_WONH

Nucleotide sequence

CATATGCACGCGGCTACTATCCCGCGCGAGGCACAGGCTCACCGTTCCGTCCTGGTCCGCGC
CGCGCGTCTGGAATGGGGTCTGGGTGCACCGGTTGCCACCTTCGCGGCGCAAGTACACCAGG
AATCTGAGTGGCGCCCGGATGCTGTCTCTCCGGTGGGCGCCCAGGGTCTGGCACAGTTTATG
CCGAGCACGGCTCGTTGGCTGCCGTCCGTTGCGCCGCAGACCGGTCAGCCGGCTCCATTTAA
CCCGGCGTGGGCGCTGCGTGCTGTTGTGGCGTACGACCTGTGGCTGCACCAGCGCGTACGTG
CAGCTACCCCGTGTGACCGTATGGCCATGGCTCTGGCAGCATACAACGGTGGCCTGGGCTGG
GTTCAGCGTGACGTTCGTCTGGCGGCAACCCGTGGTCGTAACCCAGCAGCTTGGTGGGGCAA
CGTCGAAGCGGTTAACGCCGGTCGTAGCGCAAACGCATTCCGCGAGAACCGCGGCTACCCGC
GCCGCATCCTGCTGACGCTGGAACCGGTGTACGAAGCGGCTGCATGGGGCGGTGGTAGCTGC
GACGGCGGTCGTAGCCTCGAG

Amino acid sequence (predicted MW including His_6-tag = 21.39 kDa)

MHAATIPREAQAHRSVLVRAARLEWGLGAPVATFAAQVHQESEWRPDAVSPVGAQGLAQFMP
STARWLPSVAPQTGQPAPFNPAWALRAVVAYDLWLHQRVRAATPCDRMAMALAAYNGGLGWV
QRDVRLAATRGRNPAAWWGNVEAVNAGRSANAFRENRGYPRRILLTLEPVYEAAAWGGGSCD
GGRSLEHHHHHH

In silico structure prediction with InterProScan and Alphafold

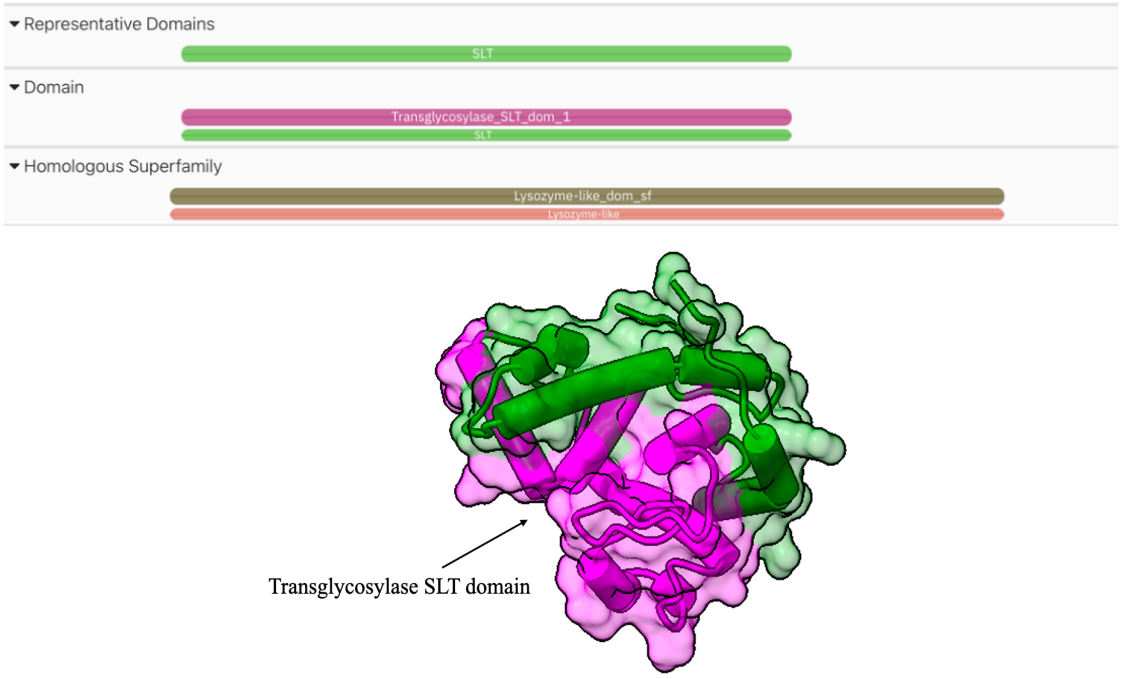

Nucleotide, amino acid sequences and *in silico* structure prediction (InterProScan, (Mulder and Apweiler, 2007) and Alphafold prediction with ChimeraX_Daily: alphafold21_predict_colab.ipynb, (Mirdita et al., 2022) of RVLD_1984 WONH. NdeI site encompassing the ATG and the XhoI site of RVLD_1984 WONH gene are highlighted in pink and green, respectively. DNA sequence was cloned in the NdeI/XhoI site of pET21a (Novagen), that allows the insertion of an in-frame His6-tag at the C-terminal of protein. SLT; Soluble Lytic Transglicosilase.
In the InterProScan figure protein representative domains are highlighted, such as SLT (lysozyme-like) domain.

RVLD_1528

Nucleotide sequence

CATATGAACAATCGCAAAAACACCGACTACATCATCATCCACTGCTCTGCTACCAAACCGTC
TATGAACATCGGTGCATACGAAATCGACCGTTGGCACCGTGAACGTGGTTGGCTGGAGATTG
GTTACCATTTCGTCGTTAAACGTAACGGCGCTATCGAACTGGGTCGTCCAATGGAAGCGGTT
GGTGCGCACGCTAAAGGCTACAACGATAAAAGCGTTTCTGTTTGCCTGATCGGCGGTGTCAA
CGATAAACTGAAACCGGATAACAACTACACGCCGGAACAGTGGACTTCTCTGGACTGCTCCA
TCAAGTTCATTAAAAAAATCTACCAGGACGCAGAAGTCATCGGCCACAATGAAGTTTCTGAC
AAAGCTTGTCCGTCCTTCAACGTGCGCAACTACATGAGCGAAAAAGTCTCCAACTTTTGGCT
CGAG

Amino acid sequence (predicted MW including His_6-tag = 17.28 kDa)

MNNRKNTDYIIIHCSATKPSMNIGAYEIDRWHRERGWLEIGYHFVVKRNGAIELGRPMEAVG
AHAKGYNDKSVSVCLIGGVNDKLKPDNNYTPEQWTSLDCSIKFIKKIYQDAEVIGHNEVSDK
ACPSFNVRNYMSEKVSNFWLEHHHHHH

In silico structure prediction with InterProScan and Alphafold

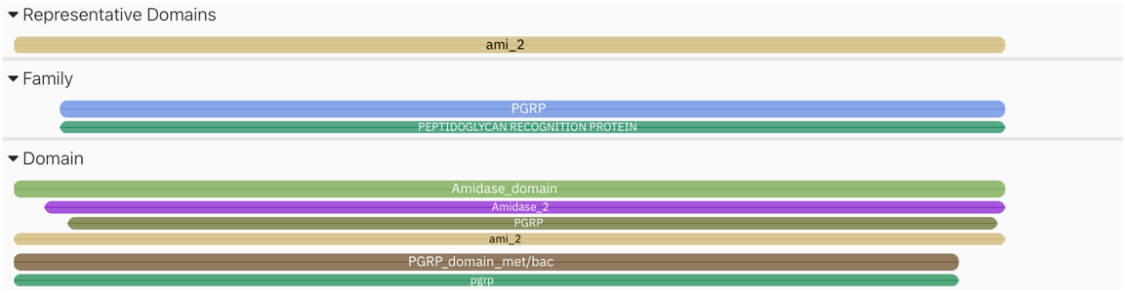

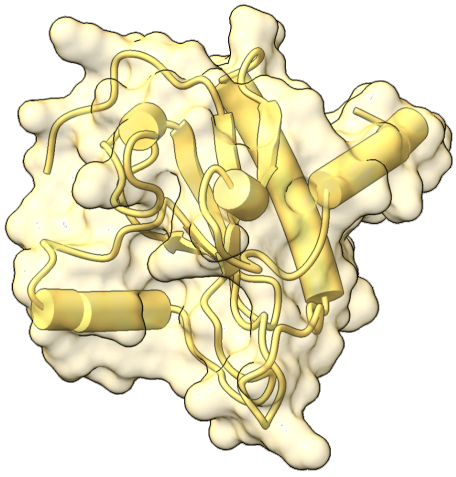

Nucleotide, amino acid sequences and *in silico* structure prediction (InterProScan, (Mulder and Apweiler, 2007) and Alphafold prediction with ChimeraX_Daily: alphafold21_predict_colab.ipynb, (Mirdita et al., 2022) of RVLD_1528. NdeI site encompassing the ATG and the XhoI site of RVLD_1528 gene are highlighted in pink and green, respectively. DNA sequence was cloned in the NdeI/XhoI site of pET21a (Novagen), that allows the insertion of an in-frame His6-tag at the C-terminal of protein. PGRP: Peptidoglycan recognition protein
In the InterProScan figure protein representative domains are highlighted, such as amidase domain.

RVLD_1985

Nucleotide sequence

CATATGCACAGCGCGCCGGCCATTCCTATGCAAGCTATCCAGTACCGCAGCCAGCTGATGCG
CGAAGCTCGTGCGCAGTGGGGTCTGAGCGCGCCGACTGCAACTTTCGCGGCGCAGGTGCACC
AGGAATCTGGTTGGAACGCAGACGCCGTTTCCCCGGTGGGCGCGCAGGGCCTGGCTCAGTTT
ATGCCGTCTACCGCTCGTTGGCTGCCAACCGTGGCTTCCGACACCGGCAAACCACTGCCATT
CAACCCAGGCTGGGCTCTGCGCGCTCTGGTCACCTACGATCGTTGGCTGTGGCAGCGTGTCC
AAGCCGTGACCCCATGCGATCGCATGGCGCTGGCGCTGGCAGCGTATAACGGTGGTCTGGGC
TGGGTTCAGCGTGATGCACGTCTGGCTGCTGCTCGCGGTCTGGATGCTCGCCGTTGGTGGGA
CAACGTTGAGACGGTGAACGCGGGCCGTTCTGCGAACGCCAAGCGTGAAAACCGTGGCTATC
CGCGTCGCATCCTGCTGACCCTGGAACCGGCATACATGGCAGCCGGTTGGGGTGGCGGCATG
TGTCATGAACTCGAG

Amino acid sequence (predicted MW including His_6-tag = 21.53 kDa)

MHSAPAIPMQAIQYRSQLMREARAQWGLSAPTATFAAQVHQESGWNADAVSPVGAQGLAQFM
PSTARWLPTVASDTGKPLPFNPGWALRALVTYDRWLWQRVQAVTPCDRMALALAAYNGGLGW
VQRDARLAAARGLDARRWWDNVETVNAGRSANAKRENRGYPRRILLTLEPAYMAAGWGGGMC
HELEHHHHHH

In silico structure prediction with InterProScan and Alphafold

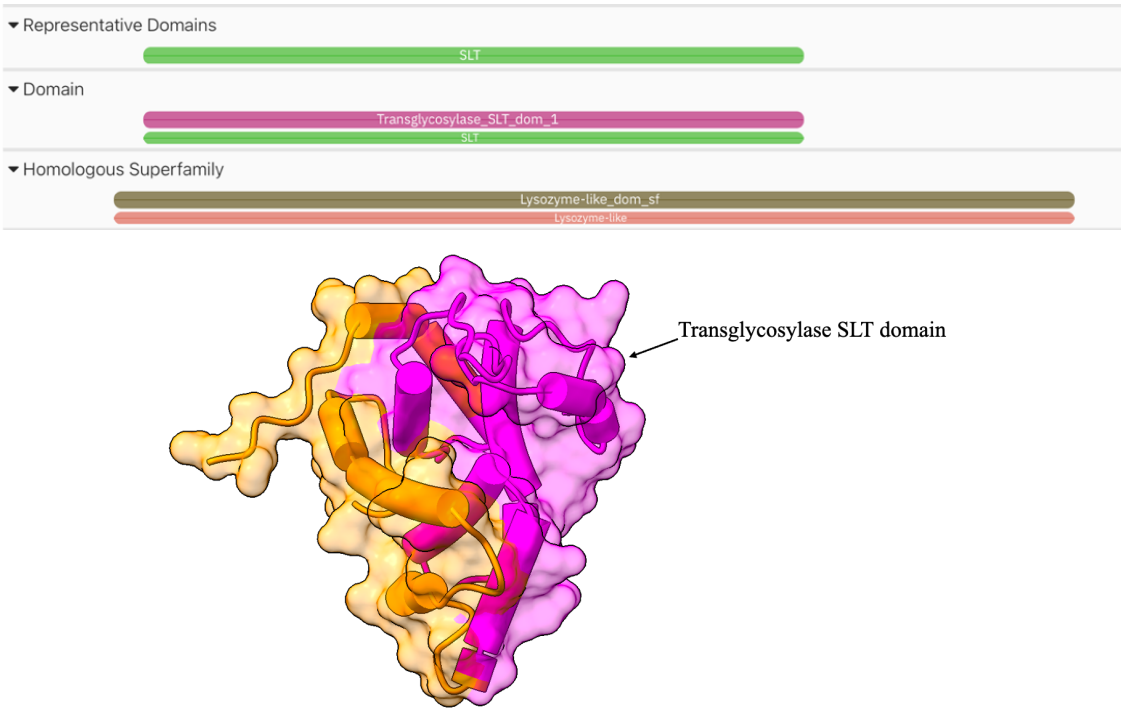

Nucleotide, amino acid sequences and *in silico* structure prediction (InterProScan, (Mulder and Apweiler, 2007) and Alphafold prediction with ChimeraX_Daily: alphafold21_predict_colab.ipynb, (Mirdita et al., 2022) of RVLD_1985. NdeI site encompassing the ATG and the XhoI site of RVLD_1985 gene are highlighted in pink and green, respectively. DNA sequence was cloned in the NdeI/XhoI site of pET21a (Novagen), that allows the insertion of an in-frame His6-tag at the C-terminal of protein. SLT; Soluble Lytic Transglicosilase.
In the InterProScan figure protein representative domains are highlighted, such as SLT (lysozyme-like) domain.

RVLD_1983_WONH

Nucleotide sequence

CATATGGCGGAAGTGACCATTCCGCGTGCTGCACAGCAGTACCGTGCGACCCTGGTTCGTGC
TGCTCATGCCACCTGGGGTCTGGATGCACCGGTTGCGGTATTTGCTGCCCAGGTTCACACGG
AGAGCTGGTGGCGTAACGACACCGTGTCCCATGTGGGTGCCCAGGGTCTGGCTCAGTTCATG
CCAGCTACCGCTCGCTGGCTGCCGTCTGTTGCGCCGGAGACTGGTAAACCGGCTCCGTTTAA
CCCGGGTTGGTCCCTGCGTGCTCTGTGTGTTTACGATAAGTGGCTGTGGGACCGCGTTGCCG
GCCATTCTGATTTCGAACGTATGGCGTTCACCCTGTCCGCTTATAACGGTGGCCTGGGTTGG
GTGAACCGTGATCGTAAGAAGGCTCGTGCTCTGGGCGTTGACGATCGCCGCTGGTTCGGTGC
AGTTGAAAACGTTAACGCGGGTCGTTCCAAGGCCGCTTTCCGTGAAAACCGTAACTATCCGC
GTCTGATCCTGGAGGAACGCCAGTACGCATACATCAAAGCAGGCTGGGGTCCGGGCGTGGAA
GATGAAGCGCGTCTGCTCGAG

Amino acid sequence (predicted MW including His_6-tag = 22.18 kDa)

MAEVTIPRAAQQYRATLVRAAHATWGLDAPVAVFAAQVHTESWWRNDTVSHVGAQGLAQFMP
ATARWLPSVAPETGKPAPFNPGWSLRALCVYDKWLWDRVAGHSDFERMAFTLSAYNGGLGWV
NRDRKKARALGVDDRRWFGAVENVNAGRSKAAFRENRNYPRLILEERQYAYIKAGWGPGVED
EARLLEHHHHHH

In silico structure prediction with InterProScan and Alphafold

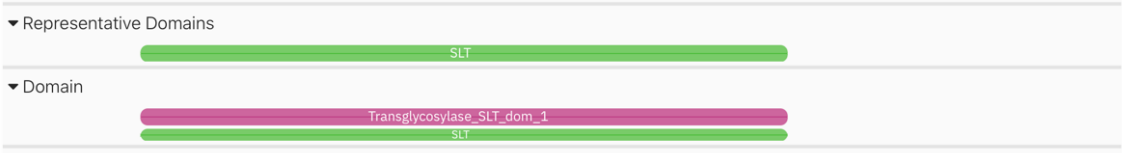

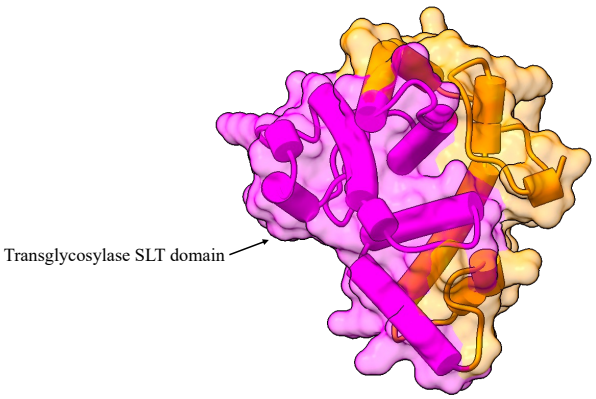

Nucleotide, amino acid sequences and *in silico* structure prediction (InterProScan, (Mulder and Apweiler, 2007) and Alphafold prediction with ChimeraX_Daily: alphafold21_predict_colab.ipynb, (Mirdita et al., 2022) of RVLD_1983 WONH. NdeI site encompassing the ATG and the XhoI site of RVLD_1983 WONH gene are highlighted in pink and green, respectively. DNA sequence was cloned in the NdeI/XhoI site of pET21a (Novagen), that allows the insertion of an in-frame His6-tag at the C-terminal of protein. SLT; Soluble Lytic Transglicosilase.
In the InterProScan figure protein representative domains are highlighted, such as SLT (lysozyme-like) domain.

Chapter 3 references

- Antonova NP, Vasina DV, Lendel AM, Usachev EV, Makarov VV, Gintsburg AL, Tkachuk AP, Gushchin VA. **(2019)**. Broad Bactericidal Activity of the *Myoviridae*Bacteriophage Lysins LysAm24, LysECD7, and LysSi3 against Gram-Negative ESKAPE Pathogens. Viruses;11(3):284. doi: 10.3390/v11030284.
- Bisen M, Kharga K, Mehta S, Jabi N, Kumar L. **(2024)**. Bacteriophages in nature: recent advances in research tools and diverse environmental and biotechnological applications. Environ Sci Pollut Res Int. 31(15):22199-22242. doi: 10.1007/s11356-024-32535-3.
- Bradford MM. **(1976)**. A rapid and sensitive method for the quantitation of microgram quantities of protein utilizing the principle of protein-dye binding. Anal Biochem. 72:248-54. doi: 10.1006/abio.1976.9999. PMID: 942051.
- Briers Y, Cornelissen A, Aertsen A, Hertveldt K, Michiels CW, Volckaert G, Lavigne R. **(2008)**. Analysis of outer membrane permeability of Pseudomonas aeruginosa and bactericidal activity of endolysins KZ144 and EL188 under high hydrostatic pressure. FEMS Microbiol Lett. 280(1):113-9. doi: 10.1111/j.1574-6968.2007.01051.x.
- Briers Y, Lavigne R. **(2015).** Breaking barriers: expansion of the use of endolysins as novel antibacterials against Gram-negative bacteria. Future Microbiol 10:377–390. http://dx.doi.org/10.2217/fmb.15.8.
- Briers Y, Schmelcher M, Loessner MJ, Hendrix J, Engelborghs Y, Volckaert G, Lavigne R. **(2009)**. The high-affinity peptidoglycan binding domain of Pseudomonas phage endolysin KZ144. Biochem Biophys Res Commun. 383(2):187-91. doi: 10.1016/j.bbrc.2009.03.161
- Briers Y, Volckaert G, Cornelissen A, Lagaert S, Michiels CW, Hertveldt K, Lavigne R. **(2007)**. Muralytic activity and modular structure of the endolysins of Pseudomonas aeruginosa bacteriophages phiKZ and EL. Mol Microbiol. 65(5):1334-44. doi: 10.1111/j.1365-2958.2007.05870.x.
- Briers Y, Walmagh M, Grymonprez B, Biebl M, Pirnay JP, Defraine V, Michiels J, Cenens W, Aertsen A, Miller S, Lavigne R. **(2014a)**. Art-175 is a highly efficient antibacterial against multidrug-resistant strains and persisters of Pseudomonas aeruginosa. Antimicrob Agents Chemother. 58(7):3774-84. doi: 10.1128/AAC.02668-14.
- Briers Y, Walmagh M, Lavigne R. **(2011)**. Use of bacteriophage endolysin EL188 and outer membrane permeabilizers against Pseudomonas aeruginosa. J Appl Microbiol. 110(3):778-85. doi: 10.1111/j.1365-2672.2010.04931.x.
- Briers Y, Walmagh M, Van Puyenbroeck V, Cornelissen A, Cenens W, Aertsen A, Oliveira H, Azeredo J, Verween G, Pirnay J-P, Miller S, Volckaert G, Lavigne R. **(2014b)**. Engineered endolysin-based "artilysins" to combat multidrug-resistant gram-negative pathogens. mBio 5:e01379-14. http://dx.doi.org/10.1128/mBio.01379-14
- Brunelle JL, Green R. **(2014)**. Coomassie blue staining. Methods Enzymol.;541:161-7. doi: 10.1016/B978-0-12-420119-4.00013-6. PMID: 24674070.
- Butler ET, Chamberlin MJ. **(1982)**. Bacteriophage SP6-specific RNA polymerase. I. Isolation and characterization of the enzyme. J Biol Chem. 25;257(10):5772-8. PMID: 7040372.
- Chang Y. **(2020)**. Bacteriophage-Derived Endolysins Applied as Potent Biocontrol Agents to Enhance Food Safety. *Microorganisms*. 8(5):724. doi:10.3390/microorganisms8050724
- Clokie MR, Millard AD, Letarov AV, Heaphy S. **(2011)**. Phages in nature. *Bacteriophage*. 1(1):31-45. doi:10.4161/bact.1.1.14942

- Czaplewski L, Bax R, Clokie M, Dawson M, Fairhead H, Fischetti VA, Foster S, Gilmore BF, Hancock RE, Harper D, Henderson IR, Hilpert K, Jones BV, Kadioglu A, Knowles D, Ólafsdóttir S, Payne D, Projan S, Shaunak S, Silverman J, Thomas CM, Trust TJ, Warn P, Rex JH. **(2016)**. Alternatives to antibiotics-a pipeline portfolio review. Lancet Infect Dis. 16(2):239-51. doi: 10.1016/S1473-3099(15)00466-1.
- d'Hérelle F. **(1917)**. Sur un microbe invisible antagoniste des bacilles dysentérique. Acad Sci Paris. 165:373–5.
- de Romero MF, Urdaneta S, Barrientos M, Romero G. **(2004)**. Correlation Between Desulfovibrio Sessile Growth and OCP, Hydrogen Permeation, Corrosion Products and Morphological Attack on Iron, Paper No. 04576, CORROSION, NACE International
- De Smet J, Hendrix H, Blasdel BG, Danis-Wlodarczyk K, Lavigne R. **(2017)**. Pseudomonas predators: understanding and exploiting phage-host interactions. Nat Rev Microbiol. 15(9):517-530. doi: 10.1038/nrmicro.2017.61.
- Defraine V, Schuermans J, Grymonprez B, Govers SK, Aertsen A, Fauvart M, Michiels J, Lavigne R, Briers Y. **(2016)**. Efficacy of Artilysin Art-175 against Resistant and Persistent Acinetobacter baumannii. Antimicrob Agents Chemother. 60(6):3480-8. doi: 10.1128/AAC.00285-16.
- Duyvejonck L, Gerstmans H, Stock M, Grimon D, Lavigne R, Briers Y. **(2021)**. Rapid and High- Throughput Evaluation of Diverse Configurations of Engineered Lysins Using the VersaTile Technique. *Antibiotics*. 10(3):293. https://doi.org/10.3390/antibiotics10030293
- Dy RL, Rigano LA, Fineran PC. **(2018)**. Phage-based biocontrol strategies and their application in agriculture and aquaculture. Biochem. Soc. Trans. 46, 1605–1613, https://doi.org/10.1042/bst20180178.
- Exner M, Bhattacharya S, Christiansen B, Gebel J, Goroncy-Bermes P, Hartemann P, Heeg P, Ilschner C, Kramer A, Larson E *et al.* **(2017)**. Antibiotic resistance: what is so special about multidrug-resistant Gram-negative bacteria? *GMS Hyg Infect Control*, 12 http://dx.doi.org/10.3205/dgkh000290
- Fenton M, Ross P, McAuliffe O, O'Mahony J, Coffey A. **(2010)**. Recombinant bacteriophage lysins as antibacterials. *Bioeng Bugs*.1(1):9-16. doi:10.4161/bbug.1.1.9818
- Fernández-Ruiz I, Coutinho FH, Rodriguez-Valera F. **(2018)**. Thousands of Novel Endolysins Discovered in Uncultured Phage Genomes. Front Microbiol. 9:1033. doi: 10.3389/fmicb.2018.01033.
- Fischetti VA. **(2010)**. Bacteriophage endolysins: a novel anti-infective to control Gram-positive pathogens. Int J Med Microbiol. 300(6):357-62. doi: 10.1016/j.ijmm.2010.04.002.
- Fischetti VA. **(2005)**. Bacteriophage lytic enzymes: novel anti-infectives. *Trends Microbiol*. 13(10):491-496. doi:10.1016/j.tim.2005.08.007
- Freimer EH, Krause RM, Mc CM. **(1959)**. Studies of L forms and protoplasts of group A streptococci. I. Isolation, growth, and bacteriologic characteristics. J Exp Med. 110:853-74; http://dx.doi.org/ 10.1084/jem.110.6.853
- Funahara Y, Nikaido H. **(1980)**. Asymmetric localization of lipopolysaccharides on the outer membrane of Salmonella typhimurium. Journal of bacteriology 141, 1463–1465. doi: 10.1128/jb.141.3.1463-1465.1980.
- Gerstmans H, Grimon D, Gutiérrez D, *et al*. **(2020)**. A VersaTile-driven platform for rapid hit-to-lead development of engineered lysins. *Sci Adv*. 6(23):eaaz1136. doi:10.1126/sciadv.aaz1136

- Gerstmans H, Rodríguez-Rubio L, Lavigne R, Briers Y. **(2016)**. From endolysins to Artilysin®s: novel enzyme-based approaches to kill drug-resistant bacteria. Biochem Soc Trans. 44(1):123-8. doi: 10.1042/BST20150192.
- Gondil VS, Harjai K, Chhibber S. **(2020)**. Endolysins as emerging alternative therapeutic agents to counter drug-resistant infections. *Int J Antimicrob Agents*. 55(2):105844. doi:10.1016/j.ijantimicag.2019.11.001
- Grabowski Ł, Łepek K, Stasiłojć M, Kosznik-Kwaśnicka K, Zdrojewska K, Maciąg-Dorszyńska M, Węgrzyn G, Węgrzyn A. **(2021)**. Bacteriophage-encoded enzymes destroying bacterial cell membranes and walls, and their potential use as antimicrobial agents. Microbiol Res. 248:126746. doi: 10.1016/j.micres.2021.126746.
- Groth AC, Calos MP. **(2004)**. Phage integrases: biology and applications. J Mol Biol. 335(3):667-78. doi: 10.1016/j.jmb.2003.09.082.
- Grundling A, Manson MD, Young R. **(2001)**. Holins kill without warning. Proc Natl Acad Sci U S A 98: 9348-9352
- Gutiérrez D, Briers Y. **(2021)**. Lysins breaking down the walls of Gram-negative bacteria, no longer a no-go. Curr Opin Biotechnol. 68:15-22. doi: 10.1016/j.copbio.2020.08.014.
- Helander IM, Mattila-Sandholm T. **(2000)**. Fluorometric assessment of gram-negative bacterial permeabilization. J Appl Microbiol. 88(2):213-9. doi: 10.1046/j.1365-2672.2000.00971.x.
- Hibstu Z, Belew H, Akelew Y, Mengist HM. **(2022)**. Phage Therapy: A Different Approach to Fight Bacterial Infections. *Biologics*. 16:173-186. doi:10.2147/BTT.S381237
- Janssen P, Maquelin K, Coopman R, Tjernberg I, Bouvet P, Kersters K, Dijkshoorn L. **(1997)**. Discrimination of Acinetobacter genomic species by AFLP fingerprinting. Int J Syst Bacteriol 47:1179 –1187. https://doi.org/10.1099/00207713-47-4-1179
- Jun SY, Jang IJ, Yoon S, Jang K, Yu K, Cho JY, Seong M, Jung GM, Yoon SJ, Kang SH. **(2017)**. Pharmacokinetics and Tolerance of the Phage Endolysin-Based Candidate Drug SAL200 after a Single Intravenous Administration among Healthy Volunteers. Antimicrob Agents Chemother 61:10.1128/aac.02629-16. https://doi.org/10.1128/aac.02629-16
- Little JW. **(2005)**. Lysogeny, Prophage Induction, and Lysogenic Conversion. *Phages*. https://doi.org/10.1128/9781555816506.ch3
- Liu H, Hu Z, Li M, Yang Y, Lu S, Rao X. **(2023)**. Therapeutic potential of bacteriophage endolysins for infections caused by Gram-positive bacteria. *J Biomed Sci*. 30(1):29. doi:10.1186/s12929-023-00919-1
- Loessner MJ. **(2005)**. Bacteriophage endolysins--current state of research and applications. Curr Opin Microbiol. 8(4):480-7. doi: 10.1016/j.mib.2005.06.002.
- Mirdita, M., Schütze, K., Moriwaki, Y. *et al.* **(2022)**. ColabFold: making protein folding accessible to all. *Nat Methods* 19, 679–682. https://doi.org/10.1038/s41592-022-01488-1
- Mulder, N., Apweiler, R. **(2007)**. InterPro and InterProScan. In: Bergman, N.H. (eds) Comparative Genomics. Methods In Molecular Biology™, vol 396. Humana Press. https://doi.org/10.1007/978-1-59745-515-2_5
- Murphy KC. **(2012)**. Phage recombinases and their applications. Adv Virus Res. 83:367-414. doi: 10.1016/B978-0-12-394438-2.00008-6.
- Murray E, Draper LA, Ross RP, Hill C. **(2021)**. The Advantages and Challenges of Using Endolysins in a Clinical Setting. *Viruses*. 13(4):680. doi:10.3390/v13040680
- Nakimbugwe D, Masschalck B, Atanassova M, Zewdie-Bosüner A, Michiels CW. **(2006)**. Comparison of bactericidal activity of six lysozimes at athosferic pressure and under high hydrostatic pressure. *Int J Food Microbiol*, 108:355-363.

- Nazir A, Xu X, Liu Y, Chen Y. **(2023)**. Phage Endolysins: Advances in the World of Food Safety. *Cells*. 12(17):2169. doi:10.3390/cells12172169
- Nelson D, Loomis L, Fischetti VA. **(2001)**. Prevention and elimination of upper respiratory colonization of mice by group A streptococci by using a bacteriophage lytic enzyme. *Proc Natl Acad Sci U S A*. 98(7):4107-4112. doi:10.1073/pnas.061038398
- Oliveira H, Melo LD, Santos SB, Nóbrega FL, Ferreira EC, Cerca N, Azeredo J, Kluskens LD. **(2013)**. Molecular aspects and comparative genomics of bacteriophage endolysins. J Virol. 87(8):4558-70. doi: 10.1128/JVI.03277-12.
- Oliveira H, Thiagarajan V, Walmagh M, Sillankorva S, Lavigne R, Neves-Petersen MT, Kluskens LD, Azeredo J. **(2014)**. A thermostable Salmonella phage endolysin, Lys68, with broad bactericidal properties against gram-negative pathogens in presence of weak acids. PLoS One. 9(10):e108376. doi: 10.1371/journal.pone.0108376.
- Park HS, Lin S, Voordouw G. **(2008)**. Ferric iron reduction by Desulfovibrio vulgaris Hildenborough wild type and energy metabolism mutants. Antonie Van Leeuwenhoek. 93(1-2):79-85. doi: 10.1007/s10482-007-9181-3.
- Pattnaik A, Pati S, Samal SK. **(2024)**. Bacteriophage as a potential biotherapeutics to combat present-day crisis of multi-drug resistant pathogens. Heliyon, Volume 10, Issue 18, e37489. https://doi.org/10.1016/j.heliyon.2024.e37489
- Raetz CR, Whitfield C. **(2002)**. Lipopolysaccharide endotoxins. Annu Rev Biochem. 71:635-700. doi: 10.1146/annurev.biochem.71.110601.135414.
- Rodríguez-Rubio L, Martínez B, Donovan DM, Rodríguez A, García P. **(2013)**. Bacteriophage virion-associated peptidoglycan hydrolases: potential new enzybiotics. Crit Rev Microbiol. 39(4):427-34. doi: 10.3109/1040841X.2012.723675.
- Santos SB, Costa AR, Carvalho C, Nóbrega FL, Azeredo J. **(2018)**. Exploiting Bacteriophage Proteomes: The Hidden Biotechnological Potential. Trends Biotechnol. 36(9):966-984. doi: 10.1016/j.tibtech.2018.04.006.
- São-José C. **(2018)**. Engineering of Phage-Derived Lytic Enzymes: Improving Their Potential as Antimicrobials. *Antibiotics (Basel)*. 2018;7(2):29. doi:10.3390/antibiotics7020029.
- Savva CG, Dewey JS, Moussa SH, To KH, Holzenburg A, Young R. **(2014)**. Stable micron-scale holes are a general feature of canonical holins. Mol. Microbiol. 91, 57–65. https://doi.org/10.1111/mmi.12439.
- Schmelcher M, Donovan DM, Loessner MJ. **(2012)**. Bacteriophage endolysins as novel antimicrobials. Future Microbiol. 7(10):1147-71. doi: 10.2217/fmb.12.97.
- Skerlavaj B, Benincasa M, Risso A, Zanetti M, Gennaro R. **(1999)**. SMAP-29: a potent antibacterial and antifungal peptide from sheep leukocytes. FEBS Lett. 463(1-2):58-62. doi: 10.1016/s0014-5793(99)01600-2.
- Stanley SY, Maxwell KL. **(2018)**. Phage-Encoded Anti-CRISPR Defenses. Annu Rev Genet. 52:445-464. doi: 10.1146/annurev-genet-120417-031321.
- Stone R. **(2002)**. Bacteriophage therapy. Stalin's forgotten cure. Science. 298(5594):728-31. doi: 10.1126/science.298.5594.728. PMID: 12399562.
- Sun J, Rutherford ST, Silhavy TJ, Huang KC. **(2022)**. Physical properties of the bacterial outer membrane. Nat Rev Microbiol. 20(4):236-248. doi: 10.1038/s41579-021-00638-0.
- Tabor S, Richardson CC. **(1985)**. A bacteriophage T7 RNA polymerase/promoter system for controlled exclusive expression of specific genes. Proc Natl Acad Sci U S A. 82(4):1074-8. doi: 10.1073/pnas.82.4.1074.

- Topka-Bielecka G, Dydecka A, Necel A, Bloch S, Nejman-Falen´czyk B, Wegrzyn G, Wegrzyn A. **(2021)**. Bacteriophage-Derived Depolymerases against Bacterial Biofilm. *Antibiotics*, *10*, 175. https://doi.org/10.3390/antibiotics 10020175
- Totté J, de Wit J, Pardo L, Schuren F, van Doorn M, Pasmans S. **(2017)**. Targeted anti-staphylococcal therapy with endolysins in atopic dermatitis and the effect on steroid use, disease severity and the microbiome: study protocol for a randomized controlled trial (MAAS trial). Trials. 18(1):404. doi: 10.1186/s13063-017-2118-x.
- Traczewski MM, Ambler JE, Schuch R. **(2021)**. Determination of MIC Quality Control Parameters for Exebacase, a Novel Lysin with Antistaphylococcal Activity. J Clin Microbiol. 59(7):e0311720. doi: 10.1128/JCM.03117-20.
- Twort FW. **(1915)**. An investigation on the nature of ultra-microscopic viruses. The Lancet, Volume 186, Issue 4814, 1241-1243.
- Vaara M, Nurminen M. **(1999)**. Outer membrane permeability barrier in Escherichia coli mutants that are defective in the late acyltransferases of lipid A biosynthesis. Antimicrob Agents Chemother. 43(6):1459-62. doi: 10.1128/AAC.43.6.1459.
- Vaara M. **(1992)**. Agents that increase the permeability of the outer membrane. Microbiol Rev. 56(3):395-411. doi: 10.1128/mr.56.3.395-411.1992.
- Vázquez R, Briers Y. **(2023)**. What's in a Name? An Overview of the Proliferating Nomenclature in the Field of Phage Lysins. *Cells*. 12(15):2016. doi:10.3390/cells12152016
- Watson A, Oh JT, Sauve K, Bradford PA, Cassino C, Schuch R. **(2019)**. Antimicrobial Activity of Exebacase (Lysin CF-301) against the Most Common Causes of Infective Endocarditis. Antimicrob Agents Chemother. 63(10):e01078-19. doi: 10.1128/AAC.01078-19.
- WHO. **(2020)**. Antibacterial agents in clinical and preclinical development: an overview and analysis.
- WHO. **(2023)**. Antimicrobial Resistance Facts, https://www.who.int/news-room/fact-sheets/detail/antimicrobial-resistance.
- Young R. **(1992)**. Bacteriophage lysis: mechanism and regulation. Microbiol Rev. 56(3):430-81. doi: 10.1128/mr.56.3.430-481.1992.

Chapter 4

Characterization of bacterial communities associated with seabed sediments in offshore and nearshore sites to improve Microbiologically Influenced Corrosion mitigation on marine infrastructures

Daniele Ghezzi[1,2], Gianmarco Mangiaterra[1], Arianna Scardino[1], Mauro Fehervari[3], Mauro Magnani[1], Barbara Citterio[1] and Emanuela Frangipani[1*]

[1]*Department of Biomolecular Sciences, University of Urbino Carlo Bo, Urbino (PU), Italy*

[2]*Present address: Department of Pharmacy and Biotechnology, University of Bologna, Bologna (BO), Italy*

[3]*R&D Engineering, Asset Based Services - Saipem SpA, Fano (PU), Italy*

Manuscript published in PLoS ONE on September 4th, 2024

https://doi.org/10.1371/journal.pone.0309971

Preface to Chapter 4

Microbiologically Influenced Corrosion (MIC) is a critical threat to marine infrastructures, posing significant safety and environmental risks due to structural failures and potential leakages of hazardous substances. These risks, coupled with substantial economic losses and reputational damage, underscore the necessity for proactive MIC management. Understanding site-specific microbial communities in marine sediments is essential for the safe design, installation, and maintenance of infrastructure systems in such environments. In this context, Chapter 4 describes the characterization of bacterial communities in offshore and nearshore marine sediments, with a particular focus on groups implicated in MIC processes. Results presented in this Chapter have been published as a Research Article to *PLoS One*. Using 16S rRNA sequencing and quantitative PCR targeting the *dsrA* gene, the research highlights differences in microbial profiles between nearshore sediments, enriched with sulfate-reducing bacteria (SRB) like *Desulfobulbus* and *Desulfosarcina* genera due to anthropogenic contamination, and offshore sediments, characterized by bacterial members typical of low-impact environments. The findings demonstrate that microbial communities influenced by high levels of organic compounds derived from human activities are more likely to drive MIC. This study emphasizes the importance of microbiological investigations as a preventive strategy against MIC. The profiling of sedimentary bacterial communities can identify suitable sites for infrastructure development and enable the monitoring of microbial evolution near existing installations, mitigating MIC at early stages. Advances in omic technologies have made such analyses more accessible and efficient, offering valuable tools to support infrastructure resilience and environmental sustainability.

Finally, this work advocates for the integration of microbial community characterization into MIC management practices. This proactive approach holds promise to enhance early detection and mitigation of MIC, safeguarding marine infrastructures from corrosion-induced failures.

PLOS ONE

RESEARCH ARTICLE

Characterization of bacterial communities associated with seabed sediments in offshore and nearshore sites to improve Microbiologically Influenced Corrosion mitigation on marine infrastructures

Daniele Ghezzi[1¤], **Gianmarco Mangiaterra**[1], **Arianna Scardino**[1], **Mauro Fehervari**[2], **Mauro Magnani**[1], **Barbara Citterio**[1], **Emanuela Frangipani**[1]*

1 Department of Biomolecular Sciences, University of Urbino Carlo Bo, Urbino (PU), Italy, **2** R&D Engineering, Asset Based Services—Saipem SpA, Fano (PU), Italy

¤ Current address: Department of Pharmacy and Biotechnology, University of Bologna, Bologna (BO), Italy
* emanuela.frangipani@uniurb.it

Citation: Ghezzi D, Mangiaterra G, Scardino A, Fehervari M, Magnani M, Citterio B, et al. (2024) Characterization of bacterial communities associated with seabed sediments in offshore and nearshore sites to improve Microbiologically Influenced Corrosion mitigation on marine infrastructures. PLoS ONE 19(9): e0309971. https://doi.org/10.1371/journal.pone.0309971

Editor: John M. Senko, The University of Akron, UNITED STATES OF AMERICA

Received: May 22, 2024

Accepted: August 19, 2024

Published: September 4, 2024

Data Availability Statement: The Illumina sequencing raw data were deposited in the Sequence Read Archive of NCBI under accession number PRJNA1053306, and are already available.

Funding: D.G. and G.M. salaries were co-financed by the European Union – PON Ricerca e Innovazione 2014-2020 pursuant to art. 24, lett. a, of Law 30 December 2010, n. 240 and subsequent amendments and integration and of the D. M. 10

Abstract

Microbiologically Influenced Corrosion (MIC) is one of the main threats for marine infrastructures, leading to severe safety and environmental risks associated with structural failures and/or leakages of dangerous fluids, together with potential huge economic losses and reputational damage for the involved parts. For a safe design and a proper installation of infrastructure systems in contact with the seabed, a deep knowledge of the site-specific microbial community of the sediments should be beneficial. Therefore, in addition to the simple detection or the sole quantification of Sulphate-Reducing Bacteria (SRB), the whole characterization of the microbial members involved in MIC phenomena is desirable. In this study, 16S rRNA-based comparison between bacterial communities thriving in offshore and nearshore marine sediments was performed, with a focus on the main bacterial groups putatively responsible for MIC. The nearshore sediments were significantly enriched in bacterial members associated with human and organic compounds contamination belonging to the *Bacteroidota*, *Desulfobacterota*, and *Firmicutes* phyla, while the offshore sediments hosted *Alphaproteobacteria*, *Nitrospinota*, and *Nitrospirota* members, representative of a low anthropogenic impact. Quantitative PCR targeting the *dsrA* gene and detailed community analyses revealed that the nearshore sediments were significantly enriched in SRB mainly affiliated to the *Desulfobulbus* and *Desulfosarcina* genera potentially involved in biocorrosion, compared to the offshore ones. These results suggest that the bacterial community associated with the high concentration of organic compounds derived by an elevated anthropogenic impact is likely to favour MIC. Such observations highlight the importance of microbiological investigations as prevention strategy against MIC processes, aiming both at characterizing sites for the establishment of new infrastructures and at monitoring those already installed.

August 2021, n. 1062 (CUP H31B21009620007). This work was partially financed by Saipem SpA, Fano (PU), Italy (WO # 31370240). the role of Funders, Saipem S.p.A. contributed by providing raw samples and the related environmental data.

Competing interests: The authors have declared that no competing interests exist.

Introduction

Corrosion of metal infrastructures in aquatic settings raises significant worries regarding environmental pollution, potential harm to aquatic ecosystems, degradation of infrastructure integrity, and substantial economic losses [1]. Metal abiotic deterioration is further accelerated by the involvement of biofouling and Microbiologically Influenced Corrosion (MIC), two mechanisms mediated by the biological activity of different organisms [2]. Biofouling refers to the accumulation and growth of various micro- and macro- organisms, including plants and/or animals (*e.g.*, algae, mussels, bernacles) on a specific surface [3], while MIC has been defined by the National Association of Corrosion Engineers (NACE) and the American Society for Testing and Materials (ASTM) as "*corrosion affected by the presence or activity, or both, of microorganisms*" (ASTM G193 2022) and denotes a complex process caused only by microorganisms and/or their metabolites on metallic surfaces that can accelerate corrosion by 10–1,000 times [4]. Although the potential for MIC can be found in both freshwater and seawater, the latter represents an extremely harsh corrosive environment, favoring MIC and leading to the breakdown or degradation of metallic materials also through an electrochemical reaction stimulated by the naturally high salt concentration, combined with its elevated electrical conductivity [5, 6]. Indeed, the high sulfate content of seawater (*i.e.*, 2.5–5 g L^{-1}) [7] also supports the metabolic activity of specific bacterial taxa responsible for MIC, thus indirectly boosting the corrosive process.

MIC constitutes the main significant challenge for the maintenance of marine infrastructures, deeply affecting many industrial fields, including the oil, gas and water utilities ones [8], being the direct cause of catastrophic corrosion failures with very high associated damage costs. In this regard, according to estimates by NACE International, the total cost of corrosion is *ca*. US$ 2.5 trillion/year globally, with MIC accounting for 20%–40% [9–11]. Furthermore, MIC and abiotic corrosion often occur simultaneously, making it challenging to differentiate the costs attributed to these two processes independently [12]. The key categories of bacteria linked to metal corrosion vary according to their metabolic activities, primarily encompassing Sulfate-Reducing Bacteria (SRB), Acid Producing Bacteria (APB), Sulfur-Oxidizing Bacteria (SOB), Metal-Oxidizing Bacteria (MOB), Metal-Reducing Bacteria (MRB), Slime-Forming Bacteria (SFB) and microorganisms that produce organic acids and are able to grow as biofilms [4, 13]. Usually, aerobic and facultative microorganisms tend to be found in the outer layers of the biofilm and establish the conditions that promote metal corrosion, but most corrosion has been attributed to anaerobes that are located in the inner layer of the biofilm [14]. Among these, SRB are the most reported corrosion-related microbes, as well as the best characterized. SRB play key roles in the carbon and sulfur cycles in marine environments by participating in the dissimilatory sulfate reduction process [15, 16]. They are estimated to perform half of the organic matter mineralization and degrade a variety of byproducts [17]. As a consequence of the organic matter degradation and sulfate reduction, SRB produce hydrogen sulfide (H_2S) that accumulates in sediment and diffuses towards the shallower sea layers where it promotes corrosive processes to the marine infrastructures [18]. Indeed, SRB are considered one of the main types of microorganisms responsible for MIC and can cause severe issues both in terms of hydrocarbon contaminants pollution and economic losses, causing corrosive phenomena in downstream processes of companies working on marine infrastructures and offshore oil producers [19]. Moreover, SRB are able to adhere to metal surfaces and form biofilms characterised by the presence of a thick exopolysaccharide (EPS) matrix, that contributes to the establishment of a localized, oxygen-depleted, and corrosive microenvironment. The H_2S produced by SRB reacts with the metal surface, leading to the formation of iron sulfides (FeS) that

can initiate pitting and under deposit corrosion. These localized areas of corrosion can, in turn, lead to structural damages and the eventual failure of metal components [20].

To prevent and limit MIC in marine infrastructures, multiple strategies are currently in use aiming at fighting the adhesion and biofilm formation of the microorganisms on the surfaces. The most applied approach includes the employment of chemicals before and/or during the usage of the infrastructures, which are highly effective, but also toxic for non corrosion-causing organisms present in the marine ecosystem, causing great environmental concern in the long run [13]. Additional strategies include the development of coatings appliable on the surfaces with anti-adhesion and antibiofilm capacity, but their efficacy over time is often limited [21, 22], and the cathodic protection, which is useful to reduce the migration of electron during corrosion, can occasionally promote bacterial corrosion [13]. Moreover, applicable technical standards are duly implemented during design to properly consider all known aspects of corrosion [23, 24], since operating practices may create conditions that promote the proliferation and spread of biocorrosive microorganisms, especially in offshore oil-producing platforms [25]. Moreover, in specific sites where the SRB presence and H_2S abundance have been definitely recognized in the sediments (*e.g.*, Black sea and Baltic sea), dedicated analyses are adopted to select materials and design cathodic protection of strategic infrastructures which pass through such critical environments, like large export gas pipelines [26, 27].

MIC assessment in the oil and gas industry is mainly estimated using culture-based methods (*i.e.*, Most Probable Number determination), which are biased by the complex growth conditions of SRB. Culture-independent molecular studies on bacterial communities impacting MIC are listed by NACE as non mandatory methods, although there has been much more emphasis in the past decade on the potential use of these molecular methods to aid in defining the potential risk for MIC and provide insight into microbial control strategy to list sites that requires periodic monitoring [28, 29].

Apart from these strategies, which are employed regardless of the microbiome composition of the sites, there are currently no additional standard mandatory analyses planned prior to the installation of marine infrastructures, to detect the presence of specific microorganisms potentially capable of carrying out corrosion in the sites of interest.

In this work, the microbial communities associated to anthropogenically-impacted nearshore and to less impacted offshore marine sediments were analysed through metabarcoding sequencing targeting the V3 and V4 hypervariable regions of the 16S rRNA gene to gain information on the possible proneness of these two different sites to develop MIC, affecting marine infrastructures. Furthermore, the quantification of SRB was assessed through quantitative PCR targeting the *dsrA* gene involved in the dissimilatory sulfate reduction process. Sediment samples were collected from the Trieste port and the Norwegian Barents Sea in the proximity of an oil/gas extraction platform. Trieste port is part of the contaminated Sites of National Interest, which include several areas featured by high levels of hazardous contaminants that can provoke serious damages to the environment, to the human health, and to the cultural heritage [30–32]. Indeed, ports suffer numerous dangerous environmental impacts mainly due to the discharge of petroleum-based pollutants in combination with the morphological structure of the port area, which is bordered by lands and promotes the accumulation of contaminants on site that require a complex remediation policy [33]. Conversely, the Barents Sea is an open marine system, where large amounts of dispersed organic matter from the northern Atlantic and Arctic oceans interchange, mainly precipitating on the sea bottom [34–36]. The sampling site in the Norwegian Barents Sea is featured by a different human-dependent contamination typology, which is represented by the presence of a drilling platform installed at 100 km far from the coast in the nearby of the collected sediments. These samples have been chosen as case studies to assess the microbial community composition of two differentially human-

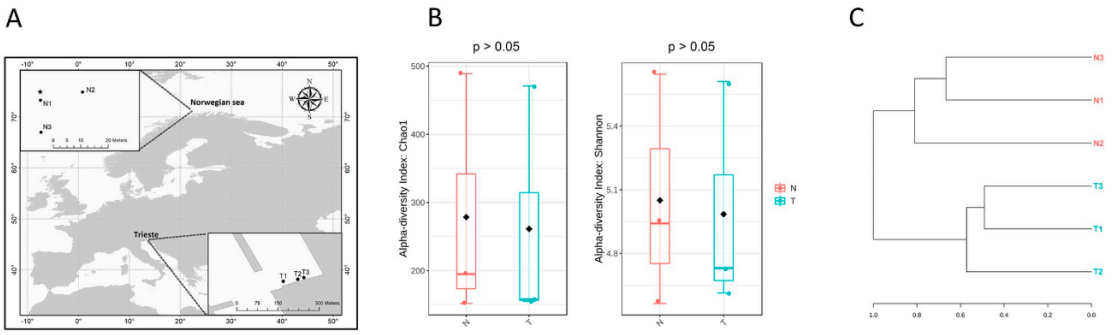

Fig 1. Samples' geographical localization and microbial diversity. A) Geographical map of Norway (N) and Trieste (T) sample sites. The star indicates the position of the Scarabeo 8 offshore semisubmersible drilling unit. B) Chao1 and Shannon indices of microbial communities at Amplicon Sequence Variant (ASV) level detected in N and T sediments. C) Dendrogram of N and T microbial communities at ASV level.

https://doi.org/10.1371/journal.pone.0309971.g001

impacted locations, to evaluate the ecological health of marine sediments and to discuss the importance of monitoring the evolution of microbial groups involved in corrosion processes, as a strategy to prevent and/or mitigate MIC.

Materials and methods

Sampling and environmental parameters

Sediments (between 100 and 200 g each) were collected in March 2021, during routine operations conducted by Saipem S.p.A., and stored in sterile containers at 4˚C during transport to the laboratory, where they were kept at -80˚C until processed. For each sediment sample, three DNA extractions were performed and pooled. Norway sediments (N1, N2, and N3) were collected from the surface of the seabed in undisturbed locations in the Goliat field at 370 m depth in the proximity of the Saipem's Scarabeo 8 offshore semisubmersible drilling rig (Fig 1A, S1 Table). N sediments were collected with a Van Veen grab sampler at 4 m South, 15 m East, and 15 m South of the platform, respectively (S1 Table, Fig 1A). Trieste (Italy) sediments (T1, T2, and T3) were collected from a seabed close to a Saipem SpA base within a 50-m port area at 8–9 m depth.

Environmental parameters were either measured in the lab upon sample reception (pH) or retrieved from dedicated databases and Saipem S.p.A. internal reports, as detailed in S2 Table. Since this work focuses on the environmental features potentiating MIC, the material of the infrastructures and the activity of the microorganisms on them were not investigated.

Total DNA extraction, 16S rRNA gene amplification and sequencing

Total DNA was extracted from around 250 mg of homogenized sample using the PowerSoil DNA Isolation Kit (Qiagen) with slight modifications, as previously described [37]. Three independent extractions were performed for each sample, and the obtained DNA was pooled. The V3 and V4 hypervariable regions of the 16S rRNA gene were amplified using 341F (`5′-CCTACGGGNGGCWGCAG-3′`) and 806R (`5′-GACTACHVGGGTATCTAATCC-3′`) primers pair [38] with 5'-Illumina adapters and for MiSeq Illumina sequencing. The amplifications were performed in 25 μl final volume containing 1x KAPA HiFi HotStart Ready Mix, 0.2 μM each primer, and 30 ng DNA (Bio-Fab Research s.r.l., Rome—Italy). The amplification program included a first DNA denaturation at 95˚C for 3 minutes, followed by 25 cycles of

denaturation at 95˚C for 30 seconds, primer annealing at 55˚C for 30 seconds, extension at 72˚C for 30 seconds, and a final extension at 72˚C for 5 minutes. Amplicons were submitted to the library preparation and Illumina MiSeq sequencing platform for indexing and pair-end sequencing (2 × 300 bp; reagent kit, v2) at the sequencing service Bio-Fab Research s.r.l.

The Illumina sequencing raw data were deposited in the Sequence Read Archive of NCBI under accession number PRJNA1053306.

Data processing

The output reads were first trimmed for their adapters and primer sequences and then checked for chimera and quality by using QIIME2 software version 2022.2.0. Reads were processed into Amplicon Sequence Variants (ASVs) using the DADA2 package version 1.14, as described in [39]. Statistical analyses, rarefaction curves, alpha and beta diversity indices calculation were performed by using Microbiome Analyst software [40] and Primer-E version 7 (Primer-E Ltd, Plymouth, UK). The taxonomic assignment of the resulting ASVs was performed by querying the ASVs against SILVA SSU database version r138.1 [41]. Eukaryotic, mitochondrial, and chloroplast sequences were removed from further analyses. Differentially abundant taxa were assessed by performing ANOVA-based single-factor analysis in Microbiome Analyst.

An unrooted phylogenetic tree was built with the neighbor-joining method, maximizing the likelihood with a gamma model distribution, and using the most abundant ASVs representative of each sample together with the most closely related sequences retrieved from the NCBI database (Best Blast Hits). MEGA11 [42] was used to construct phylogenetic trees based on ClustalW sequences alignment and neighbor-joining clustering method with 1,000 non-parametric bootstrap replicates (model: Jukes-Cantor; rates among site: uniform rates; gap/missing data treatment: pairwise deletion). iTOL was used to visualize the phylogenetic tree.

Quantitative PCR targeting the drsA gene

The SRB population was quantified in the sediment samples by qPCR assays targeting the alpha subunit of the dissimilatory sulfate reductase (*dsrA*) gene. The reactions were performed using 10 μl of the 2x QuantiNova SYBR Green PCR Master Mix (Qiagen), 2 μl of template DNA and 0.2 μM of each primer of the previously described pair DSR1-F+ (5′-ACSCACTG GAAGCACGGCGG-3′)/DSR-R (5′-GTGGMRCCGTGCAKRTTGG-3′) [43].

A calibration curve was built using 10-fold dilutions of the purified *dsrA* amplicon from the genomic DNA of *Desulfovibrio vulgaris* ATCC 29579, according to a previously validated qPCR setting [44], properly modified for this target gene. The gene copy number was determined dividing the total quantified DNA by the weight of one amplicon copy, *i.e.*, 2.42×10^{-10} ng, calculated considering the amplicon size (221 bp) and the weight of 1 bp (1.10×10^{-12} ng). Each sample was tested in duplicate in two independent reactions. The results were expressed as gene copy number per gram of sediment.

Results

Sequencing results and diversity analysis

A total of 54,771 reads were obtained of which 28,865 from the Norway (N) samples and 25,906 from the Trieste (T) samples (S1 Table). The processed ASVs were 836 and 784 for N and T microbial communities, respectively, with N2 and T2 having the highest number of ASVs (*i.e.*, 489 and 471, respectively). The rarefaction curves showed that the sequencing provided sufficient depth to investigate the microbial community composition and diversity (S1 Fig). The alpha diversity indices calculation revealed that Chao1 and Shannon mean values

were not significantly different between N and T sediments (Fig 1B), whereas Bray-Curtis analysis at ASV level revealed two clusters corresponding to the two different sample groups, with T communities being more similar among each other compared to N ones (Fig 1C).

Taxonomy composition of the microbial communities in offshore and nearshore sediments

The offshore N sediments presented 14 high abundant (>2% in at least one sample) bacterial phyla, while nearshore T sediments were composed of 10 high abundant bacterial phyla. Among these, DTB120, *Gemmatimonadota*, *Methylomirabilota*, NB1-j, *Nitrospirota*, *Planctomycetota*, and *Verrucomicrobiota* were more abundant in N, while *Campylobacterota*, *Myxococcota*, and Sva0485 prevailed in T (Fig 2A). Proteobacteria represented the most abundant phylum in both sites and was mainly composed of *Alphaproteobacteria* and *Gammaproteobacteria* classes. The average abundance (avg.) of *Gammaproteobacteria* accounted for 23% in T and 21% in N, while *Alphaproteobacteria* were highly abundant in N only (avg. 21%), and poorly present in T (avg. 2%) (Fig 2B). *Gammaproteobacteria* were distinguished between N and T at lower taxonomic levels. In N, they were taxonomically affiliated to genera of the *Pseudomonadales* order, *i.e.*, *Alcanivorax*, *Amphritea*, and C1-B045 of the *Porticoccaceae* family, and to genera of the *Steroidobacterales* order, *e.g.*, *Woeseia*. On the other hand, *Gammaproteobacteria* in T were mainly composed of unclassified genera belonging to *Thiotrichaceae*, *Thiomicrospiraceae*, and *Sedimenticolaceae* families (Fig 2 and S2 Fig). The most abundant families of *Alphaproteobacteria* in N included *Rhodobacteraceae*, *Hyphomicrobiaceae*, *Kiloniellaceae*, and unclassified *Defluviicoccales* (Fig 2 and S2 Fig). The second most abundant phylum was represented by *Actinobacteriota* in N (avg. 9%; 2% in T) and *Desulfobacterota* in T (avg. 20%; 7% in N). *Actinobacteriota* in both sites were mainly affiliated to unclassified *Actinomarinales* order (Fig 2 and S2 Fig). *Desulfobacterota* in T were composed of the *Desulfobacterales* and *Desulfobulbales* orders and *Desulfosarcina* and *Desulfobulbus* genera, whereas in N they were affiliated to the *Desulfuromonadales* order and *Geopsychrobacter* genus (Fig 2 and S2 Fig).

Bacteroidota and *Firmicutes* phyla accounted for 16% (avg.) and 9% in T, whereas in N they composed 6% and 1% of the community, respectively. In T, *Bacteroidota* were composed of *Cyclobacteriaceae* and *Flavobacteriaceae* families, whereas *Firmicutes* were composed of *Erysipelotrichaceae* (mainly *Turicibacter*), *Clostridiaceae* (mainly *Clostridium*), and *Peptostreptococcaceae* (mainly *Romboutsia*). *Campylobacterota* were also highly abundant in T only (avg. 7%) and were composed of *Sulfurimonadaceae* (mainly *Sulfurimonas*) and *Sulfurovaceae* (mainly *Sulfurovum*) families (S2 Fig).

Additional phyla present in N and T were *Planctomycetota* (avg. 4% and 1%, respectively), *Nitrospirota* (avg. 3% and <1%), *Acidobacteriota* (avg. 5% and 4%), *Myxococcota* (avg. 2% in both sites), *Chloroflexi* (avg. 4% and 7%), *Verrucomicrobiota* (avg. 2% and <1%), *Gemmatimonadota* (avg. 2% and <1%), and Sva0485 (avg. <1% and 2%) (Fig 2).

Abundant (>3% in at least one sample) classified genera belonging to these phyla included *Lutibacter* of the *Flavobacteriaceae* family (*Bacteroidota*), *Nitrospira* (*Nitrospirota*), and the acidobacterial Subgroup 10 and Subgroup 23 genera of the *Thermoanaerobaculaceae* family. Whilst all the abundant phyla in T were also present in N, some abundant phyla in N were not present in T, *i.e.*, DTB120 (avg. 2%), NB1-j (2%), and *Methylomirabilota* (3%) (S2 Fig).

Differentially abundant taxonomic analysis was performed to compare the microbial communities of the two different location and identify the bacterial taxa significantly describing each sampling location. At phylum level, T sediments were significantly ($p<0.05$) enriched in *Bacteroidota*, *Desulfobacterota*, *Firmicutes*, and Sva0485 (Fig 3A). Their affiliated genera significantly present in T were *Clostridium*, *Desulfobulbus*, and *Desulfosarcina* (Fig 3B). On the

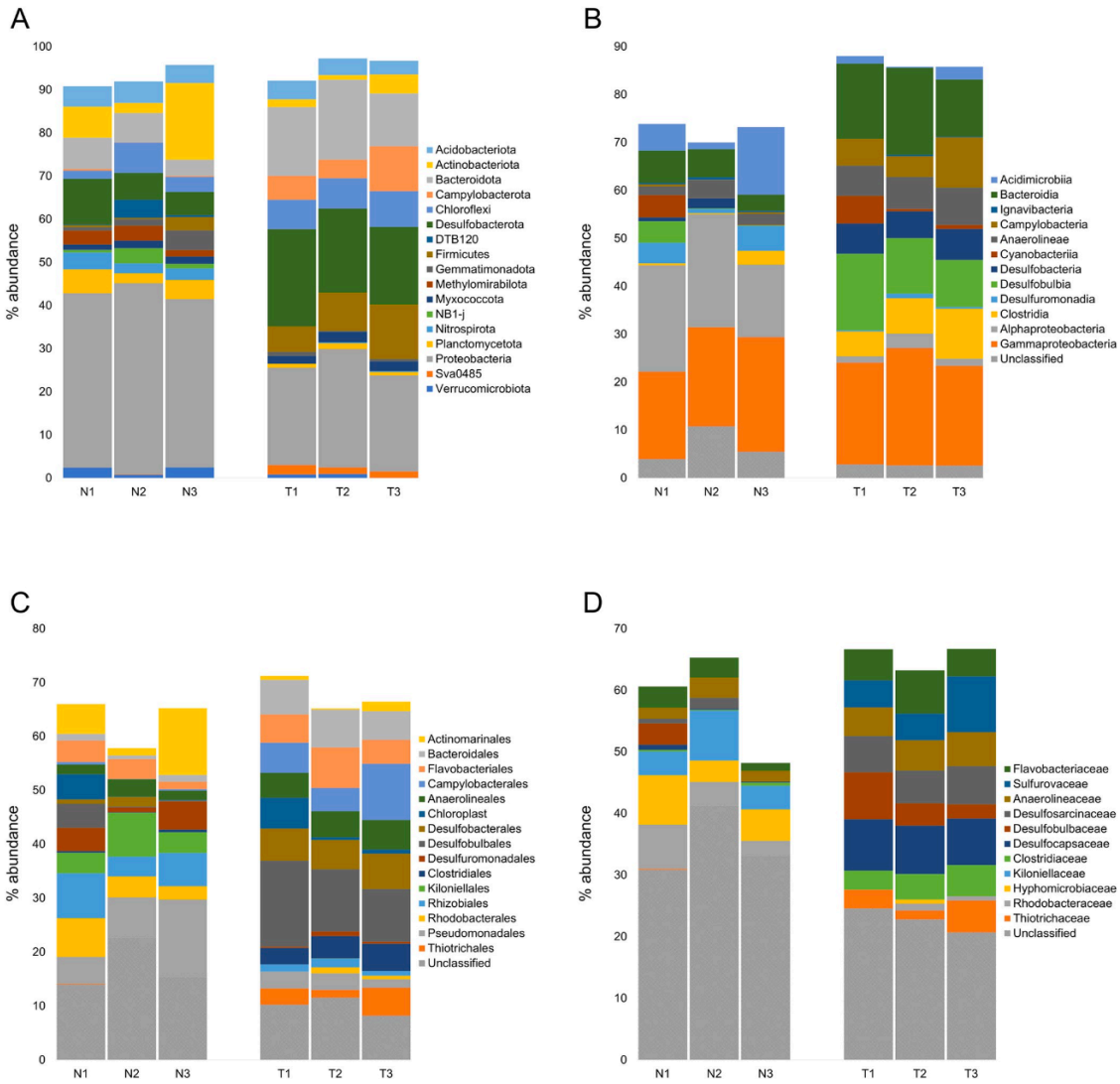

Fig 2. Microbial community composition. Taxonomy composition of offshore N and nearshore T microbial communities at A) phylum level, with abundances >2% in at least one sample, B) class, C) order, and D) family levels, with abundances >5% in at least one sample.

https://doi.org/10.1371/journal.pone.0309971.g002

other hand, N sediments were featured with the presence of *Methylomirabilota*, *Nitrospinota*, and *Nitrospirota* phyla, along with members of *Proteobacteria* (mainly of the *Alphaproteobacteria* class). At genus level, N were characterized by *Nitrospina*, *Nitrospira*, wb1_A12, and *Woeseia* (Fig 3B). Taxonomically unclassified sequences at phylum level were significantly abundant in N sediments (Fig 3A).

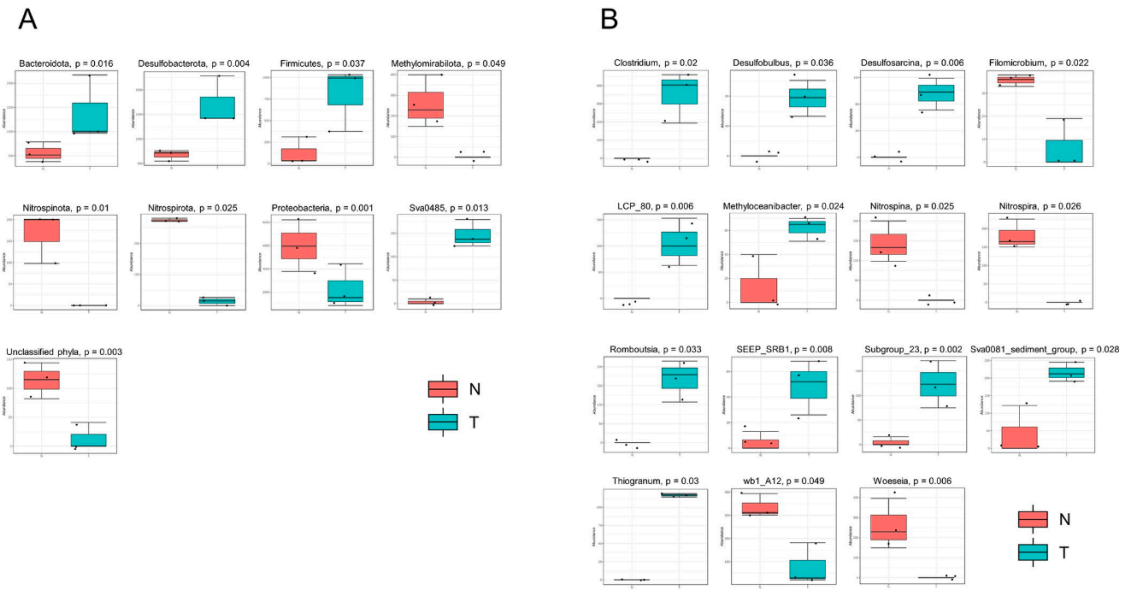

Fig 3. Microbial taxa enriched in Trieste and Norway sediments. Differentially abundant microbial phyla (A) and genera (B) between offshore N and nearshore T sediments. Only taxa significantly ($p<0.05$) enriched in N or T are shown.

https://doi.org/10.1371/journal.pone.0309971.g003

Phylogenetic analysis of the most abundant ASVs identified in offshore and nearshore sediments

The most abundant ASVs obtained from both N and T samples analyses were used to build a phylogenetic tree together with their closest cultured and uncultured relatives retrieved from the NCBI database. These ASVs were taxonomically affiliated to the dominant phyla identified in the taxonomic analysis, *i.e.*, *Proteobacteria*, *Firmicutes*, *Actinobacterota*, *Methylomirabilota*, *Chloroflexi*, and *Desulfobacterota* (Fig 4).

Methylomirabilota- and *Actinobacteriota*-affiliated ASV0004 and ASV0017, respectively, were enriched in N sediments and shared >99% with uncultured representatives retrieved from non-contaminated sediments collected from an area within the Gulf of Mexico, where in 2010 the largest oil spill at sea in history took place after the Deepwater Horizon drilling platform explosion [45, 46]. ASV0004 shared low sequence identity (88%) with an isolate belonging to Candidatus *Methylomirabilis* retrieved from a reactor with anaerobic oxidation of methane coupled with nitrite reduction, while ASV0017 shared ~88% with a strain of *Rhabdothermincola sediminis* isolated from hot spring sediments. ASV0013 abundant in N shared ~96% with a strain of *Woesia oceani* isolated from coastal sediments and >99% with uncultured bacteria retrieved from non-contaminated sediments of the Gulf of Mexico and from manganese nodules in deep sea sediments. Three additional ASVs characterizing N sediments were affiliated with the *Alphaproteobacteria* class: ASV0002, which was >99% similar to clones retrieved from non-contaminated sediments of the Gulf of Mexico and shared ~97% identity with an isolate of the *Hypomicrobium aestuarii* species; ASV0003, which shared high nucleotide identity with an uncultured representative retrieved from an oil-contaminated surface brown layer of the Gulf of Mexico and shared ~97% with bacterial isolates of *Yoonia maritima* and *Thalassobacter stenotrophicus* species; ASV0012, which was >99% similar to clones

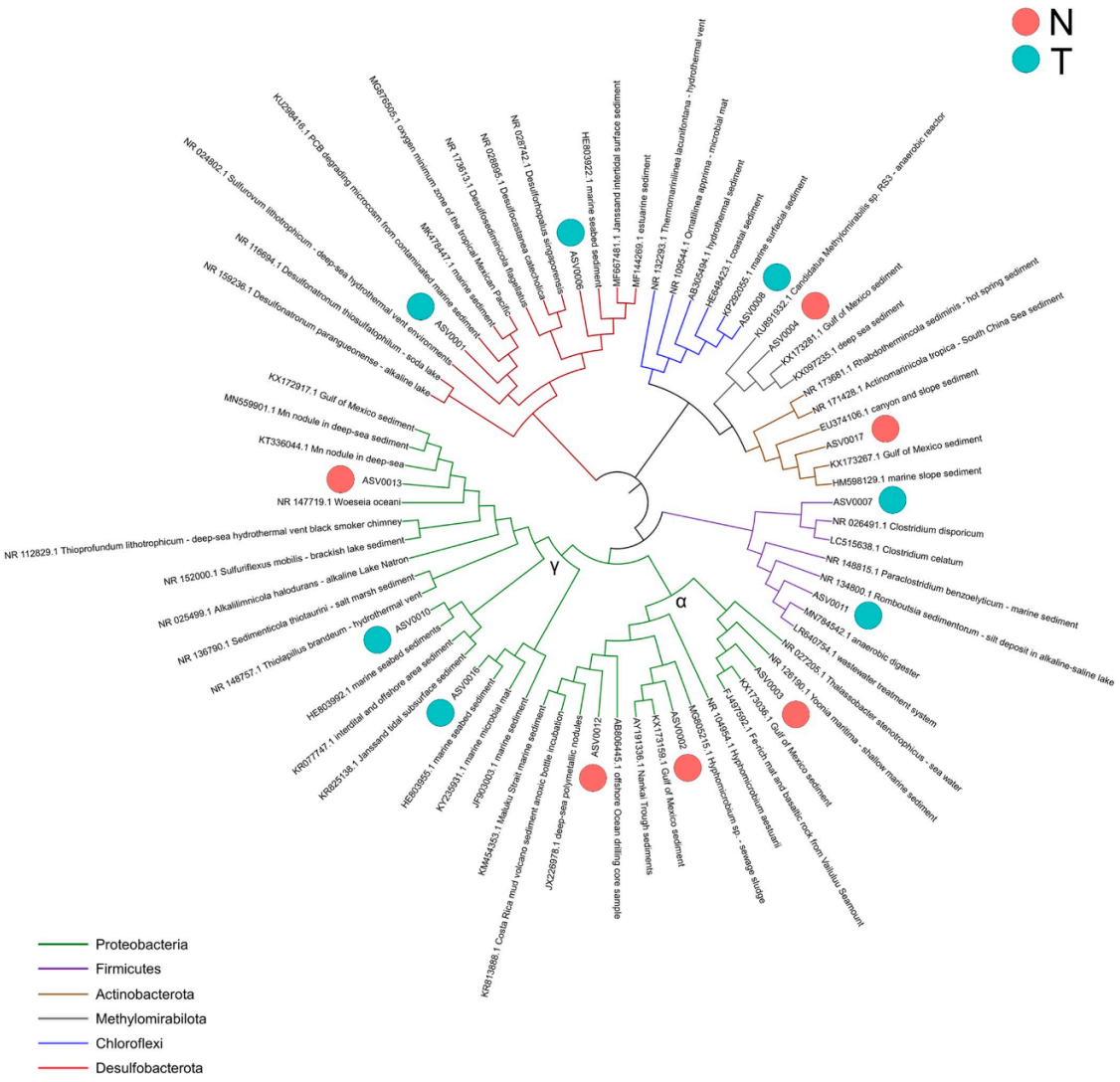

Fig 4. Phylogeny of ASVs identified from Trieste and Norway sediments. Phylogenetic tree showing the most abundant ASVs identified from offshore N and nearshore T microbial communities with their most similar sequences retrieved from the NCBI database. The ASVs characterizing N and T sediments are indicated with a red and blue dot, respectively.

https://doi.org/10.1371/journal.pone.0309971.g004

retrieved from deep sea metallic nodules and offshore drilling samples and shared ~97% identity with a *Hypomicrobium aestuarii* strain (Fig 4).

Among the seven ASVs characterizing T sediments, two were affiliated to *Desulfobacterota*, *i.e.*, ASV0001 and ASV0006. ASV0001 shared ~99% nucleotide identity with a cultured bacterial strain of *Sulfurovum lithotrophicum* isolated from deep-sea hydrothermal vents and with uncultured bacteria retrieved from contaminated marine sediments, whereas ASV0006 shared

94–95% identity with cultured strains of *Desulfosediminicola*, *Desulfocastanea*, and *Desulforhopalus* genera but formed a separated branch in the phylogenetic tree with uncultured clones from marine seabed sediments including the Janssand intertidal surface sediment (Fig 4). Additionally, the gammaproteobacterial ASV0010 and ASV0016 shared high percentage (>99%) with uncultured clones retrieved from marine sediments, including the Janssand ones (ASV0010 only), and low percentage (<93%) with cultured bacteria deposited in NCBI. ASV0010 shared ~92% with a cultured strain of *Thioprofundum lithotrophicum* isolated from a hydrothermal vent, whereas ASV0016 shared ~91% with a cultured strain of *Sedimenticola thiotaurini* isolated from a salt marsh sediment. One additional ASV characterizing T sediments was ASV0008, which shared >99% identity with uncultured clones retrieved hydrothermal and coastal sediments, and ~89% with a strain of *Thermomarinilinea lacunifontana* (belonging to the *Chloroflexi* phylum) isolated from a hydrothermal vent. Two *Firmicutes*-affiliated ASVs are indicators of anthropogenic impact of Trieste sediments, *i.e.*, ASV0007, which shared >99% identity with *Clostridium disporicum* and *Clostridium celatum* isolates, and ASV0011, which shared >99% with uncultured bacteria identified from a wastewater treatment system and cultured isolates belonging to *Romboutsia sedimentorum* species (Fig 4).

Quantification and community analysis of sulfate-reducing bacteria

Quantitative PCR targeting the *dsrA* gene, which encodes the alpha subunit of the dissimilatory sulfite reductase involved in the conversion of bisulfite to sulfide within the dissimilatory sulfate reduction pathway [47], was performed to assess the amount of SRB in both N and T sites. N sediments possessed a significant ($p < 0.01$) lower number of *dsrA* gene copies per gram compared to T sediments (1.8×10^6 and 3.5×10^7, respectively) (S3 Fig).

To identify possible significant differences among SRB between N and T, further computational analyses of the microbial communities belonging to those bacterial groups known to be potentially involved in the sulfate reduction processes were carried out (Fig 5). SRB are taxonomically affiliated to specific classes within the *Desulfobacterota*, *Firmicutes*, *Nitrospirota*, and *Thermodesulfobiota* phyla [16, 48, 49]. Our sequencing data revealed that in both N and T sediments all the SRB-associated ASVs belonged to the *Desulfobacterota* phylum. *Desulfobacterota* has been proposed as new phylum in 2020 containing the former *Deltaproteobacteria* class and *Thermodesulfobacterota* phlyum [48]. By analyzing the alpha diversity indices at ASV level affiliated to *Desulfobacterota*, richness (Chao1) and diversity (Shannon) were both significantly higher in T compared to N (Fig 5C). T sediments were significantly enriched with *Desulfobulbia* and *Desulfobacteria* classes, which were found in low abundance in N sediments (Fig 5A and 5B). On the other hand, *Desulfuromonadia* and *Syntrophobacteria* classes were slightly more abundant in N compared to T, although without statistical significance. The ASVs belonging to the *Desulfobacterota* phylum were used to build a phylogenetic tree that showed a clear clustering of T-enriching ASVs, which were mainly affiliated with the *Desulfocapsaceae*, *Desulfobulbaceae*, and *Desulfosarcinaceae* families, whereas the N-enriching ASVs were mainly affiliated with the *Desulfuromonadales* and *Syntrophobacterales* orders (Fig 5D). Differently from N-enriching ASVs, most of the ASVs characterizing T sediments were classified up to the genus level and were mainly affiliated to *Desulfobulbus* and *Desulfosarcina*. The *Desulfuromonadia*-affiliated ASVs in N belonged mainly to the Sva1033 family and *Geopsychrobacter* genus (data not shown), whereas *Syntrophobacteria*-affiliated ASVs were all classified up to the *Syntrophobacterales* order.

Discussion

MIC constitutes a concerning issue for marine infrastructures, especially the long-standing ones, such as wharves or even oil and gas pipelines, since the continuous exposure to seawater

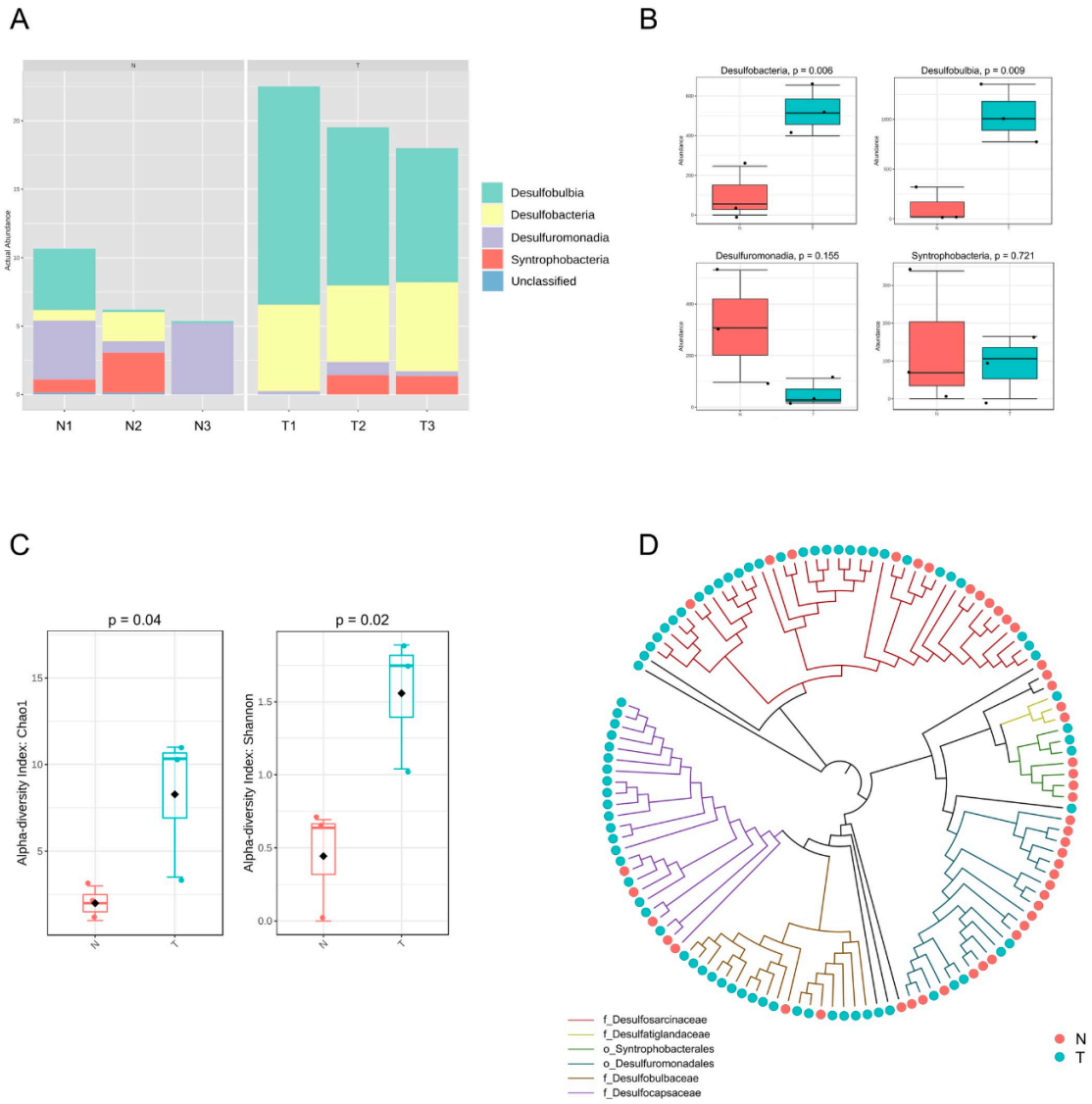

Fig 5. Diversity, taxonomy composition, and phylogenetic analysis of SRB community. A) Taxonomy analysis of *Desulfobacterota* communities at class level. B) Rank test (Anova) of the *Desulfobacterota* classes shown in panel A. C) Chao1 and Shannon diversity indices of *Desulfobacterota* communities in N and T. D) Phylogenetic tree showing all the ASVs affiliated to *Desulfobacterota* from N and T. The color of branches corresponds to orders (preceded by o_ prefix) or families (preceded by f_ prefix) reported in the legend.

https://doi.org/10.1371/journal.pone.0309971.g005

microflora leads to corrosion and is responsible for heavy damages [18, 50–52]. Currently employed strategies to prevent MIC in marine infrastructures lack comprehensive microbiological analyses of the installation sites. Additionally, no monitoring procedures aiming at studying the evolution of the microbial communities are usually performed on the sediment

sites in the nearby of already installed and operative infrastructures. To get further insights of the microbial communities associated with differentially-impacted marine sites, we analysed the microbial community composition and assessed the SRB abundance in marine sediments collected from nearshore Trieste and offshore Norwegian sites.

The presence of high levels of contaminants, low macrozoobenthic diversity, high organic matter concentration, and high numbers of hydrocarbon-degrading bacteria was reported in previous studies on water and sediments collected from the Trieste port [30, 53]. Indeed, this area possesses contaminants that exceed the legal limits fixed by the Italian government, including mercury, vanadium, zinc, total hydrocarbons, and polycyclic aromatic hydrocarbons [30–32]. By combining the experimental data on the collected sediments either performed in our laboratory or by Saipem S.p.A. sediments collected from the Trieste port area showed significantly higher concentration of total organic carbon and total hydrocarbons in T compared to N (S2 Table), indicating both a higher anthropic contamination and higher proneness to possible MIC processes in the Trieste port area. We intended to focus the attention on the marine communities inhabiting these two sites and their impact on the associated MIC hazard. Therefore, we opted not to take into account the features, characterizing the marine infrastructures (*i.e.*, their materials and coatings), which also contribute to determine the entity of MIC events.

The sediments collected at different distances of N and T sites presented similar microbial community structures among the three samples of each group, that significantly differed between the two sites. However, no significant differences were observed in terms of microbial richness and diversity between N and T. This indicates that the environmental settings of the two sites shape the taxonomy composition of the global microbial communities without affecting their richness and diversity. Conversely, the main bacterial group distribution varied greatly between N and T. Many of the differently-distributed bacterial taxa can be considered bioindicators of the health conditions of the marine sediments under analysis. Among the most abundant phyla, *Bacteroidota* and *Firmicutes* were associated with T sediments and their members suggested high human activity compared to N sediments. This was highlighted by the significantly enriched genera and most abundant ASVs in T affiliated to anaerobe species belonging to the *Clostridium* and *Rombutsia*, which are indicator of sewage solids, and which are similar to clones previously associated to wastewater treatments, anaerobic digesters, and fecal contamination [54, 55]. Trieste sediments were also characterized by the methanotrophic *Methyloceanibacter* genus, previously associated with marine sediments in the proximity of hydrothermal vents [56, 57]. Although this bacterial genus is commonly associated with hydrothermal vents, its enrichment in T can be associated with anthropogenic contamination from synthetic fertilizers that are poured into the sea [58].

Differently from T, N sediments were significantly enriched in some bacterial groups that are associated with pristine/healthy environments and poorly impacted by human contamination. In particular, N was enriched in *Nitrospinota* and *Nitrospirota* phyla and in *Nitrospina* and *Nitrospira* genera, whose members are the main responsible for the nitrification processes in marine environments by performing oxidative reaction of nitrite to nitrate [59, 60]. Moreover, these genera provide pioneering metabolic activities for the establishment of the entire microbial community and for the maintenance of the global nitrogen cycling [61]. N sediments were also significantly enriched in *Woeseia* genus, whose members are commonly found in marine sediments communities and are characterized by a facultative chemolithoautotrophic metabolism [62, 63]. Their contribution in the inorganic and organic carbon cycling is hypothesized to be crucial for the marine ecology in pristine seafloor sediments and the abundance of these microbial members in N sediments represents an additional indication of the ecological health of the offshore sampling site. Despite the most abundant bacterial taxa

retrieved from N sediments suggest a low impact of contaminants, the phylogenetic analysis of the most abundant ASVs in N sediments indicated nucleotide similarities with clones identified from the oil-contaminated marine site in the Gulf of Mexico after the Deep Horizon platform explosion in 2010 [45, 46]. These ASVs were mostly unclassified at order, family, or genus level, and were affiliated to *Alphaproteobacteria*, *Methylomirabilota*, and *Actinobacteriota*. Although similar environmental damages have never been documented in the Barents Sea sampling site, this finding suggests that the presence of the drilling platforms close to the collected sediments might contribute to the selection of these specific microbial group, which are still poorly characterized and/or have not been isolated yet.

One of the main issues of the contamination of marine sediments concerns the possible enrichment of microorganisms that can be harmful for marine pipeline systems [19, 51]. The installation of infrastructures in marine environments needs to consider the microbial community inhabiting the putative dedicated location, with the aim of preventing/retarding the establishment of MIC processes [18]. Although the main species responsible for MIC are positively selected by the formation of thick biofilms on the metal surface of infrastructures, these microorganisms are endemic and already present in the anoxic niches of the bent sediments [51]. Moreover, model studies have demonstrated that the microorganisms from marine sediments enhanced both biofouling and biocorrosion in model tank reactors [64]. Indeed, MIC management is mainly reactive rather than being proactive, including the use of physical treatments as pigging and ultraviolet irradiation, as well as broadband biocides endowed with high toxicity [65]. Very few studies have considered the evolution of the microbial community during the usage of an infrastructure over time, and no specific microbiological investigations of marine water and sediments are usually planned before the installation of marine infrastructures. Our data reveled a highly diversified microbial community between the two sites, with T sediments harboring a large number of bacteria involved in MIC, suggesting a higher susceptibility of port and harbors' infrastructures to corrosion [66]. We performed deeper analyses targeting the portion of microbial communities potentially involved H_2S production, which revealed a significant enrichment in T compared to N in terms of both relative abundance of SRB (through 16S rRNA-targeting Illumina sequencing) and total number of SRB cells quantification (through *drsA*-targeting qPCR). These data confirm that T sediments harbor a significant higher number of SRB cells compared to N sediments. Additionally, the SRB communities of the two sites were taxonomically different. T sediments were enriched in SRB species belonging to the *Desulfobulbaceae* and *Desulfosarcinaceae* families, *i.e.*, *Desulfobulbus* and *Desulfosarcina* genera. Both these genera live in anoxic environments, they are highly abundant in sediments with high concentration of organic compounds where they perform organic matter mineralization [67–69]. *Desulfosarcina* belongs to the *Desulfosarcina*/*Desulfococcus* (DSS) clade, which is considered one of the most important lineages involved in hydrocarbon degradation within marine sediments [70]. Additional SRB significantly enriched in T belonged to the Sva0485 clade, which is a marine benthic group (MBG) widely distributed in marine sediments playing a key role in carbon cycling in organic-rich marine environments and representing an important sink of acetate and hydrogen in coastal marine sediments [71–73]. If on one hand the sulfate reducing *Desulfobulbus* and *Desulfosarcina* were highly present in T and associated with high amount of organic matter in the marine sediments, the *Desulfobacterota* community in N was characterized by other SRB members that are not typically correlated with locations featured by pollution/organic compounds, and that contribute to the sulfur cycle in the marine environment. Among these, the Sva1033 family and the *Geopsychrobacter* genus were the most abundant taxa identified in N. *Geopsychrobacter* and Sva1033 members are psychrotolerant and psychrophile, respectively, are frequently associated with Antarctic and Arctic marine sediments, and possess iron-reducing capacities contributing to

the sulfur metabolism [74–76]. We are well aware that characterizing the SRB population abundance and composition is not sufficient to reliably infer the proneness of a specific site to be affected by MIC, as many other microbial phyla could contribute to this process [77, 78]. However, these data might indicate that the detection of specific microbial classes could predict the corrosion rate characterizing a defined environment, especially when suffering from anthropic impact. This seems to be the case of the T site, which also resulted enriched of bacterial groups capable of contributing to the production of corrosive sulfur species. Chemolithoautotrophic sulfur-oxidizing bacteria belonging to the *Thiogranum* genus were significantly present in T compared to N sediments, whose members were isolated from marine environments and are capable of oxidizing reduced sulfur compounds [79, 80]. Their presence in T is likely attributable to the low depth of the sampling site, in which oxygen is more available compared to the deeper sampling sites in N.

Conclusions

MIC is one of the main consequences associated with anthropic contamination of marine environments and is dependent on the establishment of specialized SRB. The investigation of the microbial communities inhabiting marine sediments is a key factor in the identification of healthy and suitable locations for the establishment of infrastructures. Further, the monitoring of the microbial community evolution in the proximity of in-use marine infrastructures should be promoted to prevent and/or mitigate MIC events. The enrichment of human-associated and sulfate-reducing bacterial members in Trieste demonstrated that this site is featured with high anthropogenic impact and is more likely to host corrosion events on installed marine infrastructures than the Norwegian site. On the other hand, some SRB members were also detected in the Norwegian sediments, suggesting that periodic monitoring of the evolution of the microbial communities at this location should be promoted and regulated to mitigate possible MIC processes. With the recent advancement of omic sequencing technologies, these analyses are now economically accessible and allow reliable results to be obtained in a very short time. Implementation of the survey already in use with microbial community studies would provide a comprehensive scenario of potential corrosion processes and represents a proactive complementary strategy to detect MIC at an early stage and to mitigate MIC already underway.

Supporting information

S1 Table. Geographical characteristics of Norway (N1-3) and Trieste (T1-3) sediments analysed in this work and sequencing results.
(DOCX)

S2 Table. Environmental parameters from N and T sample sites. TOC = Total Organic Carbon; THC = Total Hydrocarbon Concentration; PAH = Polycyclic Aromatic Hydrocarbons.
(DOCX)

S1 Fig. Rarefaction curves. Rarefaction curves of the microbial communities in offshore Norway (N) and nearshore Trieste (T) samples, showing the number of Amplicon Sequence Variants (ASVs, y axis) against the number of obtained reads (x axis).
(TIF)

S2 Fig. Most abundant microbial lineages. Microbial community composition of the offshore N and nearshore T sediments at the lowest taxonomy classification with relative abundances >3% in at least one sample. The gray scale color indicates the abundance of each taxa.
(TIF)

S3 Fig. Abundance of sulfate-reducing bacteria. Quantitative PCR targeting the *dsrA* gene from the offshore N and nearshore T sediments.
(TIF)

Acknowledgments

A specific mention goes to the crew of Saipem's Scarabeo 8 and the staff of the Trieste base for their precious commitment in the sampling, conservation, and chain of custody of the sediments used in this work, and delivery operations to the laboratories of the Department of Biomolecular Sciences of the University of Urbino.

Author Contributions

Conceptualization: Daniele Ghezzi, Barbara Citterio, Emanuela Frangipani.

Data curation: Daniele Ghezzi, Mauro Magnani, Barbara Citterio, Emanuela Frangipani.

Formal analysis: Daniele Ghezzi.

Funding acquisition: Mauro Fehervari, Mauro Magnani, Barbara Citterio, Emanuela Frangipani.

Investigation: Gianmarco Mangiaterra, Arianna Scardino, Mauro Fehervari, Emanuela Frangipani.

Methodology: Daniele Ghezzi, Gianmarco Mangiaterra, Arianna Scardino.

Project administration: Mauro Fehervari, Mauro Magnani, Barbara Citterio, Emanuela Frangipani.

Supervision: Mauro Magnani, Emanuela Frangipani.

Writing – original draft: Daniele Ghezzi, Arianna Scardino, Emanuela Frangipani.

Writing – review & editing: Daniele Ghezzi, Gianmarco Mangiaterra, Arianna Scardino, Mauro Fehervari, Mauro Magnani, Barbara Citterio, Emanuela Frangipani.

References

1. Valdez B, Ramirez J, Eliezer A, Schorr M, Ramos R, Salinas R. Corrosion assessment of infrastructure assets in coastal seas. J Mar Eng Technol. 2016; 15: 124–134. https://doi.org/10.1080/20464177.2016.1247635
2. Li Y, Ning C. Latest research progress of marine microbiological corrosion and bio-fouling, and new approaches of marine anti-corrosion and anti-fouling. Bioact Mater. 2019; 4: 189–195. https://doi.org/10.1016/j.bioactmat.2019.04.003 PMID: 31192994
3. Knisz J, Eckert R, Gieg L, Koerdt A, Lee J, Silva E, et al. Microbiologically influenced corrosion-more than just microorganisms. FEMS Microbiol Rev. 2023; 47: 1–33. https://doi.org/10.1093/femsre/fuad041 PMID: 37437902
4. Lane RA. Under the microscope: Understanding, detecting, and preventing microbiologically influenced corrosion. J Fail Anal Prev. 2005; 5: 10–12. https://doi.org/10.1361/154770205X65891/METRICS
5. Dong C, Gu X, Sun W, Wang K, Liu M, Wang J, et al. Inhibiting low-dimensional defects of titanium diboride coatings by Si incorporation: Toward enhanced corrosion resistance and mechanical properties. Appl Surf Sci. 2022; 594: 153504. https://doi.org/10.1016/J.APSUSC.2022.153504
6. Tuck B, Watkin E, Somers A, Machuca LL. A critical review of marine biofilms on metallic materials. npj Mater Degrad 2022 61. 2022; 6: 1–12. https://doi.org/10.1038/s41529-022-00234-4
7. Hülsen T, Hsieh K, Batstone DJ. Saline wastewater treatment with purple phototrophic bacteria. Water Res. 2019; 160: 259–267. https://doi.org/10.1016/j.watres.2019.05.060 PMID: 31154123

8. Jia R, Unsal T, Xu D, Lekbach Y, Gu T. Microbiologically influenced corrosion and current mitigation strategies: A state of the art review. 2019; 147: 42–58. https://doi.org/10.1016/j.ibiod.2018.11.007
9. Salgar-Chaparro SJ, Lepkova K, Pojtanabuntoeng T, Darwin A, Machuca LL. Nutrient level determines biofilm characteristics and subsequent impact on microbial corrosion and biocide effectiveness. 2020; 86: e02885–19. https://doi.org/10.1128/AEM.02885-19 PMID: 31980429
10. Wolodko J, Haile Innotech Alberta T, Khan F, Taylor C, Eckert R, Javad Hashemi S, et al. Modeling of Microbiologically Influenced Corrosion (MIC) in the oil and gas industry—past, present and future. OnePetro; 2018. p. NACE-2018-11398.
11. Beavers JA, Thompson NG. External corrosion of oil and natural gas pipelines. Corros Environ Ind. 2006; 1015–1025. https://doi.org/10.31399/ASM.HB.V13C.A0004213
12. Little BJ, Blackwood DJ, Hinks J, Lauro FM, Marsili E, Okamoto A, et al. Microbially influenced corrosion—Any progress? Corros Sci. 2020; 170: 108641. https://doi.org/10.1016/J.CORSCI.2020.108641
13. Zuo R. Biofilms: strategies for metal corrosion inhibition employing microorganisms. Appl Microbiol Biotechnol. 2007; 76: 1245–1253. https://doi.org/10.1007/s00253-007-1130-6 PMID: 17701408
14. Procópio L. The role of biofilms in the corrosion of steel in marine environments. World J Microbiol Biotechnol. 2019; 35: 73. https://doi.org/10.1007/s11274-019-2647-4 PMID: 31037431
15. Mori F, Umezawa Y. Dynamics of sulfate-reducing bacteria community structure in surface sediment of a seasonally hypoxic enclosed bay. Microbes Env. 2018; 33: 378–384. https://doi.org/10.1264/jsme2.ME18092 PMID: 30449831
16. Muyzer G, Stams AJM. The ecology and biotechnology of sulphate-reducing bacteria. Nat Rev Microbiol. 2008; 6: 441–454. https://doi.org/10.1038/nrmicro1892 PMID: 18461075
17. Plugge CM, Zhang W, Scholten JCM, Stams AJM. Metabolic flexibility of sulfate-reducing bacteria. Front Microbiol. 2011; 2. https://doi.org/10.3389/fmicb.2011.00081 PMID: 21734907
18. Liu P, Zhang H, Fan Y, Xu D. Microbially Influenced Corrosion of steel in marine environments: a review from mechanisms to prevention. Microorganisms. 2023; 11: 2299. https://doi.org/10.3390/microorganisms11092299 PMID: 37764143
19. Dang H, Xie W, Bailey J, Zhen Y, Zhang Y, Wang X, et al. Microbial diversity and community structure of sulfate-reducing and sulfur-oxidizing bacteria in sediment cores from the East China Sea. Front Microbiol. 2017;8. https://doi.org/10.3389/fmicb.2017.02133 PMID: 29163420
20. Xu D, Gu T, Lovley DR. Microbially mediated metal corrosion. Nat Rev Microbiol 2023 2111. 2023; 21: 705–718. https://doi.org/10.1038/s41579-023-00920-3 PMID: 37344552
21. Yan D, Liu J, Zhang Z, Wang Y, Zhang M, Song D, et al. Dual-functional graphene oxide-based nanomaterial for enhancing the passive and active corrosion protection of epoxy coating. Compos Part B. 2021; 222: 109075. https://doi.org/10.1016/j.compositesb.2021.109075
22. Rasheed PA, Jabbar KA, Rasool K, Pandey RP, Sliem MH, Helal M, et al. Controlling the biocorrosion of sulfate-reducing bacteria (SRB) on carbon steel using ZnO/chitosan nanocomposite as an eco-friendly biocide. 2019; 148: 397–406. https://doi.org/10.1016/j.corsci.2018.12.028
23. ANSI/NACE MR0103-2015/ISO 17945:2015. Petroleum, petrochemical and natural gas industries—metallic materials resistant to sulfide stress cracking in corrosive petroleum refining environments. 2015. Available: https://www.iso.org/standard/61077.html
24. DNV-ST-F101. Submarine pipeline systems. 2021.
25. Duncan KE, Davidova IA, Nunn HS, Stamps BW, Stevenson BS, Souquet PJ, et al. Design features of offshore oil production platforms influence their susceptibility to biocorrosion. Appl Microbiol Biotechnol. 2017; 101: 6517–6529. https://doi.org/10.1007/s00253-017-8356-8 PMID: 28597336
26. Alleyane AG, Ahrabian D, Tucher R, And Van Der Heijden H. Blue Stream. The Russia To Turkey submarine pipeline across the Black Sea. The 21th Pipeline Technology Conference. 1998.
27. Gentile M, Cattalini M, Fehervari M, Tomaselli L, Ragazzoni S, Gjedrem T. Nord Stream Project—Baltic Sea environment: hydrogen damage assessment for line pipe steel and anode material selection. 22nd International Offshore and Polar Engineering Conference. 2012.
28. Lomans BP, De Paula R, Geissler B, Kuijvenhoven CAT, Tsesmetzis N. Proposal of improved biomonitoring standard for purpose of microbiologically influenced corrosion risk assessment. Soc Pet Eng—SPE Int Oilf Corros Conf Exhib. 2016. https://doi.org/10.2118/179919-ms
29. Gieg L, Sharma M, Haile T, Hawboldt KA, Bottaro C, Modir A, et al. Standard operating procedures for sampling onshore and offshore assets for genomic, microbial, and chemical analyses and/or experiments. Fail Anal Microbiol Influ Corros. 2021; 467–486. https://doi.org/10.1201/9780429355479-30
30. Cibic T, Franzo A, Nasi F, Auriemma R, Del Negro P. The port of Trieste (Northern Adriatic Sea)-A case study of the "ecosystem approach to management." Front Mar Sci. 2017; 4: 245439. https://doi.org/10.3389/FMARS.2017.00336/BIBTEX

31. Heath E, Ogrinc N, Faganeli J, Covelli S. Sedimentary record of polycyclic aromatic hydrocarbons in the Gulf of Trieste (Northern Adriatic Sea). Water, Air, Soil Pollut Focus. 2006; 6: 605–614. https://doi.org/10.1007/s11267-006-9045-2

32. Notar M, Leskovšek H, Faganeli J. Composition, distribution and sources of polycyclic aromatic hydrocarbons in sediments of the Gulf of Trieste, Northern Adriatic Sea. Mar Pollut Bull. 2001; 42: 36–44. https://doi.org/10.1016/s0025-326x(00)00092-8 PMID: 11382982

33. Buruaem LM, Hortellani MA, Sarkis JE, Costa-Lotufo L V., Abessa DMS. Contamination of port zone sediments by metals from Large Marine Ecosystems of Brazil. Mar Pollut Bull. 2012; 64: 479–488. https://doi.org/10.1016/J.MARPOLBUL.2012.01.017 PMID: 22306311

34. Michalsen K, Dalpadado P, Eriksen E, Gjøsæter H, Ingvaldsen RB, Johannesen E, et al. Marine living resources of the Barents Sea—Ecosystem understanding and monitoring in a climate change perspective. Mar Biol Res. 2013; 9: 932–947. https://doi.org/10.1080/17451000.2013.775459

35. Brioukhanov AL, Vitaly Kadnikov V, Rusanov II, Novigatskiy AN, Kanapatskiy TA, et al. Phylogenetic diversity in sulphate-reducing bacterial communities from oxidised and reduced bottom sediments of the Barents Sea. 2022; 115: 801–820. https://doi.org/10.1007/s10482-022-01733-9 PMID: 35435634

36. Lind S, Ingvaldsen RB, Furevik T. Arctic warming hotspot in the northern Barents Sea linked to declining sea-ice import. Nat Clim Chang 2018 87. 2018; 8: 634–639. https://doi.org/10.1038/s41558-018-0205-y

37. Cappelletti M, Ghezzi D, Zannoni D, Capaccioni B, Fedi S. Diversity of methane-oxidizing bacteria in soils from "Hot Lands of Medolla" (Italy) featured by anomalous high-temperatures and biogenic CO2 emission. Microbes Environ. 2016; 31: 1–9. https://doi.org/10.1264/jsme2.ME16087 PMID: 27645100

38. Caporaso JG, Lauber CL, Walters WA, Berg-Lyons D, Lozupone CA, Turnbaugh PJ, et al. Global patterns of 16S rRNA diversity at a depth of millions of sequences per sample. Proc Natl Acad Sci U S A. 2011; 108: 4516–4522. https://doi.org/10.1073/pnas.1000080107 PMID: 20534432

39. Ghezzi D, Filippini M, Cappelletti M, Firrincieli A, Zannoni D, Gargini A, et al. Molecular characterization of microbial communities in a peat-rich aquifer system contaminated with chlorinated aliphatic compounds. Environ Sci Pollut Res Int. 2021; 28: 23017–23035. https://doi.org/10.1007/s11356-020-12236-3 PMID: 33438126

40. Chong J, Liu P, Zhou G, Xia J. Using MicrobiomeAnalyst for comprehensive statistical, functional, and meta-analysis of microbiome data. Nat Protoc. 2020; 15: 799–821. https://doi.org/10.1038/s41596-019-0264-1 PMID: 31942082

41. Quast C, Pruesse E, Yilmaz P, Gerken J, Schweer T, Yarza P, et al. The SILVA ribosomal RNA gene database project: improved data processing and web-based tools. Nucleic Acids Res. 2013; 41: D590–D596. https://doi.org/10.1093/nar/gks1219 PMID: 23193283

42. Tamura K, Stecher G, Kumar S. MEGA11: Molecular Evolutionary Genetics Analysis Version 11. Mol Biol Evol. 2021; 38: 3022. https://doi.org/10.1093/molbev/msab120 PMID: 33892491

43. Kondo R, Nedwell DB, Purdy KJ, de Queiroz Silva S. Detection and enumeration of sulphate-reducing bacteria in estuarine sediments by Competitive PCR. Geomicrobiol J. 2004; 21: 145–157. https://doi.org/10.1080/01490450490275307

44. Mangiaterra G, Amiri M, Di Cesare A, Pasquaroli S, Manso E, Cirilli N, et al. Detection of viable but non-culturable Pseudomonas aeruginosa in cystic fibrosis by qPCR: a validation study. BMC Infect Dis. 2018; 18. https://doi.org/10.1186/s12879-018-3612-9 PMID: 30587160

45. Camilli R, Reddy CM, Yoerger DR, Van Mooy BAS, Jakuba M V., Kinsey JC, et al. Tracking hydrocarbon plume transport and biodegradation at deepwater horizon. Science (80-). 2010; 330: 201–204. https://doi.org/10.1126/science.1195223 PMID: 20724584

46. Dang H, Liu Z, Teske A, Yang T, McKay L, Speare K, et al. Distinct bacterial communities in surficial seafloor sediments following the 2010 Deepwater Horizon Blowout. Front Microbiol. 2016; 7: 1384. https://doi.org/10.3389/fmicb.2016.01384 PMID: 27679609

47. Bradley AS, Leavitt WD, Johnston DT. Revisiting the dissimilatory sulfate reduction pathway. Geobiology. 2011; 9: 446–457. https://doi.org/10.1111/j.1472-4669.2011.00292.x PMID: 21884365

48. Waite DW, Chuvochina M, Pelikan C, Parks DH, Yilmaz P, Wagner M, et al. Proposal to reclassify the proteobacterial classes Deltaproteobacteria and Oligoflexia, and the phylum Thermodesulfobacteria into four phyla reflecting major functional capabilities. Int J Syst Evol Microbiol. 2020; 70: 5972–6016. https://doi.org/10.1099/ijsem.0.004213 PMID: 33151140

49. Frolov EN, Gololobova A V, Klyukina AA, Bonch-Osmolovskaya EA, Pimenov N V, Chernyh NA, et al. Diversity and activity of sulfate-reducing prokaryotes in Kamchatka Hot Springs. 2021; 9: 2072. https://doi.org/10.3390/microorganisms9102072 PMID: 34683394

50. Fatah MC, Diaz A, Darwin A. Corrosion assessment of a leakage pipeline in the seabed: A case study. J Phys Conf Ser. 2019;1402. https://doi.org/10.1088/1742-6596/1402/6/066001

51. Smith M, Bardiau M, Brennan R, Burgess H, Caplin J, Ray S, et al. Accelerated low water corrosion: the microbial sulfur cycle in microcosm. npj Mater Degrad. 2019; 3:37. https://doi.org/10.1038/s41529-019-0099-9

52. Wang Z, Li Y, Ren J, Xu W, Yang L. Investigating the effects of environment, corrosion degree, and distribution of corrosive microbial communities on service-life of refined oil pipelines. Environ Sci Pollut Res. 2022; 29: 52204–52219. https://doi.org/10.1007/s11356-022-19556-6 PMID: 35260983

53. Covelli S, Petranich E, Pavoni E, Signore S. Can sediments contaminated by mining be a source of mercury in the coastal environment due to dredging? Evidence from thermo-desorption and chemical speciation. Bull Environ Contam Toxicol. 2021; 106: 942–948. https://doi.org/10.1007/s00128-021-03159-x PMID: 33655405

54. Quach NT, Dam HT, Tran DM, Vu THN, Nguyen QV, Nguyen KT, et al. Diversity of microbial community and its metabolic potential for nitrogen and sulfur cycling in sediments of Phu Quoc island, Gulf of Thailand. Brazilian J Microbiol. 2021; 52: 1385. https://doi.org/10.1007/S42770-021-00481-8 PMID: 33856662

55. Skanavis C, Yanko WA. Clostridium perfringens as a potential indicator for the presence of sewage solids in marine sediments. Mar Pollut Bull. 2001; 42: 31–35. https://doi.org/10.1016/s0025-326x(00)00087-4 PMID: 11382981

56. Vekeman B, Kerckhof FM, Cremers G, de Vos P, Vandamme P, Boon N, et al. New Methyloceanibacter diversity from North Sea sediments includes methanotroph containing solely the soluble methane monooxygenase. Environ Microbiol. 2016; 18: 4523–4536. https://doi.org/10.1111/1462-2920.13485 PMID: 27501305

57. Takeuchi M, Katayama T, Yamagishi T, Hanada S, Tamaki H, Kamagata Y, et al. Methyloceanibacter caenitepidi gen. nov., sp. nov., a facultatively methylotrophic bacterium isolated from marine sediments near a hydrothermal vent. Int J Syst Evol Microbiol. 2014; 64: 462–468. https://doi.org/10.1099/ijs.0.053397-0 PMID: 24096357

58. Kuloyo O, Ruff SE, Cahill A, Connors L, Zorz JK, Hrabe de Angelis I, et al. Methane oxidation and methylotroph population dynamics in groundwater mesocosms. Environ Microbiol. 2020; 22: 1222. https://doi.org/10.1111/1462-2920.14929 PMID: 32017377

59. Lücker S, Nowka B, Rattei T, Spieck E, Daims H. The genome of Nitrospina gracilis illuminates the metabolism and evolution of the major marine nitrite oxidizer. Front Microbiol. 2013; 4. https://doi.org/10.3389/fmicb.2013.00027 PMID: 23439773

60. Mueller AJ, Jung MY, Strachan CR, Herbold CW, Kirkegaard RH, Wagner M, et al. Genomic and kinetic analysis of novel Nitrospinae enriched by cell sorting. ISME J. 2021; 15: 732. https://doi.org/10.1038/s41396-020-00809-6 PMID: 33067588

61. Haaijer SCM, Ji K, van Niftrik L, Hoischen A, Speth D, Jetten MSM, et al. A novel marine nitrite-oxidizing Nitrospira species from Dutch coastal North Sea water. Front Microbiol. 2013; 4. https://doi.org/10.3389/fmicb.2013.00060 PMID: 23515432

62. Hoffmann K, Bienhold C, Buttigieg PL, Knittel K, Laso-Pérez R, Rapp JZ, et al. Diversity and metabolism of Woeseiales bacteria, global members of marine sediment communities. ISME J. 2020; 14: 1042. https://doi.org/10.1038/s41396-020-0588-4 PMID: 31988474

63. Mußmann M, Pjevac P, Krüger K, Dyksma S. Genomic repertoire of the Woeseiaceae/JTB255, cosmopolitan and abundant core members of microbial communities in marine sediments. ISME J. 2017; 11: 1276. https://doi.org/10.1038/ismej.2016.185 PMID: 28060363

64. Duncan KE, Dominici LE, Nanny MA, Davidova IA, Harriman BH, Suflita JM. Microbial communities in model seawater-compensated fuel ballast tanks: biodegradation and biocorrosion stimulated by marine sediments. Corros Mater Degrad. 2024; 5: 1–26. https://doi.org/10.3390/CMD5010001/S1

65. Wang D, Zhou E, Xu D, Lovley DR. Burning question: Are there sustainable strategies to prevent microbial metal corrosion? Microb Biotechnol. 2023; 16: 2026–2035. https://doi.org/10.1111/1751-7915.14347 PMID: 37796110

66. Forsyth RA. Microbial induced corrosion in ports and harbors worldwide. Ports 2010 Build Past, Respect Futur—Proc 12th Triannual Int Conf. 2010; 932–939. https://doi.org/10.1061/41098(368)96

67. Kharrat H, Karray F, Bartoli M, Hnia WB, Mhiri N, Fardeau M-L, et al. Desulfobulbus aggregans sp. nov., a novel sulfate reducing bacterium isolated from marine sediment from the Gulf of Gabes. Curr Microbiol. 2017; 74: 449–454. https://doi.org/10.1007/s00284-017-1211-4 PMID: 28213662

68. Watanabe M, Higashioka Y, Kojima H, Fukui M. Desulfosarcina widdelii sp. nov. and Desulfosarcina alkanivorans sp. nov., hydrocarbon-degrading sulfate-reducing bacteria isolated from marine sediment and emended description of the genus Desulfosarcina. Int J Syst Evol Microbiol. 2017; 67: 2994–2997. https://doi.org/10.1099/ijsem.0.002062 PMID: 28820122

69. Jurado V, D'Angeli I, Martin-Pozas T, Cappelletti M, Ghezzi D, Luis Gonzalez-Pimentel J, et al. Dominance of Arcobacter in the white filaments from the thermal sulfidic spring of Fetida Cave (Apulia,

southern Italy). Sci Total Environ. 2021; 800: 149465. https://doi.org/10.1016/j.scitotenv.2021.149465 PMID: 34391144

70. Kleindienst S, Herbst FA, Stagars M, Von Netzer F, Von Bergen M, Seifert J, et al. Diverse sulfate-reducing bacteria of the Desulfosarcina/Desulfococcus clade are the key alkane degraders at marine seeps. ISME J. 2014; 8: 2029. https://doi.org/10.1038/ismej.2014.51 PMID: 24722631

71. D'Angeli IM, Ghezzi D, Leuko S, Firrincieli A, Parise M, Fiorucci A, et al. Geomicrobiology of a seawater-influenced active sulfuric acid cave. Plos One. 2019. https://doi.org/10.1371/journal.pone.0220706 PMID: 31393920

72. Dyksma S, Lenk S, Sawicka JE, Mußmann M. Uncultured Gammaproteobacteria and Desulfobacteraceae account for major acetate assimilation in a coastal marine sediment. Front Microbiol. 2018; 9. https://doi.org/10.3389/FMICB.2018.03124/FULL

73. Dyksma S, Pjevac P, Ovanesov K, Mussmann M. Evidence for H2 consumption by uncultured Desulfobacterales in coastal sediments. Environ Microbiol. 2018; 20: 450–461. https://doi.org/10.1111/1462-2920.13880 PMID: 28772023

74. Wunder LC, Aromokeye DA, Yin X, Richter-Heitmann T, Willis-Poratti G, Schnakenberg A, et al. Iron and sulfate reduction structure microbial communities in (sub-)Antarctic sediments. ISME J. 2021; 15: 3587. https://doi.org/10.1038/s41396-021-01014-9 PMID: 34155335

75. Baloza M, Henkel S, Kasten S, Holtappels M, Molari M. The impact of sea ice cover on microbial communities in Antarctic shelf sediments. Microorganisms. 2023; 11. https://doi.org/10.3390/microorganisms11061572 PMID: 37375074

76. Holmes DE, Nicoll JS, Bond DR, Lovley DR. Potential role of a novel psychrotolerant member of the family Geobacteraceae, Geopsychrobacter electrodiphilus gen. nov., sp. nov., in electricity production by a marine sediment fuel cell. Appl Environ Microbiol. 2004; 70: 6023. https://doi.org/10.1128/AEM.70.10.6023-6030.2004 PMID: 15466546

77. Mouser PJ, Borton M, Darrah TH, Hartsock A, Wrighton KC. Hydraulic fracturing offers view of microbial life in the deep terrestrial subsurface. FEMS Microbiol Ecol. 2016; 92: fiw166. https://doi.org/10.1093/femsec/fiw166 PMID: 27507739

78. Ma Y, Zhang Y, Zhang R, Guan F, Hou B, Duan J. Microbiologically influenced corrosion of marine steels within the interaction between steel and biofilms: a brief view. Appl Microbiol Biotechnol. 2020; 104: 515–525. https://doi.org/10.1007/s00253-019-10184-8 PMID: 31807887

79. Mori K, Suzuki KI, Yamaguchi K, Urabe T, Hanada S. Thiogranum longum gen. nov., sp. nov., an obligately chemolithoautotrophic, sulfur-oxidizing bacterium of the family Ectothiorhodospiraceae isolated from a deep-sea hydrothermal field, and an emended description of the genus Thiohalomonas. Int J Syst Evol Microbiol. 2015; 65: 235–241. https://doi.org/10.1099/ijs.0.070599-0 PMID: 25336721

80. Liau P, Kim C, Saxton MA, Malkin SY. Microbial succession in a marine sediment: Inferring interspecific microbial interactions with marine cable bacteria. Environ Microbiol. 2022; 24: 6348. https://doi.org/10.1111/1462-2920.16230 PMID: 36178156

Supporting informations

S1 Table. Geographical characteristics of Norway (N1-3) and Trieste (T1-3) sediments analysed in this work and sequencing results.

Sediment	Location	Coordinates	no. reads	no. ASVs
N1	Norway	22°18.4999'E 71°18.2653'N	7,141	152
N2	Norway	22°18.5082'E 71°18.2669'N	11,530	489
N3	Norway	22°18.5001'E 71°18.259'N	10,194	195
T1	Trieste	13°45.6361'E 45°39.8362'N	6,305	155
T2	Trieste	13°45.6646'E 45°39.8404'N	11,702	471
T3	Trieste	13°45.6766'E 45°39.8438'N	7,899	158

S2 Table. Environmental parameters from N and T sampling area. TOC = Total Organic Carbon; THC = Total Hydrocarbon Concentration; PAH = Polycyclic Aromatic Hydrocarbons.

Site	pH[a]	Temperature[b] (°C)	Salinity[c] (g/kg)	TOC (%)	THC (mg/kg)	PAH (µg/kg)
N	7.08 ± 0.2	4.2 ± 0.4 (3.9)	35.1 ± 0.0	< 1[d]	5.03 ± 0.8[d]	211 ± 4[d]
T	7.28 ± 0.2	15.3 ± 5.7 (6.9)	36.7 ± 0.9	2.30 ± 0.4[e]	151 ± 70.3[e]	> 500[f]

[a] Data experimentally measured in lab, upon samples reception.

[b] Values represent the annual seawater temperature at the sampled depth (*i.e.,* 400 mt for N and 10 mt for T), the values in parentheses are indicative of the month of March in which samples were collected. These data were extracted from the NOAA World Ocean Atlas 13 (WOA13) database (https://www.nodc.noaa.gov/OC5/woa13/woa13data.html), and provided by Saipem S.p.A.

[c] Values represent the annual seawater salinity at the sampled depth (*i.e.,* 400 mt for N and 10 mt for T). These data were extracted from the NOAA World Ocean Atlas 13 (WOA13) database (https://www.nodc.noaa.gov/OC5/woa13/woa13data.html), and provided by Saipem S.p.A.

[d] Data for the N site were retrieved from mareano.no database, mediating values from sites in the nearby coordinates.

[e] Data for the T site were collected by the Istituto Nazionale di Oceanografia e di Geofisica Sperimentale (https://www.ogs.it) and provided by Saipem S.p.A. Analyzes were conducted in triplicate by Accredia accredited laboratory according to ISO 17025:2005 standard for all the analytes researched and operating with a quality system certified according to ISO 9001:2015 standard.

[f] PAH value was retrieved from literature [30-32].

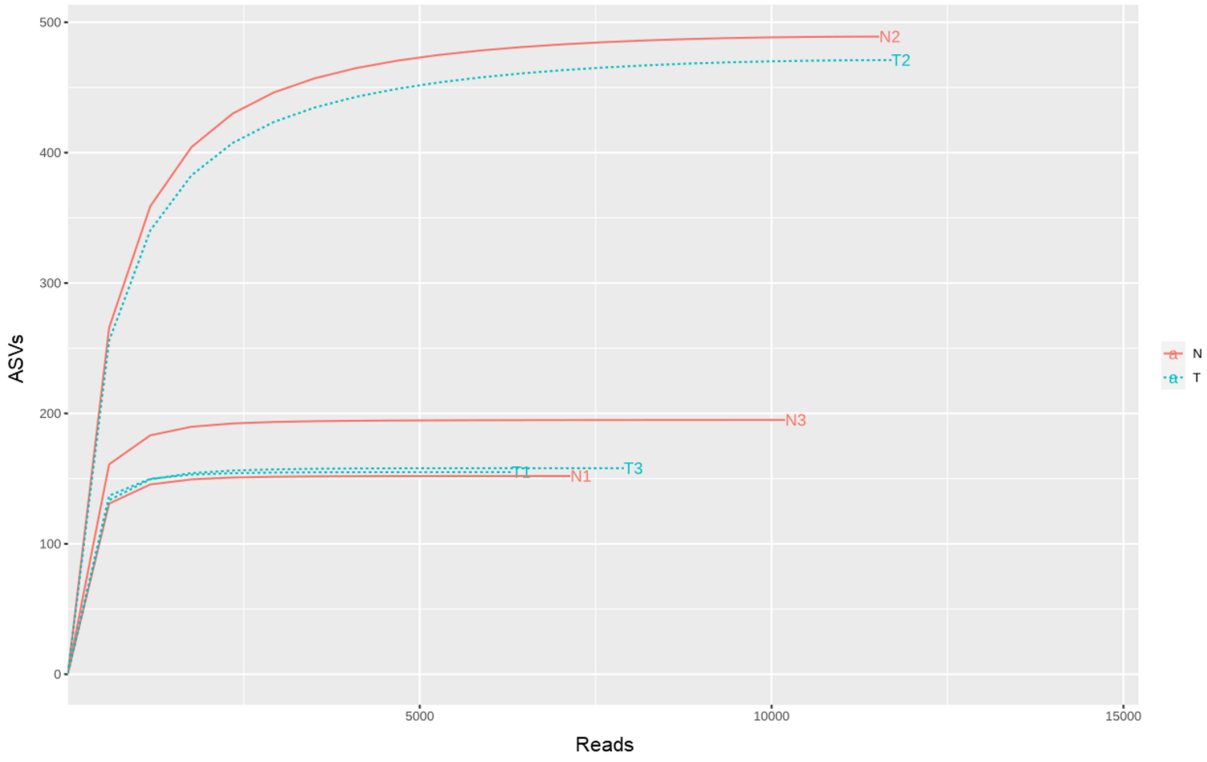

S1 Fig. Rarefaction curves. Rarefaction curves of the microbial communities in offshore Norway (N) and nearshore Trieste (T) samples, showing the number of Amplicon Sequence Variants (ASVs, y axis) against the number of obtained reads (x axis).

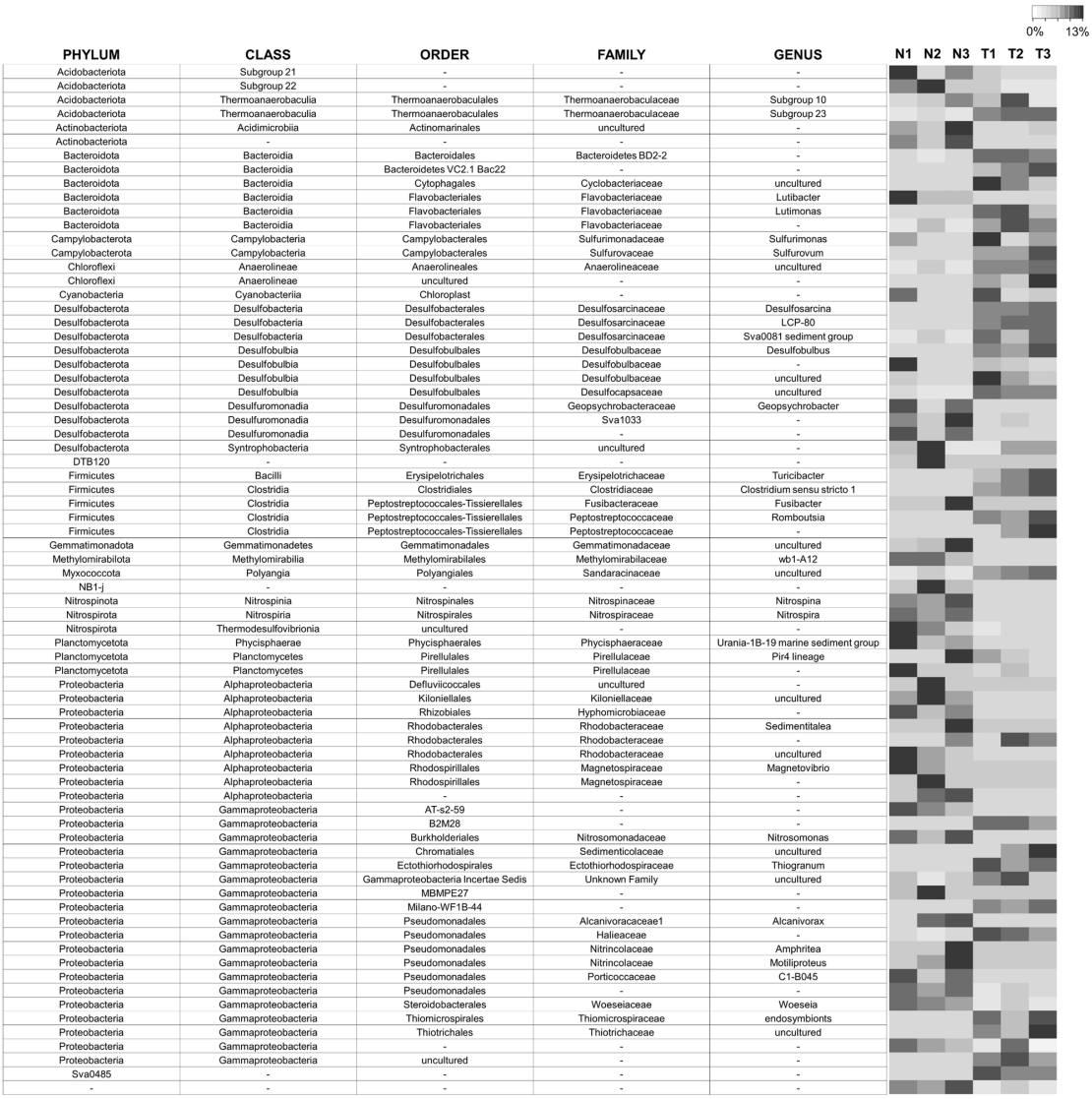

PHYLUM	CLASS	ORDER	FAMILY	GENUS	N1	N2	N3	T1	T2	T3
Acidobacteriota	Subgroup 21	-	-	-						
Acidobacteriota	Subgroup 22	-	-	-						
Acidobacteriota	Thermoanaerobaculia	Thermoanaerobaculales	Thermoanaerobaculaceae	Subgroup 10						
Acidobacteriota	Thermoanaerobaculia	Thermoanaerobaculales	Thermoanaerobaculaceae	Subgroup 23						
Actinobacteriota	Acidimicrobiia	Actinomarinales	uncultured	-						
Actinobacteriota	-	-	-	-						
Bacteroidota	Bacteroidia	Bacteroidales	Bacteroidetes BD2-2	-						
Bacteroidota	Bacteroidia	Bacteroidetes VC2.1 Bac22	-	-						
Bacteroidota	Bacteroidia	Cytophagales	Cyclobacteriaceae	uncultured						
Bacteroidota	Bacteroidia	Flavobacteriales	Flavobacteriaceae	Lutibacter						
Bacteroidota	Bacteroidia	Flavobacteriales	Flavobacteriaceae	Lutimonas						
Bacteroidota	Bacteroidia	Flavobacteriales	Flavobacteriaceae	-						
Campylobacterota	Campylobacteria	Campylobacterales	Sulfurimonadaceae	Sulfurimonas						
Campylobacterota	Campylobacteria	Campylobacterales	Sulfurovaceae	Sulfurovum						
Chloroflexi	Anaerolineae	Anaerolineales	Anaerolineaceae	uncultured						
Chloroflexi	Anaerolineae	uncultured	-	-						
Cyanobacteria	Cyanobacteriia	Chloroplast	-	-						
Desulfobacterota	Desulfobacteria	Desulfobacterales	Desulfosarcinaceae	Desulfosarcina						
Desulfobacterota	Desulfobacteria	Desulfobacterales	Desulfosarcinaceae	LCP-80						
Desulfobacterota	Desulfobacteria	Desulfobacterales	Desulfosarcinaceae	Sva0081 sediment group						
Desulfobacterota	Desulfobulbia	Desulfobulbales	Desulfobulbaceae	Desulfobulbus						
Desulfobacterota	Desulfobulbia	Desulfobulbales	Desulfobulbaceae	-						
Desulfobacterota	Desulfobulbia	Desulfobulbales	Desulfobulbaceae	uncultured						
Desulfobacterota	Desulfobulbia	Desulfobulbales	Desulfocapsaceae	uncultured						
Desulfobacterota	Desulfuromonadia	Desulfuromonadales	Geopsychrobacteraceae	Geopsychrobacter						
Desulfobacterota	Desulfuromonadia	Desulfuromonadales	Sva1033	-						
Desulfobacterota	Desulfuromonadia	Desulfuromonadales	-	-						
Desulfobacterota	Syntrophobacteria	Syntrophobacterales	uncultured	-						
DTB120	-	-	-	-						
Firmicutes	Bacilli	Erysipelotrichales	Erysipelotrichaceae	Turicibacter						
Firmicutes	Clostridia	Clostridiales	Clostridiaceae	Clostridium sensu stricto 1						
Firmicutes	Clostridia	Peptostreptococcales-Tissierellales	Fusibacteraceae	Fusibacter						
Firmicutes	Clostridia	Peptostreptococcales-Tissierellales	Peptostreptococcaceae	Romboutsia						
Firmicutes	Clostridia	Peptostreptococcales-Tissierellales	Peptostreptococcaceae	-						
Gemmatimonadota	Gemmatimonadetes	Gemmatimonadales	Gemmatimonadaceae	uncultured						
Methylomirabilota	Methylomirabilia	Methylomirabilales	Methylomirabilaceae	wb1-A12						
Myxococcota	Polyangia	Polyangiales	Sandaracinaceae	uncultured						
NB1-j	-	-	-	-						
Nitrospinota	Nitrospinia	Nitrospinales	Nitrospinaceae	Nitrospina						
Nitrospirota	Nitrospiria	Nitrospirales	Nitrospiraceae	Nitrospira						
Nitrospirota	Thermodesulfovibrionia	uncultured	-	-						
Planctomycetota	Phycisphaerae	Phycisphaerales	Phycisphaeraceae	Urania-1B-19 marine sediment group						
Planctomycetota	Planctomycetes	Pirellulales	Pirellulaceae	Pir4 lineage						
Planctomycetota	Planctomycetes	Pirellulales	Pirellulaceae	-						
Proteobacteria	Alphaproteobacteria	Defluviicoccales	uncultured	-						
Proteobacteria	Alphaproteobacteria	Kiloniellales	Kiloniellaceae	uncultured						
Proteobacteria	Alphaproteobacteria	Rhizobiales	Hyphomicrobiaceae	-						
Proteobacteria	Alphaproteobacteria	Rhodobacterales	Rhodobacteraceae	Sedimentitalea						
Proteobacteria	Alphaproteobacteria	Rhodobacterales	Rhodobacteraceae	-						
Proteobacteria	Alphaproteobacteria	Rhodobacterales	Rhodobacteraceae	uncultured						
Proteobacteria	Alphaproteobacteria	Rhodospirillales	Magnetospiraceae	Magnetovibrio						
Proteobacteria	Alphaproteobacteria	Rhodospirillales	Magnetospiraceae	-						
Proteobacteria	Alphaproteobacteria	-	-	-						
Proteobacteria	Gammaproteobacteria	AT-s2-59	-	-						
Proteobacteria	Gammaproteobacteria	B2M28	-	-						
Proteobacteria	Gammaproteobacteria	Burkholderiales	Nitrosomonadaceae	Nitrosomonas						
Proteobacteria	Gammaproteobacteria	Chromatiales	Sedimenticolaceae	uncultured						
Proteobacteria	Gammaproteobacteria	Ectothiorhodospirales	Ectothiorhodospiraceae	Thiogranum						
Proteobacteria	Gammaproteobacteria	Gammaproteobacteria Incertae Sedis	Unknown Family	uncultured						
Proteobacteria	Gammaproteobacteria	MBMPE27	-	-						
Proteobacteria	Gammaproteobacteria	Milano-WF1B-44	-	-						
Proteobacteria	Gammaproteobacteria	Pseudomonadales	Alcanivoracaceae1	Alcanivorax						
Proteobacteria	Gammaproteobacteria	Pseudomonadales	Halieaceae	-						
Proteobacteria	Gammaproteobacteria	Pseudomonadales	Nitrincolaceae	Amphritea						
Proteobacteria	Gammaproteobacteria	Pseudomonadales	Nitrincolaceae	Motiliproteus						
Proteobacteria	Gammaproteobacteria	Pseudomonadales	Porticoccaceae	C1-B045						
Proteobacteria	Gammaproteobacteria	Pseudomonadales	-	-						
Proteobacteria	Gammaproteobacteria	Steroidobacterales	Woeseiaceae	Woeseia						
Proteobacteria	Gammaproteobacteria	Thiomicrospirales	Thiomicrospiraceae	endosymbionts						
Proteobacteria	Gammaproteobacteria	Thiotrichales	Thiotrichaceae	uncultured						
Proteobacteria	Gammaproteobacteria	-	-	-						
Proteobacteria	Gammaproteobacteria	uncultured	-	-						
Sva0485	-	-	-	-						
-	-	-	-	-						

S2 Fig. Most abundant microbial lineages. Microbial community composition of the offshore N and nearshore T sediments at the lowest taxonomy classification with relative abundances >3% in at least one sample. The gray scale color indicates the abundance of each taxa.

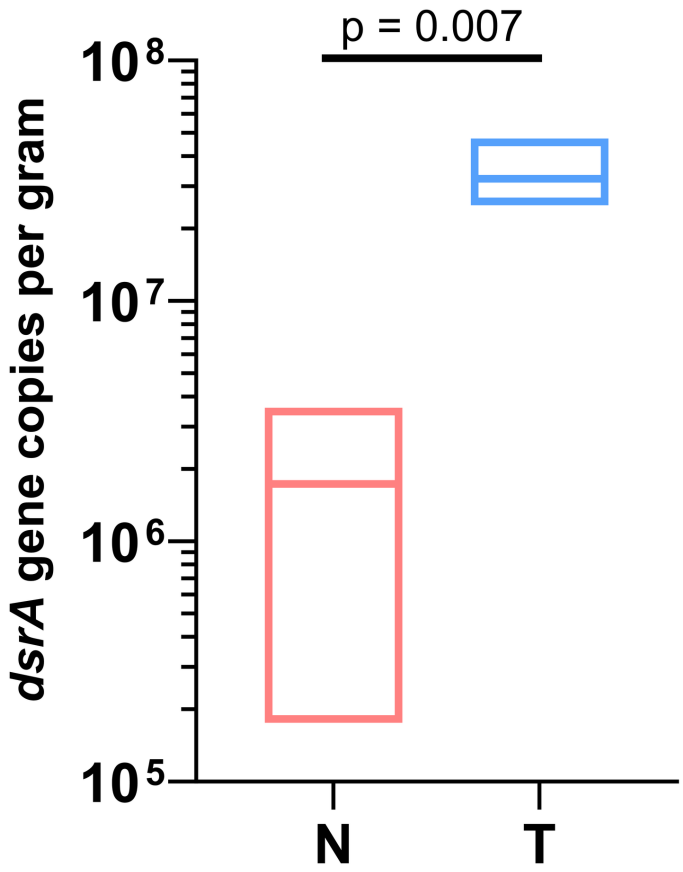

S3 Fig. Abundance of sulfate-reducing bacteria. Quantitative PCR targeting the *dsrA* gene from the offshore N and nearshore T sediments.

Chapter 5

Concluding remarks and future perspectives

Microbiologically influenced corrosion (MIC) poses a significant challenge due to the presence and/or activity of microorganisms (NACE-ASTM G193, 2022). This process impacts various industries, including marine infrastructures, gas and oil pipelines, and water treatment systems (Coetser, 2005; Skovhus et al., 2017; Kiani Khouzani et al., 2019). While conventional MIC mitigation strategies, such as chemical biocides and cathodic protection, have been effective, they often present environmental, economic, and regulatory challenges (Videla, 2002; Javaherdashti, 2017). To overcome these limitations, the development of eco-friendly alternatives has become increasingly important. Green corrosion inhibitors, such as plant-derived extracts, are particularly promising. These inhibitors offer key advantages, including low toxicity, biodegradability, and a reduced environmental impact (Hossain et al., 2019). Moreover, their adoption aligns with global efforts toward sustainability and circular economy principles, making them a desirable option for modern corrosion management.

The work presented in this thesis aimed to contribute to the development of novel methods for MIC prevention, mitigation and control. For this purpose, two complementary approaches have been pursued, namely the potential use of essential oils in eradicating biofilms-grown of *Desulfovibrio vulgaris*, as well as an innovative strategy based on the production of recombinant endolysins.

Among the various microorganisms involved in corrosion processes, such as fungi, algae, and archaea, bacteria have been the most extensively studied contributors (Lane, 2005). Sulfate reducing bacteria (SRB) represent the main players in this process, by adhering and proliferating as biofilms in the inner surface of metal infrastructures, and producing metabolites (*i.e.,* H_2S and FeS) that accelerate corrosion (Postgate, 1965; Telegdi et al., 2017). We have focused our studies on *D. vulgaris*, a representative SRB species, to investigate the dynamics of biofilm formation on different surfaces (Chapter 2), with the aim of researching the biofilm-eradication properties of eco-friendly biocides such as essential oils and plant extracts, as part of MIC-mitigation strategies. Cinnamaldehyde has been chosen as a proof of concept due to its well-known antimicrobial properties and its effectiveness as a corrosion inhibitor. Its anti-corrosion activity is attributed to the formation of a protective macroscopic film on metal surfaces (Hossain et al., 2019). However, while the antimicrobial activity of EOs or their components is well-documented, there is very limited knowledge about their application on microorganisms involving in MIC, especially on biofilm-growing SRB (Korenblum et al., 2013; Bhola et al., 2014; Souza et al., 2017). We have successfully demonstrated for the first

time that cinnamaldehyde exhibited comparable efficacy to the well-known reference biocide, glutaraldehyde, which is however toxic to the environment, particularly to aquatic ecosystems (Sano et al., 2005; Pereira et al., 2014). Cinnamaldehyde (*i.e.,* 12.5 µg/ml) inhibited the growth and killed planktonic *D. vulgaris* cells and, more importantly, almost completely disrupted biofilm-grown cells at 50 µg/ml, by reducing biomass (> 90 %), surface area (> 85 %) and thickness (> 60 %). These findings are particularly relevant for strategies aimed at mitigating microbial corrosion, since sessile cells within biofilms are notoriously more difficult to eradicate than planktonic ones. Interestingly, we were able to show that cinnamaldehyde effectively disrupts pre-formed *D. vulgaris* biofilms also on metal coupons, paving the way for further studies on its long-term effects and performance under different environmental conditions. Indeed, while cinnamaldehyde has demonstrated significant potential in lab-scale studies, its widespread adoption will face challenges related to scalability and variability in performance under diverse field conditions. Moreover, although SRB have historically been the primary focus of MIC research due to their prominent role in corrosion processes, other microbial groups also contribute significantly, and should be taken into account to better mimic the natural population dynamics responsible for MIC. The composition of microbial consortia in a given location is influenced by a variety of biotic and abiotic factors, including temperature, physiochemical properties, nutrient availability and fluid mixing (Dang and Lovell, 2016). Regarding the attached or biofilm-forming microbial consortia, it is widely recognized that microorganisms attach and form biofilm in a sequential manner. The formation of a biofilm can provide significant advantages to the community, such as improved resistance to environmental stressors and biocides (Bridier et al., 2011; Burmølle et al., 2014). Furthermore, the presence of diverse species within a consortium fosters interspecies cooperation, where certain species may supply nutrients or create habitats critical for the survival and growth of others. Among these natural population dynamics, aerobic iron-oxidizing bacteria (IOB) play a notable role in MIC. IOB oxidize ferrous ions (Fe^{2+}) to ferric ions (Fe^{3+}), using oxygen as the terminal electron acceptor, and this biologically-mediated oxidation occurs at a much faster rate than abiotic processes (Liu et al., 2016). IOB are known to accelerate the dissolution and localized corrosion of steels, and their interaction with SRB can exacerbate pitting corrosion (Xu et al., 2008). Oxygen consumption by IOB within biofilms creates anaerobic microenvironments, supporting the proliferation of SRB, which further facilitate and intensify corrosion processes. In addition to SRB and IOB, other microbial consortia, such as SRB and acid producing bacteria (APB),

also play a significant role in MIC. SRB and APB consortia have demonstrated resistance to biocides commonly used in water treatment (Pereira et al., 2021), highlighting the limitations of conventional chemical biocides. Future studies should explore the effects of cinnamaldehyde on these microbial consortia to evaluate its dual antibacterial and anti-corrosive activity. Specifically, the corrosion inhibition properties of cinnamaldehyde against these bacteria both individually and in mixed consortia should be investigated and monitored in long-term experiments. Moreover, to simulate environmental conditions where MIC occurs and provide valuable insights into cinnamaldehyde efficacy, research should examine biofilm formation, corrosion behavior, and the disruptive and anti-corrosion activity of cinnamaldehyde in a nutrient-rich artificial seawater as growth medium (Tran et al., 2020). Finally, advanced tools such as Scanning Electron Microscopy (SEM) should also be employed to assess cinnamaldehyde effectiveness in mitigating corrosion on metal surfaces. By fostering interdisciplinary collaboration and integrating cutting-edge science with sustainability principles, the next generation of MIC mitigation strategies will be able to address diverse microbial threats while minimizing the environmental impact. Advancing eco-friendly solutions like cinnamaldehyde not only tackles current challenges but also paves the way for sustainable and innovative approaches to combat MIC.

The second approach investigated in this thesis is based on an innovative strategy that regards the production of recombinant endolysins specific for *D. vulgaris*, as part of the development of green biocides to be used as a replacement for conventional toxic ones utilized in MIC control and mitigation. Endolysins are hydrolytic enzymes encoded by bacteriophages during their lytic cycle, targeting the peptidoglycan (PG) layer of both Gram-positive and Gram-negative bacteria, thus promoting cell osmotic lysis (Sao-José, 2018). Endolysins present a fast lytic activity against bacteria when they are exogenously applied as recombinant proteins (Vásquez and Briers, 2023). Moreover, these enzymes have garnered significant attention for their efficacy against clinically-relevant pathogens. Indeed, recombinant lysins were applied as "Enzybiotics" to eliminate bacterial infections and have been already assayed both *in vitro* and in *clinical trials*, and interestingly, the development of bacterial resistance has never been observed (Fischetti, 2005; Fenton et al., 2010; Briers et al., 2014; Chang, 2020 Murray et al., 2021; Liu et al., 2023). Given the many potential applications of endolysins, several biotechnology companies have started to investigate the use of phage-derived and engineered lysins in various fields. Indeed, endolysins have been applied not only as novel therapeutics,

but also as novel food preservation tools in the field of food safety (Dy et al., 2018; Nazir et al., 2023). Endolysins stand out as promising biocontrol agents due to their minimal biohazard potential for both human health and the environment. Extensive research has demonstrated their safety in human and animal models, with enzymatic inactivation deemed sufficient to prevent any environmental damage (HERA, 2007). Furthermore, the lack of hazardous effects on the human body suggests, by analogy, that their disposal and/or accumulation poses no detrimental effect to the environment. Being readily biodegradable, endolysins are environmentally friendly and do not present a biohazard concern, making them a sustainable option for various applications (Nelson et al., 2012). The last trend of enzymatic application is the eco-friendly remediation of xenobiotic-dependent pollution. Hydrolases have been shown to be efficient and safe when applied in different bioremediation scenarios, mainly because of their availability, their being economical and eco-friendly and their tolerance to the addition of water-miscible solvents (Bhandari et al., 2021). However, the potential of endolysins for the biocontrol in aquaculture and other environmentally relevant contexts, particularly those impacted by MIC, remains largely unexplored (De Romero et al., 2004). To fill this gap, this thesis focused on selecting and *in vitro* testing endolysins specific for *D. vulgaris* (Chapter 3), targeting various PG structures. The aim was to identify potential endolysins as green biocides as part of corrosion-mitigation strategies. Promising preliminary results highlighted the potential of different endolysins (*i.e.,* amidases, peptidases and soluble-lytic transglycosylases) to kill *D. vulgaris* planktonic cells permeabilized with chloroform. The latter treatment has been crucial to destabilizing the outer membrane (OM) of *D. vulgaris*, thus enabling the endolysins to access and degrade the PG layer. These results pave the way for developing engineered endolysins specifically targeting *D. vulgaris* and endowed with a permeabilizing peptide. To this aim, an outer membrane peptide (OMP) (Briers et al., 2011) could be included to mimic the membrane-destabilizing effect of chloroform, thus allowing *D. vulgaris* recombinant endolysins to cross the OM, reach and degrade the PG target. A promising approach to achieve this goal may involve the construction of *D. vulgaris* specific lysins libraries using the VersaTile technique (Gerstmans et al., 2020; Duyvejonck et al., 2021). The specific *D. vulgaris* engineered endolysins obtained with VersaTile could provide a more effective mean to mitigate SRB-associated issues, offering a novel and innovative strategy for controlling MIC, bypassing the use of conventional toxic biocides.

Finally, another strategy for MIC mitigation and control could include testing the synergistic antimicrobial activity of EOs and/or their components, such as cinnamaldehyde, with endolysins, since their combined application may yield enhanced results by leveraging their complementary mechanisms of action (Chang et al., 2017; Kim et al., 2024; Tyagi et al., 2024).

Chapter 5 references

- Bhandari S, Poudel DK, Marahatha R, Dawadi S, *et al*. **(2021)**. Microbial Enzymes Used in Biormediation. Journal of Chemistry, 1, 8849512. https://doi.org/10.1155/2021/8849512
- Bhola SM, Alabbas FM, Bhola R, *et al*. **(2014)**. Neem extract as an inhibitor for biocorrosion influenced by sulfate reducing bacteria: A preliminary investigation. Engineering Failure Analysis 36, 92-103. https://doi.org/10.1016/j.engfailanal.2013.09.015.
- Bridier A, Briandet R, Thomas V, Dubois-Brissonnet F. **(2011)**. Resistance of bacterial biofilms to disinfectants: a review. *Biofouling*, *27*(9), 1017–1032. https://doi.org/10.1080/08927014.2011.626899
- Briers Y, Walmagh M, Grymonprez B, Biebl M, Pirnay JP, Defraine V, Michiels J, Cenens W, Aertsen A, Miller S, Lavigne R. **(2014)**. Art-175 is a highly efficient antibacterial against multidrug-resistant strains and persisters of Pseudomonas aeruginosa. Antimicrob Agents Chemother. 58(7):3774-84. doi: 10.1128/AAC.02668-14.
- Briers Y, Walmagh M, Lavigne R. **(2011)**. Use of bacteriophage endolysin EL188 and outer membrane permeabilizers against Pseudomonas aeruginosa. J Appl Microbiol. 110(3):778-85. doi: 10.1111/j.1365-2672.2010.04931.x.
- Burmølle M, Ren D, Bjarnsholt T, Sørensen SJ. **(2014)**. Interactions in multispecies biofilms: do they actually matter?. *Trends in microbiology*, *22*(2), 84–91. https://doi.org/10.1016/j.tim.2013.12.004
- Chang Y, Yoon H, Kang DH, Chang PS, Ryu S. **(2017)**. Endolysin LysSA97 is synergistic with carvacrol in controlling Staphylococcus aureus in foods. *International journal of food microbiology*, *244*, 19–26. https://doi.org/10.1016/j.ijfoodmicro.2016.12.007
- Chang Y. **(2020)**. Bacteriophage-Derived Endolysins Applied as Potent Biocontrol Agents to Enhance Food Safety. *Microorganisms*. 8(5):724. doi:10.3390/microorganisms8050724
- Coetser SE, Cloete TE. **(2005)**. Biofouling and Biocorrosion in Industrial Water Systems. *Critical Reviews in Microbiology*, *31*(4), 213–232. https://doi.org/10.1080/10408410500304074
- Dang H, Lovell CR. **(2016)**. Microbial Surface Colonization and Biofilm Development in Marine Environments. *Microbiology and molecular biology reviews : MMBR*, *80*(1), 91–138. https://doi.org/10.1128/MMBR.00037-15
- de Romero MF, Urdaneta S, Barrientos M, Romero G. **(2004)**. Correlation Between Desulfovibrio Sessile Growth and OCP, Hydrogen Permeation, Corrosion Products and Morphological Attack on Iron, Paper No. 04576, CORROSION, NACE International
- Duyvejonck L, Gerstmans H, Stock M, Grimon D, Lavigne R, Briers Y. **(2021)**. Rapid and High- Throughput Evaluation of Diverse Configurations of Engineered Lysins Using the VersaTile Technique. *Antibiotics*. 10(3):293. https://doi.org/10.3390/antibiotics10030293
- Dy RL, Rigano LA, Fineran PC. **(2018)**. Phage-based biocontrol strategies and their application in agriculture and aquaculture, Biochem. Soc. Trans. 46; 1605–1613, https://doi.org/10.1042/bst20180178.
- Fenton M, Ross P, McAuliffe O, O'Mahony J, Coffey A. **(2010)**. Recombinant bacteriophage lysins as antibacterials. *Bioeng Bugs*. 1(1):9-16. doi:10.4161/bbug.1.1.9818
- Fischetti VA. **(2005)**. Bacteriophage lytic enzymes: novel anti-infectives. *Trends Microbiol*. 13(10):491-496. doi:10.1016/j.tim.2005.08.007

- Gerstmans H, Grimon D, Gutiérrez D, *et al*. **(2020)**. A VersaTile-driven platform for rapid hit-to-lead development of engineered lysins. *Sci Adv*. 6(23):eaaz1136. doi:10.1126/sciadv.aaz1136
- HERA. **(2007)**. Human and environmental risk assessment on ingredients of household cleaning products – Subtilisins (Proteases). Edition 2.0.A
- Hossain SMZ, Al-Shater A, Kareem SA, *et al*. **(2019)**. Cinnamaldehyde as a Green Inhibitor in Mitigating AISI 1015 Carbon Steel Corrosion in HCl. Arab J Sci Eng 44, 5489–5499. https://doi.org/10.1007/s13369-019-03793-y
- Javaherdashti R. **(2017)**. Microbiologically Influenced Corrosion: An Engineering Insight, 2nd ed. Springer International Publishing, AG, Cham, Switzerland. http://dx.doi.org/10.1007/978-3-319-44306-5
- Kiani Khouzani M, Bahrami A, Hosseini-Abari A, Khandouzi M, Taheri P. **(2019)**. Microbiologically Influenced Corrosion of a Pipeline in a Petrochemical Plant. *Metals*.; 9(4):459. https://doi.org/10.3390/met9040459
- Kim J, Kim S, Wang J, Anh J. **(2024)**. Synergistic antimicrobial activity of essential oils in combination with phage endolysin against Salmonella Typhimurium in cooked ground beef. Food Control, 157, 110187. https://doi.org/10.1016/j.foodcont.2023.110187
- Korenblum E, Regina de Vasconcelos Goulart F, de Almeida Rodrigues I, Abreu F, Lins U, Alves PB, Blank AF, Valoni E, Sebastián GV, Alviano DS, Alviano CS, Seldin L. **(2013)**. Antimicrobial action and anti-corrosion effect against sulfate reducing bacteria by lemongrass (Cymbopogon citratus) essential oil and its major component, the citral. AMB Express. 3(1):44. doi: 10.1186/2191-0855-3-44.
- Lane RA. **(2005)**. Under the microscope: Understanding, detecting, and preventing microbiologically influenced corrosion. *J. Fail. Anal. Prev.*;5, 10–12.
- Liu H, Gu T, Zhang G, Cheng Y, Wang H, Liu H. **(2016)**. The effect of magneticfield on biomineralization and corrosion behavior of carbon steel induced by iron-oxidizing bacteria. Corrosion Science, 102, 93-102. https://doi.org/10.1016/j.corsci.2015.09.023
- Liu H, Hu Z, Li M, Yang Y, Lu S, Rao X. **(2023)**. Therapeutic potential of bacteriophage endolysins for infections caused by Gram-positive bacteria. *J Biomed Sci*. 30(1):29. doi:10.1186/s12929-023-00919-1
- Murray E, Draper LA, Ross RP, Hill C. **(2021)**. The Advantages and Challenges of Using Endolysins in a Clinical Setting. *Viruses*. 13(4):680. doi:10.3390/v13040680
- NACE-ASTM G193-**2022**, Standard Terminology and Acronyms Relating to Corrosion.
- Nazir A, Xu X, Liu Y, Chen Y. **(2023)**. Phage Endolysins: Advances in the World of Food Safety. *Cells*. 12(17):2169. doi:10.3390/cells12172169
- Nelson DC, Schmelcher M, Rodriguez-Rubio L, *et al*. **(2012)**. Endolysins as antimicrobials. Adv. Virus Res. 83:299–365. doi: 10.1016/B978-0-12-394438-2.00007-4
- Pereira GF, Pilz-Junior HL, Corção G. **(2021)**. The impact of bacterial diversity on resistance to biocides in oilfields. Scientific reports, 11(1), 23027. https://doi.org/10.1038/s41598-021-02494-7
- Pereira SPP, Oliveira R, Coelho S, Musso C, Soares AMVM, Domingues I, Nogueira AJA. **(2014)**. From sub cellular to community level: Toxicity of glutaraldehyde to several aquatic organisms. Science of the Total Environment 470–471.
- Postgate JR. **(1965)**. Recent Advances in the Study of the Sulfate-Reducing Bacteria, Bacteriological Reviews, Vol 26, No 4.

- Sano LL, Krueger AM, Landrum PF. **(2005)**. Chronic toxicity of glutaraldehyde: differential sensitivity of three freshwater organisms. Aquatic Toxicology 71, 283–296. doi:10.1016/j.aquatox.2004.12.001
- São-José C. **(2018)**. Engineering of Phage-Derived Lytic Enzymes: Improving Their Potential as Antimicrobials. *Antibiotics (Basel)*. 7(2):29. doi:10.3390/antibiotics7020029.
- Skovhus T, Enning D, Lee J. **(2017)**. Microbiologically influenced corrosion in the upstream oil and gas industry. 1st Edn. Boca Raton FL: CRC Press. http://doi:10.1201/9781315157818
- Souza PM, Goulart FRV, Marques JM, Bizzo HR, Blank AF, Groposo C, Sousa MP, Vólaro V, Alviano CS, Moreno DSA, Seldin L. **(2017)**. Growth Inhibition of Sulfate-Reducing Bacteria in Produced Water from the Petroleum Industry Using Essential Oils. Molecules. 22(4):648. doi: 10.3390/molecules22040648.
- Telegdi J, Shaban A, Trif L. **(2017)**. Microbiologically influenced corrosion (MIC). *Trends in Oil and Gas Corrosion Research and Technologies*. 191-214.
- Tran Thi Thuy T, Kannoorpatti K, Padovan A, Thennadil S. **(2020)**. Effect of Alkaline Artificial Seawater Environment on the Corrosion Behaviour of Duplex Stainless Steel 2205. *Applied Sciences*, *10*(15), 5043. https://doi.org/10.3390/app10155043
- Tyagi JL, Gupta P, Ghate MM, Kumar D, Poluri KM. **(2024)**. Assessing the synergistic potential of bacteriophage endolysins and antimicrobial peptides for eradicating bacterial biofilms. *Archives of microbiology*, *206*(6), 272. https://doi.org/10.1007/s00203-024-04003-6
- Vázquez R, Briers Y. **(2023)**. What's in a Name? An Overview of the Proliferating Nomenclature in the Field of Phage Lysins. *Cells*. 12(15):2016. doi:10.3390/cells12152016
- Videla HA. **(2002)**. Prevention and control of biocorrosion. Int. Biodeterior. Biodegrad. 49, 259–270. https://doi.org/10.1016/S0964-8305(02)00053-7
- Xu C, Zhang Y, Cheng G, Zhu W. **(2008)**. Pitting corrosion behavior of 316L stainless steel in the media of sulphate-reducing and iron-oxidizing bacteria. Mater Charact 59:245–255. doi:10.1016/j.matchar.2007.01.001

Acknowledgments

This PhD thesis is the result of years of hard work, sacrifices, and overcoming both personal and scientific challenges. There were many sleepless nights thinking about experiments and solutions, and long day in the lab with collogues who became friends.

First of all, I would like to thank my supervisor, Prof. Emanuela Frangipani, for giving me the opportunity to join in her lab. Her expertise, availability, and immense humanity have been invaluable. I feel lucky to have learned so much from her, both professionally and personally. No matter what challenges came our way, our goal was always to do excellent research and work well together.

I am also grateful to Dr. Mauro Fehervari of SAIPEM s.p.a. for the many fruitful discussions that significantly contributed to this project.

A special thanks goes to Dr. Sarah Hijazi for her friendship and constant support in lab.

During these three years of PhD, I was lucky to meet wonderful colleagues and friends like Veronica, Francesco, and Asja. Their presence made this PhD journey easier by creating moments of laughter, celebrations, and dinners that I will always treasure.

A heartfelt thanks goes to Dr. Caterina Ciacci, or "Milo". I learned so much from her, and she became a true friend who supported me at every step and always made me smile.

I would also like to thank everyone in the Hygiene Section: Prof.s Giorgio Brandi, Giuditta Schiavano, Giulia Amagliani, Mauro De Santi, Maurizio Sisti, and the technicians Raffaella, Valentina, and Manuela. You all brightened my days, and it was a pleasure to know you.

My gratitude also goes to Prof. Rob Lavigne for giving me the opportunity to spend three months of my PhD in Leuven, Belgium. There, I met fantastic people and found a highly stimulating work environment.

Of course, I want to thank my family for always supporting me and putting up with me during this PhD period, always respecting my choices.

A special mention goes to my angel, my grandfather Filippo, who recently passed away but remains in our hearts. I hope I have made you proud.

Lastly, I want to thank my partner, Camillo, the love of my life, who has always been by my side. You are my superhero and the superhero of our son, Mattia, the most precious gift life has given us. I look forward to a wonderful life together, full of health and happiness.